



THE HONG KONG  
POLYTECHNIC UNIVERSITY

香港理工大學

Pao Yue-kong Library

包玉剛圖書館

---

## Copyright Undertaking

This thesis is protected by copyright, with all rights reserved.

**By reading and using the thesis, the reader understands and agrees to the following terms:**

1. The reader will abide by the rules and legal ordinances governing copyright regarding the use of the thesis.
2. The reader will use the thesis for the purpose of research or private study only and not for distribution or further reproduction or any other purpose.
3. The reader agrees to indemnify and hold the University harmless from and against any loss, damage, cost, liability or expenses arising from copyright infringement or unauthorized usage.

### IMPORTANT

If you have reasons to believe that any materials in this thesis are deemed not suitable to be distributed in this form, or a copyright owner having difficulty with the material being included in our database, please contact [lbsys@polyu.edu.hk](mailto:lbsys@polyu.edu.hk) providing details. The Library will look into your claim and consider taking remedial action upon receipt of the written requests.

PHARMACOLOGICAL INHIBITION OF  
GLIOBLASTOMA CELL PROLIFERATION,  
MIGRATION AND INVASION

ZHAO HUAFU

Ph.D

The Hong Kong Polytechnic University

2015



The Hong Kong Polytechnic University  
Department of Health Technology and Informatics

**Pharmacological Inhibition of  
Glioblastoma Cell Proliferation,  
Migration and Invasion**

**ZHAO Huafu**

A thesis submitted in partial fulfilment of the requirements  
for the degree of Doctor of Philosophy

June 2015



# CERTIFICATE OF ORIGINALITY

I hereby declare that this thesis is my own work and that, to the best of my knowledge and belief, it reproduces no material previously published or written, nor material that has been accepted for the award of any other degree or diploma, except where due acknowledgement has been made in the text.

\_\_\_\_\_ (Signed)

ZHAO Huafu \_\_\_\_\_ (Name of student)



## **Abstract**

Glioblastoma multiforme is the most aggressive and malignant primary brain tumor, characterized by rapid growth, extensive infiltration to neighboring normal brain parenchyma, and angiogenesis. Patients with glioblastoma have poor prognosis since the whole tumor is barely completely removed. Thus, identification of novel molecules or more effective drugs targeting glioblastoma migration and invasion is urgently needed. The phosphatidylinositol 3-kinase (PI3K)/Akt signaling pathway plays a pivotal role in the development and survival of many cancers including glioblastoma. Selective inhibitors against class I<sub>A</sub> PI3K catalytic isoforms (p110 $\alpha$ , p110 $\beta$  and p110 $\delta$ ) are attractive options for glioblastoma treatment because they display less off-target effects and toxicities. Considering that the inhibition of PI3K isoforms might be compensated by other signaling pathways, and subsequently compromise their inhibitory effects, combination treatment strategies on glioblastoma cells were also investigated. Since JNK pathway is also essential to cancer cell viability and motility, and has a crosstalk with the PI3K/Akt pathway, concurrent inhibition of PI3K and JNK may exhibit synergism. Firstly, this study investigated the roles of p110 $\alpha$ , p110 $\beta$  and p110 $\delta$  in glioblastoma cells using their respective inhibitors PIK-75, TGX-221 and CAL-101. Combination effects of p110 isoforms and JNK inhibition on glioblastoma cell proliferation, migration and invasion were then evaluated. Results showed that p110 $\alpha$ , p110 $\beta$  and p110 $\delta$  have distinct roles in the pathological processes in glioblastoma. PIK-75 was sufficient to suppress

glioblastoma cell viability, migration and invasion, whereas TGX-221 only reduced migration, and CAL-101 just moderately inhibited proliferation and migration. Compared with CAL-101, siRNA-induced knockdown of *PIK3CD* significantly suppressed glioblastoma cell proliferation, migration and invasion without affecting Akt phosphorylation level. According to these results, a competition model of p110 $\alpha$ , p110 $\beta$  and p110 $\delta$  was proposed, in which p110 $\beta$  and p110 $\delta$  may compete with p110 $\alpha$  for RTK binding sites. Furthermore, PIK-75 antagonized with JNK inhibitor SP600125, whereas TGX-221 and CAL-101 displayed synergistic inhibitory effects with SP600125 on glioblastoma cell proliferation and migration through inactivation of Akt, zyxin and FAK, leading to the blockade of lamellipodia and membrane ruffles formation. No synergistic effect on invasion was observed in all combinations. And a crosstalk model between PI3K isoforms and JNK was also proposed based on the competition model.

Myricetin is a natural flavonoid that exhibits potent anti-oxidative, anti-inflammatory, anti-diabetic and anti-cancer activities. It targets Akt, MEK1, MKK4, JAK1, RSK2 and Fyn and inhibits their activation in an ATP-competitive or -noncompetitive manner. These suggest that myricetin may be a safe and potent therapeutic drug for glioblastoma treatment. However, the role of myricetin in the regulation of glioblastoma cell viability and motility is not fully clarified. This study showed that myricetin was sufficient to suppress glioblastoma cell proliferation, whereas it displayed lower cytotoxicity to normal astrocytes. It also significantly inhibited migration and invasion capacities of glioblastoma cells by targeting class I<sub>A</sub>

PI3K catalytic isoforms and JNK. However, Myricetin was not able to sensitize glioblastoma cells to low concentrations of temozolomide. Nevertheless, it is still a promising therapeutic approach for treating glioblastoma multiforme.

In summary, combined inhibition of p110 $\beta$ /p110 $\delta$  and JNK, as well as myricetin can suppress proliferation and motility of glioblastoma cells, indicating that they may be attractive options for glioblastoma treatment.

## List of Publications

### Scientific Journal Papers

1. **Zhao HE**, Wang J, To SST. The phosphatidylinositol 3-kinase/Akt and c-Jun N-terminal kinase signaling in cancer: alliance or contradiction? (review). *Int J Oncol*. 2015; 47(2): 429-436.
2. **Zhao HE**, Wang J, Chen ZP, To SST. Distinct PI3K isoforms synergize with JNK in the regulation of glioblastoma cell proliferation and migration through Akt, zyxin and FAK. (Submitted to *Scientific Report*, Under Revision, Manuscript SREP-15-08984)
3. Wang G, Wang J, Wu W, To SST, **Zhao HE**, Wang J. Advances in lipid-based drug delivery: enhancing efficiency for hydrophobic drugs. *Expert Opin Drug Deliv*. 2015; 5:1-25.

### International Conference Abstracts

1. **Zhao HE**, Wang J, To SST. Synergistic effect of PI3K $\delta$  inhibitor CAL-101 and JNK inhibitor SP600125 on glioblastoma cell proliferation. American Association for Cancer Research Annual Meeting 2015. Philadelphia, US.
2. **Zhao HE**, Wang J, To SST. PI3K $\beta$  isoform synergizes with JNK to mediate glioblastoma cell proliferation and migration through Akt and FAK. Cold Spring Harbor Asia Conference, 2015. Suzhou, China.

## Acknowledgements

I would like to express my sincerest appreciation to my chief supervisor Dr. Shing-Shun Tony To, for providing me with a valuable opportunity to pursue my PhD study. His patient guidance, positive encouragement and ceaseless support help me through many problems, setbacks and challenges. I have learned a lot from his hard work and the way of addressing issues, and received invaluable experience and training throughout my entire PhD study.

I would like to thank Dr. Wang Jing (Department of Neurosurgery/Neuro-oncology, Sun Yat-sen University Cancer Center) for her precious suggestions and comments to the study design, and reviewing my manuscripts.

I would like to thank Prof. Benjamin Yung, Prof. Shea-Ping Yip, Dr. Parco Siu, Dr. Daniel Sze, Dr. Polly Leung, Dr. Cesar Wong, Dr. Lawrence Chan and Dr. Helen Law for their lectures, instructions and suggestions in my PhD study.

I would like to thank Dr. Wang Gang (Shanghai Eighth People Hospital) for his technical training in HPLC and preparation of nanoparticle drug carrier.

I would like to thank Mrs. Sharon Ho, Mrs Aileen Wong, Mrs. Grace Tang, Mrs. Brenda Cheung, Mrs Michelle Ng and all the other technical staff for their assistance.

I would like to thank Mr. David Lau, Mr. Tommy Chan, Ms. Kathy Kwan, Ms. Doris Kwok, Ms. Vangie Chung and other staff in the general office for their assistance in my PhD study.

## Acknowledgements

---

I would like to thank my team members including the final-year project students and MSc students for giving support for my study and their understanding of my guidance.

I would like to thank all the research students in our department and other friends for their helps and sharing of ideas and experience.

I would like to thank the Department of Health Technology and Informatics for providing an advanced laboratory and research environment, and giving me financial support to attend conferences. I would also like to thank the Hong Kong Polytechnic University (Central Grant RTH4) to undertake my research project.

Last but not the least, I would like to thank my parents, my wife, my son and my sister for their great love and unconditional support during my PhD study.

## Table of Contents

<b>Abstract</b> .....	I
<b>List of Publications</b> .....	IV
<b>Acknowledgements</b> .....	V
<b>Table of Contents</b> .....	VII
<b>List of Figures</b> .....	XIII
<b>List of Tables</b> .....	XVIII
<b>List of Abbreviations</b> .....	XIX
<b>Chapter 1 Literature review</b> .....	1
1.1 Overview of glioblastoma multiforme.....	1
1.1.1 Classification and characteristics of glioma.....	3
1.1.2 Genetic aberrations in glioblastoma multiforme .....	5
1.1.3 Therapeutic strategies for glioblastoma multiforme.....	8
1.1.3.1 Temozolomide .....	8
1.1.3.2 Anti-angiogenic therapies.....	9
1.1.3.3 Epidermal growth factor receptor (EGFR)-targeted therapies.....	11
1.2 Overview of phosphatidylinositol 3-kinase (PI3K)/Akt signaling pathway...	13
1.2.1 Canonical PI3K/Akt signaling pathway.....	13
1.2.2 PI3K family .....	16

## Table of Contents

---

1.2.2.1	Class I <sub>A</sub> PI3Ks .....	18
1.2.2.2	Class I <sub>B</sub> PI3Ks .....	20
1.2.3	Roles of class I <sub>A</sub> PI3K isoforms in glioblastoma .....	21
1.2.4	Roles of Akt in glioblastoma .....	25
1.2.5	<i>EGFR</i> amplification and <i>PTEN</i> mutation in glioblastoma .....	29
1.2.6	PI3K inhibitors .....	31
1.3	Overview of c-Jun N-terminal kinase (JNK) signaling pathway .....	34
1.3.1	Mitogen-activated protein kinases (MAPKs) pathway .....	34
1.3.2	Activation of JNK signaling .....	37
1.3.3	JNK signaling in cell migration and invasion .....	38
1.3.4	Roles of JNK signaling in glioblastoma .....	40
1.3.5	Crosstalk between PI3K/Akt and JNK pathways .....	42
1.3.6	Combination therapy targeting PI3K/Akt and Ras-mediated MAPK pathways .....	46
1.4	Overview of myricetin .....	47
1.4.1	Anti-oxidant and anti-inflammatory activities of myricetin.....	49
1.4.2	Anti-cancer activity of myricetin.....	50
1.4.3	Molecular targets of myricetin .....	51
1.5	Rationales and objectives of this study .....	52
<b>Chapter 2</b>	<b>Materials and methods</b> .....	<b>54</b>
2.1	Cell lines.....	54
2.2	Cell culture .....	56

## Table of Contents

---

2.3	Drug treatment .....	56
2.4	Cell proliferation assay (MTT method) .....	59
2.5	Determination of combination index (CI).....	59
2.6	Wound healing assay .....	61
2.7	Immunofluorescence .....	61
2.8	Boyden chamber migration assay .....	62
2.9	Invasion assay .....	62
2.10	Protein extraction .....	63
2.11	BCA protein assay.....	63
2.12	Western blotting .....	65
2.13	Preparation of myricetin-Sepherose 4B .....	65
2.14	<i>Ex vivo</i> pull-down assay .....	66
2.15	RNA isolation.....	66
2.16	Quantification of isolated RNA .....	67
2.17	cDNA synthesis .....	68
2.18	Quantitative Real-time PCR (qRT-PCR) .....	68
	2.18.1 Primer design .....	68
	2.18.2 SYBR Green qRT-PCR.....	70
	2.18.3 TaqMan qRT-PCR.....	70
2.19	RNA interference .....	71
2.20	Statistical analysis .....	73

**Chapter 3 Distinct roles of PI3K catalytic isoforms in glioblastoma ..74**

3.1 Expression pattern of PI3K/Akt pathway molecules in glioblastoma cell lines..... 74

3.2 Effect of isoform-selective PI3K inhibitors on glioblastoma cell proliferation.....77

3.3 Inhibition of p110 $\alpha$ , p110 $\beta$ , or p110 $\delta$  suppresses glioblastoma migration ..86

3.4 Inhibition of p110 $\alpha$  is sufficient to inhibit glioblastoma cell invasion .....93

3.5 Knockdown of p110 $\delta$  shows distinct effect on Akt signaling and invasion in glioblastoma cells.....95

3.6 Discussion ..... 104

3.6.2 Distinct expression pattern of PI3K/Akt pathway molecules in glioblastoma cells ..... 104

3.6.3 The p110 $\alpha$  isoform plays a more crucial role in glioblastoma than p110 $\beta$  and p110 $\delta$ ..... 105

3.6.4 The p110 $\delta$  isoform may compete with p110 $\alpha$  and p110 $\beta$  for RTK binding..... 108

3.6.5 Knockdown of *PIK3CD* inhibits glioblastoma cell migration and invasion ..... 111

**Chapter 4 Combined inhibition of PI3K catalytic isoforms and JNK in glioblastoma.....114**

4.1 Inhibition of JNK suppresses glioblastoma cell proliferation and JNK signaling..... 114

4.2	Combination effects of isoform-selective PI3K inhibitors and JNK inhibitor on glioblastoma cell proliferation .....	119
4.3	Combination effects of isoform-selective PI3K inhibitors and JNK inhibitor on glioblastoma cell migration and invasion.....	129
4.4	Discussion .....	140
4.4.1	A crosstalk model between class I <sub>A</sub> PI3K catalytic isoforms and JNK .....	140
4.4.2	Inhibition of zyxin and FAK contributes to the synergism .....	143
<b>Chapter 5</b>	<b>Anti-cancer effects of myricetin on glioblastoma .....</b>	<b>146</b>
5.1	Myricetin suppresses glioblastoma cell proliferation .....	146
5.2	Myricetin blocks glioblastoma cell migration and invasion through targeting PI3K and JNK.....	151
5.3	Myricetin does not sensitize glioblastoma cells to temozolomide.....	156
5.4	Discussion .....	164
5.4.1	Myricetin is a natural flavonoid with potent anti-cancer activity... ..	164
5.4.2	Combination treatment of myricetin and temozolomide .....	166
<b>Chapter 6</b>	<b>General discussion and conclusions .....</b>	<b>170</b>
6.1	Introduction.....	170
6.2	Regulation of cancer cell migration by FAK and zyxin signaling .....	170
6.3	Therapeutic implications of pharmacological inhibition and siRNA-induced gene silencing .....	173

## Table of Contents

---

6.4 Drug resistance to single agent and implications for combination therapies .....	177
6.5 Anti-cancer effect and therapeutic implications of natural flavonoids.....	178
6.6 Conclusions .....	180
6.7 Suggestions for future research .....	181
<b>Appendix</b> .....	184
<b>References</b> .....	187

## List of Figures

Figure 1.1: Distribution of primary brain and CNS tumors by histological characteristics in CBTRUS statistical report .....	2
Figure 1.2: Genetic aberrations of primary and secondary glioblastoma .....	7
Figure 1.3: Simplified scheme demonstrating different activation manners of class I <sub>A</sub> and class I <sub>B</sub> PI3K subunits .....	15
Figure 1.4: Domain structures of class I, II and III PI3Ks .....	17
Figure 1.5: Simplified scheme showing the process of Akt activation and its downstream pathway molecules .....	28
Figure 1.6: Simplified scheme showing activation of MAPK pathways .....	36
Figure 1.7: Simplified scheme demonstrating different crosstalks between PI3K/Akt and JNK pathways .....	45
Figure 1.8: Chemical structures of flavonoid and the representative flavonols including myricetin, quercetin, kaempferol and fisetin.....	48
Figure 3.1: Expression pattern of PI3K/Akt pathway molecules in human glioblastoma cell lines .....	76
Figure 3.2: Divergent effects of PIK-75, TGX-221 and CAL-101 on glioblastoma cell proliferation .....	78
Figure 3.3: Effects of isoform-selective PI3K inhibitors on cell proliferation in glioblastoma cells and normal human astrocytes .....	80
Figure 3.4: Effects of isoform-selective PI3K inhibitors on Akt signaling in	

## List of Figures

---

glioblastoma cells.....	82
Figure 3.5: Effect of CAL-101 on Akt signaling in glioblastoma cells at different time points .....	84
Figure 3.6: Effect of CAL-101 on Akt signaling in glioblastoma cells after 48- and 72-hr incubation .....	85
Figure 3.7: Glioblastoma cell proliferation was inhibited by mitomycin C.....	88
Figure 3.8: Inhibitory effect of isoform-selective PI3K inhibitors on migration in U-87 MG glioblastoma cells.....	89
Figure 3.9: Inhibitory effect of isoform-selective PI3K inhibitors on migration in U-373 MG glioblastoma cells.....	90
Figure 3.10: Inhibitory effects of isoform-selective PI3K inhibitors on lamellipodia and membrane ruffles formation in glioblastoma cells.....	92
Figure 3.11: Inhibition of p110 $\alpha$ blocked glioblastoma cell invasion .....	94
Figure 3.12: Optimization of siRNA transfection efficiency.....	96
Figure 3.13: Knockdown of <i>PIK3CD</i> in glioblastoma cells .....	98
Figure 3.14: Effect of <i>PIK3CD</i> gene knockdown on glioblastoma cell proliferation	100
Figure 3.15: Effect of <i>PIK3CD</i> gene knockdown on glioblastoma cell migration and invasion.....	102
Figure 3.16: The siRNA duplexes against <i>PIK3CD</i> influenced the expression of <i>ADAMTS1</i> , <i>P130Cas</i> , <i>ITGB1</i> , and <i>ITGB3</i> .....	103
Figure 3.17: Schematic diagram demonstrating a competition model of p110 $\alpha$ and p110 $\beta$ against RTK-binding sites .....	110

Figure 4.1: Expression pattern of JNK pathway in glioblastoma cells and effect of JNK inhibitor SP600125 on glioblastoma cell proliferation.....	116
Figure 4.2: Inhibitory effect of JNK inhibitor SP600125 on JNK signaling in glioblastoma cells.....	117
Figure 4.3: SP600125 inhibited c-Jun phosphorylation in a time-dependent manner .....	118
Figure 4.4: Combination effects of isoform-selective PI3K inhibitors and SP600125 on glioblastoma cell proliferation.....	120
Figure 4.5: Combination effects of isoform-selective PI3K inhibitors and SP600125 on glioblastoma cell proliferation and signal transduction.....	126
Figure 4.6: Combination effects of isoform-selective PI3K inhibitors and SP600125 on U-373 MG glioblastoma cell proliferation .....	127
Figure 4.7: Combination effects of isoform-selective PI3K inhibitors and SP600125 on cell proliferation in normal human astrocytes.....	128
Figure 4.8: SP600125 potentiates inhibitory effects of isoform-selective PI3K inhibitors on glioblastoma cell migration .....	132
Figure 4.9: Combination effects of isoform-selective PI3K inhibitors and SP600125 on migration of U-373 MG glioblastoma cells .....	134
Figure 4.10: SP600125 potentiates inhibitory effects of isoform-selective PI3K inhibitors on lamellipodia and membrane ruffles formation.....	136
Figure 4.11: Combination effects of Isoform-selective PI3K inhibitors and SP600125 on focal adhesion and cytoskeleton-related signaling .....	138

Figure 4.12: Combination effects of isoform-selective PI3K inhibitors and SP600125 on glioblastoma cell invasion .....	139
Figure 4.13: Schematic diagram showing a model of combined inhibition of class I <sub>A</sub> PI3K catalytic isoforms and JNK.....	142
Figure 5.1: Effect of myricetin on proliferation in glioblastoma cells and human astrocytes.....	148
Figure 5.2: Myricetin influenced glioblastoma cell morphology .....	149
Figure 5.3: Effect of myricetin on PI3K/Akt and JNK signaling in glioblastoma cells .....	150
Figure 5.4: Inhibitory effect of myricetin on directional migration of glioblastoma cells .....	152
Figure 5.5: Inhibitory effect of myricetin on glioblastoma cell transmigration .....	153
Figure 5.6: Inhibitory effect of myricetin on glioblastoma cell invasion.....	154
Figure 5.7: Myricetin directly binds to PI3K and JNK .....	155
Figure 5.8: Effect of temozolomide on glioblastoma cell proliferation .....	157
Figure 5.9: Combination effect of myricetin and temozolomide on glioblastoma cell proliferation .....	159
Figure 5.10: Combination effect of myricetin and temozolomide on directional migration of glioblastoma cells.....	161
Figure 5.11: Combination effect of myricetin and temozolomide on glioblastoma cell transmigration .....	162
Figure 5.12: Combination effect of myricetin and temozolomide on glioblastoma cell	

invasion.....163

## List of Tables

Table 1.1: WHO grading and characteristics of glioma .....	4
Table 1.2: Comparison of studies investigating <i>PIK3CA</i> mutations in glioblastoma.	23
Table 1.3: PI3K inhibitors in clinical trials (data from ClinicalTrials.gov).....	33
Table 2.1: Characteristics of human glioblastoma cell lines [284, 285] .....	55
Table 2.2: Characteristics of isoform-selective PI3K inhibitors.....	58
Table 2.3: Characteristics of JNK inhibitor SP600125.....	58
Table 2.4: Combination index values and their indications.....	60
Table 2.5: Preparation of diluted BSA standards.....	64
Table 2.6: Primer sequence and characteristics of primers.....	69
Table 2.7: Sequences of siRNA duplexes targeting <i>PIK3CD</i> gene .....	72
Table 4.1: Combination index (CI) for cell viability in U-87 MG glioblastoma cells treated with combinations of SP600125 and PIK-75, TGX-221 or CAL-101 .....	121
Table 4.2: Combination index (CI) for cell viability in U-87 MG cells treated with PIK-75 and SP600125 at a fixed ratio of 1:40.....	122
Table 5.1: Combination index (CI) for cell viability in U-87 MG cells treated with myricetin and temozolomide .....	158

## List of Abbreviations

4EBP	Eukaryotic initiation factor 4E-binding protein
ABCD1 (MDR1)	Multidrug resistance 1
ABCG2	ATP-binding cassette subfamily G member 2
ABD	Adaptor-binding domain
ADAMTS1	A disintegrin and metalloprotease with thrombospondin motifs 1
AML	Acute myeloid leukemia
AP-1	Activator protein-1
ASK1	Apoptosis signal-regulating kinase-1
ATCC	American Type Culture Collection
ATF2	Activating transcription factor 2
ATP	Adenosine triphosphate
BAD	Bcl-2-associated death promoter
Bax	Bcl2-associated x protein
BCAR1	Breast cancer anti-estrogen resistance protein 1
Bcl-2	B-cell lymphoma-2
bFGF	Basic fibroblast growth factor
BMK1	Big mitogen activated protein kinase 1
BSA	Bovine serum albumin
Cas	Crk-associated substrate

## List of Abbreviations

---

CBTRUS	Central Brain Tumor Registry of the United States
CDC42	Cell division control protein 42
CDK	Cyclin-dependent kinase
CI	Combination index
CLL	Chronic lymphocytic leukemia
CML	Chronic myeloid leukemia
CNS	Central nervous system
COX-2	Cyclooxygenase-2
CRC	Colorectal carcinoma
CRISPR	Clusters of regularly interspaced short palindromic repeat
DLK	Dual leucine zipper-bearing kinase
DMSO	Dimethyl sulfoxide
ECM	Extracellular matrix
EDTA	Ethylene diamine tetraacetic acid
EGF	Epidermal growth factor
EGFR	EGF receptor
EGFRvIII	EGFR variant III
ELK1	ETS-like transcription factor 1
Ena/VASP	Enabled/vasodilator-stimulated phospho-protein
EPS8	Epidermal growth factor substrate 8
ERK	Extracellular signal-regulated kinase
FA	Fraction affected

## List of Abbreviations

---

FAK	Focal adhesion kinase
FBS	Fetal bovine serum
FDA	Food and Drug Administration
FGFR	Fibroblast growth factor receptor
FOXO	Forkhead box protein
GAPDH	Glyceraldehyde 3-phosphate dehydrogenase
GBM	Glioblastoma multiforme
GDP	Guanosine diphosphate
GIST	Gastrointestinal stromal tumor
GPCR	G-protein-coupled receptor
G-protein	GTP-binding protein
GSK3	Glycogen synthase kinase 3
GTP	Guanosine triphosphate
H&N	Head and neck cancer
HCC	Hepatocellular carcinoma
HEPES	4-(2-hydroxyethyl)-1-piperazineethanesulfonic acid
HER2	Human epidermal growth factor receptor 2
HGF	Hepatocyte growth factor
HIF-1 $\alpha$	Hypoxia inducible factor-1 alpha
HPK1	Haematopoietic progenitor kinase 1
HRP	Horseradish peroxidase
IC <sub>50</sub>	Half maximal inhibitory concentration

## List of Abbreviations

---

IDH1	Isocitrate dehydrogenase 1
IFN- $\gamma$	Interferon-gamma
IGF-1	Insulin-like growth factor-1
IKK	I $\kappa$ B kinase
IL	Interleukin
JAK	Janus kinase
JIP	JNK interacting protein
JLP	JNK-interacting leucine zipper protein
JNK	c-Jun N-terminal kinase
LOH	Loss of heterozygosity
MAPK	Mitogen-activated protein kinase
MAPKK (MAP2K, MEK)	MAP kinase kinase
MAPKKK (MAP3K, MEKK)	MAP kinase kinase kinase
MAPKKKK (MAP4K)	MAP kinase kinase kinase kinase
MDM2	Murine double minute 2
MEF	Mouse embryonic fibroblast
MGMT	O <sup>6</sup> -methylguanine-DNA methyltransferase
MKK4 (SEK1)	MAPK kinase 4 (SAPK/ERK kinase 1)
MKK7 (SEK2)	MAPK kinase 7 (SAPK/ERK kinase 2)
MLK	Mixed-lineage kinase
MMP	Matrix metalloproteinase
mTOR	Mammalian target of rapamycin

## List of Abbreviations

---

mTORC1	mTOR complex 1
mTORC2	mTOR complex 2
MTT	3-(4,5-dimethylthiazol-2-yl)-2,5-diphenyltetrazolium bromide
NF- $\kappa$ B	Nuclear factor- $\kappa$ B
NHL	Non-Hodgkin's lymphoma
NSCLC	Non-small cell lung cancer
p27 <sup>kip1</sup> (CDKN1B)	Cyclin-dependent kinase inhibitor 1B
PBS	Phosphate-buffered saline
PCNA	Proliferating cell nuclear antigen
PDGF	Platelet derived growth factor
PDGFR	PDGF receptor
PDK	Phosphoinositide-dependent kinase
PH	Pleckstrin homology
PI3K	Phosphatidylinositol 3-kinase
PKB, Akt	Protein kinase B
POSH	Plenty of SH3
PtdIns	Phosphatidylinositol
PtdIns(3)P	Phosphatidylinositol-3-phosphate
PtdIns(3,4)P <sub>2</sub>	Phosphatidylinositol-3,4-bisphosphate
PtdIns(3,4,5)P <sub>3</sub> , PIP <sub>3</sub>	Phosphatidylinositol 3,4,5-triphosphate
PtdIns(4)P	Phosphatidylinositol-4-phosphate

## List of Abbreviations

---

PtdIns(4,5)P <sub>2</sub> , PIP <sub>2</sub>	Phosphatidylinositol 4,5-bisphosphate
PTEN	Phosphatase and tensin homolog deleted on chromosome 10
RBD	Ras-binding domain
RCC	Renal cell carcinoma
RhoA	Ras homolog gene family member A
RISC	RNA-induced silencing complex
RNAi	RNA interference
ROS	Reactive oxygen species
RSK2	Ribosomal S6 kinase 2
RTK	Receptor tyrosine kinase
S6K (p70 RSK)	p70 ribosomal S6 kinase
SEM	Standard error of mean
SAPK	Stress-activated protein kinase
SDS	Sodium dodecyl sulfate
SDS-PAGE	SDS-polyacrylamide gel electrophoresis
Ser	Serine
SH2	Src homology 2
SH3	Src homology 3
shRNA	Short hairpin RNA
siRNA	Small interfering RNA
STAT3	Signal transducer and activator of transcription 3

## List of Abbreviations

---

TALEN	Transcription activator-like effector nuclease
TBS	Tris-buffered saline
Thr	Threonine
TIMP	Tissue-inhibitor of metalloproteinase
TMZ	Temozolomide
TNF	Tumor necrosis factor
TPA	12-O-Tetradecanoylphorbol-13-acetate
TRAIL	TNF-related apoptosis-inducing ligand
TSC	Tuberous sclerosis complex
Tyr	Tyrosine
uPA	Urokinase plasminogen activator
UTR	Untranslated region
UV	Ultraviolet
VEGF	Vascular endothelial growth factor
VEGFR	VEGF receptor
WHO	World Health Organization
WT	Wild type
YXXM	Tyr-xaa-xaa-met
ZFN	Zinc finger nuclease
$\alpha$ -MEM	Minimum essential medium alpha



## Chapter 1 Literature review

### 1.1 Overview of glioblastoma multiforme

Glioblastoma multiforme (GBM), also known as glioblastoma, is the most common and aggressive malignant primary tumor in central nervous system (CNS). It accounts for approximate 54.0% of gliomas and 15.8% of all primary CNS tumors according to the Central Brain Tumor Registry of the United States (CBTRUS) statistical report (Figure 1.1) [1]. Glioblastoma is prevalent in male, Caucasian, and adults at the age >65 years in developed countries. The incidence rate of glioma is 6.03 new cases per 100,000 populations per year, while the incidence rate of glioblastoma is the highest in malignant brain tumors, with 3.19 new cases per 100,000 populations per year [1, 2]. In Hong Kong, 124 new cases of glioma and 52 new cases of glioblastoma were diagnosed from 2008 to 2009. The incidence rate of glioblastoma in Hong Kong is about 0.74 new cases per 100,000 populations per year [3]. Due to its malignancy, the prognosis for patients with glioblastoma is very poor, with a median overall survival of approximately 3 month without any treatment. The survival rate of glioblastoma is one of the worst among all human cancers. The 1-year, 2-year and 5-year relative survival rate for GBM patients is approximately 36%, 13.6% and 5.7%, respectively [1].

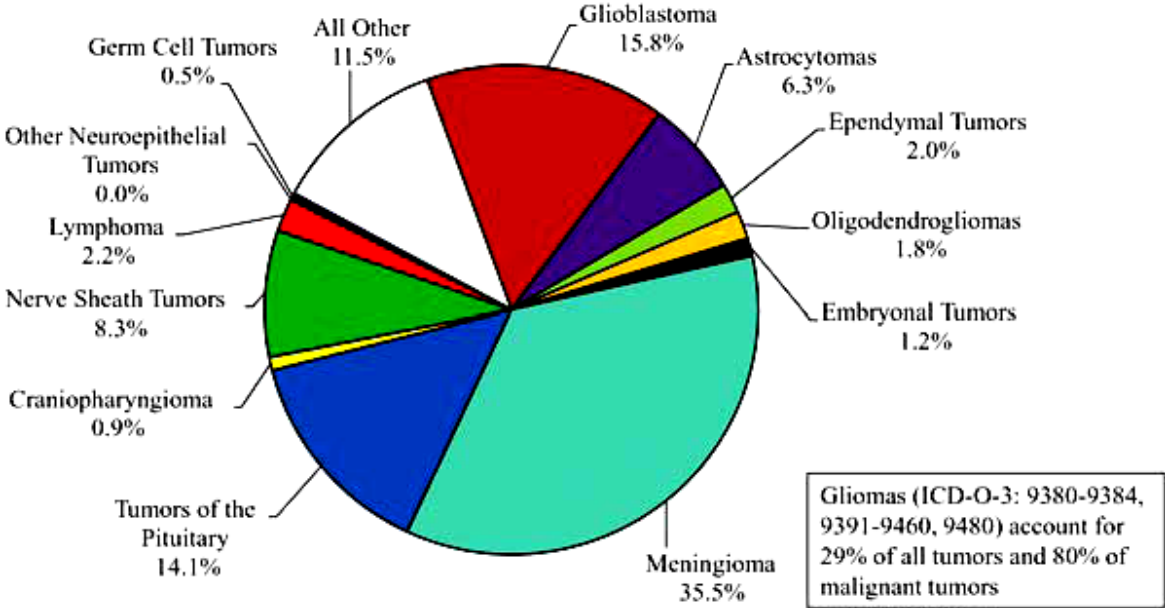


**Figure 1.1: Distribution of primary brain and CNS tumors by histological characteristics in CBTRUS statistical report [1].**

### **1.1.1 Classification and characteristics of glioma**

Glioma is a type of brain tumor that arises from glial cells including astrocytes, ependymal cells, and oligodendrocytes etc. Glial cells, also known as neuroglia, are non-neuronal cells providing support, protection, nutrients and oxygen for the neurons. According to the specific type of glial cells, glioma is mainly classified into astrocytoma, ependymoma and oligodendroglioma, which is derived from astrocytes, ependymal cells and oligodendrocytes, respectively. Since astrocytes are the most common type of glial cells in CNS, astrocytoma is the most common type of glioma. According to the histological features, astrocytoma is further divided into subependymal giant cell astrocytoma, pilocytic astrocytoma, pilomyxoid astrocytoma, diffuse astrocytoma, pleomorphic xanthoastrocytoma, anaplastic astrocytoma, and glioblastoma multiforme. The World Health Organization (WHO) classification of CNS tumor is the most widely used classification of glioma which classifies glioma into four histological tiers of malignancy as described in Table 1.1 [4]. Patients with grade I glioma usually have favorable prognosis and long-term survival following complete surgical resection, whereas patients with grade IV glioma have poor prognosis even though they received surgical removal of tumor followed by radiotherapy and chemotherapy.

Table 1.1: WHO grading and characteristics of glioma [4].

	WHO grading	Tumors	Characteristics
Glioma	Grade I	Subependymal giant cell astrocytoma	Low proliferative rate and non-infiltrative; benign tumor; high probability of cure following complete surgical resection.
		Pilocytic astrocytoma	
	Grade II	Pilomyxoid astrocytoma	Relative low proliferative but generally infiltrative activities; well-differentiated; tend to evolve into grade III or higher grade of malignancy; recurrence is common.
		Diffuse astrocytoma	
		Pleomorphic xanthoastrocytoma	
		Oligodendroglioma	
		Ependymoma	
	Grade III	Anaplastic astrocytoma	Malignant tumor with nuclear atypia and active mitosis; undifferentiated; rapid growth; high invasiveness.
		Anaplastic oligodendroglioma	
		Anaplastic oligoastrocytoma	
		Anaplastic ependymoma	
	Grade IV	Glioblastoma multiforme	High malignancy and aggressiveness; nuclear atypia and active mitosis; undifferentiated; rapid growth; pseudopalisading necrosis; abundant new blood vessels formation.
		Gliosarcoma	

### 1.1.2 Genetic aberrations in glioblastoma multiforme

Glioblastoma is classified as grade IV glioma according to the WHO grading system, and can be further grouped into two distinct subtypes. Primary (*de novo*) glioblastoma is prevalent in elderly people, accounting for 95% of glioblastoma. It develops rapidly without any clinical or histological evidence of a less malignant precursor lesion. Secondary glioblastoma is rare in elderly patients but often diagnosed in young people. Distinct from primary glioblastoma, secondary glioblastoma develops slowly and progresses from grade II or III gliomas, which has a better prognosis [5]. Although these two subtypes of glioblastoma are histological indistinguishable, they have distinct genetic and epigenetic profiles which are more objective and reliable for clinical diagnosis. Representative genetic aberrations of primary glioblastoma include *EGFR* (*epidermal growth factor receptor*) amplification (~35%), *PTEN* (*phosphatase and tensin homolog deleted on chromosome ten*) mutation (~25%), *TP53* mutation (~30%) and loss of heterozygosity (LOH) on chromosome 10q (~70%) and 10p (~50%), whereas *IDH1* (*isocitrate dehydrogenase 1*) mutation (>80%), LOH 1p/19q (>75%) and 10q (>60%), and *TP53* mutation (~65%) are the signatures of secondary glioblastoma (Figure 1.2) [5-7].

Loss of heterozygosity on chromosome 10 is one of the most frequent genetic aberrations in both primary and secondary glioblastoma. Entire loss of alleles 10q and 10p is common in primary glioblastoma, and partial LOH 10q is also frequent in anaplastic astrocytoma, accounting for 35% - 60% [7]. Deletions of 10p14-15, 10q23-24 (*PTEN*) and 10q25-qter loci are frequently found in primary glioblastoma,

indicating the location of tumor suppressor genes on chromosome 10 [8, 9]. Besides, simultaneous deletion of chromosomes 1p and 19q is common in secondary glioblastoma, associated with elevated sensitivity to chemotherapeutic agents and longer overall survival [10]. This indicates that two or more genes located on chromosomes 1p and 19q are of importance to suppress secondary glioblastoma development.

Other frequent genetic aberrations in primary glioblastoma are *EGFR* amplification and *PTEN* mutation, both of which are involved in phosphatidylinositol 3-kinase (PI3K)/Akt signaling pathway. Detailed information of these two genetic aberrations is discussed in section 1.2.5.

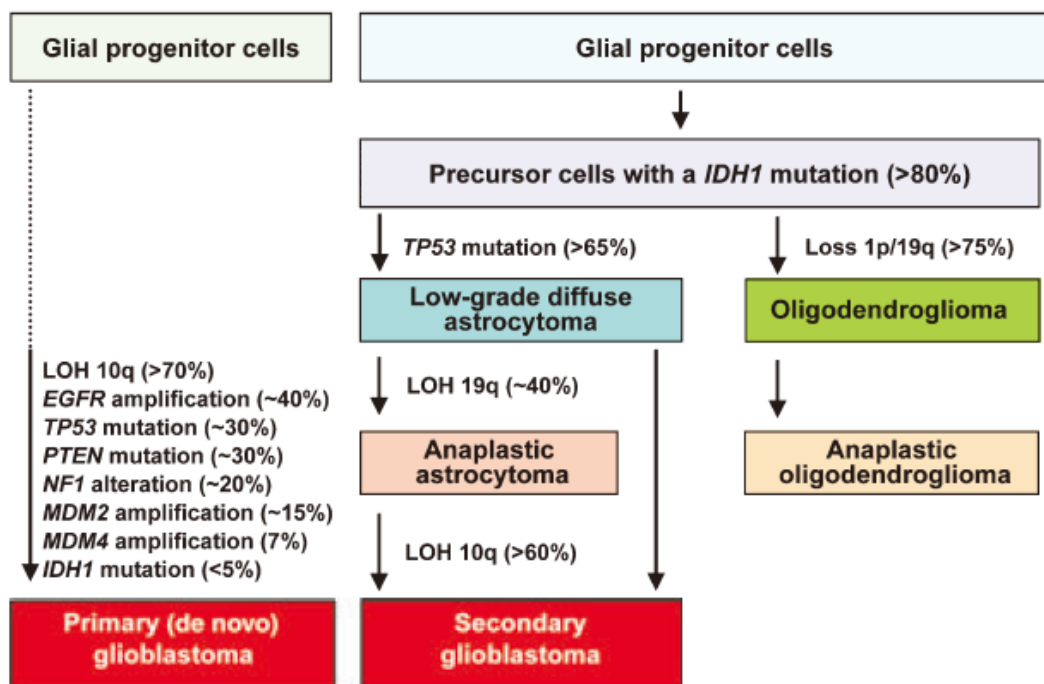


Figure 1.2: Genetic aberrations of primary and secondary glioblastoma [7].

### **1.1.3 Therapeutic strategies for glioblastoma multiforme**

Glioblastoma multiforme is characterized by rapid growth, extensive infiltration to neighboring brain tissues, pseudopalisading necrosis, and angiogenesis, which contribute to the poor prognosis. Conventional therapies for glioblastoma include maximal surgical resection followed by adjuvant radiotherapy and chemotherapy. Surgical resection alone has limited therapeutic efficacy for glioblastoma because it is impossible to completely remove the tumor entity, owing to the infiltrative nature of glioblastoma. Even though patients are administered with concomitant radiotherapy and chemotherapy (temozolomide), the prognosis remains poor, with the median overall survival in the range of 9-15 months [11-14]. Therefore, to control the rapid growth and extensive infiltration of glioblastoma, and improve the prognosis of patients, it is necessary to develop novel therapeutic strategies.

#### **1.1.3.1 Temozolomide**

Temozolomide (Temodar™, TMZ), a DNA-alkylating agent, is one of the most effective chemotherapeutic agents against glioblastoma currently. It can be rapidly absorbed into cancer cells and decomposed into 3-methyl-(triazene-1-yl)imidazole-4-carboximide, which reacts with water and releases methyldiazonium cation. Reactive methyldiazonium cation is able to methylate DNA at O<sup>6</sup>- or N<sup>7</sup>-guanine and N<sup>3</sup>-adenine, resulting in mispairing with thymine during DNA replication. The DNA mismatch pairs ultimately cause in DNA damage and trigger cancer cell death [15, 16]. However, O<sup>6</sup>-methylguanine-DNA

methyltransferase (MGMT) or O<sup>6</sup>-alkylguanine-DNA alkyltransferase is able to remove the alkyl/methyl group at O<sup>6</sup>- guanine and repair DNA damage [15, 16]. When patients with the promoter of *MGMT* being methylation, their MGMT level is decreased, resulting in a more favorable prognosis with temozolomide treatment. Their median survival increases to 21.7 months when treated with radiotherapy and concomitant temozolomide, compared with 15.3 months when treated with radiotherapy only. However, patients whose tumor contains a non-methylated *MGMT* promoter have no significant increase in survival [17, 18].

### **1.1.3.2 Anti-angiogenic therapies**

Anti-angiogenic therapy is taken for a promising novel therapy for glioblastoma, since angiogenesis is essential to rapid growth and tumor progression of glioblastoma through provision of oxygen and nutrients. Angiogenesis is a physiological process that new blood vessels sprout from pre-existing vessels driven by external stimulation including a variety of growth factors. Vascular endothelial growth factor (VEGF) family and their receptors (VEGFR) are regarded as the major factors contributing to angiogenesis in glioblastoma. VEGFR-1 and VEGFR-2 are overexpressed in high-grade glioma and activated by VEGF-A. Bevacizumab (Avastin™), a monoclonal antibody against VEGF-A, is an anti-angiogenic agent approved by the U.S. Food and Drug Administration (FDA) for cancer treatment. Evidence shows that radiotherapy and concurrent temozolomide along with bevacizumab is effective and well-tolerated in recurrent and newly diagnosed

glioblastoma, which coincides with a better progression-free survival than convention therapy [19]. However, overall survival doesn't improve, suggesting that bevacizumab tends to increase the incidence of tumor recurrence [20]. Currently, combined therapy with bevacizumab and irinotecan (Camptosar™) exhibits better response rate and progression-free survival rate in patients with recurrent glioblastoma than bevacizumab alone [21, 22]. However, patients with newly diagnosed glioblastoma do not benefit from this neoadjuvant chemotherapy [23, 24]. Although bevacizumab is capable of decreasing glioblastoma angiogenesis and vascular supply, hypoxia and glycolysis are also increased, leading to elevated tumor invasion capacity [25]. Therefore, anti-angiogenic escape in anti-VEGF therapy is still a crucial issue for glioblastoma treatment, which may leads to unfavorable prognosis of patients.

Besides VEGF, basic fibroblast growth factor (bFGF), platelet derived growth factor (PDGF), as well as their receptors are also involved in glioblastoma angiogenesis. Therefore, chemotherapeutic agents targeting these growth factors and their receptors may suppress glioblastoma angiogenesis and give rise to more effective treatment. For example, thalidomide is an angiogenesis inhibitor that decreases expression of VEGF and bFGF in glioblastoma [26]. Sorafenib (Nexavar™) is a multi-kinase inhibitor of VEGFR, PDGFR and Raf kinase for the treatment of renal cell carcinoma (RCC) and liver cancer [27]. Sunitinib (Sutent™) is a multi-kinase inhibitor targeting receptor tyrosine kinase (RTK) including PDGFR and VEGFR. It has been approved by FDA for RCC and gastrointestinal stromal tumor

(GIST) treatment [28]. Pazopanib (Votrient™) is also a multi-kinase inhibitor targeting FGFR, PDGFR and VEGFR and has been approved for RCC and soft tissue sarcoma treatment [29]. Sorafenib, sunitinib and pazopanib are currently in the phase II clinical trials for glioblastoma treatment.

### **1.1.3.3 Epidermal growth factor receptor (EGFR)-targeted therapies**

Epidermal growth factor (EGF) is a growth factor that promotes cell growth and differentiation through binding to its membrane receptor EGFR. EGFR, also known as HER1/Erb1, is a member of ErbB family consisting of EGFR/HER1 (Erb1), HER2/c-neu (ErbB2), HER3 (ErbB3), and HER4 (ErbB4). It contains an extracellular domain, a transmembrane domain, an intracellular tyrosine kinase domain, and a C-terminal domain. When EGF binds to the extracellular domain, two inactive EGFR monomers pair together to form an active homodimer. This results in conformational alteration that activates the tyrosine kinase domain, and autophosphorylation at tyrosine residues in the C-terminal domain. The phosphorylated tyrosine residues provide docking sites for proteins containing Src homology 2 (SH2) domains, and subsequently initiate signal transduction, such as through the PI3K/Akt signaling pathway [30, 31].

Aberration of EGFR/PI3K/Akt signaling is common in glioblastoma. Therapeutic strategies targeting EGFR include monoclonal antibodies and tyrosine kinase inhibitors. The most widely used monoclonal antibodies are cetuximab (Erbix™) and panitumumab (Vectibix™), both of which block ligand binding and prevent EGFR

dimerization by targeting the extracellular domain of EGFR [32, 33]. Cetuximab and panitumumab are approved by FDA for the treatment of colorectal cancer with wild-type *KRAS* [34, 35]. A phase II study of cetuximab combined with radiotherapy and temozolomide for the treatment of recurrent glioblastoma demonstrates that patients with wild-type *EGFR* tumor have more favorable prognosis than those with *EGFR* mutation [36]. Tyrosine kinase inhibitors such as gefitinib (Iressa™), erlotinib (Tarceva™) and canertinib are small molecules that reversibly or irreversibly compete with adenosine triphosphate (ATP) binding sites in the tyrosine kinase domain of EGFR. Gefitinib and erlotinib are reversible tyrosine kinase inhibitors that are approved for the treatment of non-small cell lung cancer (NSCLC), and have entered phase I/II clinical trials for glioblastoma treatment [37, 38]. However, resistance to EGFR-targeted therapies in glioblastoma is common. Compared with a historical cohort of glioblastoma patients treated with radiotherapy alone, patients treated with radiotherapy combined with gefitinib have no overall survival benefit [39]. In a phase II trial, patients with newly diagnosed glioblastoma also do not benefit from radiotherapy and concurrent temozolomide plus erlotinib [40].

## **1.2 Overview of phosphatidylinositol 3-kinase (PI3K)/Akt signaling pathway**

### **1.2.1 Canonical PI3K/Akt signaling pathway**

The PI3K/Akt signaling pathway plays a central role in the regulation of signal transduction, which mediates various biological processes including cell proliferation, survival, metabolism, motility and angiogenesis. Generally, activation of PI3K/Akt pathway starts with activation of receptor tyrosine kinases (RTKs) or G protein-coupled receptors (GPCRs), which results in PI3Ks activation. The ligands of RTKs are growth factors, cytokines, or hormones including insulin, insulin-like growth factor-1 (IGF-1), EGF, FGF, PDGF and VEGF etc. In quiescent cells, regulatory subunits of PI3K usually bind to the catalytic subunits, which maintain the stability of PI3K and restrict its lipid kinase activities. When a ligand binds to its corresponding RTK, the intracellular C-terminal kinase domain of RTK undergoes conformational alterations and autophosphorylation, which provides binding sites for PI3K regulatory subunits. The interaction between RTK and PI3K regulatory subunits subsequently relieves the inhibitory effect on the catalytic subunits, leading to elevated lipid kinase activity of PI3K (Figure 1.3). Besides, GPCRs are a group of seven-transmembrane spanning receptors that bind to heterotrimeric G proteins including  $\alpha$ ,  $\beta$ , and  $\gamma$  subunits. GPCR undergoes conformational alterations when a ligand binds to it, leading to its bound GDP being converted to GTP [41]. The  $G\alpha$  subunit together with GTP is then dissociated from the  $G\beta\gamma$  dimer to trigger  $G\alpha$ -specific signal transduction,

while  $G\beta\gamma$  recruits PI3K regulatory subunits to the membrane and interacts with RAS to activated PI3K (Figure 1.3) [42]. Activation of PI3K results in conversion of phosphatidylinositol 4,5-bisphosphate (PtdIns(4,5)P<sub>2</sub>, PIP<sub>2</sub>) to phosphatidylinositol 3,4,5-triphosphate (PtdIns(3,4,5)P<sub>3</sub>, PIP<sub>3</sub>) in plasma membrane. Subsequently, PIP<sub>3</sub> binds to the pleckstrin homology (PH) domain of Akt and anchors it to the plasma membrane. Akt at amino acid residues threonine 308 (Thr308) and serine 473 (Ser473) are then phosphorylated by phosphoinositide-dependent kinase (PDK)-1 and -2, leading to its complete activation. Activated Akt, in turn, phosphorylates downstream pathway molecules to mediate metabolism, cell growth, angiogenesis, motility and apoptosis [43].

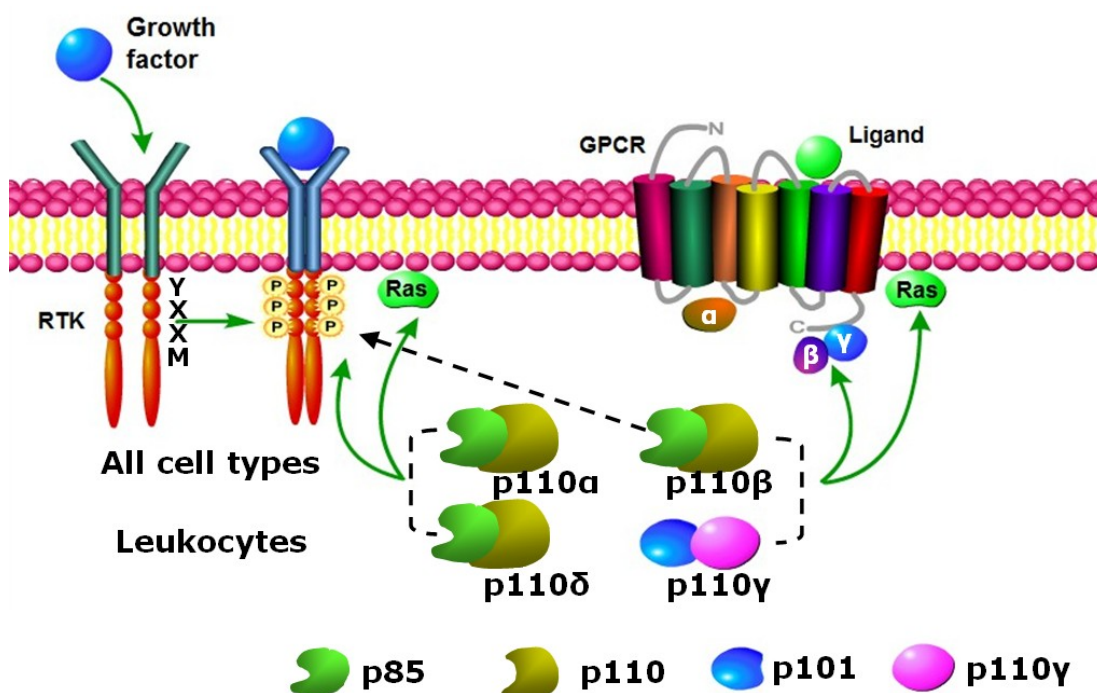


**Figure 1.3: Simplified scheme demonstrating different activation manners of class I<sub>A</sub> and class I<sub>B</sub> PI3K subunits (modified from [44]).** Class I<sub>A</sub> PI3K is composed of a p85 regulatory subunit and three p110 catalytic subunits (p110α, p110β, and p110δ). Class I<sub>B</sub> PI3K consists of a p101 regulatory subunit and a p110γ catalytic subunit activated by GPCRs. Isoforms p110α and p110β are ubiquitously expressed, while p110δ and p110γ are primarily expressed in leukocytes. Besides, p110α and p110δ are activated by RTKs, while p110β and p110γ mainly respond to GPCRs activation. Arrow with dashed line represents that p110β can also be activated by several types of RTKs.

## 1.2.2 PI3K family

PI3Ks are lipid kinases that are capable of phosphorylating phosphatidylinositol (PtdIns) at the 3' position of the inositol ring. According to the primary structure and *in vitro* lipid substrate specificity, the PI3K family is divided into three classes: Class I, II and III. Class I PI3K is further classified into two subclasses. Class I<sub>A</sub> PI3K is a heterodimer consisting of an 85 kDa regulatory subunit (p85) and a 110 kDa catalytic subunit (p110) [43]. The regulatory p84/p101 and catalytic p110 $\gamma$  subunits compose the class I<sub>B</sub> PI3K. Class I<sub>A</sub> and I<sub>B</sub> PI3Ks distinctly respond to different receptors activation. The p110 $\alpha$ , p110 $\beta$  and p110 $\delta$  subunits are activated by RTKs, while p110 $\gamma$  is activated by GPCRs (Figure 1.3) [45, 46]. Other classes of PI3Ks are structurally distinct from class I PI3K. Class II PI3K is composed of a single p110-like subunit distinguished by an additional C-terminal C2 domain. It converts phosphatidylinositol-4-phosphate (PtdIns(4)P) and phosphatidylinositol (PtdIns) to phosphatidylinositol-3,4-bisphosphate (PtdIns(3,4)P<sub>2</sub>) and PtdIns(3)P, respectively. Class III PI3K lacks a Ras-binding domain and produce PtdIns(3)P from PtdIns (Figure 1.4).

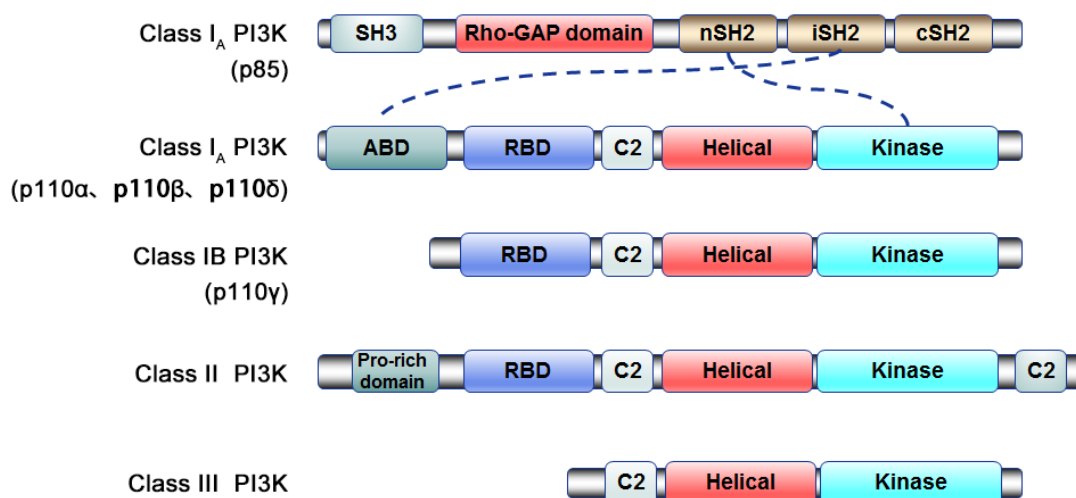


**Figure 1.4: Domain structures of class I, II and III PI3Ks (modified from [47]).**

The p85 subunits contain a Rho-GAP domain, three Src homology 2 (SH2) domains, and an NH<sub>2</sub>-terminal Src homology 3 (SH3) domain. The SH2 domains include an NH<sub>2</sub>-terminal SH2 domain (nSH2) and a C-terminal SH2 domain (cSH2) that flank an intervening-SH2 (iSH2). All catalytic subunits of class I<sub>A</sub> PI3K (p110α, p110β and p110δ) harbor an N-terminal adaptor-binding domain (ABD), a Ras-binding domain (RBD), a C2 domain, a helical domain and a catalytic kinase domain. Dashed lines represent that ABD interacts with iSH2 domain of the p85 regulatory subunit, while nSH2 domain binds to the helical domain of the p110 isoforms, leading to inhibition on PI3K kinase activity. The p110γ isoform of class I<sub>B</sub> PI3K lacks the ABD. Class II PI3K is composed of a single p110-like subunit distinguished by an additional C-terminal C2 domain, while the RBD is absent in class III PI3K.

### 1.2.2.1 Class IA PI3Ks

Three genes *PIK3R1*, *PIK3R2*, and *PIK3R3* encode five variants of the p85 isoforms: p85 $\alpha$ , p55 $\alpha$ , p50 $\alpha$ , p85 $\beta$ , and p55 $\gamma$ . They contain an N-terminal Src homology 3 (SH3) domain and three Src homology 2 (SH2) domains, including an N-terminal (nSH2) and a C-terminal (cSH2) domains that flank an intervening-SH2 (iSH2) domain. The SH3 domain binds to proline-rich sequences, while the nSH2 domain binds preferentially to the phosphorylated tyrosine residues in Tyr-Xaa-Xaa-Met (YXXM) motif, which is located in the C-terminal kinase domain of RTKs [48]. When the nSH2 domain of p85 binds to YXXM motif in RTKs, p85 at Tyr688 is phosphorylated, resulting that inhibition on p110 catalytic subunits is rescued and the lipid kinase activity of PI3K is elevated [49].

The class IA PI3K catalytic subunits (p110 $\alpha$ , p110 $\beta$  and p110 $\delta$ ) are encoded by *PIK3CA*, *PIK3CB* and *PIK3CD*, respectively. The p110 $\alpha$  and p110 $\beta$  isoforms are ubiquitously expressed, whereas p110 $\delta$  is primarily expressed in leukocytes (Figure 1.3) [50]. The p110 $\alpha$ , p110 $\beta$  and p110 $\delta$  isoforms share a similar structure: an N-terminal adaptor-binding domain (ABD), a Ras-binding domain (RBD), a C2 domain, a helical domain and a catalytic kinase domain (Figure 1.4). The p110 isoforms bind to the p85 regulatory subunits through ABD, while the C2 domain anchors to the plasma membrane, and the helical domain serves as a rigid scaffold around RBD, C2 and kinase domains [51, 52]. In addition, direct interaction between GTP-bound Ras and RBD leads to elevated catalytic activities of p110 isoforms [53].

Mutations of *PIK3CA* in 10 of 20 exons are common in diverse types of cancers

including ovarian, breast, liver, colorectal and brain cancers [54-59]. About 80% of *PK3CA* mutations occur in hot spot helical (at E542K and E545K residues in exon 9) and C-terminal kinase (at H1047R residue in exon 20) domains [60]. The majority of *PIK3CA* mutants (14 of 15 cases) in different types of cancer show gain of PI3K function, which leads to the constitutive activation of p110 $\alpha$  and Akt, and promotes the recruitment of p110 $\alpha$  to membrane phospholipids [61]. These findings suggest that p110 $\alpha$  plays an oncogenic role in human cancers. Studies have shown that helical and kinase domain mutations induce gain of PI3K function via distinct mechanisms. Gain of function triggered by helical domain mutation is independent of binding to p85 subunit but requires interaction with GTP-Ras. In contrast, activation of p110 $\alpha$  through kinase domain mutation largely depends on the interaction with p85 [62].

Both p110 $\alpha$  and p110 $\beta$  are activated by RTKs but they display different preference to RTK activation. Inhibition of p110 $\alpha$ , not p110 $\beta$ , results in the blockade of PGDF-induced actin rearrangement in porcine aortic endothelial cells, whereas inhibition of p110 $\beta$ , not p110 $\alpha$ , suppresses actin rearrangement induced by insulin [63]. Further evidence shows that p110 $\beta$  plays an essential role in insulin signaling in a kinase-independent manner [64, 65]. In addition, p110 $\beta$  is also activated by GPCRs (Figure 1.3) [66]. Activation of Akt is induced by the ligands of GPCRs in p110 $\gamma$ -null fibroblasts, while inhibition of p110 $\beta$  suppresses Akt phosphorylation, suggesting that p110 $\beta$  also responds to GPCR activation and may be redundant with p110 $\gamma$  [66].

Due to the constitutive activation and ubiquitous expression, p110 $\alpha$  plays a predominant role in RTK-mediated Akt signaling. Although the p110 $\delta$  subunit is also activated by RTKs, it may serve as a compensatory molecule to p110 $\alpha$  in Akt signaling, since p110 $\delta$  is enriched in leukocytes but not ubiquitously expressed [67]. Recently, a study shows that the cSH2 domain of p85 $\alpha$  displays a novel isoform-selective regulatory function [68]. Full inactivation of p110 $\delta$  requires the binding of nSH2 and cSH2 domains of p85 $\alpha$ , whereas the p110 $\alpha$  activity can't be inhibited by binding to the cSH2 domain [68]. This indicates that p110 $\delta$  is not redundant and may act on Akt signaling through a different mechanism. A cluster of novel and inducible *PIK3CD* promoters have been identified, and p110 $\delta$  expression is induced by tumor necrosis factor  $\alpha$  (TNF- $\alpha$ ) in endothelial cells and fibroblasts through activation of these promoters [69]. A highly conserved genomic region of *PIK3CD* displays higher promoter activity in leukocytes than non-leukocytes, where the binding sites for leukocyte-specific transcription factors may be located [70]. These findings provide a possible explanation for the high enrichment of p110 $\delta$  in leukocytes.

### **1.2.2.2 Class I<sub>B</sub> PI3Ks**

The class I<sub>B</sub> PI3K is enriched in hematopoietic cells and plays a pivotal role in GPCR-mediated Akt signaling, inflammation response and immune disorders. Inhibition of PI3K $\gamma$  with selective inhibitors may be a promising strategy for the treatment of inflammation and autoimmune diseases [71]. The p110 $\gamma$  isoform is

activated by GPCRs through direct interaction with G $\beta$  $\gamma$  dimer and Ras [72, 73]. It lacks N-terminal adaptor-binding domain and therefore does not interact with p85, but instead binds to p101 or its homolog p84 regulatory subunit, which has no sequence homology to p85 (Figure 1.4). Although p101 shows no inhibitory effect on p110 $\gamma$ , it is indispensable for p110 $\gamma$  activation because it facilitates the binding of p110 $\gamma$  to the plasma membrane and G $\beta$  $\gamma$  [74]. Loss of p101 is sufficient to inhibit Akt phosphorylation, and this cannot be compensated by overexpression of p110 $\gamma$  [75, 76]. In addition, each domain of p110 $\gamma$  is capable of binding to the anionic phospholipid which is involved in the membrane association of p110 $\gamma$ , and deletion of either RBD or helical domain leads to a complete loss of lipid kinase activity [77].

### 1.2.3 Roles of class IA PI3K isoforms in glioblastoma

Genetic aberrations involved in the PI3K/Akt pathway including *PTEN* mutation, *EGFR* amplification, *PIK3R1* and *PIK3CA* mutation are frequently found in glioblastoma and other types of cancer. *PIK3R1*, which encodes the p85 $\alpha$ , p55 $\alpha$ , and p50 $\alpha$  isoforms, is mutated in colon, ovarian, endometrial cancers and glioblastoma [78-81]. Hot spots of *PIK3R1* mutation occur in the iSH2 or nSH2 domains of p85 $\alpha$  that interact with the ABD or helical domain of p110 isoforms. R340E and K379E mutations of *PIK3R1* in nSH2 domain, and DKRMNS560del, R574fs, and T576del mutations in iSH2 domain increase the PI3K activity, suggesting that these mutations contribute to abrogation of inhibitory effect on p110 and increased Akt phosphorylation [82, 83]. Studies show that *PIK3R1* mutation is relatively rare in

glioblastoma, accounting for 10% (9 of 91) according to The Cancer Genome Atlas report [80] and 0% (0 of 19) as described in a recent study [84]. Nevertheless, *PIK3R1* is required for Akt activation, as well as tumorigenesis and development of glioblastoma. Evidence reveals that *PIK3R1* mutations upregulate Akt activity and promote normal astrocytes converting to glioblastoma in the xenograft model [81]. In addition, shRNA-mediated *PIK3R1* silencing suppresses glioblastoma cell growth and invasion through decreasing the expression of cyclin D1, proliferating cell nuclear antigen (PCNA) and matrix metalloproteinases (MMPs) -2 and -9, and increasing the expression of tissue-inhibitor of metalloproteinase-2 (TIMP-2) and p53 [85].

*PIK3CA* mutation in glioblastoma, firstly reported by Samuels et al., is up to 27% (4 of 15) [60]. However, other studies report a relatively low *PIK3CA* mutation rate in glioblastoma, which accounts for 15% (11 of 73) [59], 7% (5 of 70) [86], 4% (6 of 139) [87], 5% (5 of 97) [88] and 10% (10 of 105) [89] (Table 1.2). Interestingly, *PIK3R1* and *PIK3CA* mutations are mutually exclusive in glioblastoma, whereas it is opposite in endometrial cancer, indicating that the pattern of genetic aberrations contributing to tumorigenesis and tumor development are distinct in different types of cancer [79, 80]. Although the structure and sequence of p110 $\beta$  and p110 $\delta$  are highly homologous to p110 $\alpha$ , no *PIK3CB* or *PIK3CD* mutation has been found in human cancers yet.

**Table 1.2: Comparison of studies investigating *PIK3CA* mutations in glioblastoma**

	Samuels Y, et al. 2004	Gallia GL et al. 2006	Hartmann C, et al. 2005	Kita D, et al. 2007	Knobbe CB, et al. 2005	Parsons DW, et al. 2008
Samples with <i>PIK3CA</i> mutations, n (%)	4 (27%)	11(15%)	5(7%)	6(4%)	5 (5%)	10(10%)
Source	Primary tumors	Primary tumors (38%); Xenografts (9%); Cell lines (13%)	Primary tumors	Primary tumors (5%); Secondary tumors (3%)	Primary tumors	Primary tumors; Xenografts
No. samples	15	73	70	139	97	105
Age range (years)	NR	0.4-78	51.1 (mean age)	55.7 (mean age)	10-83	NR
Mutation location	Exon 4, 5, 13, 20	Exon 1, 4, 7, 9, 20	Exon 1, 9, 20	Exon 9, 20	Exon 1, 2, 5, 20	NR
<i>PIK3CA</i> amplification	NR	0/73	NR	17/139	0/97	0/22

Abbreviations: NR, not reported;

The p110 $\alpha$ , p110 $\beta$  and p110 $\delta$  isoforms exhibit distinct roles in different pathological processes in cancer cells. The p110 $\alpha$  isoform is required for tumor cell proliferation, migration and invasion, whereas p110 $\beta$  is essential to cell survival and tumorigenesis [64, 90-92]. Selective gene knockdown and isoform-selective inhibitors are helpful to investigate the individual role of class I<sub>A</sub> PI3K catalytic subunits. Knockdown of *PIK3CA* significantly inhibits cell viability, migration and invasion in medulloblastoma and glioblastoma cells [90, 91]. The p110 $\alpha$  subunit is also required for invasion of breast cancer cells through mediating invadopodia formation [93]. In addition, tumor cell growth is effectively suppressed *in vitro* and *in vivo* by using the p110 $\alpha$  isoform-selective inhibitors A66, BYL719 or PIK-75, while apoptosis and cell cycle arrest are promoted [94-97].

The p110 $\beta$  isoform plays a crucial role in tumor cell growth, metabolism and tumorigenesis. Knockdown of *PIK3CB* suppresses cell proliferation and induces apoptosis in ovarian cancer and glioblastoma *in vitro* and *in vivo* [92, 98]. Overexpression of p110 $\beta$  induces oncogenic transformation in chicken embryo fibroblasts [99]. Knockout of p110 $\beta$  leads to dysfunction of insulin metabolism and suppresses prostate cancer cell proliferation and tumor formation induced by *PTEN* loss [64]. Clinical studies show that overexpression of p110 $\beta$  is found in 15% of invasive breast cancer (48 of 315 cases) and 28% of colorectal cancer (23 of 82 cases), correlated with poor overall survival [100, 101].

Due to the high expression level in leukocytes, the p110 $\delta$  subunit is a promising therapeutic target for hematologic malignancies including leukemia, lymphoma and

multiple myeloma [102, 103]. Recently, overexpression of p110 $\delta$  is also observed in solid tumor cells such as glioblastoma, neuroblastoma, breast and prostate cancers, indicating that inhibition of p110 $\delta$  may also be an attractive option for cancer treatment [104-108]. Inhibition of p110 $\delta$  suppresses proliferation and promotes apoptosis of neuroblastoma cells through inactivation of p70 ribosomal protein S6 kinase (S6K) and decreased expression of B-cell lymphoma 2 (Bcl-2) [106]. In addition, targeting p110 $\delta$  in p110 $\delta$ -overexpressed prostate and breast cancer cells contributes to PTEN activation and suppression of Akt signaling, leading to retarded cell proliferation [107]. Our previous study shows that p110 $\delta$  is overexpressed in 50% of high grade glioma cell lines (6 of 12), and knockdown of p110 $\delta$  inhibits migration and invasion of glioblastoma cells by decreasing focal adhesion kinase (FAK) expression [104]. These findings indicate that p110 $\delta$  is also essential to cancer cell growth and motility.

#### **1.2.4 Roles of Akt in glioblastoma**

Akt, also known as protein kinase B (PKB), is a serine/threonine-specific kinase consisting of an N-terminal pleckstrin-homology (PH) domain, a central kinase domain and a C-terminal regulatory domain that contains a hydrophobic motif [109]. Three isoforms of Akt (Akt1/PKB $\alpha$ , Akt2/PKB $\beta$  and Akt3/PKB $\gamma$ ) are homologous to protein kinases A, G and C within their kinase domains. Akt1 and Akt2 are ubiquitously expressed, while Akt3 only shows high expression in brain and testis. When PI3K is activated, Akt is recruited to the plasma membrane through the

association of PH domain with PIP3, suggesting that the PH domain is crucial for activation of Akt (Figure 1.5). Full activation of Akt requires phosphorylation at both Thr308 and Ser473. PIP3 also recruits PDK-1 to the membrane by interacting with its PH domain, which then phosphorylates Akt at Thr308 in the activation loop to partially activate Akt [110, 111]. PDK-2, also known as mTOR complex 2 (mTORC2), is a complex of mammalian target of rapamycin (mTOR) and Rictor responsible for Akt phosphorylation at Ser473 in the hydrophobic motif [112]. Akt plays a central role in the regulation of various cellular functions such as cell proliferation, motility, survival, and metabolism, by phosphorylating a number of downstream molecules (Figure 1.5). It mediates protein synthesis by phosphorylating tuberous sclerosis complex (TSC) and then activating mTOR. mTOR and its partner Raptor bind to p70 S6K and eukaryotic initiation factor 4E-binding protein (4EBP), leading to their phosphorylation and initiation of protein translation [113]. Forkhead box protein (FOXO) family is also phosphorylated by Akt, resulting in the inactivation of FOXO and the formation of FOXO and 14-3-3 protein complex. The complex is subsequently sequestered in the cytoplasm and thereby inhibits the transcription of pro-apoptotic genes such as *FasL* and *BIM* [114]. Likewise, Akt phosphorylates the Bcl-2-associated death promoter (BAD), a pro-apoptotic member of Bcl-2 family, leading to the sequestration of BAD from the mitochondrial membrane by 14-3-3 proteins, which then allows the release of Bcl-2 and inhibits Bax-triggered apoptosis [115].

Akt also plays a pivotal role in tumorigenesis, development and progression of

glioblastoma. Aberrant activation of Akt induced by *PTEN* mutation is documented in a variety of cancers such as thyroid, lung, breast, ovarian cancers and glioblastoma [116-120]. Evidence shows that activation of both Ras and Akt is essential to tumorigenesis through the recruitment of a set of specific mRNAs to the ribosomes, which encode proteins involved in growth, transcription regulation, intercellular interactions, and morphology [121]. Co-activation of oncoprotein Ras and Akt in neural progenitors and astrocytes induces glioblastoma formation *in vivo*, whereas activation of either Ras or Akt does not [122]. Additional expression of a constitutively activated form of Akt in grade III anaplastic astrocytoma, which expresses E6/E7, Ras and human telomerase reverse transcriptase, leads to *in vivo* formation of glioblastoma [123]. Further, constitutively activated Akt and Ras in tumor-bearing mice are required for the maintenance of glioblastoma, whereas inhibition of Akt leads to tumor remission and prolonged survival of mice [124].

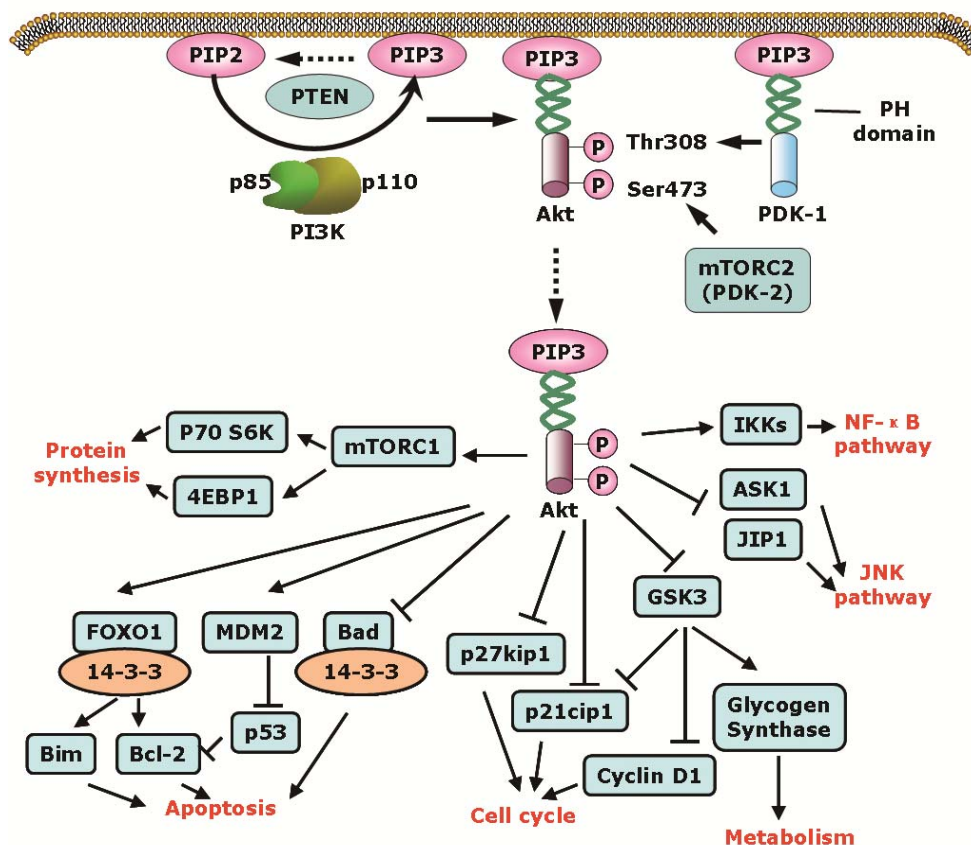


**Figure 1.5: Simplified scheme showing the process of Akt activation and its downstream pathway molecules.** Activated PI3Ks generate PIP3 from PIP2, leading to the binding of PIP3 to the PH domain of Akt and recruitment of Akt to the plasma membrane. PIP3 also recruits PDK-1 to the plasma membrane through binding to its PH domain, which then phosphorylates Akt at Thr308. Subsequently, Akt is completely activated through phosphorylation at Ser473 by PDK-2/mTORC2. Activated Akt phosphorylates a variety of downstream pathway molecules including mTOR, GSK3 (glycogen synthase kinase 3), BAD, IKK (IκB kinase) and FOXO1 to regulate cancer cell growth, proliferation, motility, survival, and metabolism.

### 1.2.5 *EGFR* amplification and *PTEN* mutation in glioblastoma

EGFR, a member of RTKs family, plays a key role in the activation of PI3K/Akt signaling. Compared with secondary glioblastoma, *EGFR* amplification (36% versus 8% of cases) and EGFR overexpression (>60% versus <10% of cases) are more common in primary glioblastoma [5, 125]. Approximate 98% of primary glioblastomas with *EGFR* amplification also exhibit EGFR overexpression, while 70% - 90% of those with EGFR overexpression show *EGFR* amplification, indicating a strong correlation between *EGFR* amplification and EGFR overexpression [125, 126]. Evidence shows that EGFR amplification and overexpression in glioblastoma are associated with poor prognosis of patients, especially in young people [126, 127]. The most common type of *EGFR* mutation in glioblastoma is *EGFR* variant III mutation (*EGFRvIII*) (45% to 60% of cases also have *EGFR* amplification), which is also known as  $\Delta$ *EGFR* or *de2-7EGFR*, and characterized by an in-frame deletion in exons 2-7 [126, 128]. This mutation produces a truncated EGFR protein without the extracellular ligand-binding domain, leading to its ligand-independent constitutive activation [129]. Constitutively active EGFRvIII promotes glioblastoma growth, angiogenesis and tumorigenicity by activating multiple cellular signaling pathways such as PI3K/Akt, MAPK/ERK, and NF- $\kappa$ B pathways [130-132]. Glioblastoma xenograft containing EGFRvIII mutant displays higher PI3K and Akt activities, and greater tumor volumes than those with wild-type EGFR [133]. In addition, EGFRvIII overexpression promotes angiogenesis and tumor growth in glioblastoma by increasing angiopoietin-like 4 expression [130]. Shinojima et al. reported that

EGFRvIII overexpression in the presence of *EGFR* amplification is a strong indicator of poor survival prognosis [126]. However, a recent study shows that EGFRvIII is not a significant prognostic indicator of patients treated with radiotherapy and adjuvant temozolomide [134].

Phosphatase and tensin homolog deleted on chromosome 10 (PTEN), also known as MMAC-1 or TEP-1, is a protein with both lipid phosphatase and tyrosine phosphatase activities. Wild-type PTEN acts as a tumor suppressor by dephosphorylating PIP3 to PIP2 and blocking the recruitment of Akt to the plasma membrane, which subsequently suppresses Akt activation in cancer [135, 136]. *PTEN* gene is located on a region of chromosome 10q23, which is highly susceptible to mutation in human cancers. Thus, *PTEN* mutation and loss of PTEN are common in a wide range of cancers including glioblastoma, gastric, prostate, lung and ovarian cancers [137-141]. *PTEN* mutation is common in primary glioblastoma (15% to 40%) and associated with poor prognosis [5, 137, 142], whereas it is rare in secondary glioblastoma (<4%) [143]. Loss of PTEN function is capable of promoting glioblastoma cell proliferation, survival, invasion and migration by activating Akt and downstream signaling pathways. Studies showed that wild-type PTEN inhibits Akt phosphorylation and increases the expression of the cyclin-dependent kinase inhibitor 1B (p27<sup>kip1</sup>), resulting in the blockade of glioblastoma cell proliferation and tumorigenesis through G1-cycle arrest [144, 145]. PTEN also regulates the expression level and transcriptional activity of p53 in both phosphatase-dependent and -independent manners to control DNA damage repair and cell cycle. PTEN is

able to bind to the tumor suppressor p53, regulate its transcriptional activity, increase its stability and protect it from the murine double minute 2 (MDM2)-mediated proteasomal degradation [146, 147]. In addition, PTEN directly binds to FAK, dephosphorylates FAK at Tyr397 and subsequently inhibits p130Cas phosphorylation, leading to retarded glioblastoma cell migration and invasion [148, 149]. PTEN also prevents NF- $\kappa$ B binding to the FAK promoter through inhibition of PI3K/Akt signaling [150]. Ectopic expression of wild-type PTEN inhibits glioblastoma cell invasion by decreasing the expression of the MMP-2 and -9, and increasing the expression of TIMP-1 and -2 [151]. Further, PI3K inhibitors do not imitate the inhibitory effect of PTEN on cell invasion, indicating that this inhibitory effect depends on the tyrosine phosphatase activity of PTEN, rather than its lipid phosphatase activity [152].

### **1.2.6 PI3K inhibitors**

Due to the importance of class I PI3Ks in tumor growth and development, small molecular inhibitor targeting PI3Ks may be a promising approach for cancer treatment. According to their isoform selectivity, PI3K inhibitors are generally classified into pan-PI3K, isoform-selective or dual PI3K/mTOR inhibitors.

Wortmannin and LY294002 are known as the first generation of potent pan-PI3K inhibitors, which target all class I<sub>A</sub> p110 isoforms with half maximal inhibitory concentration (IC<sub>50</sub>) of 1 nM and 1.4  $\mu$ M respectively [153, 154]. The other pan-PI3K inhibitors include quercetin and demethoxyviridin. However, wortmannin

and LY294002 are of limited use clinically due to their poor pharmaceutical properties (insolubility and short half-life), off-target effects and unacceptable toxicities in animal studies [155, 156]. A new generation of pan-PI3K inhibitors with more favorable safety, efficacy and pharmacokinetics such as GDC-0941, GDC-0032, BKM120, PX-866 and XL147 have been developed and entered into clinical trials (Table 1.3). Selective inhibitors against p110 isoforms that may display less off-target effects and toxicities are attractive options for cancer treatment. Several isoform-selective PI3K inhibitors including BYL719 and CAL-101 have entered phase I/II clinical trials. They exhibit anti-proliferative and pro-apoptotic activities in solid tumors and hematologic malignancies [157-160].

The mTOR pathway is activated by PI3K/Akt signaling in response to growth factor stimulation to regulate metabolism, protein translation and autophagy [161]. Rapamycin and its analogues fail to serve as an effective therapeutic approach, because they inhibit mTORC1 rather than mTORC2, and trigger a negative feedback loop to augment Akt activation [162]. Therefore, dual inhibition of PI3K and mTORC1/2 may be more effective than rapamycin alone. Dual PI3K/mTOR inhibitors such as NVP-BEZ235, GSK2126458, XL765 and SF1126 are currently being tested in clinical trials (Table 1.3).

Table 1.3: PI3K inhibitors in clinical trials (data from ClinicalTrials.gov)

Classification	Drug name	Target(s)	Tumor(s)	Clinical trials	References
Pan-PI3K inhibitors	Pictilisib (GDC-0941)	p110- $\alpha$ , - $\beta$ , - $\delta$ , - $\gamma$	Breast, colorectal, gastric, prostate and ovarian cancers, NSCLC, melanoma, NHL	Phase I/II	[163]
	Taselisib (GDC-0032)	p110- $\alpha$ , - $\delta$ , - $\gamma$	Breast and squamous cell lung cancer	Phase I	[164]
	Buparlisib (BKM120)	p110- $\alpha$ , - $\beta$ , - $\delta$ , - $\gamma$	Breast, prostate, and ovarian cancer, GBM, CRC, NSCLC, GIST, B-cell lymphoma	Phase I/II	[165-169]
	PX-866	p110- $\alpha$ , - $\beta$ , - $\delta$ , - $\gamma$	Ovarian and prostate cancer, melanoma, GBM, NSCLC	Phase II	[170-172]
	XL147	p110- $\alpha$ , - $\beta$ , - $\delta$ , - $\gamma$	Breast cancer, endometrial, and ovarian cancer, GBM, lymphoma	Phase I/II	[173]
Isoform-selective inhibitors	BYL719	p110 $\alpha$	Breast, ovarian, H&N, melanoma, esophageal carcinoma, GIST	Phase I/II	[159]
	Idelalisib (CAL-101)	p110 $\delta$	CLL, NHL, hematologic malignancies	Phase III	[160, 174, 175]
Dual PI3K/mTOR inhibitors	BEZ235 (NVP-BEZ235, Dactolisib)	p110- $\alpha$ , - $\beta$ , - $\delta$ , - $\gamma$ /mTOR	Breast, prostate, and endometrial cancer, RCC, GBM	Phase I/II	[176, 177]
	Omipalisib (GSK2126458, GSK458)	p110- $\alpha$ , - $\beta$ , - $\delta$ , - $\gamma$ /mTOR	Solid tumors	Phase I	[178]
	XL765	p110- $\alpha$ , - $\beta$ , - $\delta$ , - $\gamma$ /mTOR	Breast cancer, NSCLC, lymphoma, GBM	Phase I/II	[179, 180]
	SF1126	p110- $\alpha$ , - $\beta$ , - $\delta$ /mTOR, integrin	B-cell malignancies, GIST, CRC, ovarian cancer, neuroblastoma	Phase I	[181, 182]

NHL, Non-Hodgkin's lymphoma; CLL, chronic lymphocytic leukemia; NSCLC, non-small cell lung cancer; CRC, colorectal carcinoma; GBM, glioblastoma; GIST, gastrointestinal stromal tumor; H&N, head and neck cancer; RCC, renal cell cancer.

### **1.3 Overview of c-Jun N-terminal kinase (JNK) signaling pathway**

The c-Jun N-terminal kinase (JNK), also known as stress-activated protein kinase (SAPK), can be activated in response to a wide variety of stress stimuli such as ultraviolet (UV) irradiation, heat shock, toxins, cytokines and growth factors. In mammals, JNK is encoded by *JNK1 (MAPK8)*, *JNK2 (MAPK9)* and *JNK3 (MAPK10)* genes, each of which is located on a different chromosome. Due to the alternative splicing of the mRNA 3'-coding region, at least ten isoforms have been identified: *JNK1* (four isoforms), *JNK2* (four isoforms) and *JNK3* (two isoforms). *JNK1* and *JNK2* isoforms are ubiquitously expressed, while *JNK3* isoforms are mainly expressed in brain, heart and testis [183, 184]. These isoforms are presented as 54 kDa and 46 kDa proteins that recognize and interact with different substrates [184]. However, the functional differences between these ten isoforms are unknown yet.

#### **1.3.1 Mitogen-activated protein kinases (MAPKs) pathway**

Mitogen-activated protein kinases (MAPKs) family is a group of highly conserved protein kinases including extracellular signal-regulated kinase (ERK), the 38 kDa protein kinase (p38), JNK, and the big mitogen activated protein kinase 1 (BMK1)/ERK5. MAPK signaling pathways are involved in the regulation of various cellular functions including cell proliferation, apoptosis, mitosis and gene expression. Generally, activation of MAPK signaling pathways is initiated when a ligand binds to its receptor, and leads to the recruitment of adaptor proteins and activation of small GTP-binding proteins (G-proteins). The protein kinase cascade consisting of up to

four tiers of kinases is subsequently activated. The MAPKKKKs (MAP4Ks) phosphorylate and activate the MAPKKKs (MAP3Ks or MEKKs). MAP3Ks then phosphorylate and activate the MAPKKs (MAP2Ks or MEKs), which in turn phosphorylate and activate the MAPKs. Activated MAPKs translocate to the nucleus, phosphorylate and interact with their specific substrates (Figure 1.6) [185].

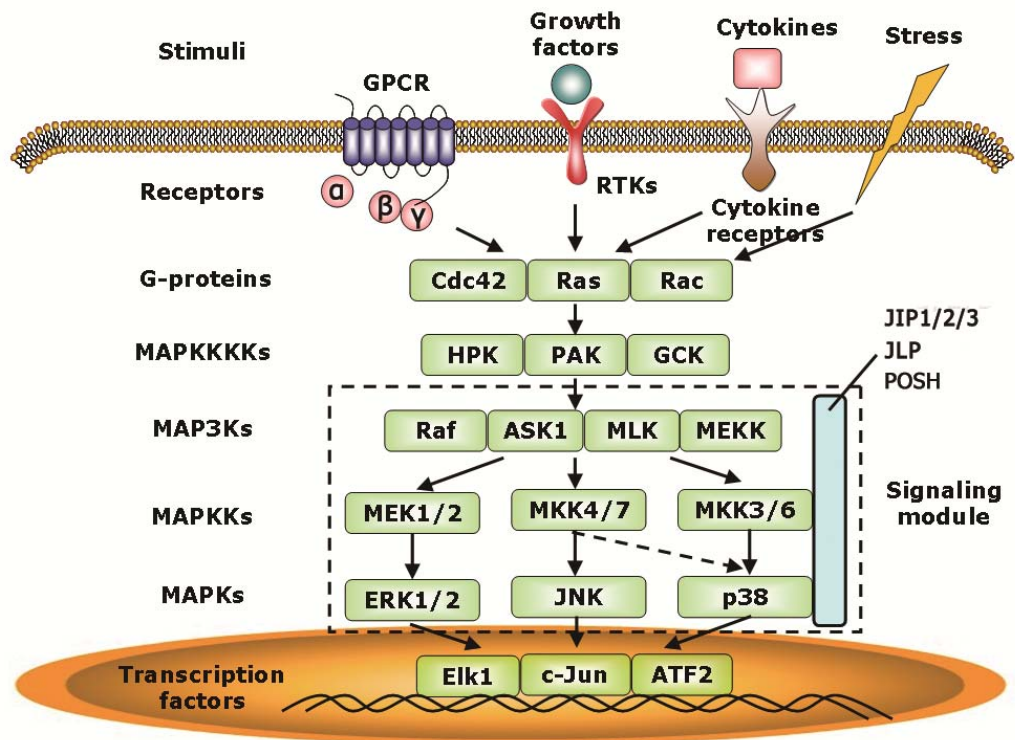


**Figure 1.6: Simplified scheme showing activation of MAPK pathways.** The main MAPK family includes ERK, JNK and p38, which is activated by stress, cytokines and growth factors. Generally, activation of MAPK signaling pathway starts with receptor activation, leading to the activation of G-proteins such as cell division control protein 42 (CDC42), Ras and Rac. The protein kinase cascade that consists of up to four tiers of kinases is subsequently activated. The scaffold proteins such as JNK interacting protein (JIP), JNK-interacting leucine zipper protein (JLP), and plenty of SH3 (POSH) etc. interact with specific members of MAP3Ks, MAPKs and MAPKs to form a module that facilitates signaling. The activated MAPKs translocate to the nucleus and phosphorylate specific transcription factors including ETS-like transcription factor 1 (ELK1), c-Jun and activating transcription factor-2 (ATF2).

### 1.3.2 Activation of JNK signaling

Rho family of GTPases is a family of small signaling G proteins (~21 kDa) such as cell division control protein 42 (CDC42), Rac, Ras and Ras homolog gene family member A (RhoA), which activate MAP4Ks in JNK signaling [186]. The MAP4Ks activate MAP3Ks such as the Raf kinase [187], apoptosis signal-regulating kinase 1 (ASK1) [188], MAPK kinase kinase 1/4 (MEKK1/4) [189] and mixed-lineage kinase (MLK) [190], which then phosphorylate two MAPK kinases, MKK4 (SAPK/ERK kinase 1, SEK1) and MKK7 (SAPK/ERK kinase 2, SEK2). MKK4 and MKK7 sequentially phosphorylate JNK at tyrosine and threonine residues respectively, leading to the full activation of JNK [191, 192]. Evidence shows that MKK4 and MKK7 are not redundant in the activation of JNK signaling. JNK activation induced by various stress stimuli is attenuated in either *MKK4*<sup>-/-</sup> or *MKK7*<sup>-/-</sup> cells, indicating that MKK4 and MKK7 collaborate with each other to activate JNK [192]. In addition, MKK4 and MKK7 respond distinctly to the stimulus. UV irradiation and anisomycin activate both MKK4 and MKK7, whereas only MKK7 is activated upon the stimulation of tumor necrosis factor (TNF) and interleukin-1 (IL-1), suggesting that MKK7 is required for cytokine-induced JNK activation [193]. Activated JNK not only phosphorylates cytoplasmic proteins, but also translocates into the nucleus and phosphorylates a number of transcription factors such as c-Jun, JunB, JunD, activating transcription factor 2 (ATF2), p53, and signal transducer and activator of transcription 3 (STAT3). c-Jun, the first identified substrate of JNK, is activated when the amino acid residues Ser63 and Ser73 in its N-terminus are phosphorylated by

JNK, leading to elevated stability and activity. The Jun (c-Jun, JunB and JunD) subfamily is able to interact with the Fos (c-Fos, FosB, Fra1 and Fra2) subfamily to form the activator protein-1 (AP-1) dimer. AP-1 then binds to the promoters of numerous genes and controls their transcriptional activities [194, 195].

Scaffold proteins play essential roles in the regulation of MAPK signaling pathways. JNK interacting protein (JIP), JNK-interacting leucine zipper protein (JLP), and plenty of SH3 (POSH) are identified as the scaffold proteins involved in JNK signaling. They interact with specific members of the JNK signaling cascade and form a module to facilitate signal transduction (Figure 1.6) [196]. JIP1 is the first identified scaffold protein in the JNK pathway, but not involved in p38 or ERK signaling. It recruits JNK, MKK7, MLK3, dual leucine zipper-bearing kinase (DLK) and haematopoietic progenitor kinase-1 (HPK1) to form the signaling module [197, 198]. Recruitment of JNK to JIP1 and its subsequent phosphorylation by JNK are required for the activation of the JNK-signaling module via MLK3 and MKK7 [199]. JIP1 also interacts with the dual-specificity phosphatases M3/6 and MAPK phosphatase 7 (MKP7) and leads to dephosphorylation of JNK, suggesting that JNK activation is mediated by JIP1 in a dynamic pattern via assembly of both the stimulatory upstream kinases and inhibitory phosphatases [200].

### **1.3.3 JNK signaling in cell migration and invasion**

The JNK signaling pathway mediates various cellular events such as cell proliferation, inflammation, and apoptosis upon activation of stress stimuli. It has

been found that lack of JNK1 leads to decreased proliferation through downregulating c-Jun activity, whereas absence of JNK2 promotes cell proliferation in fibroblasts by increasing c-Jun stability, revealing the opposite roles of JNK isoforms in the regulation of cell proliferation and c-Jun activity [201, 202]. In addition, depending on the cell type and stimulus, JNK1 and JNK2 may act as pro-apoptotic or anti-apoptotic molecules [203-205].

JNK signaling is also required for cell migration and invasion. Evidence shows that MEKK1 is required for the activation of JNK, but not other MAPKs, and inhibition of MEKK1 suppresses migration and lamellipodia formation in mouse embryonic fibroblasts (MEFs) or embryonic stem cells, suggesting that JNK signaling is essential to cell migration [206, 207]. Paxillin, a component of focal adhesion complexes involved in cell migration and adhesion, is a target of JNK1. JNK1 phosphorylates paxillin at Ser178 and then promotes rapid migration in keratocytes and Schwann cells [208, 209]. Also, JNK1 binds to and phosphorylates  $\beta$ -catenin at Ser-37 and Thr41, accompanied by dissociation of  $\alpha$ -catenin from the  $\beta$ -catenin/E-cadherin complex, leading to the blockade of cell-cell junction and increased migration in keratinocytes [210, 211]. Inhibition of JNK1 significantly suppresses migration of hepatocellular carcinoma and gastric cancer cells, indicating that JNK1 is also crucial for cancer cell migration [212, 213]. JNK2 seems to control cell migration via a distinct mechanism. The JIP-based peptide inhibitors selectively targeting JNK2 inhibit c-Jun phosphorylation and cell migration in breast cancer cells [214]. Evidence shows that the expression of epidermal growth factor

substrate 8 (EPS8), a key regulator of EGFR-mediated actin modelling, is increased in the absence of JNK2, resulting in reduced migration in mouse mammary tumor cells [215]. Furthermore, JNK2 regulates the localization of EPS8 at membrane ruffles and promotes their formation [215].

Activation of JNK is also essential to cancer cell invasion. Knockdown of MLK3 expression represses JNK activation and cell invasion in ovarian and gastric cancer cells through decreasing the expression of MMP-1, -2, -9 and -12 [213, 216]. Besides, inhibition of JNK decreases the phosphorylation of c-Jun and prohibits c-Jun/AP-1 binding to the promoter of MMP-1, leading to reduced MMP-1 activity and cell invasion in osteosarcoma and hepatocellular carcinoma (HCC) cells [217, 218]. Inhibition of either JNK1 or JNK2 is sufficient to impair breast cancer and HCC cell invasion [212, 219]. Overexpression of constitutively active JNK1 or JNK2 potentiates cell invasion and induces epithelial-mesenchymal transition in breast cancer cells [220]. Thus, both JNK1 and JNK2 are capable of inducing cancer cell migration and invasion, likely through different mechanisms.

#### **1.3.4 Roles of JNK signaling in glioblastoma**

JNK plays a pivotal role in the survival and progression of glioblastoma. Studies observe that JNK is constitutively activated in high-grade glioma: 90% in glioblastoma (58 of 64), 63% in anaplastic astrocytoma (30 of 48) and 18% in low-grade glioma (11 of 63), whereas the phosphorylation of JNK is not found in normal astrocytes or oligodendrocytes [221, 222]. In addition, more than 75% of

glioma with JNK activation are accompanied by EGFR or EGFRvIII overexpression [221, 222]. These findings suggest that activation of JNK is positively correlated with the histological grade of glioma and is responsive to EGFR activation. Besides, inhibition of Rac1 prohibits cell growth and induces apoptosis in glioblastoma cells but not in normal astrocytes, which can be rescued by activation of MEKK1 [223].

JNK1, JNK2 and JNK3 play distinct roles in cancer. Studies demonstrate that JNK1 is required for tumor formation, growth and development in gastric and colon cancers [224, 225]. Activation of JNK1 is involved in migration and invasion of HCC cells, associated with short survival of HCC patients [212, 226]. Compared with JNK1, JNK2 is of more importance to Ras- or EGFR-induced tumor transformation, growth and survival [227-229]. Inhibition of JNK2 in glioblastoma cells suppresses cell growth, DNA synthesis, and induces cell cycle arrest in S phase [230]. More importantly, highly constitutive activation and autophosphorylation of all JNK2 (JNK2 $\alpha$ 1, JNK2 $\alpha$ 2, JNK2 $\beta$ 1 and JNK2 $\beta$ 2) and JNK3 $\alpha$ 2 isoforms are observed in glioblastoma cells in the absence of upstream kinases MKK7 or MEKK1, whereas the activities of the other JNK isoforms are low [231]. In addition, the 54 kDa JNK2 isoforms (JNK2 $\alpha$ 2 and JNK2 $\beta$ 2) are predominantly expressed in all glioblastoma samples (19 of 19), and JNK2 $\alpha$ 2 possesses the highest kinase activity [231]. Similarly, a study also shows that JNK2 $\alpha$ 2 isoform is expressed in 88.2% (15 of 17) of glioblastoma, and effectively promotes glioblastoma cell proliferation and tumorigenesis [232]. These indicate that JNK2 isoforms, especially JNK2 $\alpha$ 2, have dominant expression and constitutive activities in glioblastoma, and play more vital

roles than JNK1.

The exact role of JNK3 in cancer is not fully understood yet, but it is suggested to serve as a tumor suppressor in glioblastoma. Loss of JNK3 expression by epigenetic silencing is found in brain tumors, gastric cancer, hepatocellular carcinoma, lymphoma, and H&N carcinoma [233-235]. Ectopic expression of JNK3 significantly impairs the colony formation ability of breast cancer cells [234]. In addition, overexpression of wild-type JNK3 suppresses C6 glioma cell proliferation and increases the stability and activity of p27<sup>kip</sup>, indicating that JNK3 is a candidate tumor suppressor in glioblastoma [236].

### **1.3.5 Crosstalk between PI3K/Akt and JNK pathways**

PI3K/Akt and JNK signaling pathways do not act independently to mediate cellular processes and functions. Increasing evidence reveals that these two pathways interact with each other and form a regulatory network. A number of studies find that Akt antagonizes the activation of JNK and its upstream kinases MLK, ASK1 and MKK4/7 by binding to the scaffold protein JIP1. JIP1 directly binds to the PH domain of Akt, and then forms an Akt/JIP1 complex that facilitates the activation of Akt1 via PDK1, leading to the disassociation of JNK from Akt/JIP1 module and inactivation of JNK [237-240]. Besides, Akt also interacts with and phosphorylates MLK3 at Ser674 [241, 242], ASK1 at Ser83 [243, 244], and MKK4 at Ser78 and Ser80 [245, 246], leading to their decreased kinase activities.

Conversely, evidence shows that JNK activation is frequently accompanied by

activation of PI3K and Akt in several types of cancers such as glioblastoma, cervical carcinoma and prostate cancer [232, 247, 248]. One possible explanation is that JNK is constitutively activated in some cancers. Studies reveal that JNK2 isoforms are constitutively active in glioblastoma and non-small cell lung carcinoma [222, 231, 232, 249]. Overexpression of JNK2 $\alpha$ 2, not JNK1 $\alpha$ 1, augments Akt phosphorylation in glioblastoma cells [232]. The other possible explanation is that both PI3K/Akt and JNK signaling activation are associated with overexpression of EGFR or EGFRvIII and loss of PTEN function. Since both PI3K/Akt and JNK pathways are responsive to EGF stimulation, overexpression of wild-type EGFR or EGFRvIII can give rise to the activation of these two pathways in cancer [132, 229, 250]. EGF-induced activation of Akt and JNK are inhibited by a PI3K inhibitor wortmannin or a dominant-negative mutant of PI3K, suggesting that PI3K also regulates the kinase activity of JNK [247]. It has been demonstrated that JNK and c-Jun activities are constitutively elevated in *PTEN*<sup>-/-</sup> MEFs and prostate cancer cells, which are suppressed by the PI3K inhibitor, whereas expression of wild-type PTEN relieves this inhibitory effect [248]. Moreover, the transcriptional activity of *PTEN* is regulated by c-Jun. The *c-Jun*<sup>-/-</sup> fibroblasts exhibit elevated mRNA and protein levels of PTEN, accompanied by inactivation of Akt in both *TP53*<sup>-/-</sup> and *TP53*<sup>+/+</sup> cancer cells, suggesting that PTEN is negatively regulated by c-Jun in a p53-independent manner [251]. Supporting evidence shows that c-Jun inhibits *PTEN* transcription by binding to a variant AP-1 site in its promoter [251]. Besides, c-Jun/AP-1 also increases the transcriptional activity of PDK-1 that activates its downstream target Akt, suggesting that JNK regulates Akt activity

through the JNK/c-Jun/PDK1/Akt axis [252].

Taken together, although Akt inhibits JNK signaling through association with JIP1, simultaneous activation of both Akt and JNK is also found in cancers with constitutively active forms of JNK, which is positively regulated by EGFR/EGFRvIII and PI3K, and is negatively mediated by PTEN (Figure 1.7).

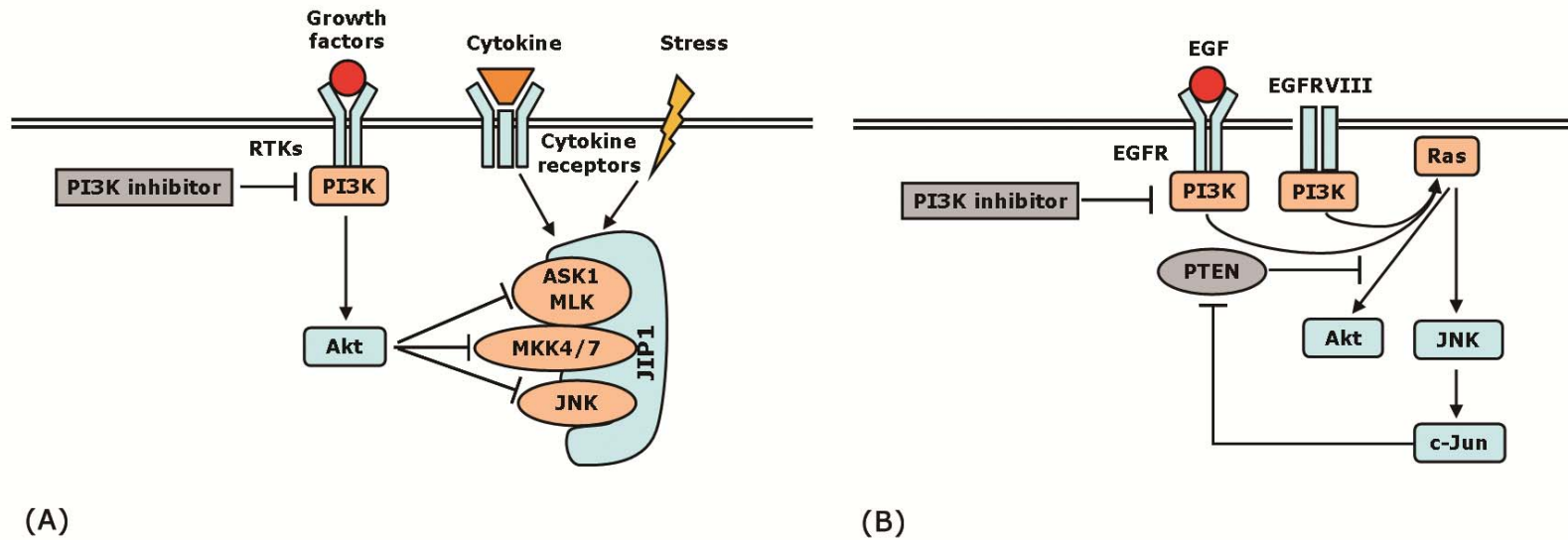


**Figure 1.7: Simplified scheme demonstrating different crosstalks between PI3K/Akt and JNK pathways.** (A) Activation of PI3K/Akt signaling inhibits stress- and cytokine-induced JNK activation. Akt antagonizes the activation of JNK and its upstream kinases MLK, ASK1 and MKK4/7 by binding to the scaffold protein JIP1. The PI3K inhibitor can activate JNK signaling through inactivation of Akt. (B) Co-activation of Akt and JNK is exhibited in the context of EGF stimulation, EGFR or EGFRvIII overexpression, as well as loss of *PTEN*. The PI3K inhibitors and wild-type *PTEN* inhibit both Akt and JNK activation. Activated c-Jun by JNK can bind to the promoter sequence of *PTEN*, resulting in the inhibition of *PTEN* transcription and activation of Akt.

### **1.3.6 Combination therapy targeting PI3K/Akt and Ras-mediated MAPK pathways**

Since Ras is capable of interacting with the catalytic isoforms of PI3K to activate PI3K/Akt and MAPK pathways, combination therapies targeting these two pathways may have synergism in cancer treatment [253]. Evidence shows that combined inhibition of p110 $\delta$  and MEK (MAPK/ERK kinase) suppresses phosphorylation of both Akt and ERK, and has synergistic cytotoxicity in human acute myeloid leukemia progenitors [254]. The results of a phase I trial suggest that patients receiving combination therapies targeting PI3K/Akt and Ras/Raf/MEK/ERK pathways may have better prognosis [255]. PI3K/Akt and MKK4/JNK pathways cooperate to regulate cancer cell survival. Concurrent inhibition of p85 $\alpha$  and MKK4 synergistically suppresses cell proliferation and promotes apoptosis in lung cancer cells, indicating that combination therapies targeting these two pathways might be more effective [256, 257]. However, combination effects of the class I<sub>A</sub> PI3K catalytic isoforms and JNK inhibition on glioblastoma cells are not clear.

## 1.4 Overview of myricetin

Myricetin (3,5,7-Trihydroxy-2-(3,4,5-trihydroxyphenyl)-4-chromenone) is a member of natural flavonoid abundant in vegetables, fruits, onions, nuts, berries, tea and red wine. Flavonoid is a class of polyphenol that consists of two substituted benzene rings connected by a chain of three carbon atoms and an oxygen bridge (Figure 1.8). According to the chemical structure, especially the difference in the 3' position of C ring, flavonoid is divided into six subclasses including flavone, flavanone, flavanol, flavonol, anthocyanin and isoflavonoid [258]. Myricetin, as well as quercetin, kaempferol and fisetin, belong to the flavonol subclass. The chemical structures of these flavonols are shown in Figure 1.8. Myricetin exhibits potent anti-oxidant, anti-inflammatory, anti-diabetic, neuroprotective and anti-cancer activities. Quercetin, which differs from myricetin by one hydroxyl group (-OH), is permeable to the blood-brain barrier [259]. Therefore, it is possible that myricetin is able to do the same, making it a promising therapeutic strategy for glioblastoma treatment.

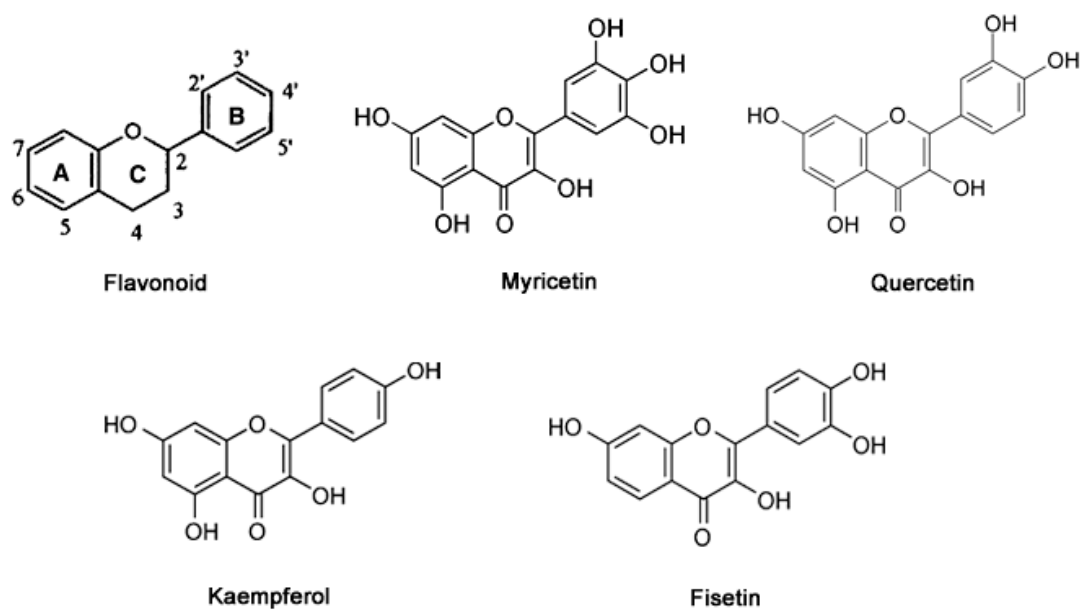


**Figure 1.8: Chemical structures of flavonoid and the representative flavonols including myricetin, quercetin, kaempferol and fisetin.**

### 1.4.1 Anti-oxidant and anti-inflammatory activities of myricetin

Flavonols including myricetin, quercetin and kaempferol are capable of scavenging reactive oxygen species (ROS), suppressing lipid peroxidation and chelating redox-active metals. Evidence shows that myricetin prevents fibroblasts from H<sub>2</sub>O<sub>2</sub>-induced DNA damage through suppressing intracellular ROS generation and increasing the activities of antioxidant enzymes like superoxide dismutase and catalase [260]. The configuration and total number of B-ring -OH in flavonoid determine the free radical scavenging capacity. Hydroxyl groups on the B-ring are able to donate hydrogen and an electron to radicals to generate more stable products. Generally, the total number of hydroxyl groups is positively correlated with the anti-oxidant activity of flavonoid [261]. The 3' and 4' hydroxyl groups on the B-ring are of more importance than 5' -OH to the radical scavenging activity [262]. Therefore, the anti-oxidant activity of myricetin is much higher than kaempferol, but is close to quercetin [263].

Myricetin also possesses potent anti-inflammatory activity on acute and chronic inflammation. Studies show that myricetin not only suppresses the expression of cytokines such as interleukins (ILs) -6 and -8, interferon- $\gamma$  (IFN- $\gamma$ ) and TNF- $\alpha$  in the inflammation response, but also inhibits cytokine-induced apoptosis and cell death [264-266]. An *in vivo* study demonstrates that myricetin suppresses inflammation such as xylene-induced ear edema and cotton pellet granuloma, and decreases the number of leukocytes [267]. The anti-oxidant and anti-inflammatory activities of myricetin may contribute to its anti-cancer effect by modulating the tumor

microenvironment.

#### **1.4.2 Anti-cancer activity of myricetin**

The most studied biological activity of myricetin is its anti-cancer activity. Myricetin inhibits cell transformation in mouse epidermal cells by targeting PI3K/Akt, MEK/ERK and Janus kinase 1 (JAK1)/STAT3 signaling pathways [268-270]. An *in vivo* study shows that myricetin protects mice from the occurrence of UVB-induced skin cancer via downregulating cyclooxygenase-2 (COX-2) expression and Fyn kinase activity [271]. Analysis of structure-activity relationships shows that 3'- and 4'-OH on the B-ring play an important role in the inhibitory effect of myricetin on EGF-induced cell transformation through inactivation of PI3K and AP-1 [272]. Myricetin also exerts anti-proliferative, pro-apoptotic, anti-invasive and anti-angiogenic effects on a variety of cancers. It induces apoptosis of pancreatic cells through activation of caspases-3/-9 and inactivation of Akt. Tumor growth and metastasis to lung are also suppressed by myricetin in an orthotopic pancreatic tumor model [273]. Myricetin inhibits bladder cancer cell viability through G2/M cell cycle arrest by decreasing the expression of Cdc2 and cyclin B1, and attenuates cell invasion by downregulating MMP-9 activity [274]. It mitigates cell proliferation and invasion and promotes apoptosis in esophageal carcinoma cells *in vitro*, as well as tumor growth in tumor xenografts by reducing activity of ribosomal S6 kinase 2 (RSK2) [275]. It also decreases the activities of MMP-2, urokinase plasminogen activator (uPA), ERK and AP-1 to suppress migration and invasion in colorectal and

lung cancer cells [276, 277]. In addition, myricetin is able to suppress UVB-induced angiogenesis by decreasing the activities of MMP-9, MMP-13 and hypoxia inducible factor-1 $\alpha$  (HIF-1 $\alpha$ ) in a mouse skin cancer model [278]. These findings suggest that myricetin is a promising therapeutic drug with potent anti-cancer effects.

To date, few studies report the anti-cancer effects of myricetin on glioblastoma, especially on cell migration and invasion. Studies show that combination of myricetin and tumor necrosis factor-related apoptosis-inducing ligand (TRAIL) induces apoptosis of glioblastoma cells via increasing caspases-8/-9 and caspases-3/-7 activities and decreasing c-FLIP and Bcl-2 expression [279]. In addition, myricetin inhibits peroxide production, COX-2/PGE2 expression and MMP-9 activity to block TPA-induced migration and invasion in glioblastoma cells [280]. Besides, although combination of quercetin and temozolomide displays synergism to inhibit glioblastoma cell viability and promote apoptosis by decreasing Hsp27 expression [281, 282], little is known about whether myricetin can sensitize glioblastoma cells to temozolomide.

### **1.4.3 Molecular targets of myricetin**

A number of target proteins of myricetin are recently identified, including Akt, MEK1, MKK4, JAK1, RSK2 and Fyn. Myricetin directly binds to the ATP binding sites of Akt, MKK4 and Fyn with hydrogen bonds, and then blocks their activation by competing with ATP [268, 271, 283]. Myricetin interacts with MEK1 in an ATP-noncompetitive manner, and the binding site is similar to the MEK1-selective

inhibitor PD184352 [269]. RSK2 is a substrate kinase located in the signal transduction between ERK and the transcription factors. Myricetin is able to bind to the N-terminal domain of RSK2, which is essential to transducing the RSK2 activation signal to the transcription factors [275]. In addition, myricetin directly binds to the catalytic domain of JAK1 to inhibit its activation [270]. Taken together, myricetin is promising therapeutic drug with broad spectrum that acts in either ATP-competitive or ATP-noncompetitive manner.

### **1.5 Rationales and objectives of this study**

Glioblastoma is characterized by rapid growth, extensive infiltration to neighboring normal brain parenchyma, and new blood vessel formation. Thus, migration and invasion are potential therapeutic targets for glioblastoma treatment. PI3K/Akt pathway involved in a variety of biological processes including cell proliferation, metabolism, motility, survival and angiogenesis, is a promising target for glioblastoma treatment. Selective inhibitors for class I<sub>A</sub> PI3K isoforms that may display less off-target effects and toxicities are attractive options. However, the exact roles of p110 $\alpha$ , p110 $\beta$  and p110 $\delta$ , as well as their interactions in glioblastoma are not fully elucidated yet. Considering that inhibition of PI3K isoforms might be compensated by other signaling pathways, and subsequently compromise the inhibitory effects, combination treatment strategies by dual inhibition of PI3K and JNK were investigated in this study. Numerous studies provide a clear rationale for the combined inhibition, including: (1) JNK pathway also plays an important role in the

survival and motility of glioblastoma cells, (2) constitutively active forms of JNK, as well as co-activation of both Akt and JNK is found in glioblastoma, (3) EGFR/PI3K/PTEN/Akt pathway has crosstalk with JNK/c-Jun pathway, which is regulated by EGFR/EGFRvIII and PTEN, (4) combination inhibition of PI3K/Akt and MKK4/JNK pathways effectively suppresses lung cancer cell proliferation.

Therefore, the objectives of this study are (1) to investigate the roles of class I<sub>A</sub> PI3K catalytic isoforms (p110 $\alpha$ , p110 $\beta$  and p110 $\delta$ ) in the regulation of glioblastoma cell viability and motility, (2) to evaluate the combination effects of PI3K isoforms and JNK inhibition on glioblastoma cell proliferation, migration and invasion, (3) to study the effects of myricetin on glioblastoma cell viability and motility, and (4) to investigate whether myricetin can sensitize glioblastoma cells to temozolomide.

## Chapter 2 Materials and methods

### 2.1 Cell lines

Normal human astrocytes were obtained from ScienCell Research Laboratories. Four human glioblastoma cell lines (U-87 MG, U-118 MG, U-138 MG, and A-172) were purchased from American Type Culture Collection (ATCC). The other four glioblastoma cell lines (U-343 MG, U-373 MG, SK-MG3 and LN-Z308) and two paediatric glioblastoma cell lines (GBM6840 and GBM2603) were kindly provided by Prof. HK Ng (Prince of Wales Hospital, The Chinese University of Hong Kong). The characteristics of all glioblastoma cell lines are listed in Table 2.1.

**Table 2.1: Characteristics of human glioblastoma cell lines [284, 285]**

<b>Cell line</b>	<b>Age/Gender</b>	<b>Tumor grade</b>	<b><i>PTEN</i> status</b>	<b><i>TP53</i> status</b>	<b>Tumorigenicity</b>
U-87 MG	44 years/Female	Grade IV	Splicing variant/deletion	WT	Yes
U-118 MG	50 years/Male	Grade IV	Splicing defect	Substitution/missense	Yes
U-138 MG	47 years/Male	Grade IV	Splicing variant/deletion	Substitution/missense	No
U-343 MG	54 years/Male	Grade III	Substitution/missense	WT	Yes
U-373 MG	50 years/Male	Grade IV	Frame shift	Substitution/missense	Yes
A-172	53 years/Male	Grade IV	WT/deletion	WT	No
SK-MG3	N/A	Grade IV	N/A	Heterozygous mutation	N/A
LN-Z308	65 years/Male	Grade IV	Deletion/frame shift	Deletion	Yes
GBM2603*	N/A	Grade IV	N/A	N/A	N/A
GBM6840*	17 years/Female	Grade IV	In-frame deletion	WT	Yes

\*, GBM6840 and GBM2603 were derived from the tumor of two paediatric GBM patients in the laboratory of the Department of Anatomical and Cellular Pathology, Prince of Wales Hospital, the Chinese University of Hong Kong. N/A, not available. WT, wild type.

## 2.2 Cell culture

Cells were cultured in minimum essential medium alpha ( $\alpha$ -MEM) supplemented with 10% (v/v) fetal bovine serum (FBS). Cells were incubated at 37°C in 5% CO<sub>2</sub> humidified atmosphere and passaged at a ratio of 1:3 every two to three days. Medium was discarded and cells were rinsed with Ca<sup>2+</sup>- and Mg<sup>2+</sup>-free phosphate-buffered saline (PBS). Cells were disassociated by Trypin-EDTA solution and then serum-containing medium was added to stop the disassociation. Cells were dispersed by pipetting medium over the cell layer surface several times. And then cells were transferred to a 15 mL conical tube and centrifuge at 200 ×g for 5 min. The supernatant was aspirated and cell pellets were resuspended with complete growth medium. Cells were transferred to new culture plates and incubated at 37°C in 5% CO<sub>2</sub>.

## 2.3 Drug treatment

Glioblastoma cells were seeded onto 6-well plates ( $2 \times 10^5$  cells per well) and incubated for 24 hr. Cells were incubated with isoform-selective PI3K inhibitors alone or in combination with SP600125 in  $\alpha$ -MEM medium supplemented with 10% FBS at 37°C. For the treatment of myricetin or temozolomide, drugs were prepared in  $\alpha$ -MEM medium supplemented with 20  $\mu$ M HEPES buffer and 10% FBS to stabilize the pH at 7.2. Glioblastoma cells were treated with myricetin at 37°C. The incubation time differed according to the requirement of assays. The solvent dimethyl sulfoxide (DMSO) at a dilution of 1:1000 (v/v) was used as a carrier control. For further protein

extraction and Western blotting, cells were rinsed with PBS and harvested. The characteristics of isoform-selective PI3K inhibitors PIK-75, TGX-221 and CAL-101, as well as JNK inhibitor SP600125 are listed in Tables 2.2 and 2.3.

Table 2.2: Characteristics of isoform-selective PI3K inhibitors

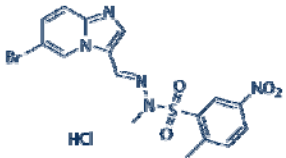
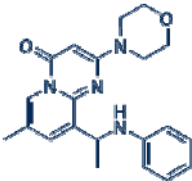
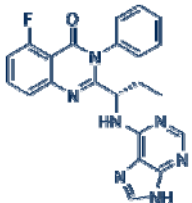
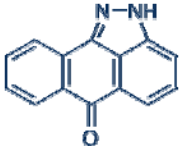
Compound	Chemical structure	IC <sub>50</sub> (nM)				Reference
		p110 $\alpha$	p110 $\beta$	p110 $\delta$	p110 $\gamma$	
PIK-75		5.8	1300	510	76	[286]
TGX-221		5000	5	211	> 3500	[287]
CAL-101		820	565	2.5	89	[158]

Table 2.3: Characteristics of JNK inhibitor SP600125

Compound	Chemical structure	IC <sub>50</sub> (nM)					Reference
		JNK1	JNK2	JNK3	MKK4	MKK7	
SP600125		40	40	90	400	5100	[288]

## 2.4 Cell proliferation assay (MTT method)

Glioblastoma cells were seeded onto 96-well plates ( $2 \times 10^3$  cells per well) and incubated for 24 hr. Then cells were treated with drugs in complete growth medium supplemented with 10% FBS for 48 hr at 37°C and DMSO (1:1000) was used as a carrier control. MTT (3-(4,5-dimethylthiazol-2-yl)-2,5-diphenyltetrazolium bromide) (5 mg/mL, 20  $\mu$ L) were added to each well, and the cells were further incubated for 4 hr at 37°C. The medium was then removed, and 150  $\mu$ L of DMSO was added to dissolve the formazan crystals formed. Finally, the absorbance at 570 nm and 620 nm was measured by BioRad BenchMark Plus™ microplate spectrophotometer. Half-maximal inhibitory concentration ( $IC_{50}$ ) value was determined by dose response curve fitting at a series of drug doses using Origin 9.0 software. Experiments were carried out in triplicate, and each independent experiment consisted of four measurements.

## 2.5 Determination of combination index (CI)

Cells were treated with two drugs alone and in combination at a fixed ratio for 48 hr. Drugs were two-fold serially diluted. Percentage of cell proliferation was determined and represented as  $A_{570-620}$  (treatment)/ $A_{570-620}$  (control)  $\times 100\%$ . The fraction affected (FA) refers to the inhibition of cell proliferation and is calculated by:  $FA = 1 - (\% \text{ cell proliferation}/100)$ . Combination effect was evaluated by combination index (CI) as described by Chou [289]. According to the FA values, CI was automated calculated by Compusyn software.  $CI < 0.9$  indicates synergistic effect;

CI > 1.1 indicates antagonistic effect; CI between 0.9 and 1.1 indicates additive effect (Table 2.4).

**Table 2.4: Combination index values and their indications [289]**

CI		Synergism/antagonism
<0.1	+++++	Very strong synergism
0.1 - 0.3	++++	Strong synergism
0.3 - 0.7	+++	Synergism
0.7 - 0.85	++	Moderate synergism
0.85 - 0.9	+	Slight synergism
0.9 - 1.1	Nearly	additive
1.1 - 1.2	-	Slight antagonism
1.2 - 1.45	--	Moderate antagonism
1.45 - 3.3	---	Antagonism
3.3 - 10	----	Strong antagonism
>10	-----	Very strong antagonism

## 2.6 Wound healing assay

Glioblastoma cells were seeded onto 12-well plates ( $3 \times 10^5$  cells per well) and were incubated for 24 hr to achieve 90%-100% confluence. Cells were pretreated with 5  $\mu\text{g}/\text{mL}$  mitomycin C for 1 hr to eliminate the interference of cell proliferation. Wounds on the confluent cells were created using a sterile 200  $\mu\text{L}$  pipette tip. After rinsing with PBS for three times, cells were treated with drugs in  $\alpha$ -MEM medium supplemented with 5% FBS and then incubated for 24 hr at 37°C. Cells were photographed immediately after inhibitor treatment (time zero) and at 12 or 24 hr after wounding. Cell migration rate was indicated as the number of cells migrated into the original wounds or the migration distance of cells relative to those in DMSO control.

## 2.7 Immunofluorescence

Glioblastoma cells were seeded onto sterile coverslips in 24-well plates ( $2.5 \times 10^4$  cells per well) and incubated for 24 hr at 37°C. After a 3-hr drug treatment, cells were fixed with 4% paraformaldehyde for 15 min and then permeabilized with 0.25% Triton X-100 for 10 min at room temperature. Coverslips were blocked with 1% BSA for 30 min and incubated with Alexa Fluor 594-conjugated phalloidin (Life Technologies) for 20 min to visualize actin filaments. Cells were air dried and mounted on a microscope slide with ProLong Gold antifade mountant with DAPI (Life Technologies). Lamellipodia were analyzed under Leica TSC SP8 confocal laser scanning microscope and membrane ruffles were observed by phase contrast microscopy. In

each case, about 200 cells were photographed and representative cells were shown. Independent experiments were carried out in triplicate.

## **2.8 Boyden chamber migration assay**

Cell migration was evaluated using the Polyester-Transwell inserts with 8  $\mu\text{m}$  pores (Corning). Briefly, glioblastoma cells ( $2.5 \times 10^4$  cells per insert) were pretreated with drugs in serum-free medium for 1 hr at 37°C and then seeded into the transwell inserts. Medium supplemented with 5% FBS in each well of companion plate was served as a chemoattractant. After a 12-hr incubation, cells on the upper surface of the membrane were removed. Cells on the lower surfaces of the membrane were fixed with absolute methanol and were then stained with 0.1% crystal violet solution. Cells were photographed under a light microscope at 50 $\times$  magnification and cells from at least 5 representative fields were counted using ImageJ software. Independent experiments were carried out in triplicate.

## **2.9 Invasion assay**

Invasiveness of glioblastoma cells was determined using BioCoat™ Matrigel™ Invasion Chamber (Corning). Briefly, the transwell inserts with 8  $\mu\text{m}$  pores and precoated Matrigel was rehydrated for 2 hr at 37°C. Medium supplemented with 5% FBS in each well of companion plate was served as a chemoattractant. After a 24-hr incubation, the matrigel layer and non-invasive cells on the upper surface of the membrane were removed. Cells on the lower surfaces of the membrane were fixed

with absolute methanol and were then stained with 0.1% (w/v) crystal violet solution. Cells were photographed under a light microscope at 50× magnification and invasive cells from at least 5 representative fields were counted using ImageJ software. Independent experiments were carried out in triplicate.

## **2.10 Protein extraction**

Glioblastoma cells were rinsed with PBS and dissociated using Trypsin-EDTA solution. The detached cells were then transferred to a 1.5 mL eppendorf tube and centrifuged at 200 ×g for 5 min at 4°C. The supernatant was discarded and the cell pellets were washed with ice-cold PBS by centrifugation at 200 ×g for 5 min at 4°C. Subsequently, the cell pellets were lysed in RIPA lysis buffer (50 mM Tris, 150 mM NaCl, 0.5% sodium deoxycholate, 0.1% SDS, 1% NP-40, 1 mM EDTA, pH 7.2) containing 1× cOmplete protease inhibitor cocktail (Roche) and 1× PhosSTOP phosphatase inhibitor cocktail (Roche). Cells were homogenized by vortexing and pipetting up and down several times. The mixture was placed on ice for 30 min with occasional vortexing. The cellular lysate was clarified by centrifugation at 12,000 ×g for 15 min at 4°C. The clarified lysate was transferred to a new eppendorf tube and stored at -80°C until analysis.

## **2.11 BCA protein assay**

Protein quantification was carried out using Pierce BCA Protein Assay Kit (Thermo Scientific). A set of diluted bovine serum albumin (BSA) standards were

prepared as shown in Table 2.5. The BCA working reagent was prepared by mixing reagent A and reagent B at a ratio of 50:1. The protein sample was also diluted in RIPA lysis buffer at 1:15 dilution, and then 25  $\mu\text{L}$  of each diluted sample or BSA standards was added into a microplate well. BCA working reagent was then added into the microplate (200  $\mu\text{L}$  per well) and the plate was mixed thoroughly. The plate was covered and incubated for 30 min at 37°C. The plate was then placed for 10 min at room temperature and the absorbance at 562 nm was measured by BioRad BenchMark Plus™ microplate spectrophotometer. A standard curve was produced by plotting the  $A_{562}$  of each BSA standard, and the protein concentration of each sample was determined using the standard curve.

**Table 2.5: Preparation of diluted BSA standards**

<b>Vial</b>	<b>Volume of RIPA buffer (<math>\mu\text{L}</math>)</b>	<b>Volume and source of BSA (<math>\mu\text{L}</math>)</b>	<b>Final BSA concentration (mg/mL)</b>
A	300	300 of 2 mg/mL BSA	1
B	150	250 of 2 mg/mL BSA	0.75
C	300	300 of vial A dilution	0.5
D	250	250 of vial C dilution	0.25
E	180	180 of vial D dilution	0.125
F	240	60 of vial E dilution	0.025
G	100	0	0 = Blank

## 2.12 Western blotting

Samples were mixed with 5× loading buffer (250 mM Tris pH6.8, 10% SDS, 0.05% bromophenol blue, 50% glycerol, 5% β-mercaptoethanol) at a ratio of 4:1. Then the samples were heat-denatured at 100°C for 5 min. Samples were separated by sodium dodecyl sulfate-polyacrylamide gel electrophoresis (SDS-PAGE). Total protein (40 μg) was loaded onto the wells of 8% polyacrylamide gel. After the electrophoresis, the proteins were electrotransferred to a PVDF membrane. The membrane was blocked for 2 hr by either 5% (w/v) non-fat milk or 5% (w/v) BSA in Tris-buffered saline with 0.1% Tween-20 (TBST, pH7.4). The membrane was then incubated overnight with primary antibodies with gentle agitation at 4°C. Primary antibodies were diluted using 5% BSA in TBST as described in the antibodies supplier's instructions. After the primary antibody incubation, the membrane was washed with TBST three times with 10 min each. The membrane was then incubated with horseradish peroxidase (HRP)-conjugated secondary antibodies at a dilution of 1:5000 for 1 hr at room temperature with gentle agitation. And then the membrane was washed again with TBST four times with 8 min each. Positive signals were visualized by Amersham™ ECL™ Select Western Blotting Detection Reagent (GE Healthcare) and recorded by ChemiDoc MP Imaging System (Bio-Rad).

## 2.13 Preparation of myricetin-Sepherose 4B

CNBr-activated Sepharose 4B powder (GE Healthcare) was washed with 1 mM HCl (pH 3.0) for 15 min. Myricetin (3 mg) was dissolved in DMSO and then coupled

to CNBr-activated Sepharose 4B beads (25 mg) in the coupling buffer (0.1 M NaHCO<sub>3</sub>, 0.5 M NaCl, pH 8.3) overnight with gentle rotation at 4°C. Excess myricetin was washed away with coupling buffer by centrifugation at 1000 rpm for 3 min at 4°C. Remaining active groups in the Sepharose beads were blocked by 0.1 M Tris-HCl buffer (pH 8.0) with 2-hr rotation at room temperature. Subsequently, the mixture was washed three times with 0.1 M acetate buffer (pH 4.0) containing 0.5 M NaCl followed by an additional wash with 0.1 M Tris-HCl buffer (pH 8.0) containing 0.5 M NaCl.

#### **2.14 *Ex vivo* pull-down assay**

Pull-down assay was performed as described by Kumamoto et al. [270]. The glioblastoma cell lysate (500 µg) was incubated with myricetin-coupled Sepharose 4B beads (100 µL, 50% slurry) at 4°C overnight in the reaction buffer (50 mM Tris-HCl, 5 mM EDTA, 150 mM NaCl, 1 mM DTT, 0.01% Nonidet P-40 and 2 µg/mL BSA containing 1× protease inhibitor cocktail, pH 7.5). The beads were then washed five times with washing buffer (50 mM Tris-HCl, 5 mM EDTA, 200 mM NaCl, 1 mM DTT, 0.02% Nonidet P-40, and 0.02 mM PMSF, pH 7.5). The proteins bound to the beads were applied to SDS-PAGE and then detected by Western blotting.

#### **2.15 RNA isolation**

Total RNA was isolated using TRIzol Reagent (Life Technologies) which (0.5 mL per well) was added directly to the cells in the 6-well plates. Cells were lysed by

pipetting the cells up and down for several times. Samples were then homogenized by incubation for 5 min at room temperature. Chloroform (0.1 mL) was added and samples were mixed by shaking the tubes several times. The mixture was then incubated for 2 min at room temperature and centrifuged at 12,000  $\times g$  for 15 min at 4°C. The colorless upper aqueous phase was carefully transferred to a new RNase-free eppendorf tube and isopropanol (0.25 mL) was added. Then the samples were incubated for 10 min at room temperature and centrifuged at 12,000  $\times g$  for 10 min at 4°C. The supernatant was removed and the RNA pellets were washed with 0.5 mL of 75% ethanol and then centrifuging at 7,500  $\times g$  for 5 min at 4°C. The supernatant was discarded and the RNA pellets were air-dried for 10 min. RNase-free water (30-50  $\mu$ L) was added to dissolve the RNA pellets and then RNA was incubated for 10 min at 55-60°C. The total RNA was stored at -80°C for further analysis.

## **2.16 Quantification of isolated RNA**

The purity and quantity of total RNA were evaluated by spectrophotometry (NanoDrop 2000, Thermo Scientific). The RNA sample (1  $\mu$ L) was loaded onto the measurement pedestal of NanoDrop 2000. The concentration of RNA was determined by the absorbance at 260 nm. The purity of RNA was evaluated by the ratio of absorbance at 260 nm and 280 nm ( $A_{260/280}$ ). The total RNA with an  $A_{260/280} > 1.8$  and  $< 2.0$  was regarded to be pure.

## 2.17 cDNA synthesis

First-strand cDNA was synthesized from 2 µg of total RNA using the Fermentas RevertAid First Strand cDNA Synthesis Kit (Thermo Scientific). According to the manufacturer's protocol, oligo(dT)<sub>18</sub> primer, reaction buffer, RNase inhibitor, dNTP mix and M-MuLV reverse transcriptase were added into RNA samples, followed by incubation for 60 min at 42°C. And then the reaction was terminated by heating at 70°C for 5 min. The cDNA product was stored at -80°C.

## 2.18 Quantitative Real-time PCR (qRT-PCR)

### 2.18.1 Primer design

The *P130Cas*, *ITGB3*, *ADAMTS1* and *GAPDH* primers for SYBR Green qRT-PCR were designed using Primer Premier 6 Software. Primers with length between 18-25 bp, GC content between 45%-55%, and the melting temperature ( $T_m$ ) between 58°C-62°C were designed. The maximum  $\Delta G$  of hairpins, self-primers and cross-primers was minimized. The PCR product with length between 80-280 bp was designed to span the exons. The primer sequences were listed in Table 2.6. As for TaqMan qRT-PCR, the specific primers for *PIK3CA* (Hs00180679\_m1), *PIK3CB* (Hs00178872\_m1), *PIK3CD* (Hs00192399\_m1), and *GAPDH* (Hs99999905\_m1) were purchased from Life Technologies.

**Table 2.6: Primer sequence and characteristics of primers**

<b>Gene</b>	<b>Primer sequence (5' to 3')</b>	<b>Tm (°C)</b>	<b>Position</b>	<b>Product length (bp)</b>
<i>P130Cas</i>	Forward: GCAATGCCTCACTGCTCTTCAGA	59.6	2218-2458	241
	Reverse: TGGGTCTTCTCAAACCTCCTTCC	60.3		
<i>ITGB1</i>	Forward: CTGCGAGTGTGGTGTCTGTAAGTG	60.2	2057-2321	265
	Reverse: CCAACAGTCGTCAACATCCTTCTCC	60.2		
<i>ITGB3</i>	Forward: AAGTGCGGCAGGTGGAGGATTA	60.0	406-655	250
	Reverse: GGCAAGCAGGTGGTCTTCATATCAT	59.8		
<i>ADAMTS1</i>	Forward: AGTTAGCCTGGTGGTGGTGAAGAT	60.0	1358-1590	233
	Reverse: ACACAGTTCCAACATCAGCCATCC	59.9		
<i>GAPDH</i>	Forward: ATGGCACCGTCAAGGCTGAGAA	60.5	344-619	276
	Reverse: TGCTGATGATCTTGAGGCTGTTGTC	60		

### **2.18.2 SYBR Green qRT-PCR**

The SYBR Green qRT-PCR was performed on ABI PRISM 7500 System (Life Technologies) using FastStart Universal SYBR Green Master Mix (Roche). According to the manufacturer's protocol, the PCR reaction mixture contained 1×SYBR Green Master Mix, template cDNA (0.05 µg) and primer pairs (0.3 µM). Cycling variables were set as follows: initiation of activation step at 95°C for 10 min, followed by 40 cycles including denaturation at 95°C (15 sec), annealing at 60°C (30 sec) and extension at 72°C (30 sec). Human GAPDH mRNA was served as an internal control for RNA normalization. The relative expression was normalized using the  $2^{-\Delta\Delta CT}$  method. Independent experiments were carried out in triplicate, and each reaction is duplicated.

### **2.18.3 TaqMan qRT-PCR**

The TaqMan qRT-PCR was performed on ABI PRISM 7500 System using Platinum Quantitative PCR SuperMix-UDG (Life Technologies) according to the manufacturer's protocol. The PCR reaction mixture was prepared as followed: 1×SuperMix-UDG, template cDNA (0.05 µg), 1×Fluorogenic Probes and Primers, and ROX reference dye. Cycling variables were set as follows: UDG incubation step at 50°C for 2 min, and initiation of activation step at 95°C for 2 min, followed by 40 cycles including denaturation at 95°C (15 sec), annealing and extension at 60°C (60 sec). Human GAPDH mRNA was used as an internal control for RNA normalization. The relative expression was normalized using the  $2^{-\Delta\Delta CT}$  method. Independent

experiments were carried out in triplicate, and each reaction was duplicated.

### **2.19 RNA interference**

Small interfering RNA (siRNA) synthetic duplexes were purchased from Qiagen and appropriate RNase-free water was added to obtain a 20  $\mu$ M solution. The AllStars Negative Control siRNA (Qiagen) with sequence not homologous to any known mammalian genes was used as a negative control. The AllStars Hs Cell Death Control siRNA duplexes (Qiagen) which target several genes that are essential to cell survival were employed as positive controls to evaluate the transfection efficiency. The target sequences of siRNA duplexes are listed in Table 2.7.

Briefly, the glioblastoma cells were seeded onto 6-well plates ( $1.5 \times 10^5$  cells per well) and incubated for 24 hr. Cells were then transfected with siRNA annealed duplexes using Lipofectamine 2000 transfection reagent (Life Technologies) according to manufacturer's instructions. The siRNA duplexes (100 pmol) and Lipofectamine 2000 (5  $\mu$ L) were separately diluted in 250  $\mu$ L of Opti-MEM I Reduced Serum Medium (Life Technologies). After a 5-min incubation, they were mixed together and incubated for 20 min at room temperature to obtain the transfection complexes. Subsequently, the cells in 6-well plates were rinsed with PBS and serum-free MEM medium was added. The transfection complexes were added drop by drop to the 6-well plate (500  $\mu$ L per well), and the resulting final concentration of siRNA was 50 nM. Cells were incubated for 12-16 hr at 37°C, and then the medium was removed and changed to the complete growth medium. Cells were further

incubated for different periods before analysis.

**Table 2.7: Sequences of siRNA duplexes targeting *PIK3CD* gene**

Gene	Product name	Catalog No.	Target sequence (5' to 3')	Position
<i>PIK3CD</i>	siPIK3CD_1	SI00071512	CAGCGTGGGCATCATCT TTAA	2524-2544
	siPIK3CD_2	SI00071519	CCCACAGGTGATCCTAA CATA	4710-4730
	siPIK3CD_5	SI02223809	CCGGTCACGCATGAAG GCAAA	4044-4064
	siPIK3CD_6	SI02223816	CGCCGTGATCGAGAAA GCCAA	1393-1413

## **2.20 Statistical analysis**

Data were presented as means  $\pm$  S.E.M and analyzed by SPSS v22.0. Curves and histograms were produced using GraphPad PRISM v5.0. Statistical comparisons among multiple groups in qRT-PCR, cell proliferation, migration and invasion assays were analyzed by One-way ANOVA and Post Hoc multiple comparison Tukey HSD test. The difference was considered to be statistically significant at  $p < 0.05$ .

## **Chapter 3 Distinct roles of PI3K catalytic isoforms in glioblastoma**

### **3.1 Expression pattern of PI3K/Akt pathway molecules in glioblastoma cell lines**

Prior to the pharmacological inhibition of PI3K isoforms on glioblastoma cells, the expression pattern of PI3K/Akt pathway molecules in these cells was investigated. Ten human glioblastoma cell lines were selected for measuring the expression levels of PI3Ks (p110 $\alpha$ , p110 $\beta$ , p110 $\delta$ , p85 $\alpha$  and p85 $\beta$ ), Akt, PTEN and EGFR, as well as the phosphorylation level of Akt. Normal astrocytes were used for comparison. A distinct expression pattern of PI3K/Akt pathway molecules among different glioblastoma cell lines was exhibited (Figure 3.1). The expression levels of p110 $\alpha$ , p110 $\beta$ , p110 $\delta$  and EGFR, as well as the phosphorylation level of Akt in most of glioblastoma cell lines were higher than those in astrocytes, indicating that they play important roles in glioblastoma. The expression of p110 $\beta$  and p85 $\beta$  were consistently high in most glioblastoma cell lines. However, the expression of p110 $\alpha$ , p110 $\delta$ , p85 $\alpha$ , Akt and EGFR among different glioblastoma cell lines varied greatly. The expression of p110 $\alpha$  and p110 $\beta$  was low in U-87 MG and U-138 MG cells, accompanied by a relatively low phosphorylation level of Akt. The expression of p110 $\delta$  was much higher in U-87 MG, U-373 MG, SK-MG3, LN-Z308, GBM2603 and GBM6840 cells.

The expression of PTEN in most primary glioblastoma cell lines was null due to its mutation, whereas it was detected in U-343 MG, A-172, GBM2603 and GBM6840

cells, as well as in astrocytes. In addition, EGFR was highly expressed in U-343 MG, A-172, SK-MG3 and GBM6840 cell lines. The distinct expression pattern of PI3K/Akt pathway in glioblastoma cell lines may contribute to their phenotype and tumorigenicity. Since U-87 MG cells have been widely used for investigating the sensitivity of glioblastoma cells to kinase inhibitors, these cells were selected for this study [94, 290]. Compared with U-87 MG cells, U-373 MG cells showed different expression of p110 $\alpha$ , p110 $\beta$  and p85 $\alpha$ , as well as *TP53* status and the phosphorylation of Akt. These two cell lines to some extent reflect the heterogeneity of glioblastoma in the clinical, thus U-373 MG cells were employed as a supplementation.

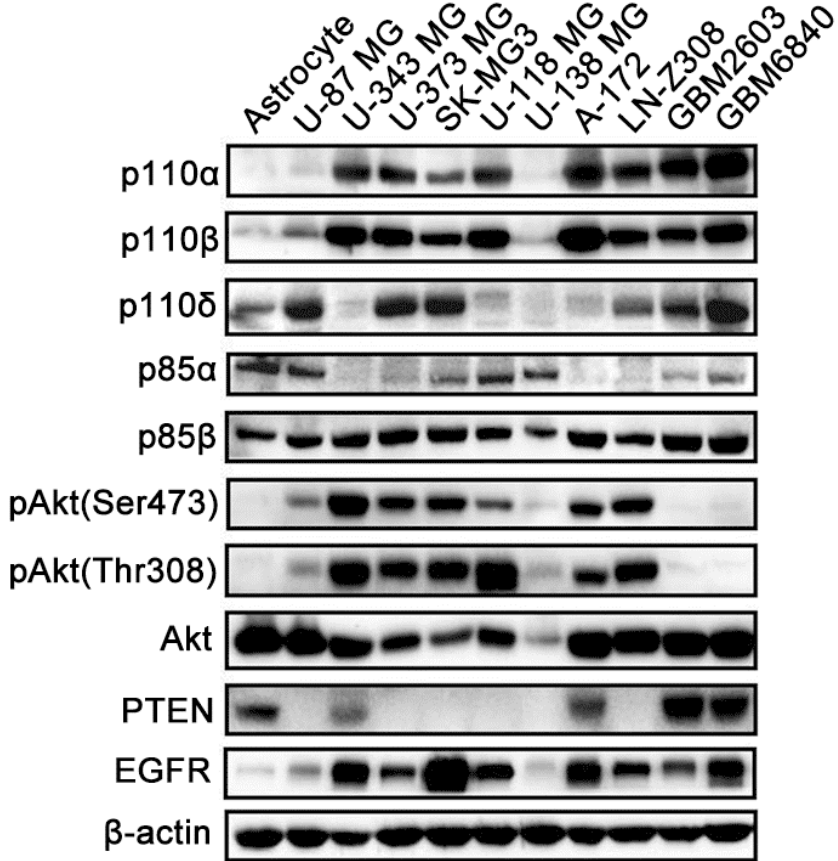


**Figure 3.1: Expression pattern of PI3K/Akt pathway molecules in human glioblastoma cell lines.** Normal astrocytes were used for comparison. The expression of β-actin was used as a loading control. GBM2603 and GBM6840 are two paediatric glioblastoma cell lines.

### **3.2 Effect of isoform-selective PI3K inhibitors on glioblastoma cell proliferation**

To investigate the divergent roles of class I<sub>A</sub> PI3K catalytic isoforms, selective inhibitors PIK-75, TGX-221 and CAL-101 against p110 $\alpha$ , p110 $\beta$  and p110 $\delta$  respectively were employed. The characteristics of these isoform-selective PI3K inhibitors is described in Table 2.2. U-87 MG and U-373 MG cells were incubated with PIK-75, TGX-221 and CAL-101 respectively at different concentrations for 48 hr. The p110 $\alpha$  inhibitor PIK-75 displayed a dose-dependent inhibitory effect on glioblastoma cell proliferation. Cell viability was reduced significantly upon PIK-75 treatment (0.0675  $\mu$ M), and greater inhibition was achieved with higher concentration (Figure 3.2A). In contrast, the p110 $\beta$  inhibitor TGX-221 did not show any significant inhibitory effect (Figure 3.2B). Compared with PIK-75, the p110 $\delta$  inhibitor CAL-101 also suppressed U-87 MG and U-373 MG cell proliferation in a dose-dependent manner but was less effective. Cell viability was significantly reduced when the concentration of CAL-101 reached 10  $\mu$ M or higher (Figure 3.2C). Compared with U-373 MG cells, U-87MG cells were more susceptible to the treatment of these three inhibitors. The IC<sub>50</sub> values of PIK-75, TGX-221 and CAL-101 against U-87 MG cells were 0.09  $\mu$ M, 484.82  $\mu$ M and 39.11  $\mu$ M respectively (Figure 3.2D). In summary, isoform-selective PI3K inhibitors PIK-75, TGX-221 and CAL-101 exerted distinct effects on glioblastoma cell proliferation.

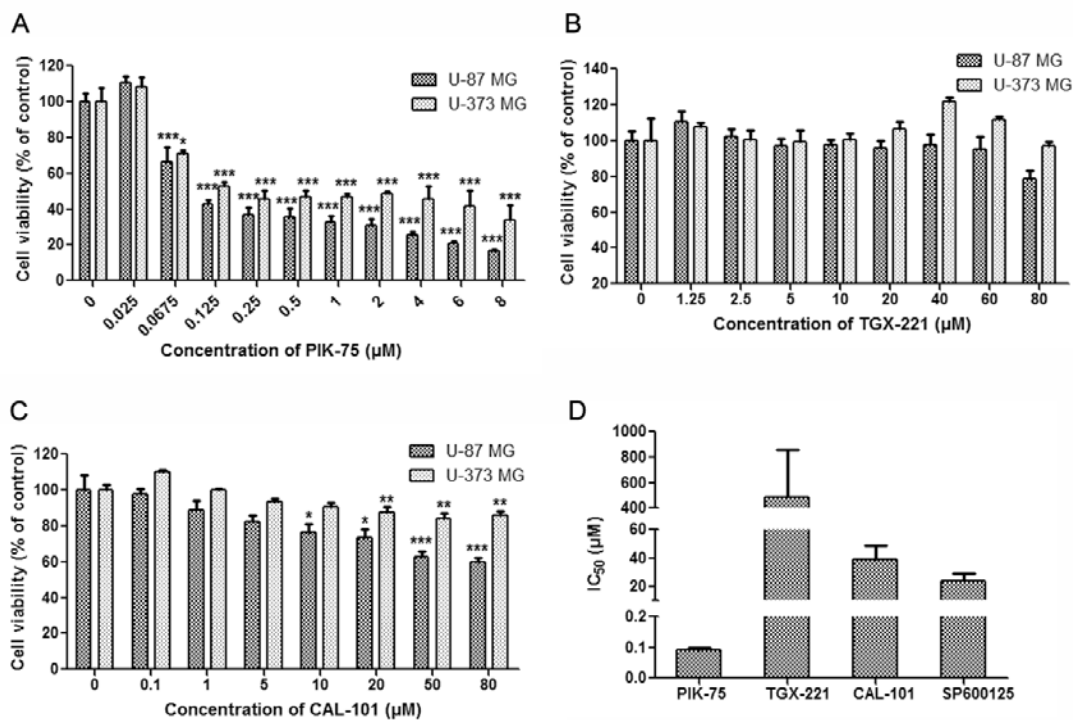


**Figure 3.2: Divergent effects of PIK-75, TGX-221 and CAL-101 on glioblastoma cell proliferation.** U-87 MG and U-373 MG cells were treated with PIK-75 (A), TGX-221 (B) or CAL-101 (C) at different concentrations for 48 hr. DMSO was used as a carrier control. Cell viability of U-87 MG and U-373 MG cells treated with PIK-75 and CAL-101 sharply decreased, whereas TGX-221 had no significant inhibitory effect (n=3; *p* values were determined by One-way ANOVA and Post Hoc multiple comparison Tukey HSD test. Comparison was performed between DMSO control and treatment groups. \*: *p* < 0.05; \*\*: *p* < 0.01; \*\*\*: *p* < 0.001). (D) IC<sub>50</sub> values of PIK-75, TGX-221 and CAL-101 against glioblastoma U-87 MG cells were determined using Origin 9.0 software.

The isoform-selective PI3K inhibitors may be toxic to normal tissues. Therefore, to investigate the cytotoxicities of these inhibitors, cell viability of normal astrocytes upon the treatment of PIK-75 (0.1  $\mu$ M), TGX-221 (20  $\mu$ M) or CAL-101 (10  $\mu$ M) from 24 to 96 hr was evaluated compared with U-87 MG and U-373 MG cells. Results showed that although cell viability of astrocytes was also inhibited by PIK-75, the toxicity was less on astrocytes than U-87 MG cells. (Figure 3.3A). No significant inhibitory effect on cell proliferation of astrocytes was observed in the treatment with TGX-221 or CAL-101. Compared with astrocytes, U-87 MG cells were more sensitive to TGX-221 and CAL-101 at 72-hr treatment (Figure 3.3B-C). The inhibitory effects of PIK-75, TGX-221 and CAL-101 on astrocytes were comparable to their effects on U-373 MG cells. In addition, the inhibitory effect of PIK-75, not TGX-221 and CAL-101, on glioblastoma cell proliferation is time-dependent (Figure 3.3).

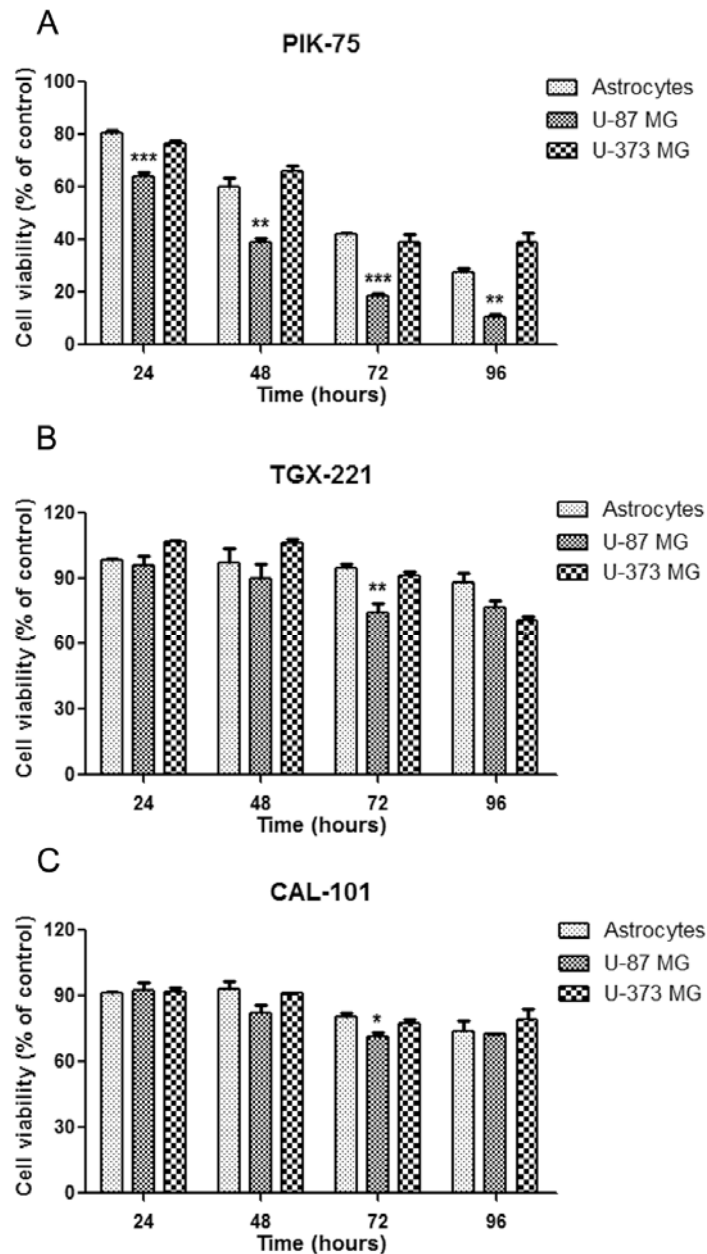


**Figure 3.3: Effects of isoform-selective PI3K inhibitors on cell proliferation in glioblastoma cells and normal human astrocytes.** U-87 MG, U-373 MG cells and human astrocytes were treated with PIK-75 (0.1  $\mu$ M), TGX-221 (20  $\mu$ M) or CAL-101 (10  $\mu$ M) for 24, 48, 72 and 96 hr respectively. DMSO was used as a carrier control. Compared with U-87 MG cells, astrocytes showed higher viabilities when treated with PIK-75 (n=3; *p* values were determined by Two-way ANOVA and Post Hoc multiple comparison Tukey HSD test. \*: *p* <0.05; \*\*: *p* <0.01; \*\*\*: *p* <0.001).

To investigate whether the effects of the isoform-selective PI3K inhibitors on glioblastoma cell proliferation was due to the suppression of Akt signaling, Akt phosphorylation level in U-87 MG cells upon treatment with PIK-75, TGX-221 and CAL-101 was determined. U-87 MG cells were treated with PIK-75, TGX-221 and CAL-101 at different concentrations for 3 hr and 24 hr respectively. The inhibitory effects of PIK-75, TGX-221 and CAL-101 on Akt phosphorylation at both Ser473 and Thr308 were dose-dependent. Treatment of PIK-75 ( $\geq 0.125 \mu\text{M}$ ), TGX-221 ( $\geq 5 \mu\text{M}$ ) and CAL-101 ( $\geq 0.5 \mu\text{M}$ ) inhibited the phosphorylation of Akt, and the phosphorylation level decreased as the concentration of inhibitors increased. Regardless of distinct effects of isoform-selective PI3K inhibitors on glioblastoma cell viability, Akt phosphorylation at both Ser473 and Thr308 were reduced after 3-hr and 24-hr treatments, indicating that these inhibitors may affect different downstream pathways of Akt to exert their different effects (Figure 3.4).

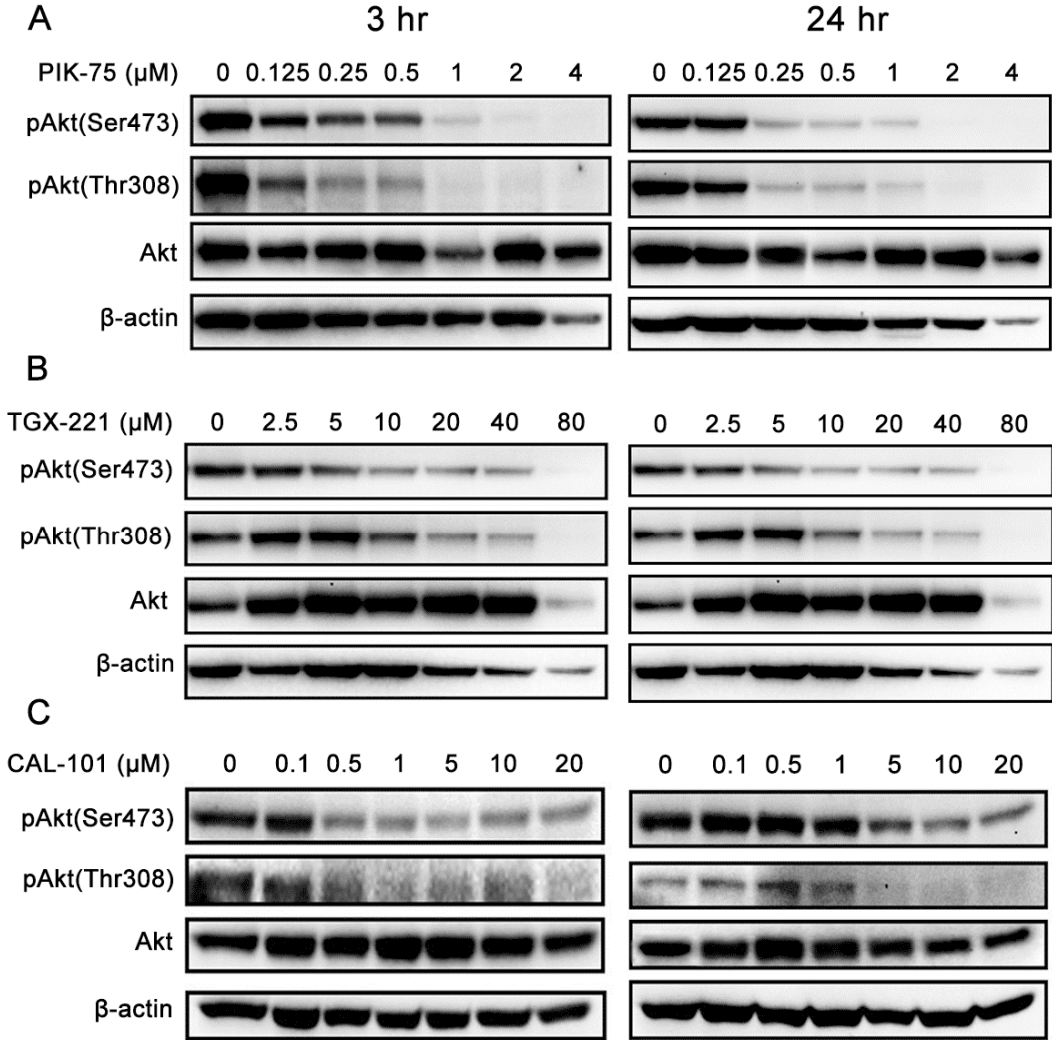


**Figure 3.4: Effects of isoform-selective PI3K inhibitors on Akt signaling in glioblastoma cells.** U-87 MG cells were treated with PIK-75, TGX-221, CAL-101 at different concentrations for 3 hr and 24 hr. DMSO was used as a carrier control. PIK-75, TGX-221 and CAL-101 dramatically inhibited Akt phosphorylation at both Ser473 and Thr308.

To investigate whether the inhibitory effect on Akt activation was time-dependent, CAL-101 was selected as the representative inhibitor. U-87 MG cells were incubated with CAL-101 at a final concentration of 1  $\mu$ M and 10  $\mu$ M for 1, 3, 6, 12, and 24 hr, respectively. CAL-101 (1  $\mu$ M) displayed inhibitory effect on Akt activation after incubation for 3 hr, whereas 10  $\mu$ M of CAL-101 strongly suppressed Akt activation from 1-hr to 24-hr incubation. Moreover, the inhibitory effect of CAL-101 became higher as time went by (Figure 3.5). These findings indicated that the inhibitory effect of CAL-101 on PI3K/Akt signaling was not only dose-dependent, but also time-dependent.

Due to the long duration of some cellular functional assays, it was necessary to determine if the isoform-selective inhibitors would lose their inhibitory effects. Therefore, U-87 MG cells were incubated with CAL-101 for 48 and 72 hr as well. Results revealed that CAL-101 (1  $\mu$ M and 10  $\mu$ M) suppressed Akt phosphorylation at Ser473 and Thr308 after incubation for 48 hr, whereas this inhibitory effect disappeared when incubation period was extended to 72 hr (Figure 3.6). This indicates that the duration of inhibitory effects was up to 48 hr only.

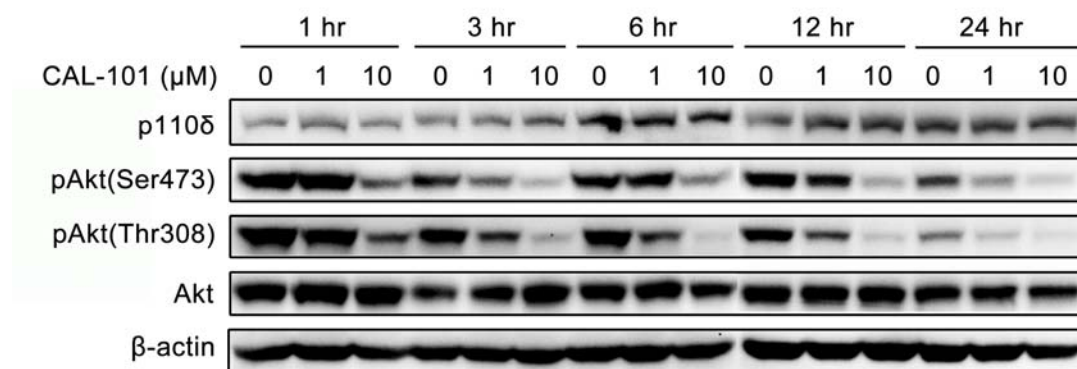


**Figure 3.5: Effect of CAL-101 on Akt signaling in glioblastoma cells at different time points.** U-87 MG cells were incubated with CAL-101 (1 μM and 10 μM) from 1 to 24 hr. Akt phosphorylation at Ser473 and Thr308 was inhibited by CAL-101 in a time-dependent manner. DMSO was used as a carrier control. The expression of β-actin was used as a loading control.

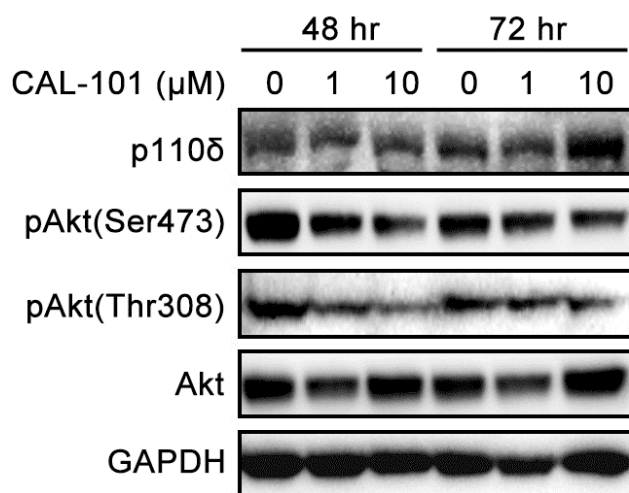


**Figure 3.6: Effect of CAL-101 on Akt signaling in glioblastoma cells after 48- and 72-hr incubation.** U-87 MG cells were incubated with CAL-101 (1  $\mu\text{M}$  and 10  $\mu\text{M}$ ) for 48 and 72 hr. Akt phosphorylation was inhibited by CAL-101 at 48 hr, whereas the inhibitory effect disappeared at 72 hr. DMSO was used as a carrier control. The expression of GAPDH was used as a loading control.

### **3.3 Inhibition of p110 $\alpha$ , p110 $\beta$ , or p110 $\delta$ suppresses glioblastoma migration**

Wound healing assay was performed to evaluate the effects of isoform-selective PI3K inhibitors on glioblastoma cell migration. U-87 MG cells were pretreated with mitomycin C prior to wound production to exclude the effect of cell proliferation. Results showed that mitomycin C at 5-10  $\mu\text{g}/\text{mL}$  effectively inhibited U-87 MG cell growth without decreasing the live cell number (Figure 3.7). Therefore, 5  $\mu\text{g}/\text{mL}$  was considered as the optimal concentration of mitomycin C to block glioblastoma cell proliferation. Cells were then treated with PIK-75 (0.1  $\mu\text{M}$ ), TGX-221 (20  $\mu\text{M}$ ) and CAL-101 (10  $\mu\text{M}$ ) after wound was generated since inhibitors at these concentrations were sufficient to inhibit Akt phosphorylation without inducing glioblastoma cell death. The migratory capacity of U-87 MG cells is presented as the number of cells migrating into the original wounds, since these cells were dispersedly distributed and it was difficult to measure the migration distance of cells. Inhibition of p110 $\alpha$ , p110 $\beta$  and p110 $\delta$  prevented U-87 MG cells migrating into the wound to different extent. The capacity of blocking migration is roughly ranked as followed: PIK-75 >TGX-221 >CAL-101 (Figure 3.8). Similar inhibitory effects were also observed in U-373 MG cells. However, due to the resistance of U-373 MG cells to these isoform-selective PI3K inhibitors, the inhibitory effect on migration was lower than those in U-87 MG cells (Figure 3.9).

Actin remodeling includes formation of lamellipodia and membrane ruffles, which are essential to cell migration. Therefore, the effect of isoform-selective PI3K

inhibitors on these parameters were assessed by labeling actin filaments after 3-hr drug treatment. Number of U-87 MG cells with lamellipodia and membrane ruffles was significantly decreased after treatment with isoform-selective PI3K inhibitors (Figure 3.10). Interestingly, TGX-221 displayed higher inhibitory effect on membrane ruffles formation than PIK-75 and CAL-110, whereas lamellipodia formation was most significantly impaired by PIK-75, suggesting that p110 $\beta$  may be required for membrane ruffles formation, while p110 $\alpha$  is essential to lamellipodia formation (Figure 3.10E-F).

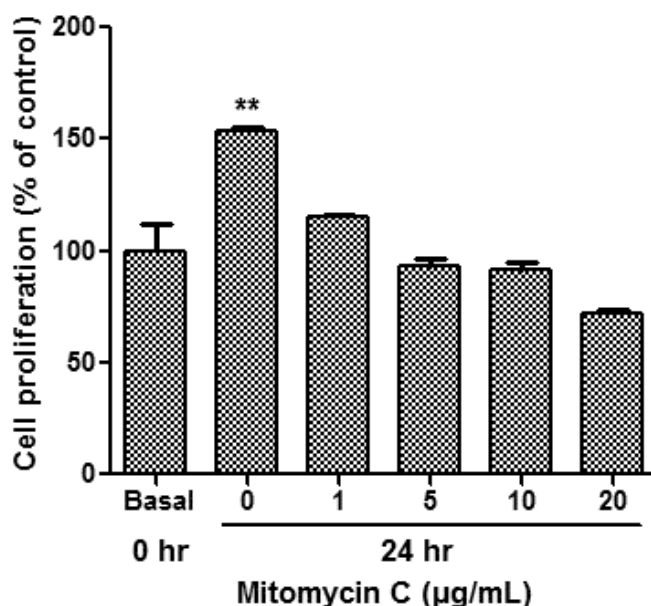


**Figure 3.7: Glioblastoma cell proliferation was inhibited by mitomycin C.**

Number of viable U-87 MG cells was counted using Vi-Cell Cell Viability Analyzer (Beckman Coulter) before and after treatment of mitomycin C for 24 hr. Cell proliferation was inhibited by mitomycin C at 5 or 10 µg/mL without impairing cell viability. MEM medium supplemented with 10% FBS was used as a negative control. (n=3; *p* values were determined by One-way ANOVA and Post Hoc multiple comparison Tukey HSD test. \*\*: *p* <0.01)

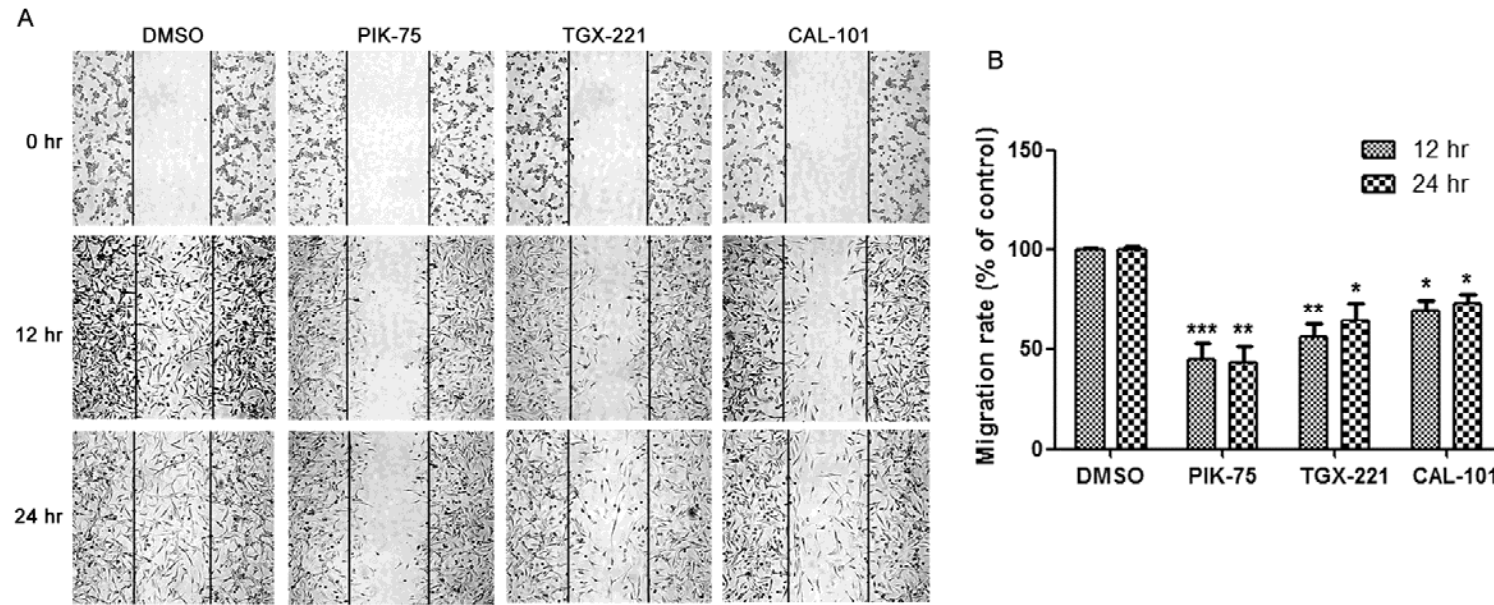


**Figure 3.8: Inhibitory effect of isoform-selective PI3K inhibitors on migration in U-87 MG glioblastoma cells.** (A) Wound healing in U-87 MG cells treated with PIK-75 (0.1  $\mu$ M), TGX-221 (20  $\mu$ M) or CAL-101 (10  $\mu$ M) for 12 and 24 hr. Cells were pretreated with 5  $\mu$ g/mL of mitomycin C for 1 hr. The lines indicate the edges of wounds generated before drug treatment (0 hr). Photographs were obtained at 50 $\times$  magnification. (B) Migration rate (%) was analyzed and expressed as the number of cells migrating into the original wounds relative to those in DMSO control. (n=3; *p* values were determined by One-way ANOVA and Post Hoc multiple comparison Tukey HSD test. \*: *p* <0.05; \*\*: *p* <0.01; \*\*\*: *p* <0.001).

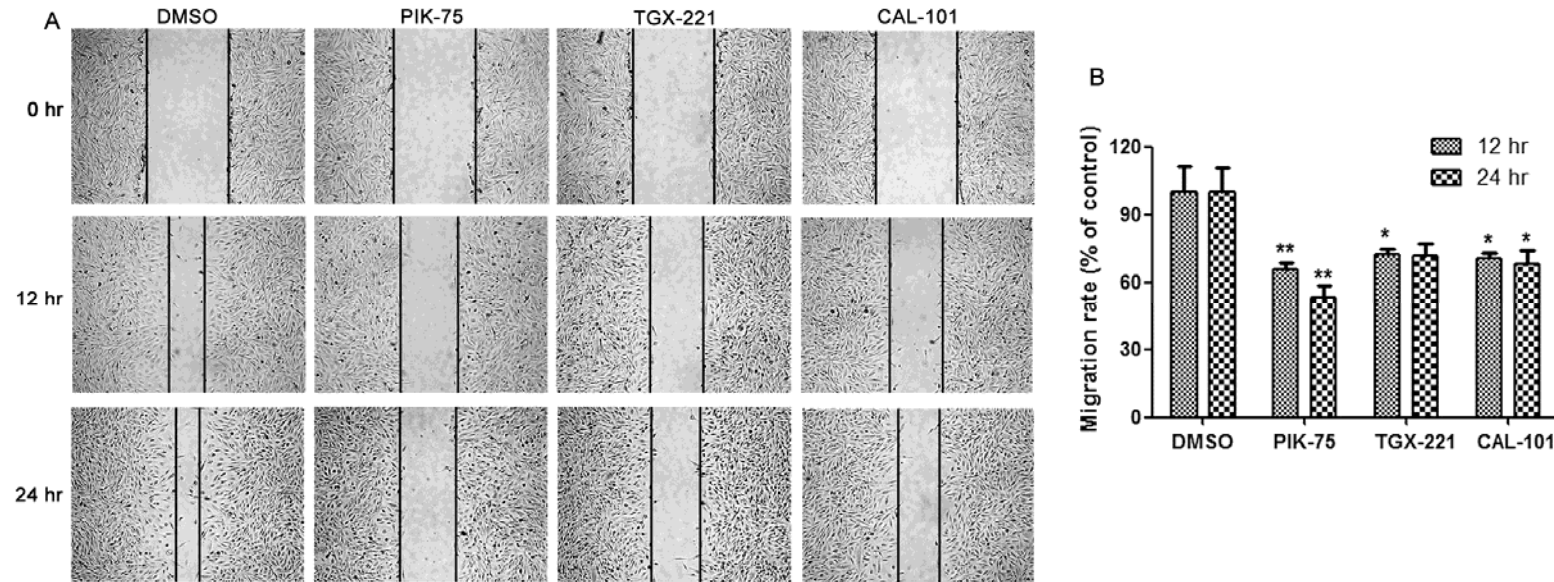


**Figure 3.9: Inhibitory effect of isoform-selective PI3K inhibitors on migration in U-373 MG glioblastoma cells.** (A) Wound healing in U-373 MG cells treated with PIK-75 (0.1  $\mu$ M), TGX-221 (20  $\mu$ M) or CAL-101 (10  $\mu$ M) for 12 and 24 hr. Cells were pretreated with 5  $\mu$ g/mL of mitomycin C for 1 hr. The lines indicate the edges of wounds generated before drug treatment (0 hr) or after 12-hr or 24-hr treatment. Photographs were obtained at 50 $\times$  magnification. (B) Wound healing distance (%) was analyzed and expressed as the migration distance of cells relative to that of DMSO control. (n=4; *p* values were determined by One-way ANOVA and Post Hoc multiple comparison Tukey HSD test. \*: *p* < 0.05; \*\*: *p* < 0.01).

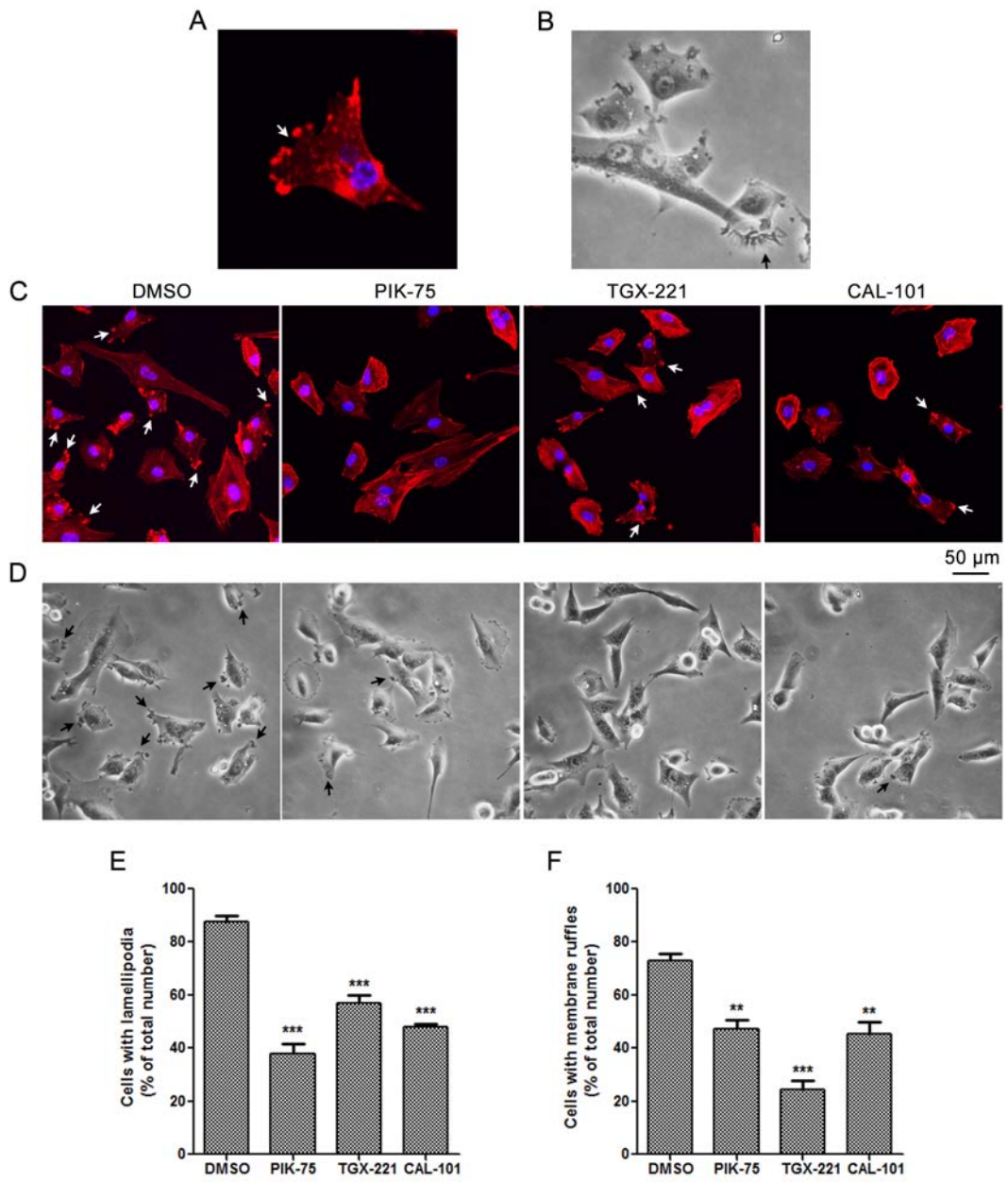


**Figure 3.10: Inhibitory effects of isoform-selective PI3K inhibitors on lamellipodia and membrane ruffles formation in glioblastoma cells. (A-B)**

Representative cells showing the lamellipodium (white arrow) and membrane ruffle (black arrow). (C) U-87 MG cells were stained with Alexa Fluor 594-conjugated phalloidin (red) upon treatment with PIK-75 (0.1  $\mu$ M), TGX-221 (20  $\mu$ M) or CAL-101 (10  $\mu$ M) for 3 hr. Lamellipodia formation was blocked by inhibition of p110 $\alpha$ , p110 $\beta$  or p110 $\delta$ . Bar = 50  $\mu$ m. (D) Phase contrast microscopy showing membrane ruffles were reduced by the treatment of isoform-selective PI3K inhibitors. Photographs were obtained at 200 $\times$  magnification. (E) Cells with lamellipodia were counted and data were expressed as the ratio of number of cells with lamellipodia over total cell number. (F) Cells with membrane ruffles were counted and data were expressed as the ratio of number of cells with membrane ruffles over total cell number. (n=3; *p* values were determined by One-way ANOVA and Post Hoc multiple comparison Tukey HSD test. \*\*: *p* <0.01; \*\*\*: *p* <0.001)

### **3.4 Inhibition of p110 $\alpha$ is sufficient to inhibit glioblastoma cell invasion**

To analyze the effects of isoform-selective PI3K inhibitors on glioblastoma cell invasion, Boyden chamber invasion assay was performed on U-87 MG cells. Cells were seeded onto Matrigel-coated invasion chamber and then treated with PIK-75 (0.1  $\mu$ M), TGX-221 (20  $\mu$ M) or CAL-101 (10  $\mu$ M) for 24 hr. Number of invasive cells was markedly decreased by PIK-75, whereas neither TGX-221 nor CAL-101 inhibited glioblastoma cell invasion (Figure 3.11).

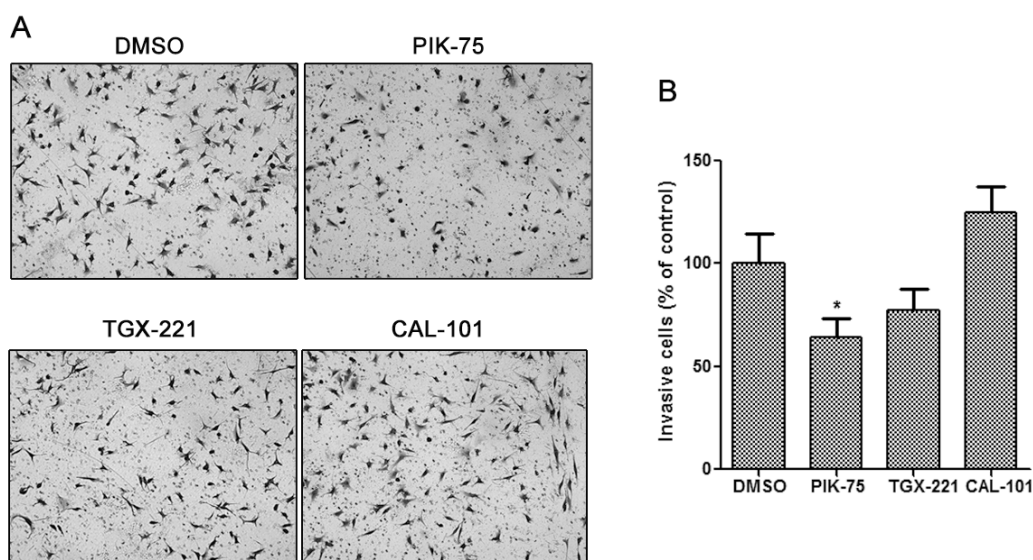


**Figure 3.11: Inhibition of p110 $\alpha$  blocked glioblastoma cell invasion.** Boyden chamber invasion assay against U-87 MG cells treated with PIK-75 (0.1  $\mu$ M), TGX-221 (20  $\mu$ M) or CAL-101 (10  $\mu$ M) for 24 hr. (A) Representative photographs showing the invasive cells that had passed through matrigel to the lower surface of the membrane at 100 $\times$  magnification. Invaded cells from 5 representative fields were counted. (B) Number of invaded cells was significantly decreased by PIK-75 (n=3; *p* values were determined by One-way ANOVA and Post Hoc multiple comparison Tukey HSD test. \*: *p* <0.05).

### **3.5 Knockdown of p110 $\delta$ shows distinct effect on Akt signaling and invasion in glioblastoma cells**

The roles of p110 $\alpha$  and p110 $\beta$  in glioblastoma have been well studied. However, the role of p110 $\delta$  and its interaction with p110 $\alpha$  and p110 $\beta$  are not fully understood. To investigate these, target-specific siRNAs against *PIK3CD* (siPIK3CD\_1, siPIK3CD\_2, siPIK3CD\_5, and siPIK3CD\_6) were employed and their sequences are shown in Table 2.7. Prior to the siRNA-induced gene knockdown experiment, the transfection efficiency was evaluated to obtain the most optimized ratio between siRNA duplexes and transfection reagent. The AllStars Hs Cell Death Control siRNA duplexes were mixed with Lipofectamine 2000 transfection reagent at a ratio of 100:5, 100:3, 100:1.5 or 50:1.5 (pmol: $\mu$ L). U-87 MG cells were incubated with the mixture for 48 hr at 37°C. Since the AllStars Hs Cell Death Control siRNA duplexes target several genes which are essential to cell survival, the higher the transfection efficiency, more cell death will be triggered. Results demonstrated that when the ratio between cell death control siRNA duplexes and Lipofectamine 2000 was 100 pmol : 5  $\mu$ L, the transfection achieved the highest efficiency (Figure 3.12).

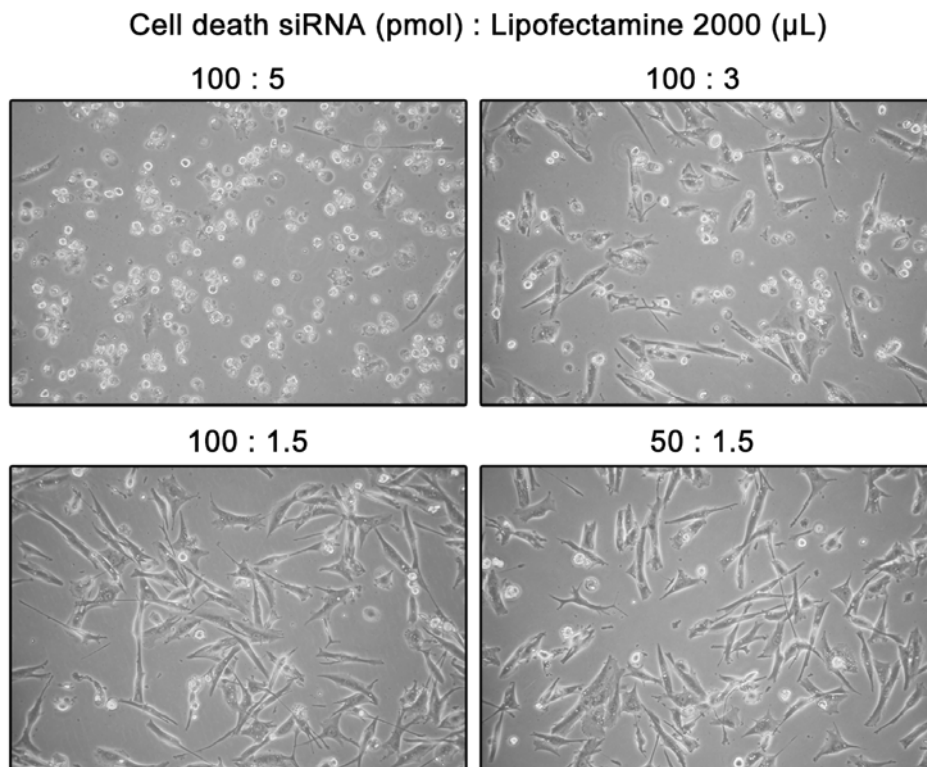


**Figure 3.12: Optimization of siRNA transfection efficiency.** The AllStars Hs Cell Death Control siRNA duplexes were mixed with Lipofectamine 2000 transfection reagent at a series of ratios. U-87 MG cells were incubated with the mixture for 48 hr at 37°C. Photographs were obtained at 100 $\times$  magnification. The transfection efficiency was higher as cells displayed higher cytotoxicity after 48-hr incubation.

To observe the effect of *PIK3CD* knockdown on PI3K/Akt signaling pathway in glioblastoma cells, U-87 MG cells were transfected with four siRNA duplexes against *PIK3CD*. Results showed that all four siPIK3CD duplexes were able to significantly decrease the protein and mRNA expression levels of *PIK3CD* (Figure 3.13A). Compared with the scramble siRNA transfection, the relative mRNA expression of *PIK3CD* was decreased to 0.28, 0.19, 0.21 and 0.19 by siPIK3CD\_1, siPIK3CD\_2, siPIK3CD\_5, and siPIK3CD\_6 respectively (Figure 3.13A, top panel). Subsequently, siPIK3CD\_2 and siPIK3CD\_6 with the highest knock-down efficiency were selected for the following studies. To evaluate the off-target effect of siPIK3CDs and their effects on Akt signaling, the expression of p110 $\alpha$  and p110 $\beta$  was measured. Compared with the scramble siRNA transfection, the transfection of siPIK3CD\_2 and siPIK3CD\_6 did not affect the expression of p110 $\alpha$ , p110 $\beta$  and Akt. Also, the phosphorylation level of Akt did not significantly change, which was distinct from the treatment of p110 $\delta$  inhibitor (Figure 3.13B).

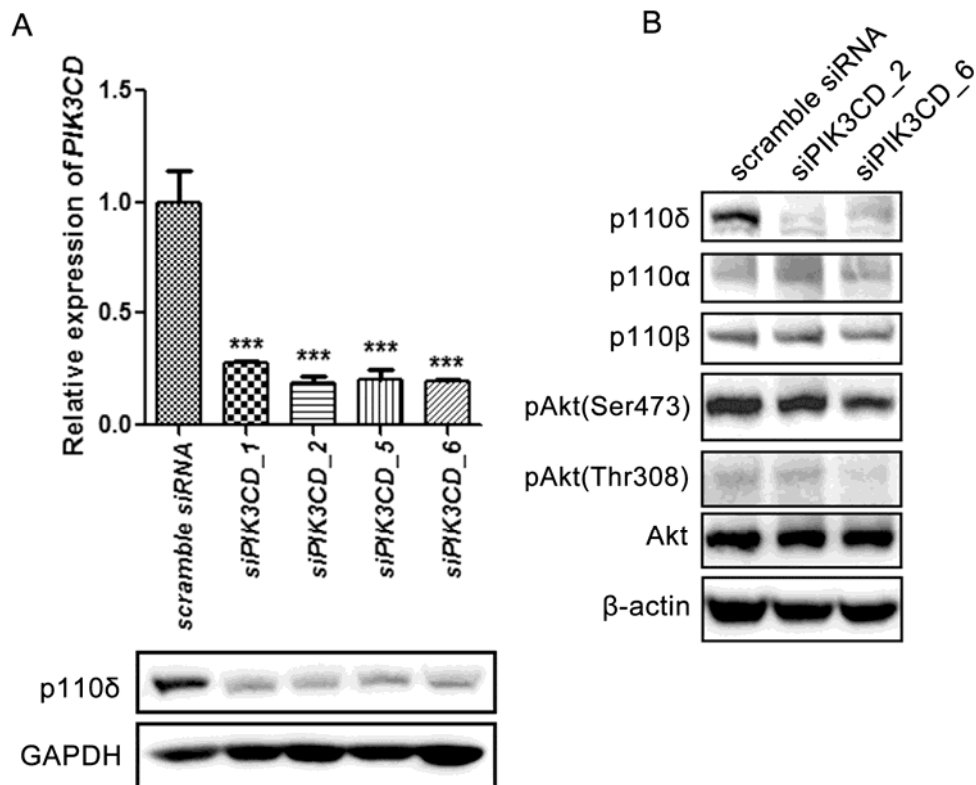


**Figure 3.13: Knockdown of *PIK3CD* in glioblastoma cells.** U-87 MG cells were incubated with the mixture of siRNA (100 pmol) and Lipofectamine 2000 (5  $\mu$ L) for 48 hr. The AllStars Negative Control siRNA duplexes were denoted as “scramble siRNA” and used as a negative control. (A) The mRNA and protein expression of p110 $\delta$  was decreased by siPIK3CD. The *GAPDH* mRNA was used a control to normalize the mRNA expression of *PIK3CD*. The protein expression of GAPDH was used as a loading control. (n=3. *p* values were determined by One-way ANOVA and Post Hoc multiple comparison Tukey HSD test. \*\*\*: *p* <0.001). (B) siPIK3CD\_2 and siPIK3CD\_6 were selected to observe their effects on Akt signaling. The expression of  $\beta$ -actin was used as a loading control.

We had observed the divergent effects between p110 $\delta$  inhibitor and *PIK3CD* gene knockdown on Akt signaling. However, it is not clear whether these two treatments also have distinct effects on glioblastoma cell proliferation, migration and invasion. Therefore, U-87 MG cells were transfected with siPIK3CD\_2 and siPIK3CD\_6 duplexes. After a 48-hr incubation, cells were trypsinized and used for cell proliferation, wound healing and invasion assays. Results showed that glioblastoma cell proliferation was significantly inhibited by siPIK3CD\_2 and siPIK3CD\_6. The inhibitory effect of siPIK3CDs on glioblastoma cell proliferation is time-dependent (Figure 3.14). In addition, cell migration was also suppressed by siPIK3CD\_2 and siPIK3CD\_6, whereas cell invasion was only blocked by siPIK3CD\_2 (Figure 3.15).

To investigate the mechanism of *PIK3CD* knockdown on glioblastoma cell migration and invasion, the mRNA expression levels of focal adhesion-related genes were measured. The mRNA expression levels of *P130Cas* and *ITGB3* were downregulated by siPIK3CD\_2 and siPIK3CD\_6, while the mRNA expression of *ITGB1* was not significantly affected, indicating that knockdown of *PIK3CD* may suppress glioblastoma cell migration via inhibition of p130Cas and integrin  $\beta$ 3 (Figure 3.16). Interestingly, the mRNA expression level of *ADAMTS1* was increased by siPIK3CD\_2, but it was decreased by siPIK3CD\_6, suggesting that it may be the reason why siPIK3CD\_2 but not siPIK3CD\_6 had inhibitory effect on glioblastoma cell invasion (Figure 3.16).

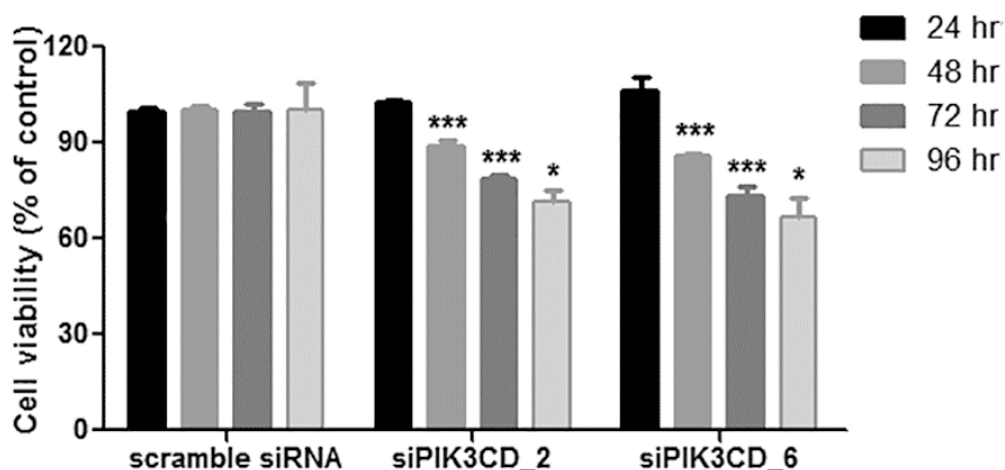


**Figure 3.14: Effect of *PIK3CD* gene knockdown on glioblastoma cell proliferation.** U-87 MG cells were transfected with siPIK3CD\_2 and siPIK3CD\_6 duplexes and then incubated for 48 hr. The AllStars Negative Control siRNA duplexes were denoted as “scramble siRNA” and used as a negative control. Cells were then seeded onto 96-well plates to perform cell proliferation assay. Cells were incubated in  $\alpha$ -MEM medium supplemented with 10% FBS for additional 24, 48, 72 and 96 hr. ( $n=3$ ;  $p$  values were determined by Two-way ANOVA and Post Hoc multiple comparison Tukey HSD test. \*:  $p < 0.05$ ; \*\*\*:  $p < 0.001$ ).

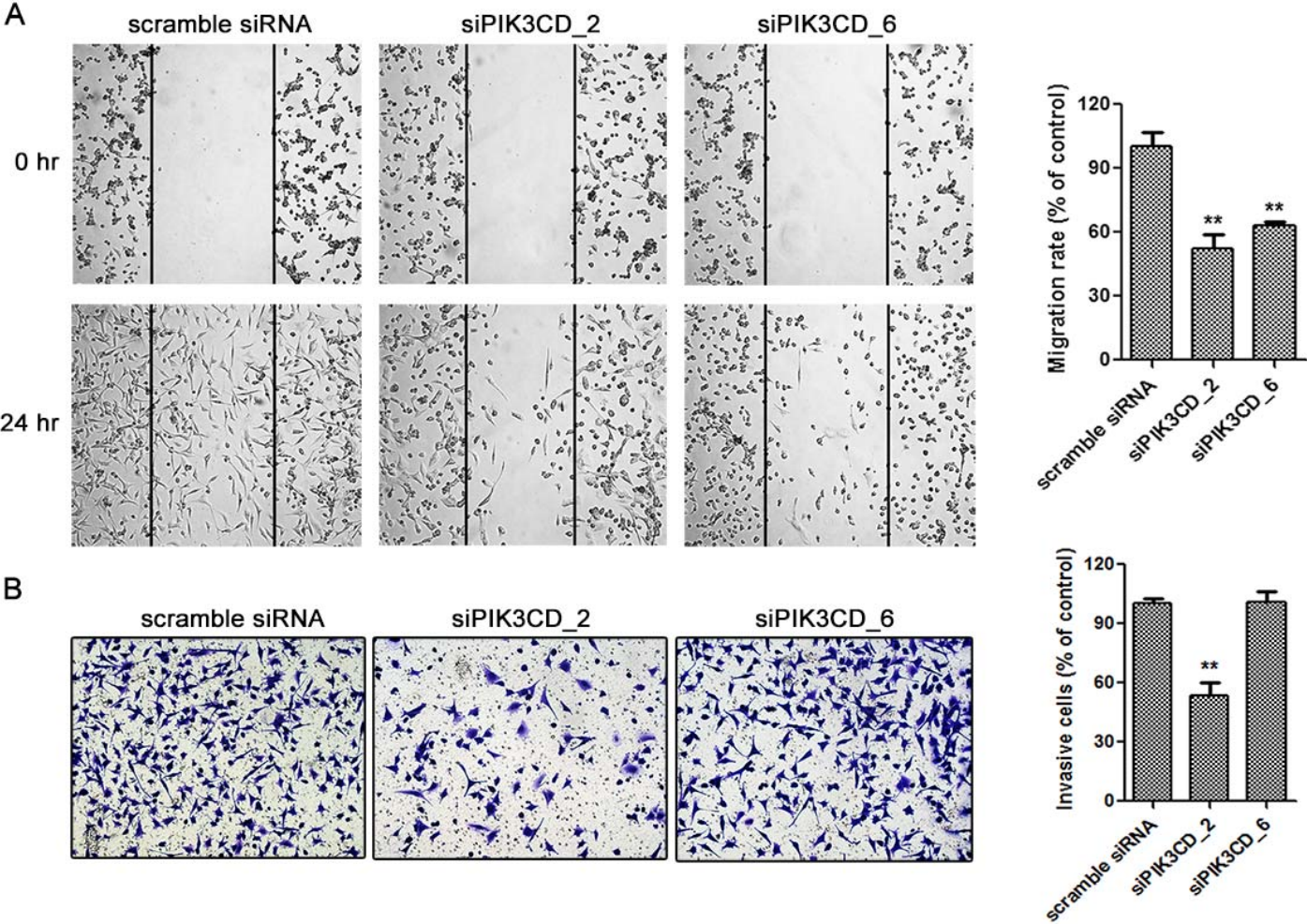


**Figure 3.15: Effect of *PIK3CD* gene knockdown on glioblastoma cell migration and invasion.** U-87 MG cells were transfected with siPIK3CD\_2 and siPIK3CD\_6 duplexes and incubated for 48 hr. The AllStars Negative Control siRNA duplexes were denoted as “scramble siRNA” and used as a negative control. (A) Cells were treated with 5  $\mu\text{g}/\text{mL}$  of mitomycin C for 1 hr and then used for wound healing assay. The lines indicate the edges of wounds generated before drug treatment (0 hr). Photographs were obtained at 50 $\times$  magnification. Migration rate (%) was analyzed and expressed as the number of cells migrating into the original wounds relative to those in DMSO control. (B) Cells were used for Boyden chamber invasion assay. Representative photographs showing the invasive cells that had passed through matrigel to the lower surface of the membrane at 100 $\times$  magnification. Invaded cells from 5 representative fields were counted. ( $n=3$ ;  $p$  values were determined by One-way ANOVA and Post Hoc multiple comparison Tukey HSD test. \*\*:  $p < 0.01$ ).

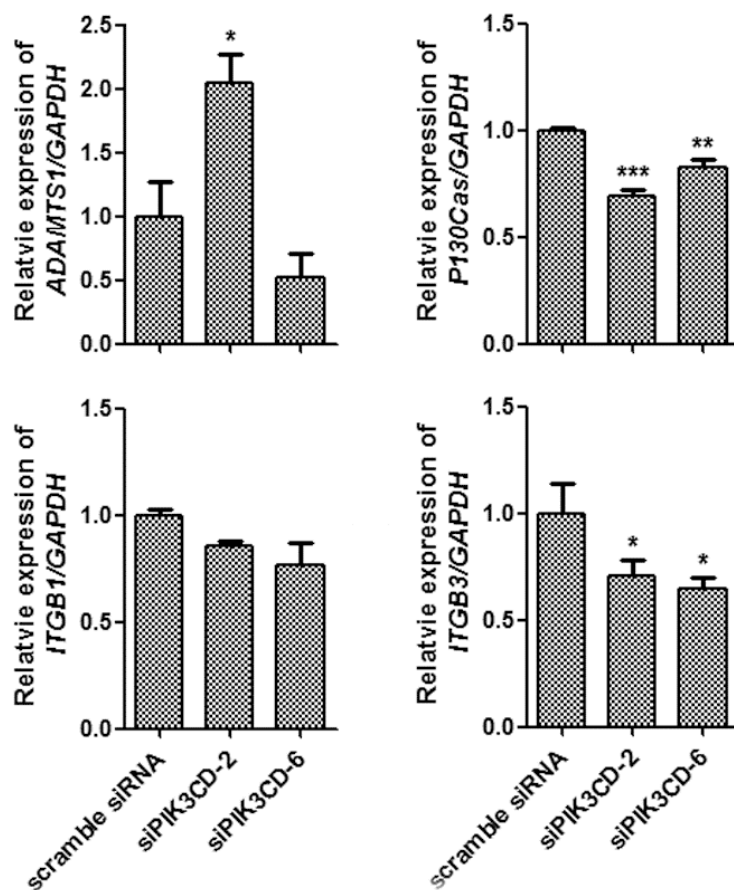


**Figure 3.16:** The siRNA duplexes against *PIK3CD* influenced the expression of *ADAMTS1*, *P130Cas*, *ITGB1*, and *ITGB3*. U-87 MG cells were transfected with siPIK3CD duplexes and incubated for 48 hr. The AllStars Negative Control siRNA duplexes were denoted as “scramble siRNA” and used as a negative control. SYBR Green qRT-PCR was performed to evaluate the effects of siPIK3CD\_2 and siPIK3CD\_6 on the mRNA expression of *ADAMTS1*, *P130Cas*, *ITGB1* and *ITGB3*. Human GAPDH mRNA was served as an internal control for RNA normalization. (n=3. *p* values were determined by One-way ANOVA and Post Hoc multiple comparison Tukey HSD test. \*: *p* < 0.05; \*\*: *p* < 0.01; \*\*\*: *p* < 0.001).

### 3.6 Discussion

#### 3.6.2 Distinct expression pattern of PI3K/Akt pathway molecules in glioblastoma cells

The expression pattern of PI3K/Akt pathway molecules varied greatly among different glioblastoma cell lines. EGFR was overexpressed in 8 out of 10 glioblastoma cell lines, compared with the expression in astrocytes. Evidence reveals that it is frequently amplified or overexpressed in primary glioblastoma [5]. Overexpression of EGFR is associated with the elevated PI3K activity, leading to the activation of Akt signaling. Mutation and loss of *PTEN* are frequently found in primary glioblastoma (15%-40%) [291]. Since most of *PTEN* mutations in cell lines are splicing variant, deletion or frame shift (Table 2.1), it is not surprised that its expression was not detected in the most of the cell lines investigated in this study. However, two paediatric glioblastoma cell lines expressed wild-type PTEN, leading to inactivation of Akt, since *PTEN* mutation is rare in paediatric glioblastoma and only one allele of *PTEN* is mutated in GBM6840 cells [143, 285]. PTEN was also detected in U-343 MG cells because its mutation in these cells is point mutation including substitution or missense, which resulted in TGT(Cys) turning to TCT(Ser) [284].

Besides, the expression of p110 $\alpha$  and p110 $\delta$  was different between glioblastoma cell lines. The distinct expression pattern of PI3K/Akt pathway molecules may contribute to the activation of Akt and downstream signaling pathways in different manners, and lead to the various phenotypes and tumorigenicity. Due to their

ubiquitous expression, p110 $\alpha$  and p110 $\beta$  may play dominant roles in Akt activation. Studies find that p110 $\delta$  is overexpressed in some solid tumors including glioblastoma [104, 105], neuroblastoma [106], breast [107] and prostate cancer [108]. We also observed high expression level of p110 $\delta$  in several glioblastoma cell lines. However, even though p110 $\delta$  expression was high in U-87 MG cells, the low expression of p110 $\alpha$  and p110 $\beta$  led to the low phosphorylation of Akt, suggesting that p110 $\delta$  has a lower lipid kinase activity.

### **3.6.3 The p110 $\alpha$ isoform plays a more crucial role in glioblastoma than p110 $\beta$ and p110 $\delta$**

To investigate the roles of class I<sub>A</sub> PI3K catalytic isoforms in glioblastoma cells, three selective inhibitors PIK-75, TGX-221 and CAL-101 were employed, which selectively targets p110 $\alpha$ , p110 $\beta$  and p110 $\delta$  respectively. These PI3K isoforms played distinct roles in glioblastoma cell proliferation, migration and invasion. Although these inhibitors all inhibited Akt phosphorylation at both Ser473 and Thr308, they may affect divergent downstream pathways. Inhibition of p110 $\alpha$  was sufficient to suppress glioblastoma cell viability, migration and invasion, whereas inhibition of p110 $\beta$  only blocked cell migration, and inhibition of p110 $\delta$  moderately impeded cell proliferation and migration. Similar findings also show that inhibition of p110 $\alpha$  suppresses proliferation and migration in glioblastoma cells, whereas inhibition of p110 $\beta$  impedes migration but not affects cell proliferation [292]. Thus, p110 $\alpha$  is of

more importance to glioblastoma cell viability and motility than p110 $\beta$  and p110 $\delta$ .

Accumulating evidence shows that the p110 isoforms exert distinct roles in Akt phosphorylation and other pathological processes [293, 294]. The p110 $\alpha$  and p110 $\beta$  isoforms display different preferences to RTK activation, and p110 $\beta$  is also activated by GPCRs [66, 295]. Gene silencing and isoform-selective inhibitors are helpful to investigate the individual role of class I<sub>A</sub> PI3K catalytic subunits. The p110 $\alpha$  isoform is required for tumor cell proliferation, migration and invasion, whereas p110 $\beta$  is essential to cell survival and tumorigenesis [64, 90-92]. Knockdown of *PIK3CA* significantly inhibits cell viability and motility in medulloblastoma and glioblastoma cells [90, 91]. The p110 $\alpha$  isoform is also vital to invasion of breast cancer cells through mediating invadopodia formation [93]. In addition, tumor cell growth is effectively suppressed *in vitro* and *in vivo* by using the p110 $\alpha$  isoform-selective inhibitors A66, BYL719 or PIK-75, while apoptosis and cell cycle arrest are promoted [94-97]. Knockdown of *PIK3CB* suppresses cell proliferation and induces apoptosis in ovarian cancer and glioblastoma *in vitro* and *in vivo*, suggesting p110 $\beta$  plays important roles in cell growth [92, 98]. However, selective p110 $\beta$  inhibitor TGX-221 does not affect cell proliferation or apoptosis, but impedes migration in glioblastoma cells [292]. Similar findings were also observed in this study. Our previous study shows that knockdown of *PIK3CB* barely suppresses glioblastoma cell migration, which is different from the selective inhibitor TGX-221 [104]. Distinct outcomes between the selective inhibitor and gene knockout may be caused by kinase-independent function of p110 $\beta$  or compensatory effect of other kinases [296,

297]. Effect of *PIK3CB* knockout or knockdown on cell migration may be compensated by other p110 isoforms such as p110 $\alpha$ , leading to the unaffected migratory capacity. Besides, mice with kinase-dead mutant of p110 $\beta$  are capable to survive to adulthood, while ablation of p110 $\beta$  leads to embryonic lethality, indicating p110 $\beta$  has kinase-independent functions [298, 299]. Therefore, even though the kinase activity of p110 $\beta$  is decreased, its kinase-independent function still exist to maintain some phenotypes such as proliferation.

Targeting p110 $\delta$  suppresses cell growth, migration and invasion in neuroblastoma and glioblastoma cells [104, 106]. Our previous study shows that knockdown of *PIK3CD* blocks glioblastoma cell migration and invasion, whereas a selective p110 $\delta$  inhibitor IC87114 only suppresses cell migration without affecting the invasive capacity [104]. In this study, similar results were also found in glioblastoma cells using two siRNAs with difference sequences targeting *PIK3CD* and the inhibitor CAL-101 with higher selectivity for p110 $\delta$ . This suggests that p110 $\delta$  also has a kinase-independent function on invasion.

Taken together, p110 $\alpha$  is most essential among three class I<sub>A</sub> PI3K catalytic isoforms, which may be due to its predominant role in RTK-mediated Akt signaling. In contrast, inhibition of p110 $\beta$  and p110 $\delta$  exerts minor influence on cellular functions of glioblastoma cells, which may be limited by the constitutive activation of p110 $\alpha$  [300].

### 3.6.4 The p110 $\delta$ isoform may compete with p110 $\alpha$ and p110 $\beta$ for RTK binding

Although the p110 $\alpha$  isoform plays a dominant role in the activation of PI3K/Akt signaling, it is hypothesized that p110 $\beta$  modulates PI3K activity in a competitive manner by competing against p110 $\alpha$  for RTK binding [301]. In this competition model, p110 $\alpha$  and p110 $\beta$  with high and low lipid kinase activities respectively competes with each other for binding to RTKs. Ablation of p110 $\alpha$  liberates binding sites for occupancy of p110 $\beta$  with low lipid kinase activity, leading to attenuated PI3K activity and Akt activation. On the contrary, knockout of p110 $\beta$  causes the compensatory effect of p110 $\alpha$ , and more active p110 $\alpha$  binds to RTKs, resulting in elevated PI3K activity and Akt activation (Figure 3.17A). If the p110 $\beta$  activity is inhibited by a selective inhibitor, inactive p110 $\beta$  still occupies the binding sites of RTKs, thus suppresses PI3K activity and Akt activation (Figure 3.17B). This model is supported by the evidence that genetic deletion of *PI3KCA* suppresses tumor formation in breast cancer, whereas loss of *PIK3CB* leads to mammary gland hyperplasia and tumorigenesis, accompanied by increased PI3K activity and Akt phosphorylation level [301]. In addition, overexpression of p110 $\beta$  blocks the EGF-induced migration in breast cancer cells, suggesting abundant p110 $\beta$  may replace p110 $\alpha$  in interacting with EGFR and results in decreased active p110 $\alpha$  [302].

Similarly, we observed that the phosphorylation of Akt at Ser473 and Thr308 was not downregulated by siPIK3CDs, whereas the p110 $\delta$ -selective inhibitor CAL-101 significantly inhibited Akt phosphorylation. We hypothesized that p110 $\delta$

may also be involved in this competition model and compete with p110 $\alpha$  and p110 $\beta$  to fine-tune PI3K activity. Therefore, knockdown of p110 $\delta$  may cause an increased or unaffected Akt phosphorylation level, compensated by more active p110 $\alpha$  and p110 $\beta$  binding to RTKs. Inhibition of p110 $\delta$  by CAL-101 suppressed Akt phosphorylation, because inactive p110 $\delta$  still occupies the RTK binding sites. Supporting evidence comes from the findings that silencing *PIK3CD* doesn't affect Akt phosphorylation in neuroblastoma cells [106].

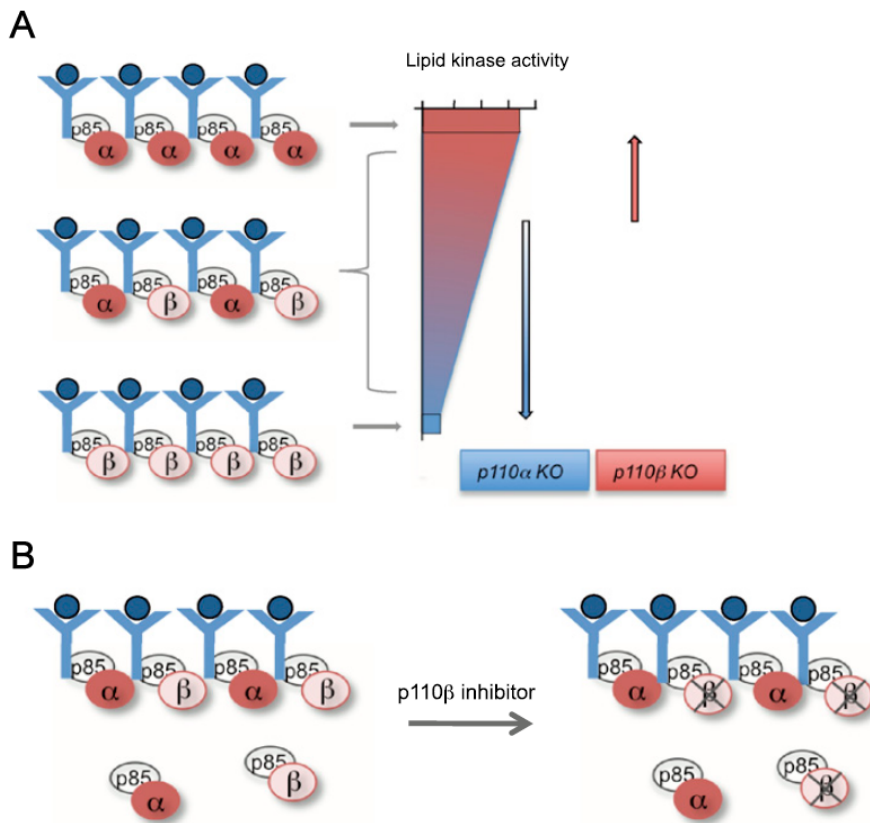


**Figure 3.17: Schematic diagram demonstrating a competition model of p110 $\alpha$  and p110 $\beta$  against RTK-binding sites [301].** In this competition model, p110 $\alpha$  and p110 $\beta$  are two PI3K isoforms with high and low lipid kinase activities, respectively. (A) Deletion of p110 $\alpha$  is expected to markedly decrease PI3K activity, whereas knockout of p110 $\beta$  releases the RTK-binding sites for more active p110 $\alpha$ , leading to increased PI3K activity and activation of Akt signaling. (B) In the presence of a selective p110 $\beta$  inhibitor, p110 $\beta$  still occupies the binding sites on receptors, consequently blocking p110 $\alpha$  binding and decreasing PI3K activity.

### 3.6.5 Knockdown of *PIK3CD* inhibits glioblastoma cell migration and invasion

Although both the p110 $\delta$  inhibitor and *PIK3CD* gene knockdown were able to impeded glioblastoma cell proliferation and migration, they displayed distinct effect on cell invasion, which may be induced by the kinase-independent function of p110 $\delta$ . Knockdown of *PIK3CD* failed to inhibit Akt phosphorylation, likely due to the compensation of p110 $\alpha$  or p110 $\beta$ , but it suppressed glioblastoma cell motility through mediating mRNA expression levels of integrin  $\beta$ 3, p130Cas and ADAMTS1. This suggests that p110 $\delta$  may exert its role in a p110 $\alpha$ - or p110 $\beta$ -independent manner, which is supported by the findings that the activation mechanism between p110 $\alpha$  and p110 $\delta$  mediated by the p85 regulatory subunit is different [68].

Integrins are transmembrane receptors that serve as bridges between cellular actin cytoskeleton and extracellular matrix (ECM) during cell adhesion, migration and invasion. Integrin interacts with intracellular adhesion molecules such as talin, paxillin,  $\alpha$ -actinin and vinculin, thereby plays a crucial role in actin reassembly, focal adhesion and migration [303]. It is also involved in cell invasion though linking to MMPs and mediating their activation [304]. Integrins are composed of  $\alpha\beta$  heterodimers that recognize various ECM ligands including fibronectin, collagen, laminin and vitronectin. Different integrin heterodimers are able to recognize different ligands. For example, integrin  $\alpha$ 7 $\beta$ 1 recognizes laminin, while the  $\alpha$ v $\beta$ 3 heterodimer interacts with fibronectin and vitronectin [305]. Higher expression levels of  $\alpha$ v $\beta$ 3,

$\alpha 5\beta 1$  integrins are found in glioblastoma than low-grade glioma and normal brain tissues, correlated with higher capacity of cell migration and invasion [306, 307]. Overexpression of integrin  $\beta 3$  promotes non-invasive prostate cancer cell migration and adhesion through activation of PI3K/Akt pathway [308]. On the contrary, silencing of *ITGB3* (encodes integrin  $\beta 3$ ) impedes migration and invasion in colorectal cancer cells [309]. We found that knockdown of *PIK3CD* decreased the mRNA expression of *ITGB3* rather than *ITGB1*, although integrin  $\beta 1$  also plays an important role in cell migration and invasion. P130Cas, also known as breast cancer anti-estrogen resistance protein 1 (BCAR1), is a member of the Crk-associated substrate (Cas) family. It serves as an adaptor protein interacting with Src kinase and FAK involved in cell motility. It has been shown that overexpression of p130Cas in MEFs promotes cell migration by increasing actin assembly at lamellipodia sites and enhancing focal adhesion turnover rate [310]. Evidence shows that integrin  $\beta 1$ /Akt/p130Cas/paxillin signaling axis plays a crucial role in the regulation of cell death and invasion [311, 312]. Integrin  $\beta 1$ -mediated Akt activation induces phosphorylation of paxillin and p130Cas through binding of FAK to integrin and then activating PI3K [311]. The mRNA expression of *p130Cas* was downregulated when *PIK3CD* was silenced. These findings suggest that p110 $\delta$  is able to regulate glioblastoma cell migration and invasion through mediating integrin  $\beta 3$  expression and integrin  $\beta 1$ /PI3K/Akt/p130Cas/paxillin axis.

ADAMTS1 (a disintegrin and metalloprotease with thrombospondin motifs 1) is a metalloprotease involved in tumor invasion and metastasis. However, the effect of

ADAMTS1 on cancer cell invasion is still in controversy. Either increased or decreased expression level of ADAMTS1 is found in various tumors [313, 314]. Overexpression of ADAMTS1 promotes bronchial epithelial tumor development and remodeling of stroma by increasing the expression of MMP-13 and fibronectin [315]. Controversial evidence also shows that deletion of ADAMTS1 promotes cell invasion and invadopodia formation in breast cancer cells by increasing the expression of VEGF and VEGFR2 [316]. The mechanism of ADAMTS1 as a pro-invasive or anti-invasive molecule is poorly understood. It may be explained by the anti-angiogenic role of ADAMTS1 through sequestering VEGF and preventing its binding to VEGFR [317, 318]. Therefore, high expression level of ADAMTS1 released in the ECM leads to VEGF arrest and reduced cell invasion. Here, we demonstrated that knockdown of *PIK3CD* by siPIK3CD\_2 increased glioblastoma cell invasion, correlated with upregulation of *ADAMTS1* expression. Conversely, siPIK3CD\_6 downregulated the mRNA expression of *ADAMTS1*, and did not affect the cell invasion. The data suggest that ADAMTS1 suppresses glioblastoma cell invasion *in vitro*, and the divergent effect between siPIK3CD\_2 and siPIK3CD\_6 may be caused by off-target effect. Since siRNA can trigger off-target effect to prevent the expression of various genes through microRNA-like silencing mechanism, siPIK3CD\_6 may bind to the 3'UTR of *ADAMTS1* gene, leading to its mRNA degradation [319].

## **Chapter 4 Combined inhibition of PI3K catalytic isoforms and JNK in glioblastoma**

### **4.1 Inhibition of JNK suppresses glioblastoma cell proliferation and JNK signaling**

JNK signaling pathway plays an important role in the survival and motility of cancer cells [212, 214, 217, 228]. The phosphorylation level of JNK in astrocytes was comparable to glioblastoma cells, indicating that JNK also plays a pivotal role in normal brain tissues. However, the phosphorylation level of c-Jun in astrocytes was much lower than glioblastoma cells, since c-Jun/AP-1 is involved in the transcriptional regulation of numerous oncogenes or tumor suppressor genes. The protein expression level of c-Jun varied greatly in glioblastoma cell lines, while its phosphorylation level was consistently high (Figure 4.1A). U-87 MG, U-373 MG, U-343 MG and SK-MG3 cells with high expression and phosphorylation levels of c-Jun were selected to evaluate the effect of JNK inhibition on proliferation in malignant glioma cells. SP600125 is a non-selective JNK inhibitor with broad spectrum against JNK1, JNK2 and JNK3. The characteristics of SP600125 is shown in Table 2.3. U-87 MG, U-373 MG, U-343 MG and SK-MG3 cells were incubated with SP600125 at different concentrations for 48 hr. SP600125 significantly suppressed glioma cell proliferation in a dose-dependent manner with  $IC_{50}$  of 20.43  $\mu$ M, 29.66  $\mu$ M, 29.82  $\mu$ M and 28.91  $\mu$ M for U-87 MG, U-373 MG, U-343 MG and SK-MG3 cells respectively (Figure 4.1B-C). U-87 MG cells were more sensitive to SP600125 than

the other glioblastoma cells.

To evaluate the effect of SP600125 on JNK signaling in glioblastoma cells, U-87 MG cells were treated with the inhibitor at a series of concentrations for 3 and 24 hr. Results demonstrated that SP600125 ( $\geq 5 \mu\text{M}$ ) decreased the phosphorylation level of c-Jun in a dose-dependent manner, whereas JNK phosphorylation was not affected (Figure 4.2). To determine whether the inhibitory effect of SP600125 on JNK signaling is time-dependent, U-87 MG cells were incubated with SP600125 at a final concentration of  $5 \mu\text{M}$  and  $20 \mu\text{M}$  for 1, 3, 6, 12, and 24 hr, respectively. SP600125 ( $5 \mu\text{M}$ ) slightly inhibited c-Jun phosphorylation after 1-hr to 24-hr treatment. In contrast, SP600125 at a higher concentration ( $20 \mu\text{M}$ ) remarkably suppressed c-Jun phosphorylation, and this inhibitory effect was more significant as time went by (Figure 4.3A). This inhibitory effect maintained till 48 hr, but it disappeared and the phosphorylation level of c-Jun was comparable to that of control group after 72-hr treatment (Figure 4.3B). These findings indicated that the inhibitory effect of SP600125 on JNK signaling was not only dose-dependent, but also time-dependent.

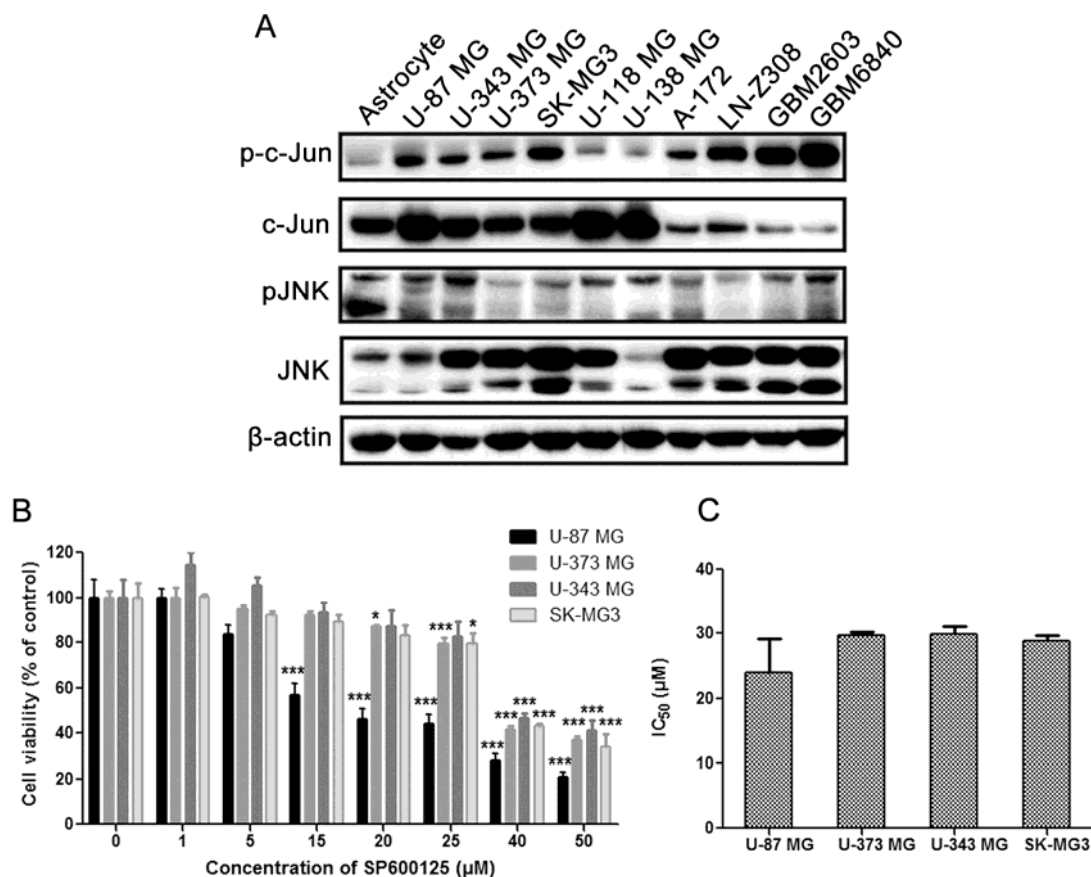


**Figure 4.1: Expression pattern of JNK pathway in glioblastoma cells and effect of JNK inhibitor SP600125 on glioblastoma cell proliferation.** (A) Protein expression and phosphorylation levels of JNK and c-Jun in astrocytes and glioblastoma cell lines. The expression of β-actin was used as a loading control. (B) U-87 MG, U-373 MG, U-343 MG and SK-MG3 cells were treated with SP600125 at different concentrations for 48 hr. DMSO was used as a carrier control. Cell proliferation was significantly inhibited by SP600125 ( $n=3$ ;  $p$  values were determined by One-way ANOVA and Post Hoc multiple comparison Tukey HSD test. \*:  $p < 0.05$ ; \*\*\*:  $p < 0.001$ ). (C) IC<sub>50</sub> values of SP600125 against glioblastoma cell lines U87-MG, U-373 MG, U-343 MG and SK-MG3, determined by dose response curve fitting using Origin 9.0 software ( $n=3$ ).

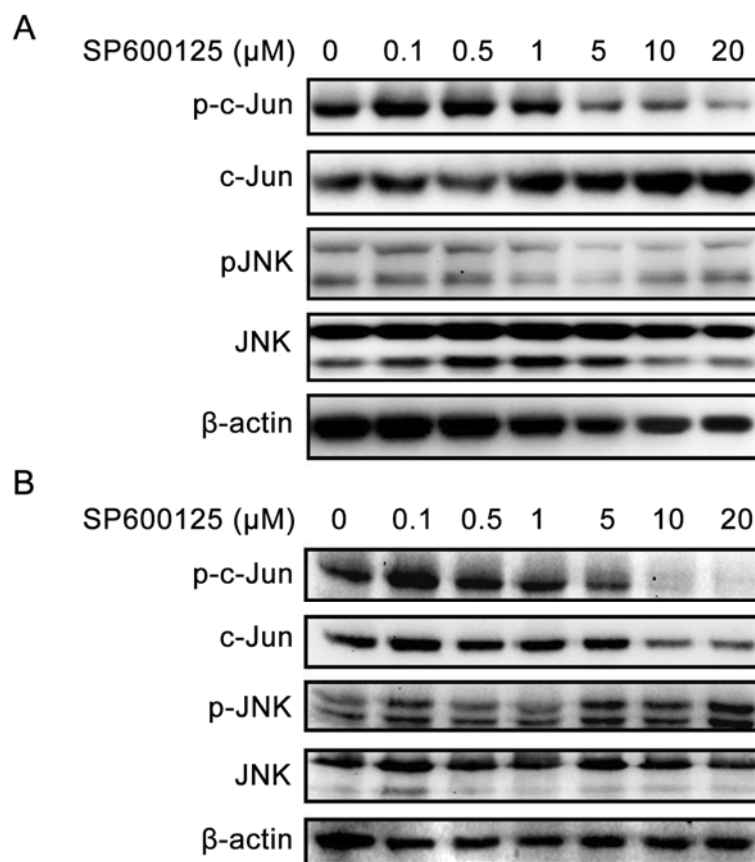


**Figure 4.2: Inhibitory effect of JNK inhibitor SP600125 on JNK signaling in glioblastoma cells.** U-87 MG cells were incubated with SP600125 at different concentrations for 3 hr (A) or 24 hr (B). DMSO were used as a carrier control. SP600125 inhibited c-Jun phosphorylation in a dose-dependent manner, without affecting the phosphorylation of JNK. The expression of  $\beta$ -actin was used as a loading control.

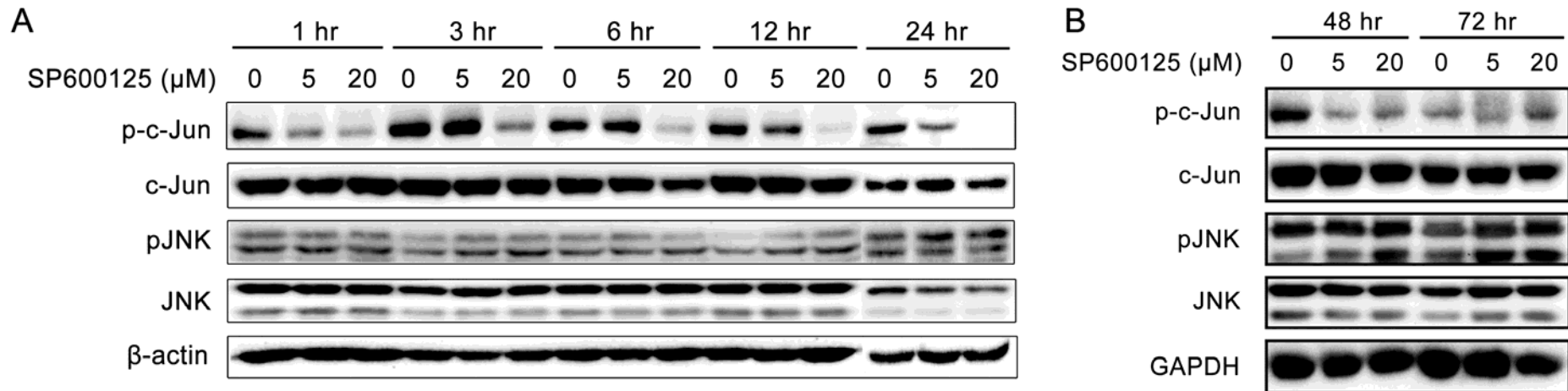


**Figure 4.3: SP600125 inhibited c-Jun phosphorylation in a time-dependent manner.** (A) U-87 MG cells were treated with SP600125 (5 μM and 20 μM) for 1 hr to 24 hr. The expression of β-actin was used as a loading control. (B) U-87 MG cells were treated with SP600125 (5 μM and 20 μM) for 48 hr and 72 hr. The expression of GAPDH was used as a loading control. DMSO was used as a carrier control.

## **4.2 Combination effects of isoform-selective PI3K inhibitors and JNK inhibitor on glioblastoma cell proliferation**

To evaluate the combination effect on glioblastoma cell proliferation, U-87 MG cells were treated with the isoform-selective PI3K inhibitors or SP600125 alone and in combination for 48 hr. PIK-75, TGX-221 and CAL-101 were combined with SP600125 at a fixed ratio according to the method described by Chou [289]. FA-CI plots were generated to evaluate the combination effect (Figure 4.4). Combination of PIK-75 and SP600125 showed antagonistic effect on U-87 MG cell proliferation with  $CI > 1.1$ , whereas TGX-221/CAL-101 combined with SP600125 exhibited a moderate synergistic effect with  $CI < 0.9$  (Table 4.1). In addition, PIK-75 consistently antagonized with SP600125 even though the ratio of PIK-75 to SP600125 increased to 1:40 (Table 4.2 and Figure 4.4B). Interestingly, TGX-221 at too low or too high concentrations did not synergize with SP600125, indicating that combination effect of TGX-221 and SP600125 is dose-dependent (Table 4.1). According to earlier findings, 0.1  $\mu\text{M}$  of PIK-75, 20  $\mu\text{M}$  of TGX-221, 10  $\mu\text{M}$  of CAL-101 and 20  $\mu\text{M}$  of SP600125 alone showed less cytotoxicities to U-87 MG cells but significant inhibition of Akt or JNK signaling. Furthermore, combination of TGX-221 and SP600125, as well as CAL-101 and SP600125 displayed synergistic effects at these concentrations. Therefore, these concentrations were chosen for the subsequent experiments.

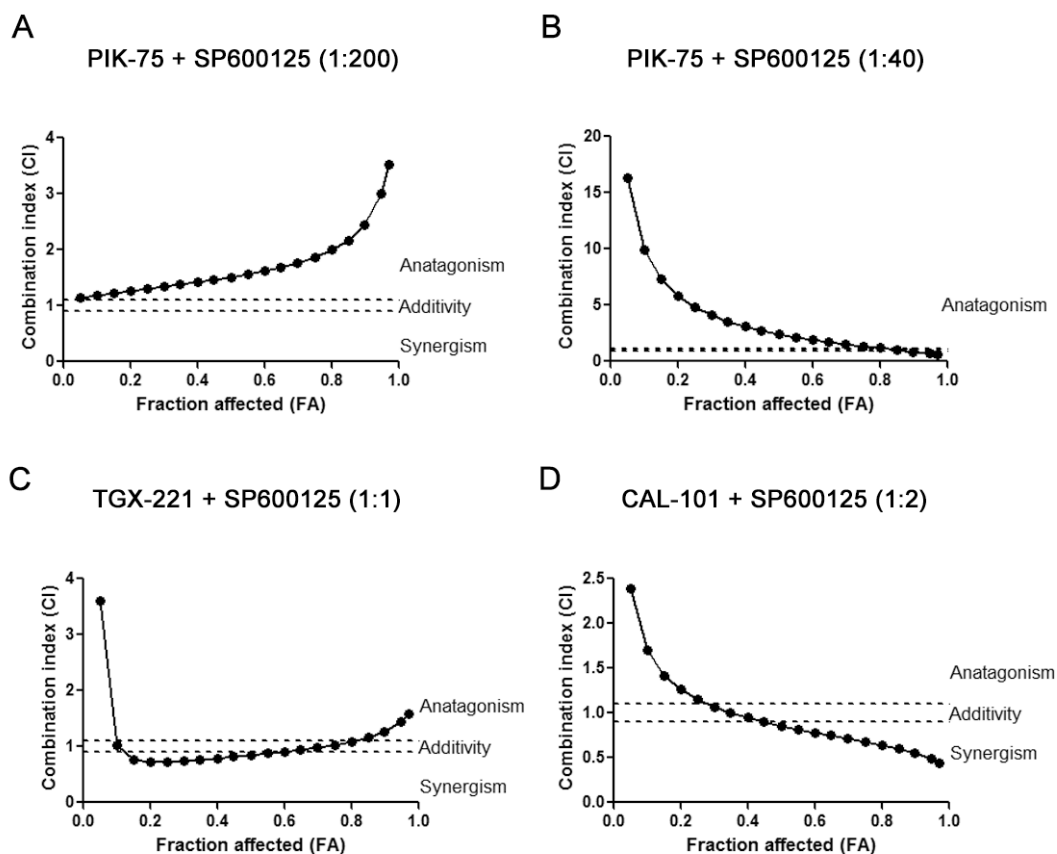


**Figure 4.4: Combination effects of isoform-selective PI3K inhibitors and SP600125 on glioblastoma cell proliferation.** FA-CI plots represent the CI values automated generated by Compusyn software. U-87 MG cells were treated with isoform-selective PI3K inhibitors and SP600125 at a fixed ratio for 48 hr. DMSO was used as a carrier control. (A-B) FA-CI plots represent the CI values of PIK-75 and SP600125 at the ratio of 1:200 or 1:40. (C) FA-CI plot represents the CI values of TGX-221 and SP600125 at the ratio of 1:1. (D) FA-CI plot represents the CI values of CAL-101 and SP600125 at the ratio of 1:2. Two dashed lines indicated the CI values of 0.9 and 1.1.

**Table 4.1: Combination index (CI) for cell viability in U-87 MG glioblastoma cells treated with combinations of SP600125 and PIK-75, TGX-221 or CAL-101 (n=3)**

PIK-75 ( $\mu\text{M}$ )	TGX-221 ( $\mu\text{M}$ )	CAL-101 ( $\mu\text{M}$ )	SP600125 ( $\mu\text{M}$ )	CI *		
				PIK-75 + SP600125	TGX-221 + SP600125	CAL-101 + SP600125
0.01	2	1	2	1.333 $\pm$ 0.169	1.252 $\pm$ 0.040	1.614 $\pm$ 0.169
0.025	5	2.5	5	1.645 $\pm$ 0.082	0.907 $\pm$ 0.005	1.263 $\pm$ 0.301
0.05	10	5	10	1.595 $\pm$ 0.061	0.837 $\pm$ 0.001	0.911 $\pm$ 0.107
0.1	20	10	20	1.568 $\pm$ 0.047	0.855 $\pm$ 0.055	0.809 $\pm$ 0.018
0.2	40	20	40	2.104 $\pm$ 0.103	1.009 $\pm$ 0.125	0.700 $\pm$ 0.049

\* Data were presented as mean  $\pm$  S.E.M. CI < 0.9 indicates synergistic effect; CI > 1.1 indicates antagonistic effect; CI between 0.9 and 1.1 indicates additive effect.

**Table 4.2: Combination index (CI) for cell viability in U-87 MG cells treated with PIK-75 and SP600125 at a fixed ratio of 1:40 (n=3)**

PIK-75 ( $\mu\text{M}$ )	SP600125 ( $\mu\text{M}$ )	CI *
0.05	2	6.457 $\pm$ 2.157
0.125	5	2.164 $\pm$ 0.412
0.25	10	1.166 $\pm$ 0.176
0.5	20	1.369 $\pm$ 0.175
1	40	1.262 $\pm$ 0.369

\* Data were presented as mean  $\pm$  S.E.M. CI < 0.9 indicates synergistic effect; CI > 1.1 indicates antagonistic effect; CI between 0.9 and 1.1 indicates additive effect.

To investigate whether the combination treatment was time-dependent, U-87 MG cells were treated with PIK-75 (0.1  $\mu$ M), TGX-221 (20  $\mu$ M) and CAL-101 (10  $\mu$ M) combined with SP600125 (20  $\mu$ M) for 24, 48, 72 and 96 hr. Combination of PIK-75 and SP600125 attenuated the inhibitory effect of PIK-75 at all the investigated time points, being in accordance with the observation that PIK-75 and SP600125 were antagonistic (Figure 4.5A). The inhibitory effects of drug combinations (TGX-221 and SP600125, CAL-101 and SP600125) on glioblastoma cell proliferation were time-dependent, and SP600125 potentiated the inhibitory effect of TGX-221 or CAL-101 at all the time points tested (Figure 4.5B-C). Taken together, combination of PIK-75 and SP600125 showed an antagonistic effect on glioblastoma cell proliferation, whereas TGX-221 or CAL-101 synergized with SP600125 in a dose- and time- dependent manner. Similar results were also found in U-373 MG cells, suggesting that the combination effect may not be cell line-specific (Figure 4.6).

Western blotting was carried out to investigate the effects of drug combination on Akt and JNK signaling. JNK inhibitor SP600125 not only inhibited c-Jun phosphorylation, but also attenuated Akt phosphorylation at Ser473 and Thr308. More importantly, combination of TGX-221 or CAL-101 and SP600125 had higher inhibition of Akt phosphorylation at Thr308, whereas Akt phosphorylation at Ser473 and c-Jun phosphorylation were not further inhibited (Figure 4.5E-F). No significant change of Akt and c-Jun phosphorylation levels was observed in the combination of PIK-75 and SP600125 (Figure 4.5D). The phosphorylation level of c-Jun was elevated by PIK-75, indicating this may be the cause of antagonism. Interestingly,

inhibition of p110 $\beta$  remarkably suppressed c-Jun phosphorylation, but no further suppression was observed when JNK was also inhibited (Fig 4.5E). This suggests that p110 $\beta$  and JNK may act on c-Jun via the same pathway.

Additionally, experiments were also conducted in normal human astrocytes to evaluate the combination effects on normal brain cells. Treatments of SP600125 alone, as well as combined with PIK-75, TGX-221 and CAL-101 showed lower cytotoxicities to astrocytes than U-87 MG cells (Figure 4.7).

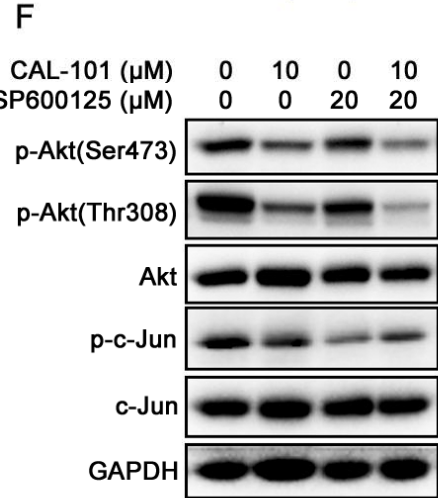
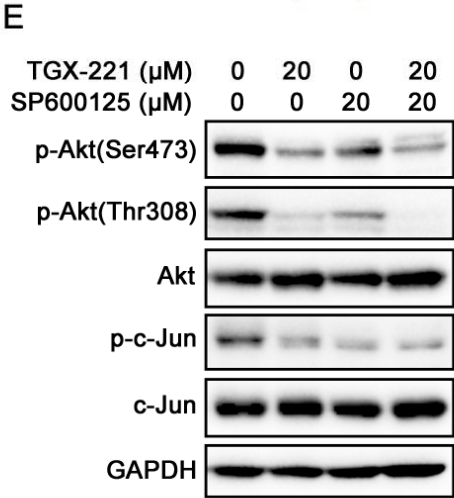
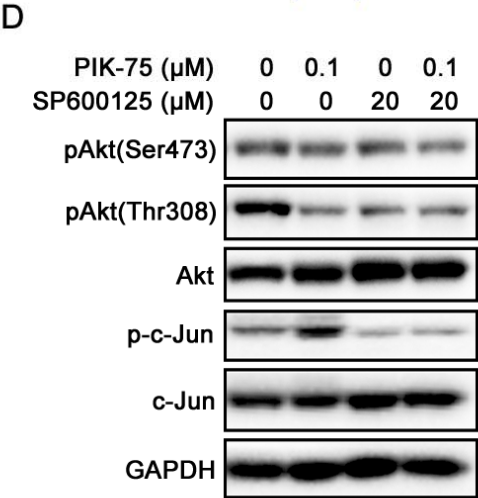
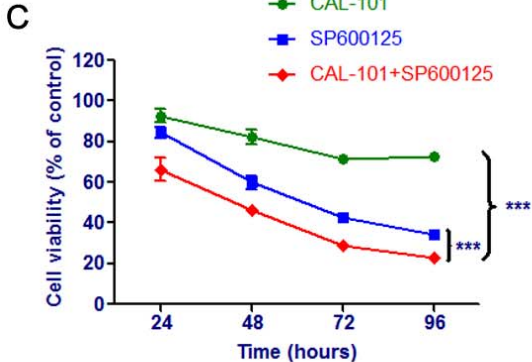
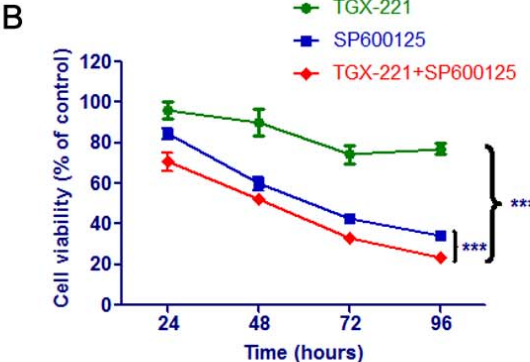
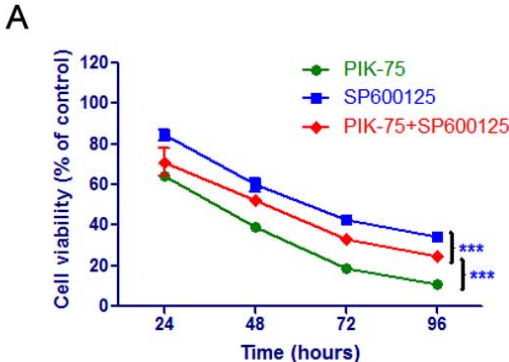


**Figure 4.5: Combination effects of isoform-selective PI3K inhibitors and SP600125 on glioblastoma cell proliferation and signal transduction.** (A-C)

U-87 MG cells were treated with PIK-75 (0.1  $\mu$ M), TGX-221 (20  $\mu$ M) or CAL-101 (10  $\mu$ M) alone and combined with SP600125 (20  $\mu$ M) for 24, 48, 72 and 96 hr respectively. DMSO was used as a carrier control. PIK-75 combined with SP600125 showed antagonistic effect, whereas SP600125 significantly synergized TGX-221 or CAL-101 (n=3; *p* values were determined by Two-way ANOVA and Post Hoc multiple comparison Tukey HSD test. \*\*\*: *p* <0.001). (D-E) U-87 MG cells were treated with PIK-75, TGX-221 or CAL-101 alone and combined with SP600125 for 3 hr. Combination of TGX-221 and SP600125, as well as CAL-101 and SP600125 exhibited higher inhibition of Akt phosphorylation at Thr308 and to a lesser extent at Ser473.

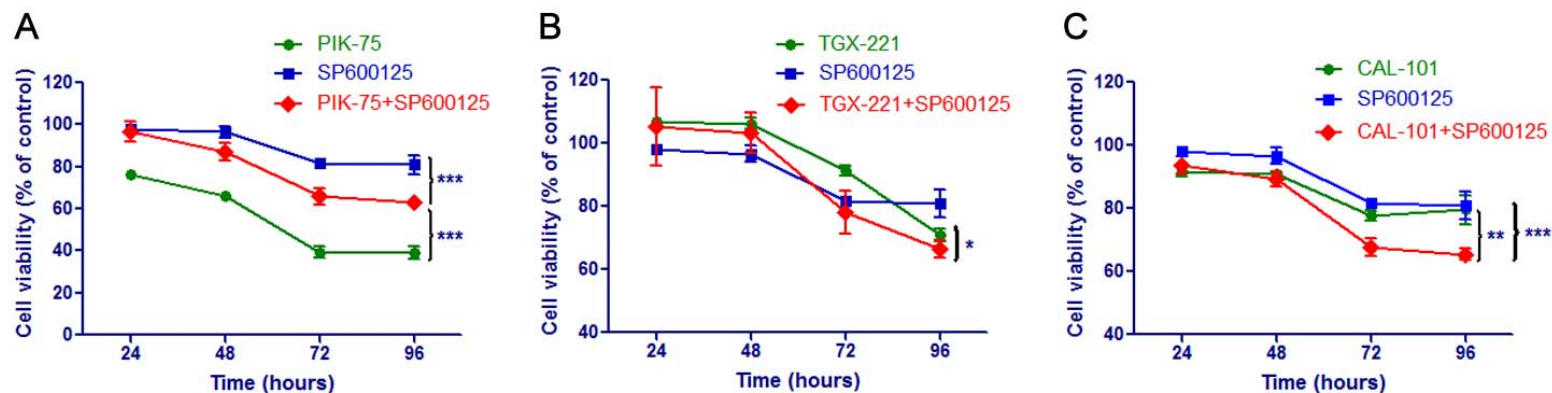


**Figure 4.6: Combination effects of isoform-selective PI3K inhibitors and SP600125 on U-373 MG glioblastoma cell proliferation.** U-373 MG cells were treated with PIK-75 (0.1  $\mu$ M), TGX-221 (20  $\mu$ M) or CAL-101 (10  $\mu$ M) alone and combined with SP600125 (20  $\mu$ M) for 24, 48, 72 and 96 hr respectively. DMSO was used as a carrier control. (A) PIK-75 combined with SP600125 showed antagonistic effect. (B) TGX-221 showed slight synergism with SP600125 at 72 hr and 96 hr. (C) CAL-101 showed synergistic effect with SP600125 at 72 hr and 96 hr. (n=3; *p* values were determined by Two-way ANOVA and Post Hoc multiple comparison Tukey HSD test. \*: *p* < 0.05; \*\*: *p* < 0.01; \*\*\*: *p* < 0.001).

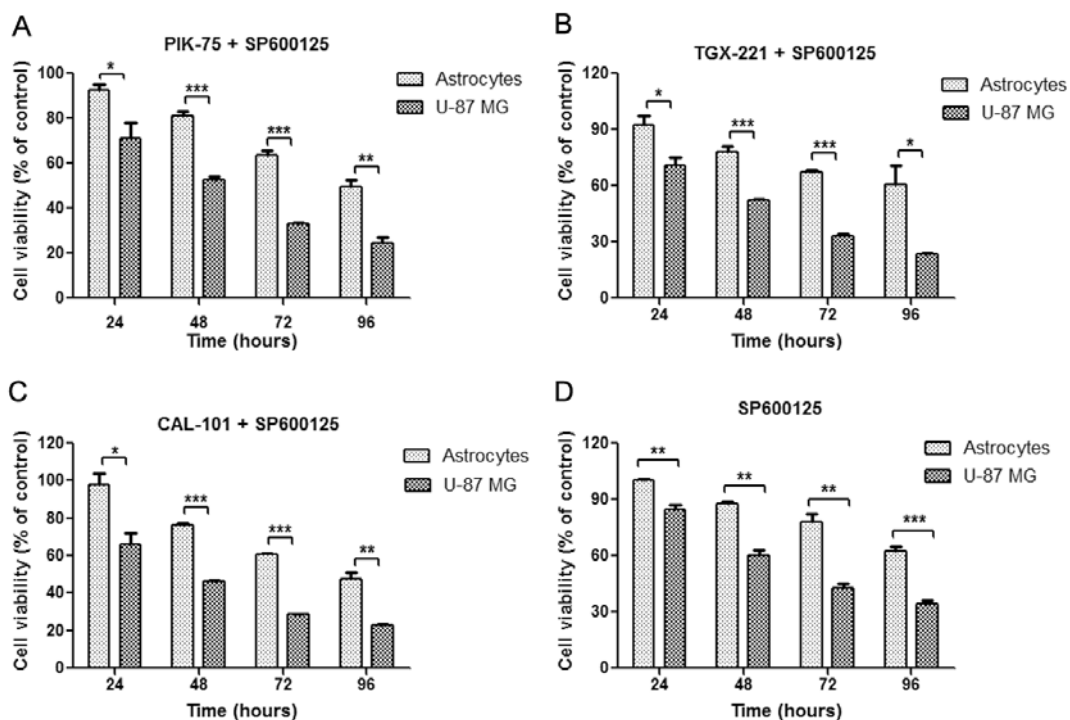


**Figure 4.7: Combination effects of isoform-selective PI3K inhibitors and SP600125 on cell proliferation in normal human astrocytes.** Glioblastoma cells U-87 MG and human astrocytes were treated with PIK-75 (0.1  $\mu$ M), TGX-221 (20  $\mu$ M) or CAL-101 (10  $\mu$ M) alone and combined with SP600125 (20  $\mu$ M) for 24, 48, 72 and 96 hr respectively. Compared with U-87 MG cells, astrocytes showed much higher viability when treated with SP600125 combined with PIK-75 (A), TGX-221 (B) or CAL-101 (C). (D) SP600125 alone also displayed less cytotoxicity to normal human astrocytes. (n=3; *p* values were determined by Independent Sample *t*-test. \*: *p* < 0.05; \*\*: *p* < 0.01; \*\*\*: *p* < 0.001).

### **4.3 Combination effects of isoform-selective PI3K inhibitors and JNK inhibitor on glioblastoma cell migration and invasion**

To investigate the combination effects of isoform-selective PI3K inhibitors and SP600125 on glioblastoma cell motility, wounds were generated on confluent U-87 MG cells, subsequently treated with PIK-75 (0.1  $\mu$ M), TGX-221 (20  $\mu$ M), or CAL-101 (10  $\mu$ M) alone and combined with SP600125 (20  $\mu$ M) for 24 hr. In order to exclude the effect of cell proliferation, cells were incubated with mitomycin C prior to wound production and inhibitor treatment. Results showed that combination of PIK-75 and SP600125 did not further inhibit glioblastoma cell migration, whereas TGX-221 or CAL-101 combined with SP600125 potentiated the inhibitory effects (Figure 4.8). Similar inhibitory effects were also observed in U-373 MG cells. However, due to the resistance of U-373 MG cells to these inhibitors, the synergistic inhibitory effects were lower than those in U-87 MG cells (Figure 4.9). In addition, TGX-221 or CAL-101 synergized with SP600125 to block the formation of lamellipodia and membrane ruffles in U-87 MG cells, whereas the combination of PIK-75 and SP600125 did not (Figure 4.10).

To elucidate the molecular mechanism contributing to the synergistic effects of isoform-selective PI3K inhibitors and JNK inhibitor on cell migration, activation of focal adhesion and cytoskeleton-related signaling network were investigated. After 24-hr drug treatment, phosphorylation level of FAK at Tyr925 in U-87 MG cells was decreased upon inhibition of p110 isoforms or JNK alone, whereas the phosphorylation level of zyxin was only reduced by inhibition of JNK (Figure 4.11A-C).

Moreover, combination of TGX-221 and SP600125 showed lower FAK phosphorylation level, while combination of CAL-101 and SP600125 displayed lower phosphorylation levels of both zyxin and FAK (Figure 4.11B-E). Additionally, expression levels of Rac1 and RhoA were not substantially affected by inhibition of p110 isoforms and JNK (Figure 4.11A-C). Thus, isoform-selective PI3K inhibitors impeded glioblastoma cell migration through blockade of FAK activation, and reduced FAK and zyxin activation contributed to the synergistic inhibitory effects on glioblastoma cell migration.

To analyze the combination effects of isoform-selective PI3K inhibitors and SP600125 on glioblastoma cell invasion, Boyden chamber invasion assay was performed on U-87 MG cells. No synergistic effect on cell invasion was found in any combination treatment (Figure 4.12).

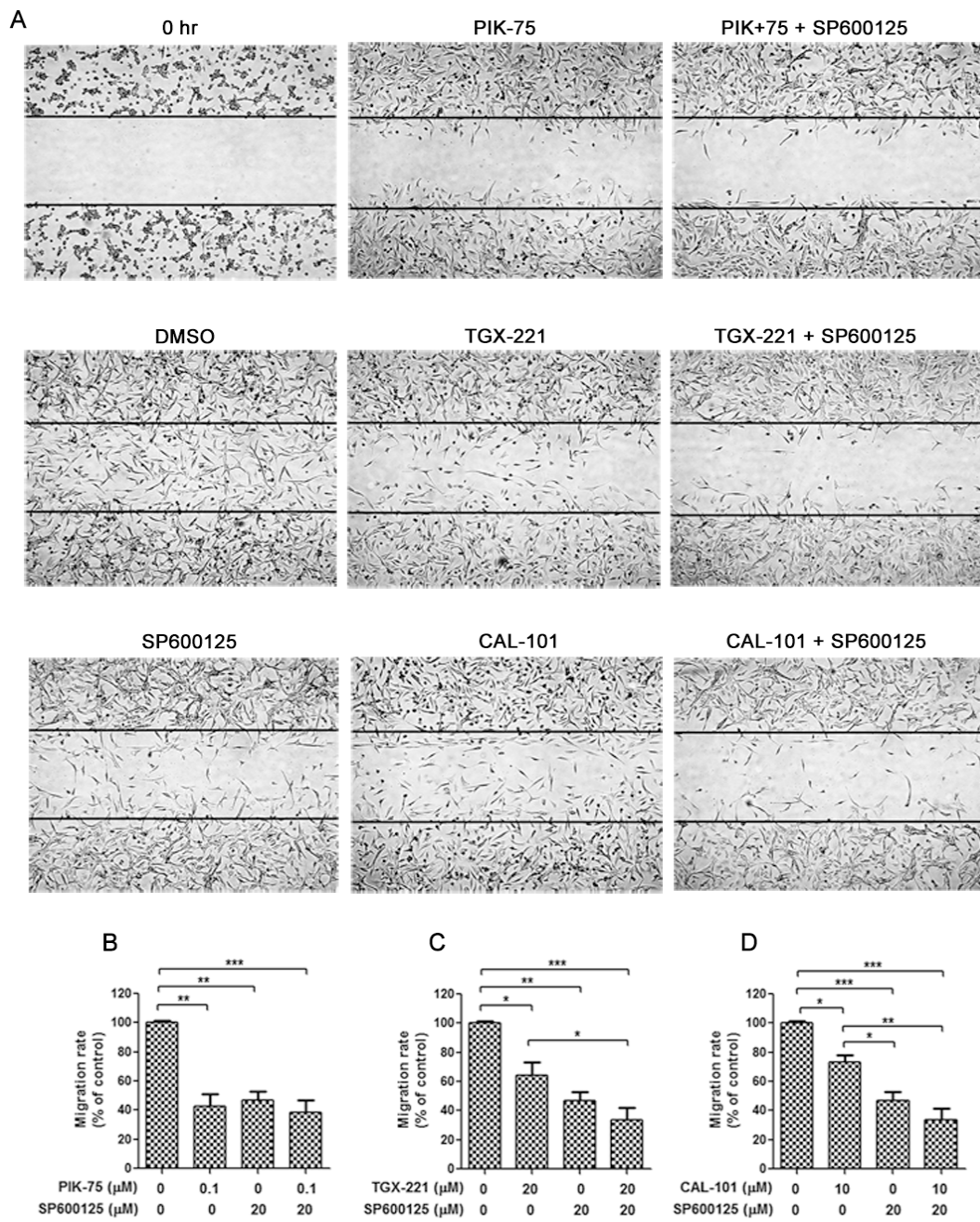


**Figure 4.8: SP600125 potentiates inhibitory effects of isoform-selective PI3K inhibitors on glioblastoma cell migration.** (A) Wound healing in U-87 MG cells treated with PIK-75 (0.1  $\mu$ M), TGX-221 (20  $\mu$ M) or CAL-101 (10  $\mu$ M) alone and combined with SP600125 (20  $\mu$ M) for 24 hr. Cells were pretreated with 5  $\mu$ g/mL of mitomycin C for 1 hr. The lines indicate the edges of wounds generated before drug treatment (0 hr). Photographs were obtained at 50 $\times$  magnification. (B-D) Migration rate (%) was analyzed and expressed as the number of cells migrating into the original wounds relative to those in DMSO control. Inhibition of migration rate was reinforced by the combined treatment of TGX-221 and SP600125, as well as CAL-101 and SP600125 (n=3; *p* values were determined by One-way ANOVA and Post Hoc multiple comparison Tukey HSD test. \*: *p* <0.05; \*\*: *p* <0.01; \*\*\*: *p* <0.001).

Chapter 4 Combined inhibition of PI3K catalytic isoforms and JNK in glioblastoma

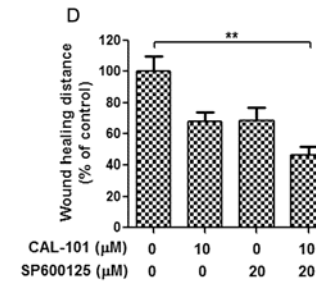
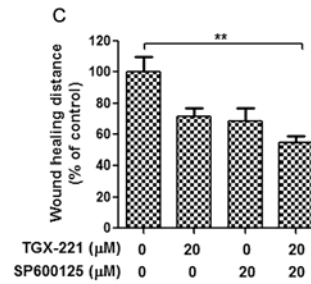
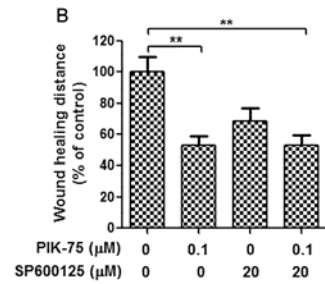
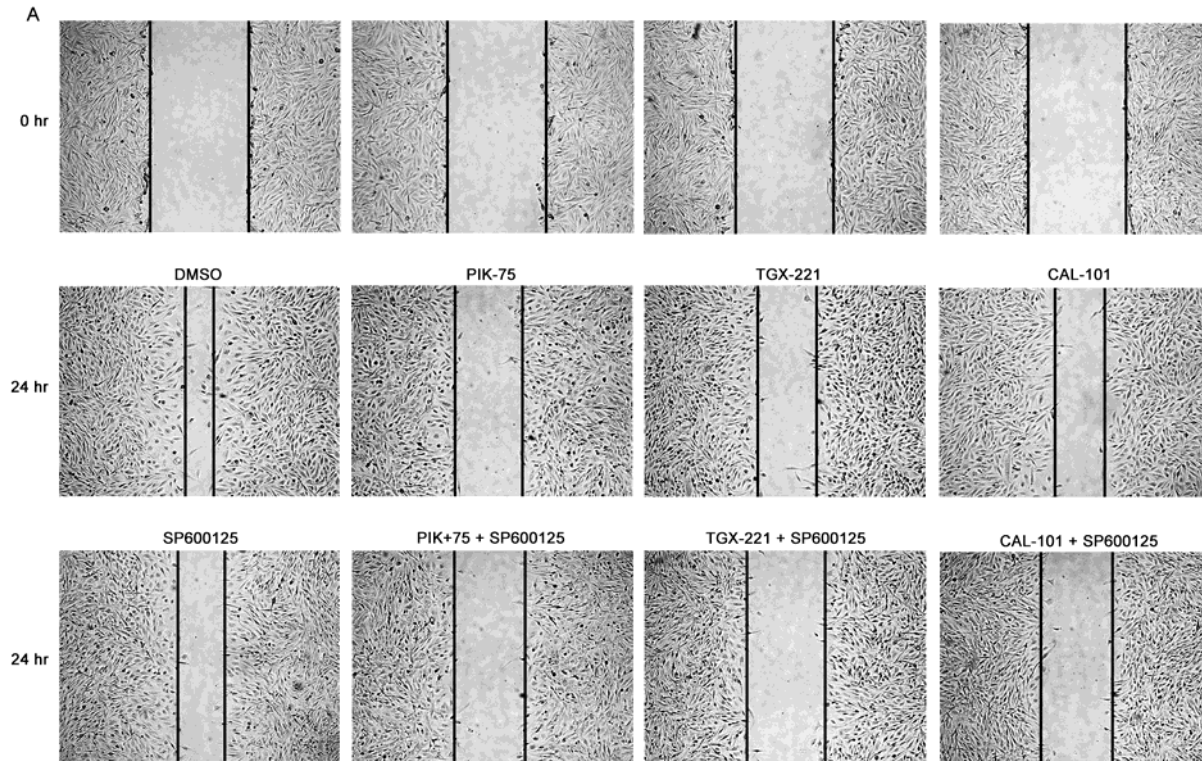
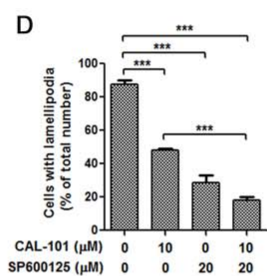
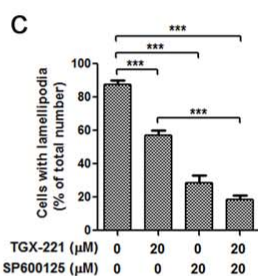
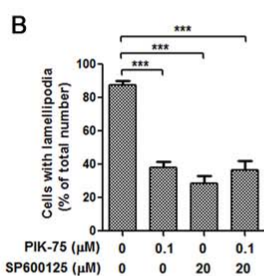
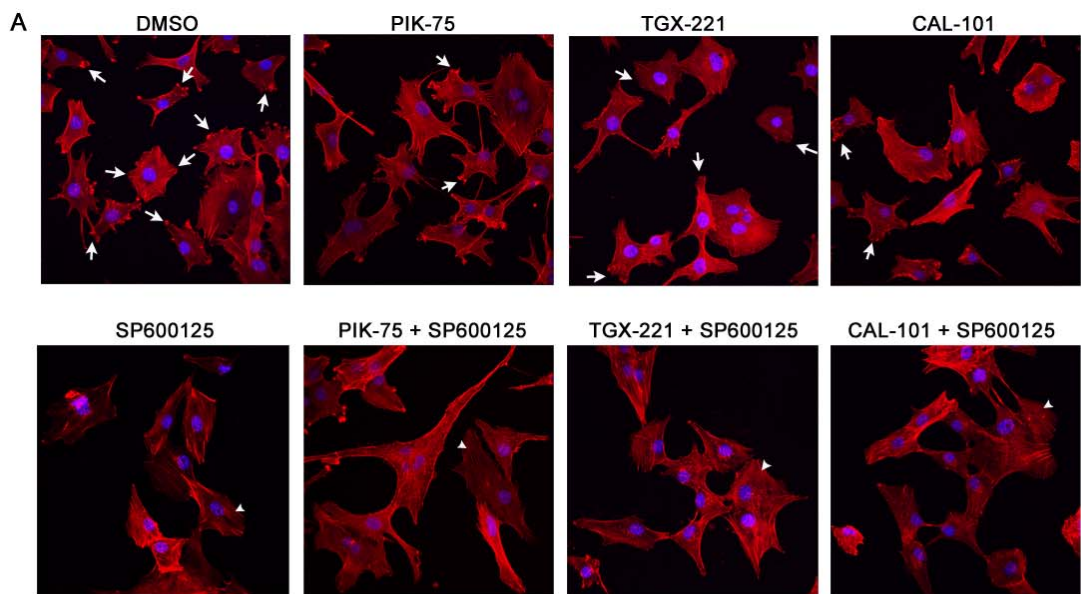


**Figure 4.9: Combination effects of isoform-selective PI3K inhibitors and SP600125 on migration of U-373 MG glioblastoma cells.** (A) Wound healing assay in U-373 MG cells treated with PIK-75 (0.1  $\mu$ M), TGX-221 (20  $\mu$ M) or CAL-101 (10  $\mu$ M) alone and combined with SP600125 (20  $\mu$ M) for 24 hr. Cells were pretreated with 5  $\mu$ g/mL of mitomycin C for 1 hr. The lines indicate the edges of wounds generated before (0 hr) or after (24 hr) drug treatment. Photographs were obtained at 50 $\times$  magnification. (B-D) Wound healing distance (%) was analyzed and expressed as the migration distance of cells relative to that of DMSO control. Combination of PIK-75 and SP600125 did not potentiate the inhibitory effect. However, cell migration was suppressed by the combined treatment of TGX-221 or CAL-101 and SP600125 (n=3; *p* values were determined by One-way ANOVA and Post Hoc multiple comparison Tukey HSD test. \*\*: *p* <0.01).



50 μm

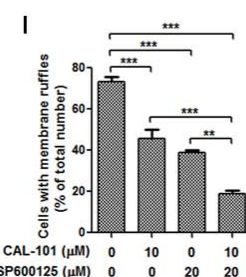
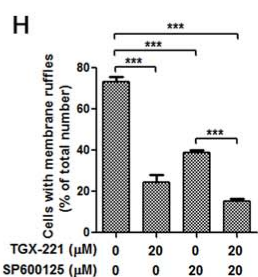
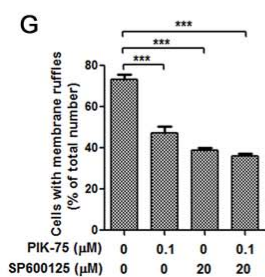
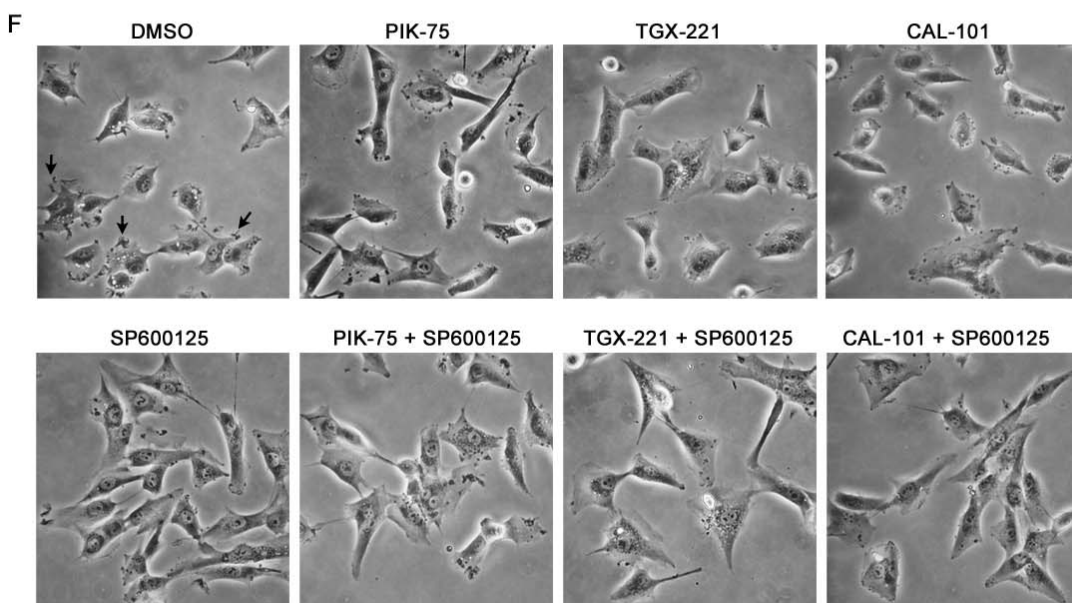


**Figure 4.10: SP600125 potentiates inhibitory effects of isoform-selective PI3K inhibitors on lamellipodia and membrane ruffles formation.** (A) U-87 MG cells stained with Alexa Fluor 594-conjugated phalloidin (red) after treatment with PIK-75 (0.1  $\mu$ M), TGX-221 (20  $\mu$ M) or CAL-101 (10  $\mu$ M) alone and combined with SP600125 (20  $\mu$ M) for 3 hr. Lamellipodia (white arrows) were decreased after inhibition of p110 $\alpha$ , p110 $\beta$ , p110 $\delta$  and JNK, while stress fibers (arrowheads) were widely developed at the presence of SP600125. Bar = 50  $\mu$ m. (B-D) Cells with lamellipodia were counted and data were expressed as the ratio of number of cells with lamellipodia over total cell number. SP600125 potentiated the inhibitory effects of TGX-221 and CAL-101 on lamellipodia formation (n=3; *p* values were determined by One-way ANOVA and Post Hoc multiple comparison Tukey HSD test. \*\*\*: *p* <0.001). (F) Phase contrast microscopy of U-87 MG cells after treatment with PIK-75, TGX-221 or CAL-101 alone and combined with SP600125 for 3 hr. Cells with membrane ruffles (black arrows) were reduced by the treatment of isoform-selective PI3K inhibitors and SP600125. Photographs were obtained at 200 $\times$  magnification. (G-I) Cells with membrane ruffles were counted and data were expressed as the ratio of number of cells with membrane ruffles over total cell number. SP600125 also enhanced the inhibitory effects of TGX-221 and CAL-101 on membrane ruffles formation (n=3; *p* values were determined by One-way ANOVA and Post Hoc multiple comparison Tukey HSD test. \*\*: *p* <0.01; \*\*\*: *p* <0.001)

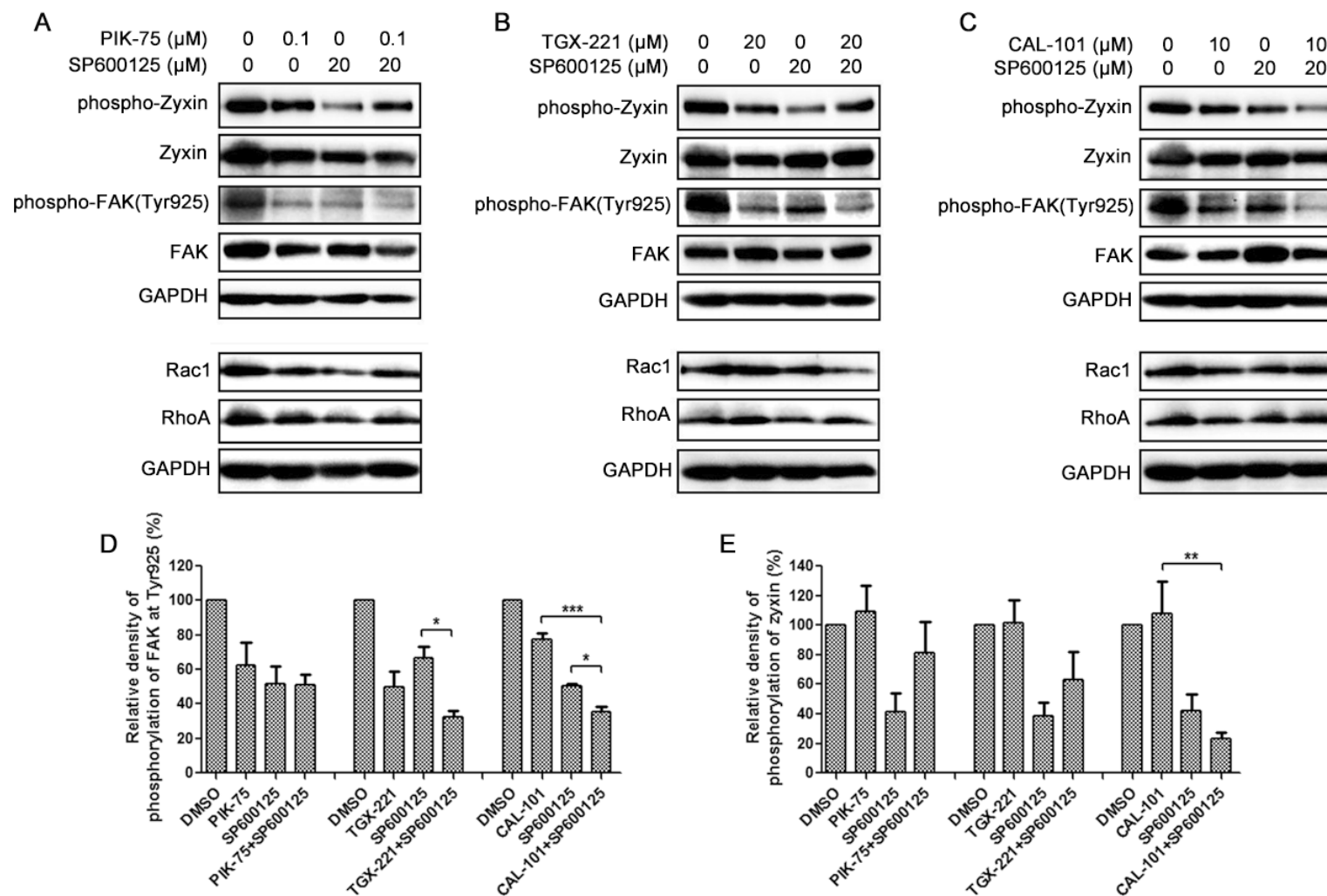


**Figure 4.11: Combination effects of Isoform-selective PI3K inhibitors and SP600125 on focal adhesion and cytoskeleton-related signaling.** (A-C) U-87 MG cells were treated with PIK-75 (0.1  $\mu$ M), TGX-221 (20  $\mu$ M) or CAL-101 (10  $\mu$ M) alone and in combination with SP600125 (20  $\mu$ M) for 24 hr. Whole cell lysates were separated by SDA-PAGE, and the phosphorylation and protein expression levels were determined by Western blotting using antibodies against the corresponding proteins. Expression of GAPDH was served as a loading control. Data are representative of three independent experiments. Density of FAK (D) and zyxin (E) phosphorylation levels were relative to total FAK and zyxin protein expression levels. (n=3; *p* values were determined by One-way ANOVA and Post Hoc multiple comparison Tukey HSD test. \*: *p* <0.05; \*\*: *p* <0.01).

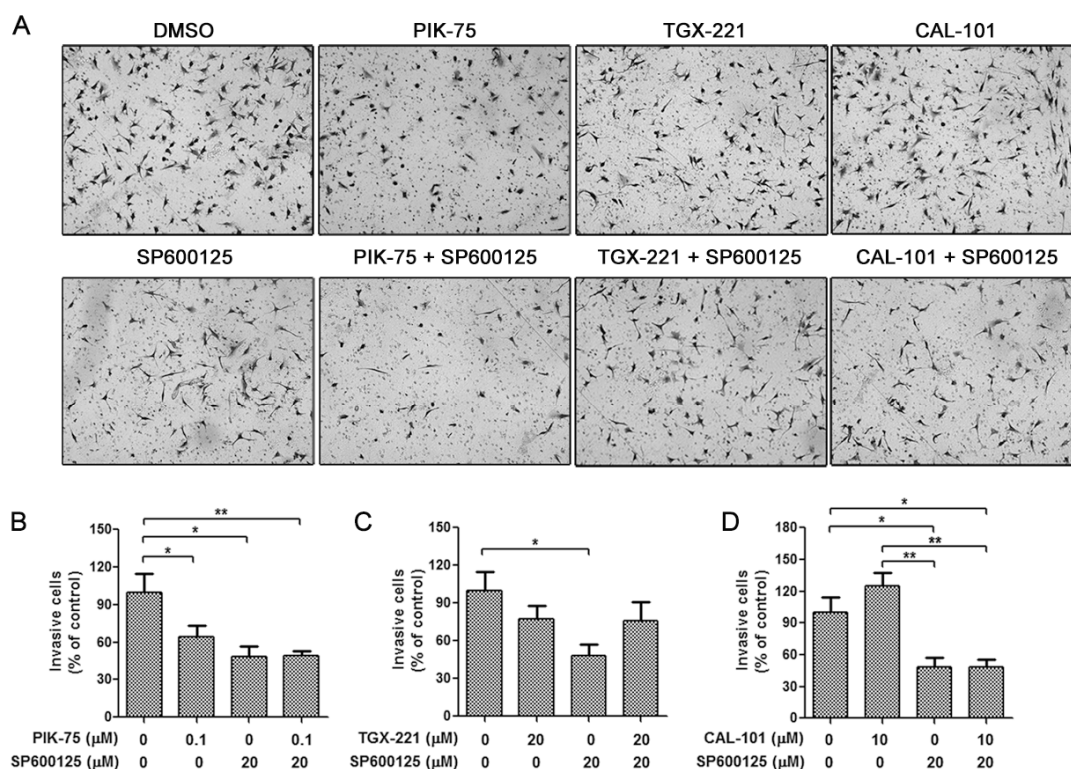


**Figure 4.12: Combination effects of isoform-selective PI3K inhibitors and SP600125 on glioblastoma cell invasion.** Boyden chamber invasion assay of U-87 MG cells treated with PIK-75 (0.1  $\mu\text{M}$ ), TGX-221 (20  $\mu\text{M}$ ) or CAL-101 (10  $\mu\text{M}$ ) alone and combined with SP600125 (20  $\mu\text{M}$ ) for 24 hr. (A) Representative photographs showing the invasive cells that had passed through matrigel to the lower surface of the membrane at 100 $\times$  magnification. Invaded cells from 5 representative fields were counted. (B-D) Number of invasive cells was significantly decreased by PIK-75 and SP600125, and all the drug combination did not enhanced the inhibitory effect ( $n=3$ ;  $p$  values were determined by One-way ANOVA and Post Hoc multiple comparison Tukey HSD test. \*:  $p < 0.05$ ; \*\*:  $p < 0.01$ ).

## 4.4 Discussion

### 4.4.1 A crosstalk model between class IA PI3K catalytic isoforms and JNK

The PI3K/Akt pathway has a crosstalk with JNK pathway, and co-activation of Akt and JNK is found in glioblastoma [232, 320]. Combination therapies targeting PI3K/Akt and Ras-mediated MAPK pathways may exert synergism for cancer treatment [253]. Evidence shows that combined inhibition of p110 $\delta$  and MEK has synergistic cytotoxicity in human acute myeloid leukemia progenitors [254]. Concurrent expression of dominant-negative p85 $\alpha$  and MKK4 is also synergistic to induce apoptosis in lung cancer cells [256]. These data suggest that combined inhibition of PI3K and JNK may also exert synergism in the regulation of cell viability and motility in glioblastoma cells. This study demonstrated that combined inhibition of p110 $\beta$  or p110 $\delta$  and JNK displayed synergistic inhibitory effects on glioblastoma cell proliferation and migration via blockade of Akt, zyxin and FAK activation. Formation of lamellipodia and membrane ruffles involved in cell migration was also suppressed. However, only PIK-75 and SP600125 suppressed glioblastoma cell invasion, but all the drug combinations had no synergistic effects, suggesting the crosstalk between PI3K and JNK on cell invasion is limited.

The ATP-competitive JNK inhibitor SP600125 was sufficient to inhibit viability, migration and invasion of glioblastoma cells through decreasing the phosphorylation levels of both c-Jun and Akt. Activated JNK can translocate into the nucleus and

phosphorylate a variety of transcription factors such as c-Jun, which is a component of transcription factor AP-1. AP-1 is able to regulate the transcriptional activity of PDK-1 and the activation of its downstream target Akt, suggesting that JNK regulates Akt activity through JNK/c-Jun/PDK1/Akt axis [252]. Interestingly, we found that only TGX-221 was able to decrease c-Jun phosphorylation, being consistent with the findings that constitutive activation of p110 $\beta$  contributes to JNK activation [247]. Our data therefore suggest that p110 $\beta$ , neither p110 $\alpha$  nor p110 $\delta$ , may be an upstream regulator of JNK signaling, possibly because they are both activated by GPCRs.

Since p110 $\alpha$  plays a dominant role in RTK-mediated Akt signaling, inhibition of p110 $\alpha$  by PIK-75 may lead to activation of p110 $\beta$  due to a compensatory effect induced by GPCR activation, and then p110 $\beta$  may activate JNK pathway to escape from p110 $\alpha$  inhibition (Figure 4.13). We also found that phosphorylation level of c-Jun was elevated by treatment of PIK-75, indicating that inhibition of p110 $\alpha$  may increase JNK activity through activation of GPCR/p110 $\beta$ /JNK axis. It explains why combined inhibition of p110 $\alpha$  and JNK was antagonism in our study. Conversely, inhibition of p110 $\beta$  blocks the activation of JNK, thus combined with inhibition of JNK leads to a synergistic effect (Figure 4.13). In addition, inhibition of p110 $\delta$  didn't affect the activity of p110 $\alpha$  and p110 $\beta$ , thus the activation of GPCR/p110 $\beta$ /JNK/c-Jun axis was not triggered. Therefore, combined inhibition of p110 $\delta$  and JNK is also synergism (Figure 4.13).

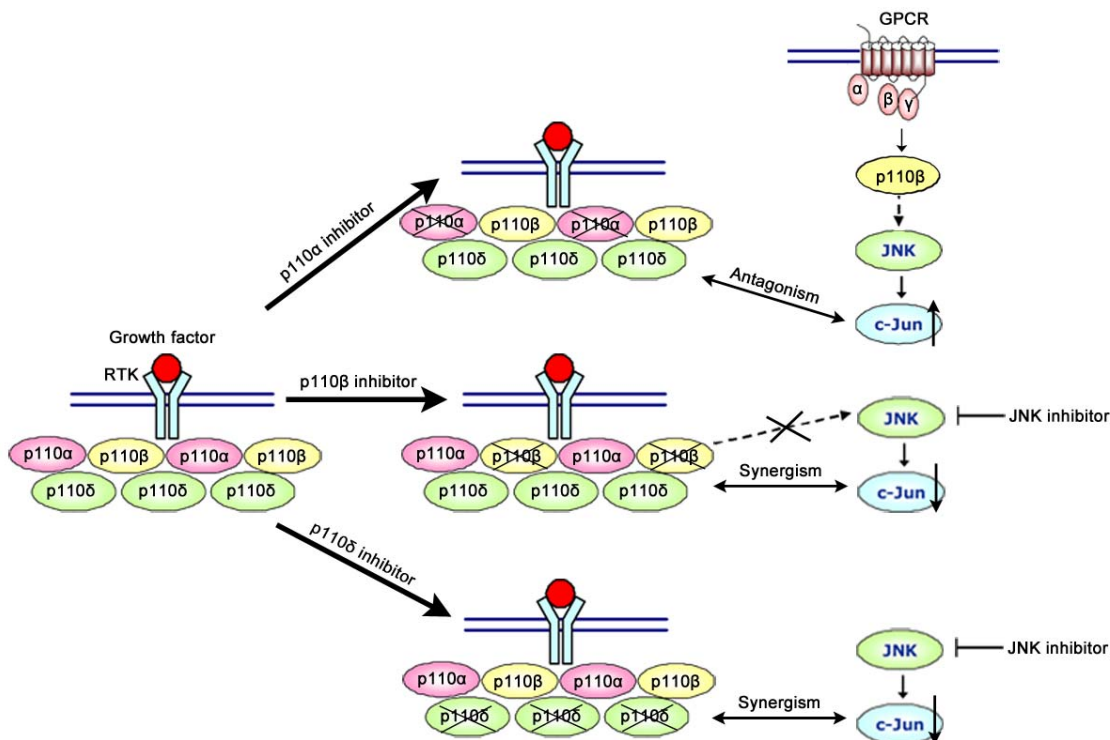


**Figure 4.13: Schematic diagram showing a model of combined inhibition of class I<sub>A</sub> PI3K catalytic isoforms and JNK.** Inhibition of p110α increased JNK activity via compensatory effect of GPCR/p110β/JNK/c-Jun axis activation, leading to an antagonism with JNK inhibition. Conversely, inhibition of p110β blocks the activation of GPCR/p110β/JNK/c-Jun axis, thus combined with inhibition of JNK leads to a synergistic effect. Inhibition of p110δ may not affect the activity of p110α and p110β, thus the activation of JNK is not triggered. Therefore, combined inhibition of p110δ and JNK is also synergism. Arrow with dashed line indicates that more than one step may be involved. Arrows beside c-Jun indicate that the activity of c-Jun is increased or decreased.

#### **4.4.2 Inhibition of zyxin and FAK contributes to the synergism**

Migration and invasion of glioblastoma cells are potential therapeutic targets for GBM treatment. Cell migration is a complicated biological process including actin polymerization, protrusion formation, adhesion complexes formation, focal adhesion turnover, and retraction at the cell rear. A variety of cytoskeletal structures including lamellipodia, filopodia, focal adhesions, stress fibers, and membrane ruffles are essential to a motile cell, providing adhesion sites and contractile forces for cell movement. Focal adhesion complexes consisting of integrin, paxillin, talin, zyxin and FAK are formed at the edges of lamellipodia to provide attachment of cell protrusion to the extracellular matrix [321]. Zyxin and FAK are known as focal adhesion proteins mediating cell-matrix adhesion and actin polymerization. Zyxin recruits Enabled/vasodilator-stimulated phospho-proteins (Ena/VASP) through N-terminal ActA proline-rich domain to regulate actin filament assembly, and facilitates focal adhesion by interacting with specific proteins through C-terminal LIM domains [322]. The interaction of LIM domains and adaptors required phosphorylation of zyxin at Ser142 [323]. Evidence shows that knockdown or inhibition of zyxin leads to blockade of cell spreading and migration [324]. Besides, zyxin is involved in stress fiber stabilization and remodeling through its recruitment to stress fibers and interaction with Ena/VASP and  $\alpha$ -actinin [325, 326]. Here, we demonstrated that SP600125 markedly decreased zyxin phosphorylation level, and bundles of stress fibers were observed upon treatment with SP600125. However, none of the

isoform-selective PI3K inhibitors did so. These suggest that phosphorylation of zyxin at Ser142/143 is involved in stress fiber stabilization, and the impacts of JNK and PI3K inhibitors on downstream signaling and actin structures are different. Moreover, combination of CAL-101 and SP600125 synergistically reduced zyxin phosphorylation level than on their own.

Activation of FAK is involved in focal adhesion, cell migration and invasion. Autophosphorylation of FAK at Tyr397 leads to recruitment of PI3K p85 subunit and phosphorylation of FAK at Tyr925, and subsequently triggers the Ras-dependent activation of MAPK pathway. FAK phosphorylation status at Tyr925 is crucial to cell migration and focal adhesion turnover. Evidence reveals that expression of nonphosphorylatable FAK at Tyr925 in *FAK*<sup>-/-</sup> mouse embryonic fibroblasts reduces phosphorylation of paxillin and activates Rac1, leading to stabilization of focal adhesion, inhibition of cell protrusion and migration [327]. In this study, isoform-selective PI3K inhibitors and SP600125 alone suppressed glioblastoma cell migration through inhibition of FAK phosphorylation at Tyr925. Combination of TGX-221 and SP600125, as well as CAL-101 and SP600125 also potentiated the inhibitory effects on FAK phosphorylation.

In conclusion, combined inhibition of p110 $\beta$  and JNK, as well as p110 $\delta$  and JNK showed synergistic inhibitory effects on glioblastoma cell proliferation and migration via Akt, zyxin and FAK inhibition, leading to blockade of lamellipodia and membrane ruffles formation. Since SP600125 is a non-selective inhibitor against JNK1, JNK2 and JNK3, we still don't know which JNK isoform is involved in the synergism with

PI3K. Future studies focusing on silencing *JNK1* and *JNK2* will provide a better understanding on how this synergism works.

## Chapter 5 Anti-cancer effects of myricetin on glioblastoma

### 5.1 Myricetin suppresses glioblastoma cell proliferation

To evaluate the anti-proliferative effect of myricetin on glioblastoma cells, glioblastoma cells U-87 MG and U-373 MG were treated with myricetin at different concentrations for 48 hr. Myricetin is a weakly acidic flavonoid that is stable at low pH, while it will degrade under alkaline conditions (pH >8.0) [328]. Therefore, myricetin was prepared in MEM medium supplemented with HEPES (pH 7.2), a more powerful buffering agent than sodium bicarbonate, to maintain the drug's stability. Human astrocytes were also treated with myricetin to determine its cytotoxicity to normal brain tissues. Results showed that myricetin ( $\geq 20 \mu\text{M}$ ) significantly decreased U-87 MG and U-373 MG cell viability in a dose-dependent manner (Figure 5.1A-B). Although myricetin also inhibited astrocytes proliferation, the cytotoxicity is much less compared with glioblastoma cells (Figure 5.1C). U-87 MG cells treated with myricetin ( $\geq 40 \mu\text{M}$ ) detached from the surface of culture dish and displayed abnormal morphologies such as cell shrinkage, chromatin condensation and blebbing, suggesting that apoptosis might have been induced. However, the majority of cells remained normal spindle shape if treated with less than  $20 \mu\text{M}$  of myricetin, indicating that cell death in glioblastoma cells was not triggered by myricetin at these doses (Figure 5.2).

To investigate the effect of myricetin on PI3K/Akt and JNK signaling, U-87 MG

cells were treated with myricetin at different concentration for 3 hr, since this is a desirable time point to detect changes in signaling activation according to the earlier data of PI3K inhibitors. Results showed that phosphorylation of Akt at Ser473 and Thr308, as well as phosphorylation of c-Jun were downregulated by myricetin ( $\geq 5 \mu\text{M}$ ), whereas the phosphorylation of JNK did not significantly change (Figure 5.3).

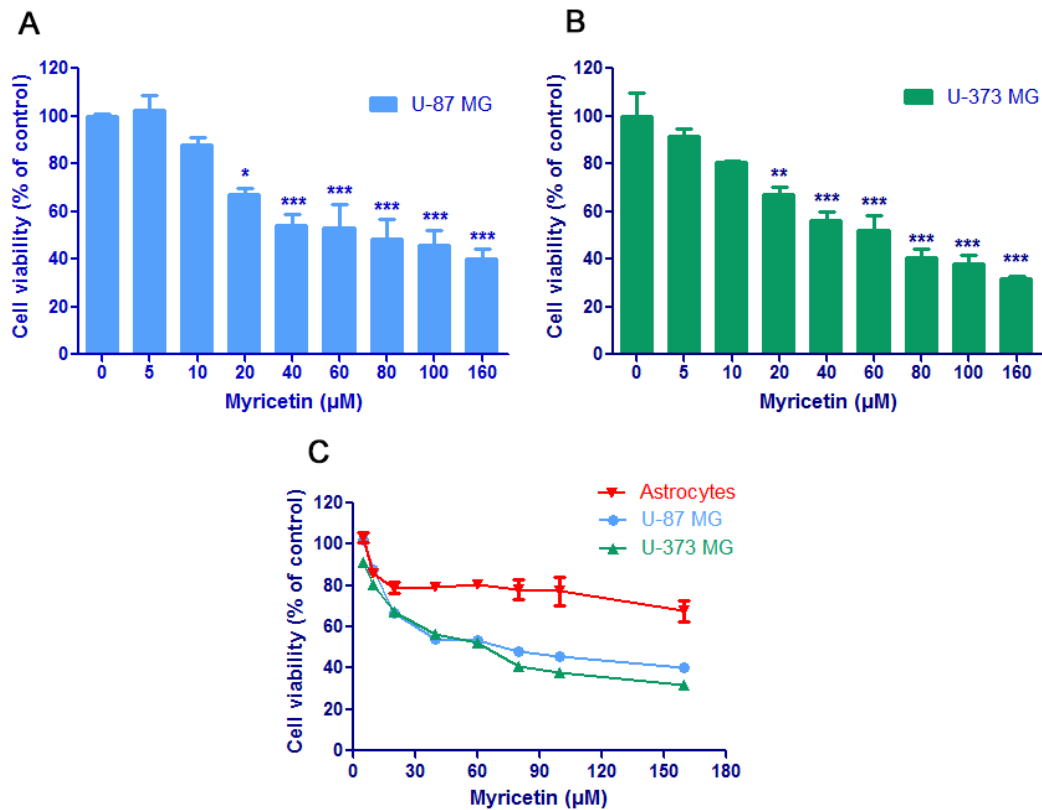


**Figure 5.1: Effect of myricetin on proliferation in glioblastoma cells and human astrocytes.** Two glioblastoma cell lines (U-87 MG and U-373 MG) and normal human astrocytes were treated with myricetin at different concentrations for 48 hr. DMSO was used as a carrier control. Myricetin significantly inhibited glioblastoma cell proliferation in U-87 MG (A) and U-373 MG (B) cells. (n=3; *p* values were determined by One-way ANOVA and Post Hoc multiple comparison Tukey HSD test. \*: *p* < 0.05; \*\*: *p* < 0.01; \*\*\*: *p* < 0.001) (C) Myricetin displayed much less toxicity on astrocytes than on glioblastoma cells.

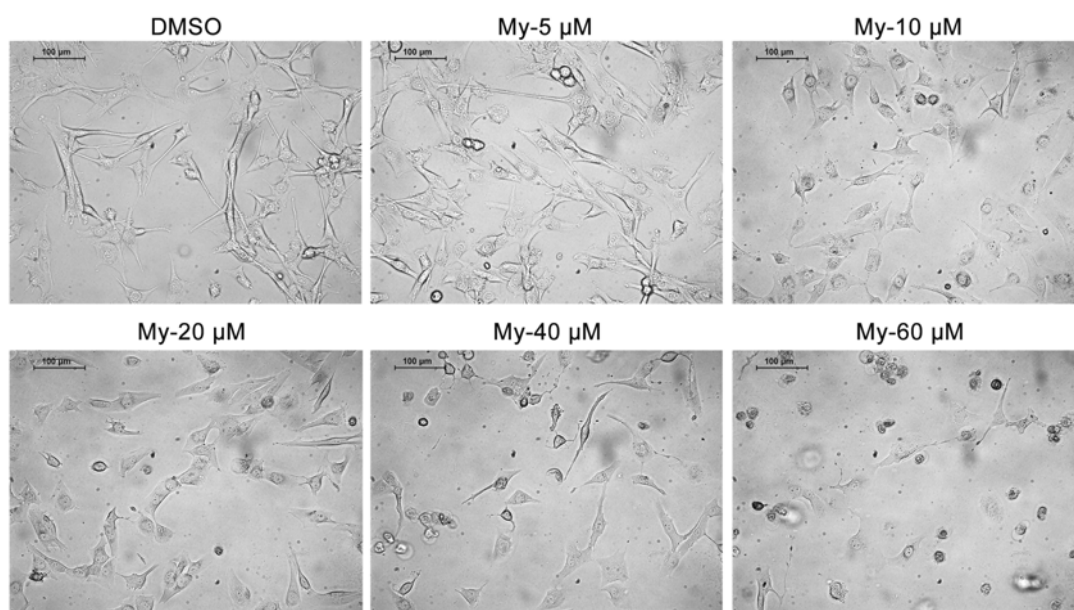


**Figure 5.2: Myricetin influenced glioblastoma cell morphology.** U-87 MG cells were incubated with myricetin (My) at different concentration for 24 hr. Cells were then photographed at 200x magnification under light microscopy. DMSO was used as a carrier control.

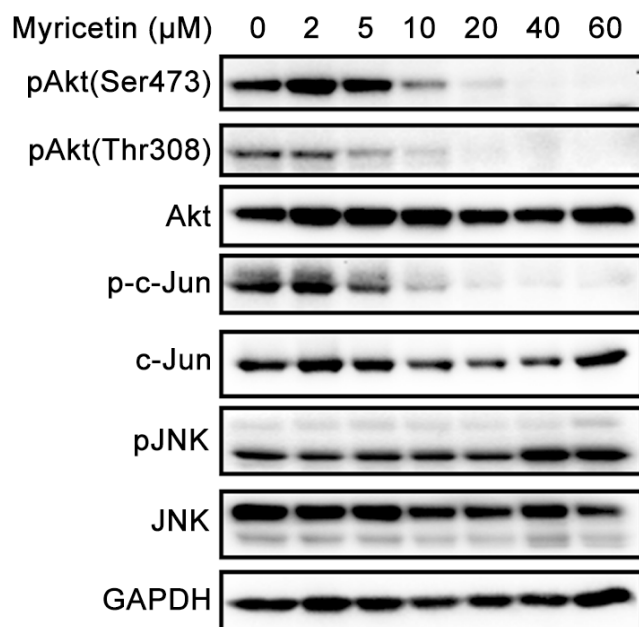


**Figure 5.3: Effect of myricetin on PI3K/Akt and JNK signaling in glioblastoma cells.** U-87 MG cells were treated with myricetin at different concentrations for 3 hr. DMSO was used as a carrier control. Expression of GAPDH was used as a loading control. The phosphorylation levels of Akt and c-Jun were decreased upon treatment with myricetin ( $\geq 5 \mu\text{M}$ ).

## 5.2 Myricetin blocks glioblastoma cell migration and invasion through targeting PI3K and JNK

Wound healing assay and transwell migration assay were performed to assess the anti-migratory effect of myricetin on glioblastoma cells. U-87 MG cells were pretreated with 5  $\mu\text{g/mL}$  of mitomycin C prior to wound production to exclude the effect of cell proliferation. Results showed that myricetin ( $\geq 10 \mu\text{M}$ ) not only prevented glioblastoma cells directionally migrating into the wounds (Figure 5.4), but also inhibited cells transmigrating through the porous membrane (Figure 5.5), indicating that glioblastoma cell migration was significantly inhibited by myricetin. In addition, transwell invasion assay was carried out to evaluate the anti-invasive effect of myricetin on U-87 MG cells. Glioblastoma cell invasion was also markedly suppressed by myricetin ( $\geq 10 \mu\text{M}$ ) (Figure 5.6).

Given that myricetin is capable of inhibiting Akt and c-Jun phosphorylation, we hypothesize that PI3K and JNK are possible targets of myricetin. To investigate the interactions between myricetin and class I<sub>A</sub> PI3K catalytic isoforms or JNK, myricetin was coupled with CNBr-Sepharose 4B beads, and then target proteins of myricetin in U-87 MG cell lysate were pulled down *ex vivo*. Results showed that p110 $\alpha$ , p110 $\beta$ , p110 $\delta$  and JNK were detected in myricetin-coupled Sepharose beads, but not in Sepharose beads alone (Figure 5.7). Akt was used as a positive control, which has been shown to bind myricetin previously, to confirm myricetin had been successfully coupled to the Sepharose beads [268].

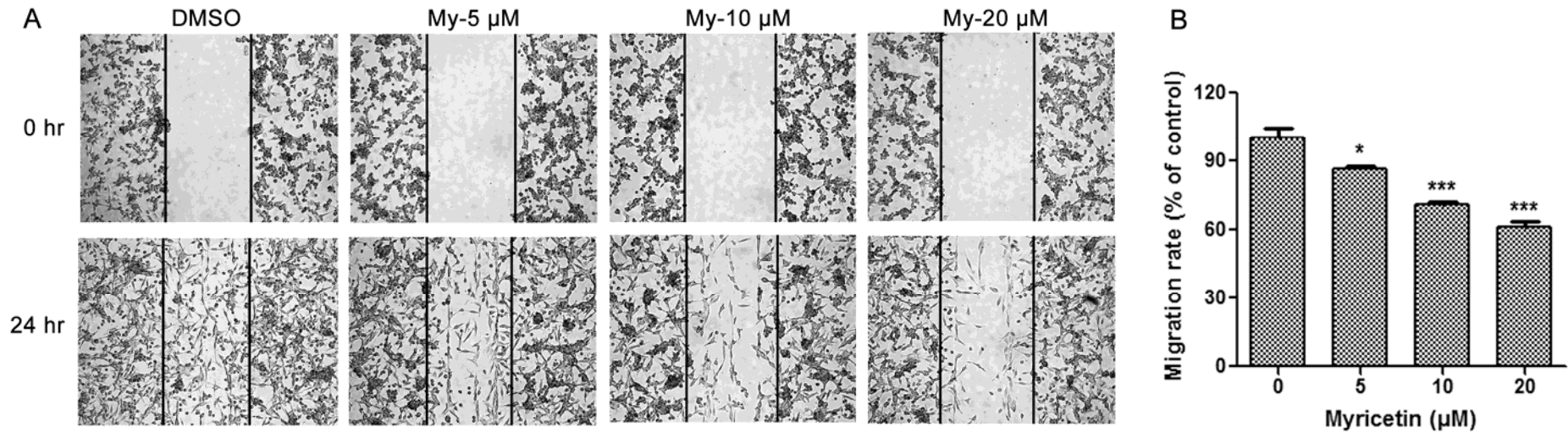


**Figure 5.4: Inhibitory effect of myricetin on directional migration of glioblastoma cells.** (A) Wound healing in U-87 MG cells treated with myricetin at different concentrations for 24 hr. Cells were pretreated with 5 μg/mL of mitomycin C for 1 hr. DMSO was used as a carrier control. The lines indicate the edges of wounds generated before drug treatment (0 hr). Photographs were obtained at 50× magnification. (B) Migration rate (%) was analyzed and expressed as the number of cells migrating into the original wounds relative to those in DMSO control. (n=3; *p* values were determined by One-way ANOVA and Post Hoc multiple comparison Tukey HSD test. \*: *p* < 0.05; \*\*: *p* < 0.01; \*\*\*: *p* < 0.001).

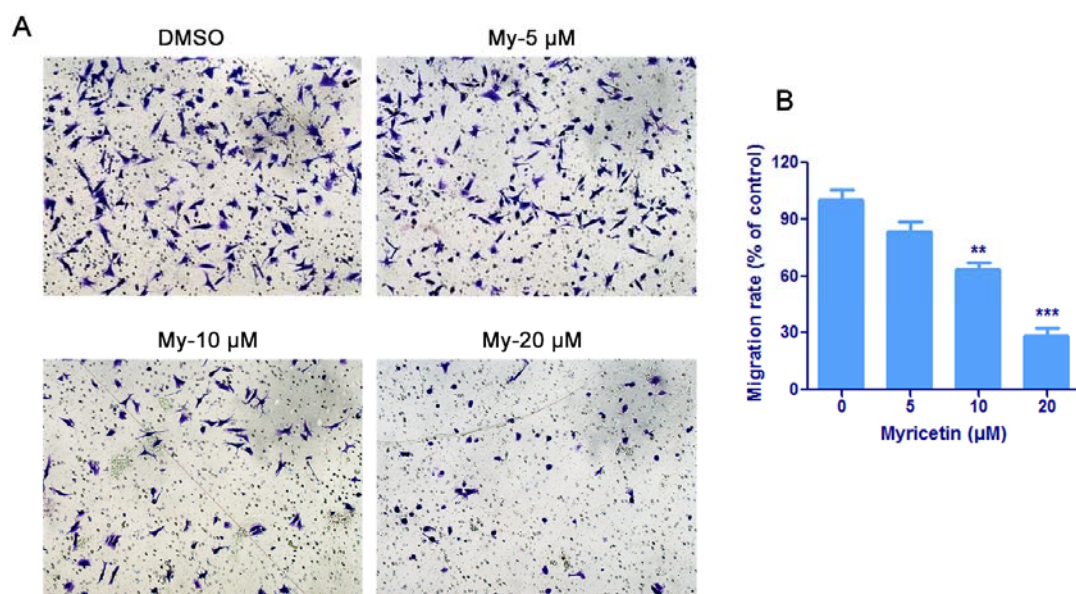


**Figure 5.5: Inhibitory effect of myricetin on glioblastoma cell transmigration.**

Boyden chamber migration assay was performed on U-87 MG cells treated with myricetin at different concentrations in serum-free medium for 24 hr. DMSO was used as a carrier control. (A) Representative photographs showing the cells that had migrated through membrane to the lower surface at 100× magnification. Cells from 5 representative fields were counted. (B) Cell migration was significantly decreased by myricetin (n=3; *p* values were determined by One-way ANOVA and Post Hoc multiple comparison Tukey HSD test. \*: *p* <0.05; \*\*: *p* <0.01).

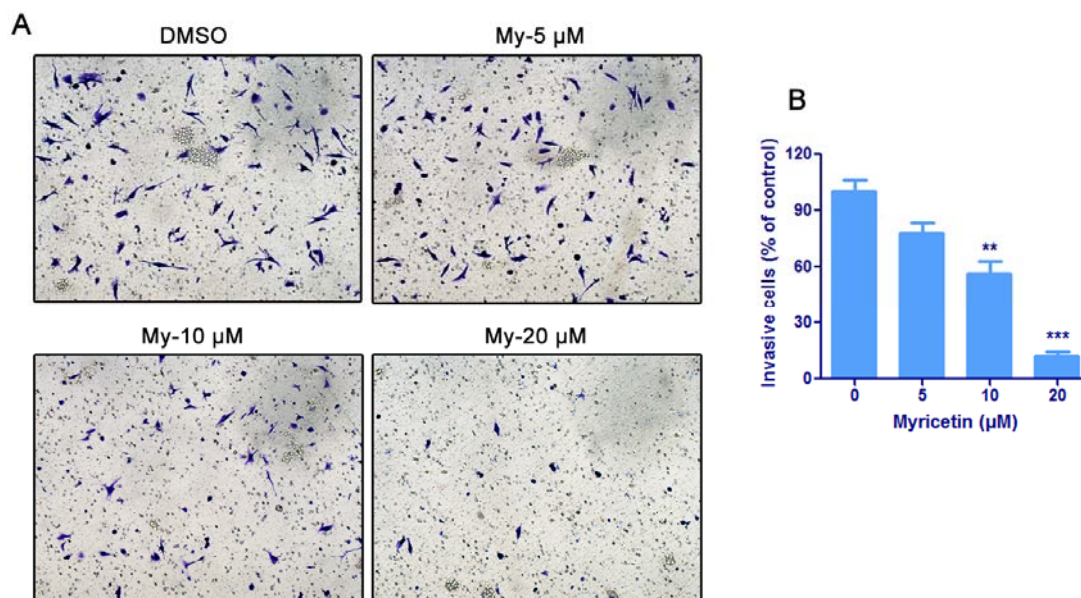


**Figure 5.6: Inhibitory effect of myricetin on glioblastoma cell invasion.** Boyden chamber invasion assay was performed in U-87 MG cells treated with myricetin at different concentrations in serum-free medium for 24 hr. DMSO was used as a carrier control. (A) Representative photographs showing the invasive cells that had passed through matrigel to the lower surface of the membrane at 100× magnification. Invaded cells from 5 representative fields were counted. (B) Number of invasive cells was significantly decreased by myricetin ( $n=3$ ;  $p$  values were determined by One-way ANOVA and Post Hoc multiple comparison Tukey HSD test. \*\*:  $p < 0.01$ ; \*\*\*:  $p < 0.001$ ).

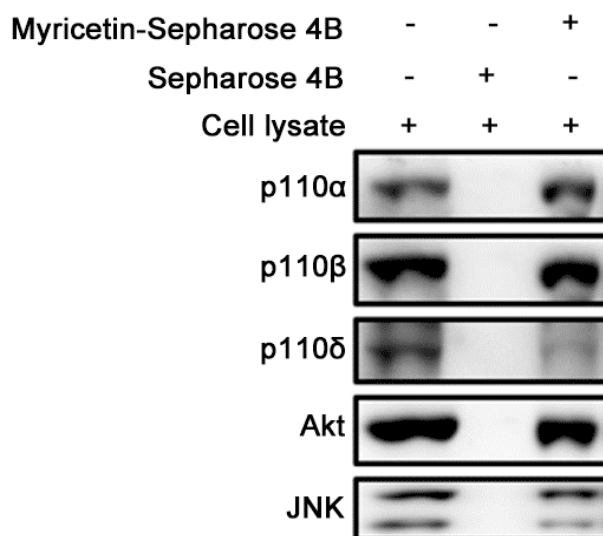


**Figure 5.7: Myricetin directly binds to PI3K and JNK.** *Ex vivo* pull-down assay was performed on U-87 MG cells. Whole cell lysate (input control), lysate with Sepharose 4B beads (negative control) and myricetin-coupled Sepharose 4B beads were applied to SDS-PAGE and then detected by Western blotting. Akt was used as a positive control, to confirm myricetin had been successfully coupled to the Sepharose beads.

### 5.3 Myricetin does not sensitize glioblastoma cells to temozolomide

Temozolomide is the most widely used chemotherapeutic agent for glioblastoma treatment. To determine the minimal effective concentration of temozolomide, its effect on proliferation of glioblastoma cells U-87 MG was investigated. Like myricetin, temozolomide was also prepared in MEM medium supplemented with HEPES (pH 7.2), since it is unstable at high alkaline pH values [15]. Results demonstrated that U-87 MG cells were sensitive to temozolomide at high concentrations ( $\geq 500 \mu\text{M}$ ), whereas temozolomide at low concentrations ( $\leq 200 \mu\text{M}$ ) did not significantly inhibit glioblastoma cell proliferation (Figure 5.8). Therefore, it would be beneficial to the patients if the sensitivity of glioblastoma cells to temozolomide could be enhanced by combination treatment.

To investigate if myricetin could sensitize glioblastoma cells to temozolomide at low concentrations, U-87 MG cells were treated with myricetin and temozolomide at a fixed ratio of 1:10, and the cell viabilities were determined by MTT method. Myricetin failed to sensitize U-87 MG cells to temozolomide ( $\leq 200 \mu\text{M}$ ) with CI  $>0.9$  (Table 5.1). The synergism was predicted to emerge when the concentrations of myricetin and temozolomide became very high (Figure 5.9). Temozolomide ( $200 \mu\text{M}$ ) alone did not suppress glioblastoma cell migration and invasion. Combined treatment of myricetin and temozolomide had no synergistic effect on either directional migration or transmigration in U-87 MG cells (Figure 5.10 and 5.11). Furthermore, myricetin did not synergize with temozolomide to inhibit cell invasion in U-87 MG cells (Figure 5.12).

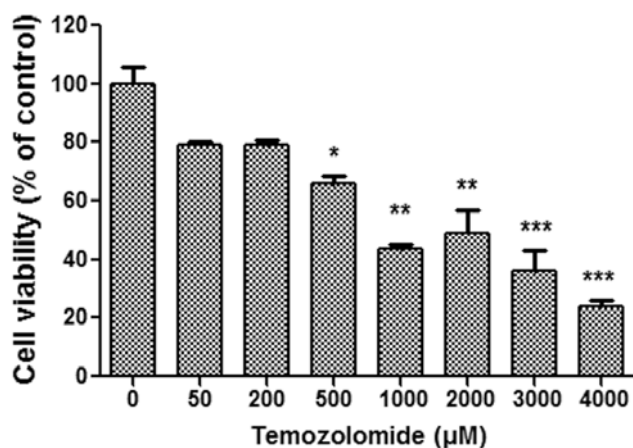


**Figure 5.8: Effect of temozolomide on glioblastoma cell proliferation.** U-87 MG cells were treated with temozolomide at different concentrations for 48 hr. DMSO at the lowest dilution (1:200) was used as a carrier control, which was comparable to the dilution of temozolomide at 4000 µM. Cell proliferation was significantly inhibited by temozolomide ( $\geq 500$  µM) ( $n=3$ ;  $p$  values were determined by One-way ANOVA and Post Hoc multiple comparison Tukey HSD test. \*:  $p < 0.05$ ; \*\*:  $p < 0.01$ ; \*\*\*:  $p < 0.001$ ).

**Table 5.1: Combination index (CI) for cell viability in U-87 MG cells treated with myricetin and temozolomide (n=3)**

<b>Myricetin (<math>\mu\text{M}</math>)</b>	<b>Temozolomide (<math>\mu\text{M}</math>)</b>	<b>FA</b>	<b>CI</b>
1	10	0.071	1.838
10	100	0.225	2.180
20	200	0.441	0.967

CI < 0.9 indicates synergistic effect; CI > 1.1 indicates antagonistic effect; CI between 0.9 and 1.1 indicates additive effect.

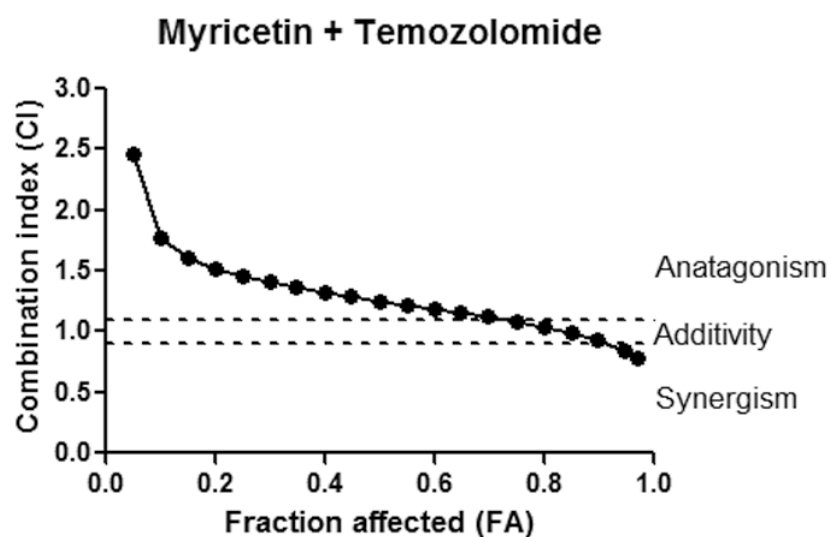


**Figure 5.9: Combination effect of myricetin and temozolomide on glioblastoma cell proliferation.** U-87 MG cells were treated with myricetin and temozolomide at a fixed ratio of 1:10 for 48 hr. FA-CI plot was automated generated by Compusyn software, representing the CI values of combination treatment of myricetin and temozolomide. Two dashed lines indicated the CI values of 0.9 and 1.1.

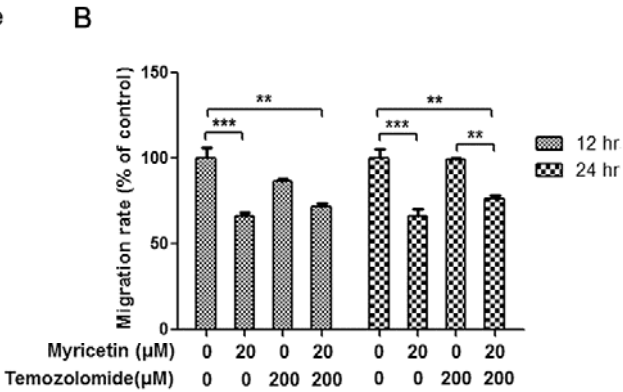
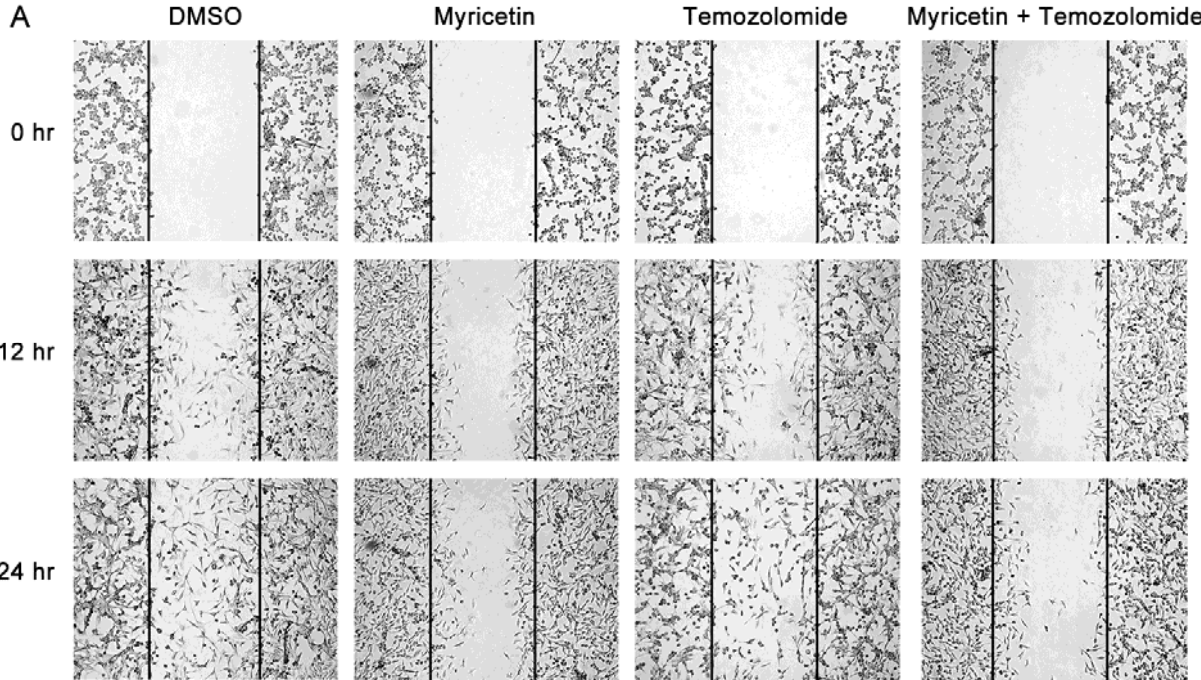


**Figure 5.10: Combination effect of myricetin and temozolomide on directional migration of glioblastoma cells.** (A) Wound healing in U-87 MG cells treated with myricetin (20  $\mu$ M) and temozolomide (200  $\mu$ M) for 24 hr. Cells were pretreated with 5  $\mu$ g/mL of mitomycin C for 1 hr. DMSO was used as a carrier control. The lines indicate the edges of wounds generated before drug treatment (0 hr). Photographs were obtained at 50 $\times$  magnification. (B) Migration rate (%) was analyzed and expressed as the number of cells migrating into the original wounds relative to those in DMSO control. (n=3; *p* values were determined by One-way ANOVA and Post Hoc multiple comparison Tukey HSD test. \*\*: *p* <0.01; \*\*\*: *p* <0.001).

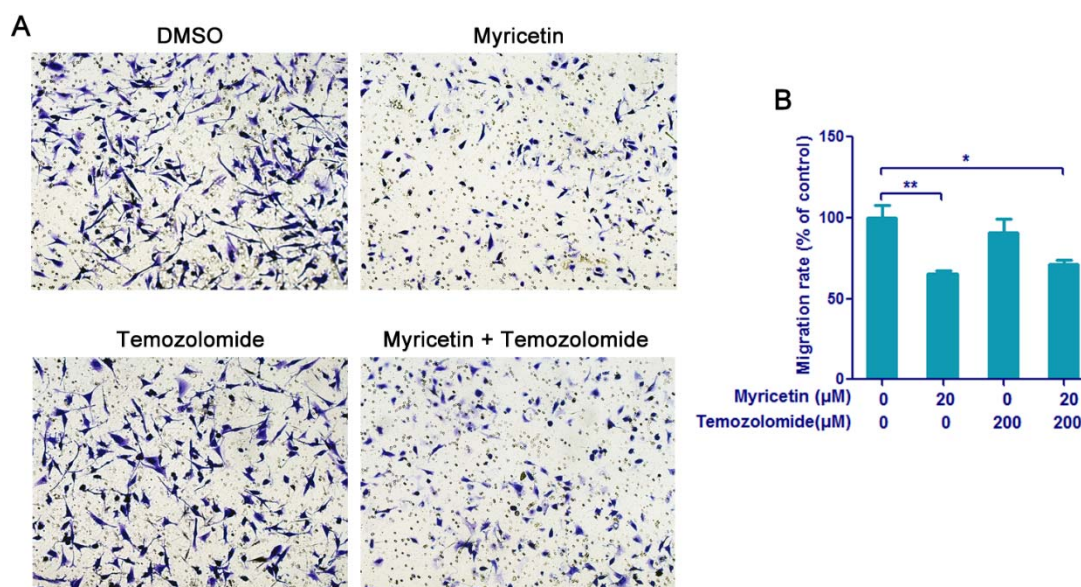


**Figure 5.11: Combination effect of myricetin and temozolomide on glioblastoma cell transmigration.** Boyden chamber migration assay in U-87 MG cells treated with myricetin (20 μM) and temozolomide (200 μM) in serum-free medium for 24 hr. DMSO was used as a carrier control. (A) Representative photographs showing the cells that had migrated through membrane to the lower surface at 100× magnification. Cells from 5 representative fields were counted. (B) Cell migration was significantly decreased by myricetin, but combination of myricetin and temozolomide did not potentiate the inhibitory effect (n=3; *p* values were determined by One-way ANOVA and Post Hoc multiple comparison Tukey HSD test.

\*: *p* < 0.05; \*\*: *p* < 0.01).

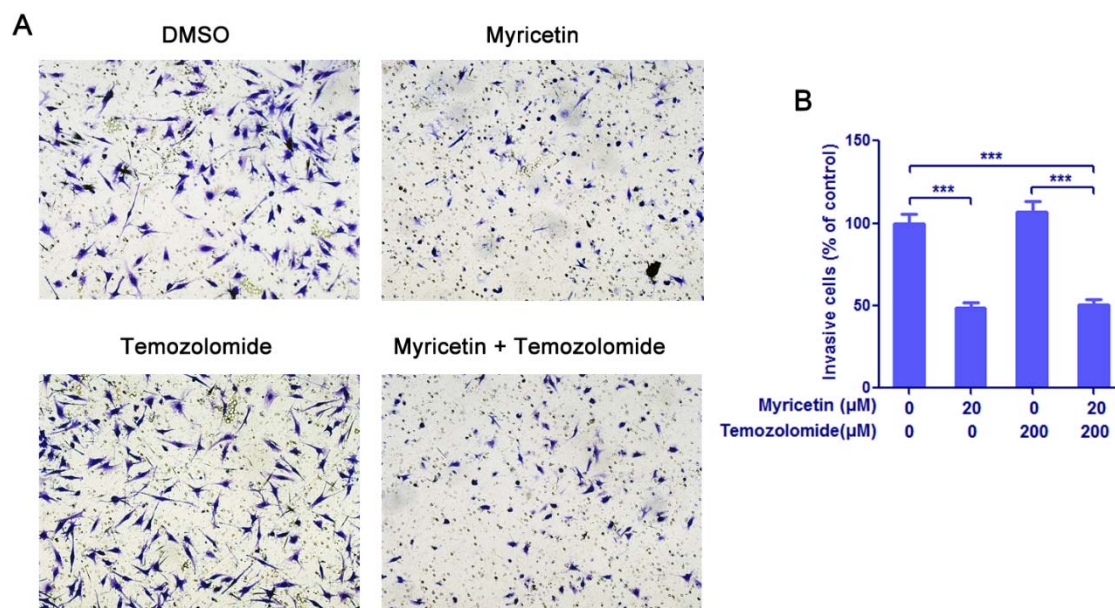


**Figure 5.12: Combination effect of myricetin and temozolomide on glioblastoma cell invasion.** Boyden chamber invasion assay of U-87 MG cells treated with myricetin (20  $\mu\text{M}$ ) and temozolomide (200  $\mu\text{M}$ ) in serum-free medium for 24 hr. DMSO was used as a carrier control. (A) Representative photographs showing the invasive cells that had passed through matrigel to the lower surface of the membrane at 100 $\times$  magnification. Invaded cells from 5 representative fields were counted. (B) Number of invasive cells was significantly decreased by myricetin, but combination of myricetin and temozolomide did not potentiate the inhibitory effect ( $n=3$ ;  $p$  values were determined by One-way ANOVA and Post Hoc multiple comparison Tukey HSD test. \*\*\*:  $p < 0.001$ ).

## 5.4 Discussion

### 5.4.1 Myricetin is a natural flavonoid with potent anti-cancer activity

Myricetin is a bioactive polyphenol that possesses anti-oxidant, anti-inflammatory and anti-cancer activities. However, most studies focus on the anti-cancer effect of quercetin, an structural analogue of myricetin, that is more abundant content in berries and tropical plants [329, 330]. Both myricetin and quercetin contain the 3' and 4' hydroxyl groups on the B-ring, while the only difference between them is the 5' -OH. The anti-oxidant activity of flavonoid is determined by the configuration and total number of B-ring -OH, which is a donor of hydrogen and an electron to radicals. It has been reported that the 3' and 4' hydroxyl groups on the B-ring play a more crucial role in the radical scavenging activity than 5' -OH, indicating the anti-oxidant activities of myricetin and quercetin are comparable [262, 263]. Another flavonol kaempferol is less abundant in tropical berries and plants, and has a lower anti-oxidant activity than myricetin and quercetin since it only contains a 4' -OH [262, 263, 329, 330]. The anti-oxidant activity of myricetin is higher than quercetin on protecting lymphocytes from oxidative DNA damage, while kaempferol is least effective [331]. Numerous studies have shown that quercetin suppresses cell proliferation, migration, invasion *in vitro* and tumor growth *in vivo* in a wide range of cancers, including breast, prostate, lung, colon and pancreatic cancers [332-336]. Evidence reveals that myricetin exerts higher inhibitory effect on prostate cancer cell proliferation and viability [337]. Myricetin and kaempferol are more

effective in suppressing medulloblastoma cell migration than quercetin through inhibition of Akt and Met activation [338]. These findings suggest that myricetin may be a more effective therapeutic drugs for cancer treatment than quercetin.

Quercetin also shows a potent anti-cancer effect on glioblastoma. It impedes glioblastoma cell proliferation and migration, and induces apoptosis through inactivating JAK1/STAT3 signaling and decreasing cyclin D1 expression and MMP-2 activity [339, 340]. Quercetin promotes apoptosis and disrupts mitochondrial membrane potential in glioblastoma cells via increasing p53 expression and activating caspases-3/-9 [341]. However, few studies report the anti-cancer effect of myricetin on glioblastoma. Evidence shows that combination of myricetin and tumor necrosis factor-related apoptosis-inducing ligand (TRAIL) induces apoptosis in glioblastoma cells via increasing caspases-8/-9 and caspases-3/-7 activities and decreasing c-FLIP and Bcl-2 expression [279]. In addition, myricetin inhibits peroxide production, COX-2/PGE2 expression and MMP-9 activity to block TPA-induced migration and invasion in glioblastoma cells [280]. We also found that myricetin was capable of suppressing glioblastoma cell proliferation, migration and invasion via blockage of PI3K/Akt and JNK signaling.

Quercetin is a natural PI3K inhibitor, of which 3'- and 4'- hydroxyl groups on the B-ring interact with PI3K by hydrogen bonds [342]. It promotes apoptosis in melanoma cells via blockade of PI3K/Akt and ERK activation [343]. Quercetin also suppresses migration and invasion of H-Ras-induced breast epithelial cells through inactivation of PI3K/Akt and MMP-2 [344]. Similar to quercetin, myricetin can directly

bind to PI3K and downregulate its kinase activity [278, 342]. However, it is unclear which PI3K isoform interacts with myricetin. Several targets of myricetin have been identified recently, including Akt, MEK1, MKK4, JAK1, Fyn and RAK2, via an ATP-competitive or -noncompetitive manner [268, 269, 271, 275, 283]. Considering that the phosphorylation levels of Akt and c-Jun were reduced by myricetin, PI3K and JNK may be the targets of myricetin. Here, we found that all the three class I<sub>A</sub> PI3K catalytic isoforms (p110 $\alpha$ , p110 $\beta$  and p110 $\delta$ ) bound to myricetin. Myricetin also interacted with JNK and decreased its activity. Therefore, class I<sub>A</sub> PI3K catalytic isoforms and JNK are identified as the targets of myricetin.

#### **5.4.2 Combination treatment of myricetin and temozolomide**

Temozolomide is the most widely used chemotherapeutic agent for glioblastoma treatment. Its efficacy is highly correlated with the MGMT promoter methylation status in GBM patients [345]. PTEN and p53 status may also influence the response of glioblastoma to temozolomide. Evidence demonstrates that loss of PTEN function confers the resistance of glioblastoma cells to temozolomide, while restoration of wild-type PTEN or inhibition of Akt activation increases the sensitivity [346]. It is supported by a cohort study that *PTEN* deletion is positively correlated with poor survival of glioblastoma patients receiving radiotherapy and concomitant temozolomide [142]. However, there are controversies on PTEN loss leading to increased sensitivity of glioblastoma cells to temozolomide [347, 348]. Double-strand breaks induced by a functional analogue of temozolomide cannot be efficiently

repaired in astrocytes with loss of PTEN, resulting in increased apoptosis [347]. It is also reported that the prognosis of GBM patients received radiotherapy and concomitant temozolomide is not associated with PTEN status [348]. Till now, there is also no clear consensus about the relationship between p53 status and sensitivity of glioblastoma cells to temozolomide. Glioblastoma cells with p53 deficiency exhibit higher sensitivity to temozolomide *in vitro* and *in vivo*, leading to prolonged cell cycle arrest, increased apoptosis and decreased viability [349-352]. Supporting evidence shows that wild-type p53 expression is not a positive prognostic factor for GBM patients [353, 354]. On the contrary, inhibition of wild-type p53 function attenuates the sensitivity of glioblastoma cells to temozolomide, leading to elevated viability, more colonies formation and decreased apoptosis [355-357]. It is also supported by studies that wild-type p53 expression is positively correlated with long survival of GBM patients [358, 359]. Taken together, the response of glioblastoma cells to temozolomide can be dependent or independent on the PTEN and p53 status.

To improve the prognosis of GBM patients, it would be an attractive option if the sensitivity of glioblastoma cells to temozolomide can be increased through combination with other drugs. Several studies report that quercetin is able to increase glioblastoma cell sensitivity to temozolomide, leading to inhibition of cell viability and induction of apoptosis by decreasing Hsp27 expression. However, these studies do not calculate the combination index, or no statistical analysis is shown between the combination and single drug treatments, thus it is unknown whether the combination effect is synergism or additivity [281, 282]. A study also shows that

quercetin combined with irradiation and temozolomide further decreases glioblastoma cell viability and promotes apoptosis compared with treatment of irradiation and temozolomide [360]. However, combination of irradiation and quercetin shows no significant difference with the combination of irradiation and temozolomide, and the combination of quercetin and temozolomide is not mentioned. Therefore, it is still unclear whether quercetin is able to synergize with temozolomide on glioblastoma cells, not to mention the combination effect of myricetin and temozolomide. We found that myricetin was not able to sensitize glioblastoma cells to temozolomide at low concentrations in the inhibition of proliferation, migration and invasion. The FA-CI plot predicted that this combined treatment only has synergistic effect when the concentrations of myricetin and temozolomide are very high, which is impossible for clinical application. Similarly, quercetin at low concentrations antagonizes with cisplatin, taxol, pirarubicin or 5-Fluorouracil on inhibition of ovarian cell viability and tumor growth, whereas quercetin at high concentrations combined with cisplatin displays no significant difference with cisplatin alone [361]. Decreased intracellular ROS level and increased SOD1 expression are detected in both ovarian cells and xenograft tumor, indicating that quercetin at low concentrations may antagonize with cisplatin through alleviating the oxidative stress induced by this chemotherapeutic agent.

Since the status of MGMT, p53 and PTEN can influence the response of glioblastoma cells to temozolomide, they may also have an impact on the combination effect of myricetin and temozolomide. Besides, glioblastoma stem-like

cells exhibit resistance to temozolomide via a MGMT-independent manner [362]. The response of these cells to temozolomide may be determined by the status of multidrug resistance 1 (MDR1, ABCB1), ATP-binding cassette subfamily G member 2 (ABCG2) and PTEN [363]. Thus, glioblastoma stem-like cells may also influence the combination effect of myricetin and temozolomide.

## **Chapter 6 General discussion and conclusions**

### **6.1 Introduction**

One of the well-known characteristics of glioblastoma multiforme is the extensive infiltration to neighboring normal brain parenchyma, correlated with highly migration and invasion capacities of tumor cells. Cell migration is a complex biological process that requires the participation of various protein kinases, scaffold proteins and extracellular matrix molecules. Inhibition of the protein kinases or lipid kinase such as PI3K and JNK, which play pivotal roles in cell motility, may be attractive options for glioblastoma treatment. Pharmacological inhibition using synthetic kinase inhibitors or natural flavonoids, as well as siRNA-induced gene silencing are promising therapeutic approaches.

### **6.2 Regulation of cancer cell migration by FAK and zyxin signaling**

Cell migration is a complicated biological process including actin polymerization, protrusion formation, adhesion complexes formation, turnover of focal adhesion, and retraction at the cell rear [321, 364, 365]. A variety of cytoskeletal structures including lamellipodia, filapodia, focal adhesion, stress fibers, and membrane ruffles are essential to a motile cell, providing adhesion sites and contractile forces for cell movement. Cell migration can be divided into multiple cyclical steps. Initially, activated by an external or internal signaling, actin polymerizes to form actin filaments, leading to the formation and forward extension of lamellipodia. Focal

adhesion complexes is then formed at the edge of lamellipodia to provide attachment of cell protrusion to the extracellular matrix. The cell body is pulled forward by the contractile tension of stress fiber, and focal adhesion turnover at the rear of cell leads to released cell-to-ECM adhesion to allow cell retraction. These steps are repeated to drive cell movement.

Focal adhesion is a cellular structure providing attachment of cells through integrin-mediated linkage of actin cytoskeleton and ECM components such as fibronectin, collagen, laminin and vitronectin. Focal adhesion complex consists of integrin clusters and other scaffold proteins like paxillin, talin, p130Cas, zyxin, vinculin and  $\alpha$ -actinin [366]. When ECM ligands bind to the extracellular domain of integrin, the latter undergoes dimerization and recruit talin, vinculin and  $\alpha$ -actinin to build the connection with actin filaments and regulate various cellular processes [303, 367]. FAK and Src kinase play crucial roles in integrin-mediated signal transduction. The cytoplasmic domain of integrin  $\beta$ 1 has been shown to interact with FAK [368]. Autophosphorylation of FAK at Tyr397 leads to its binding to the SH2 domain of Src and Fyn kinases, and then phosphorylates the focal adhesion proteins paxillin and p130Cas [369]. PI3K p85 subunit is also recruited to FAK through SH2 domain and then phosphorylation of FAK at Tyr925 in the C-terminal region triggers the Ras-dependent activation of MAPK pathway [370]. Evidence demonstrates that knockout of FAK in mouse embryonic fibroblasts inhibits cell spreading and impedes PI3K-mediated Rac1 activation, leading to altered location of Rac1 at focal adhesion [371]. These findings suggest that integrin/FAK/Src/PI3K/Rac1 signaling axis plays

an essential role in cell migration and focal adhesion.

The balance between focal adhesion formation and turnover are crucial to cell adhesion and migration. More active focal adhesion turnover than formation leads to unstable adhesion and rapid cell migration [366]. Enhanced formation and retarded turnover of focal adhesion have been shown in FAK-deficient cells [372]. FAK phosphorylation status at Tyr925 is vital to cell migration and focal adhesion turnover. Inhibition of FAK phosphorylation at Tyr925 reduces phosphorylation of paxillin and activates Rac1, leading to stabilization of focal adhesion, inhibition of cell protrusion and migration [327].

Zyxin is a zinc-binding phosphoprotein located at focal adhesion and actin cytoskeleton. It recruits Ena/VASP family through N-terminal ActA proline-rich domain to regulate actin filament assembly, and facilitates focal adhesion by interacting with specific proteins through C-terminal LIM domains [322]. Ena/VASP proteins including Mena, VASP and EVL, which are accumulated in focal adhesions, lamellipodia and filopodia, directly regulate actin polymerization and F-actin branching, protect the barbed end of actin filament from binding with capping proteins [373, 374]. Ena/VASP-deficient cells display slow movement of lamellipodia and short actin filaments, suggesting Ena/VASP proteins regulate cell migration through elongation of actin filaments and reduced protrusion of lamellipodia [373, 375]. The LIM domain is a protein domain with zinc-finger structure that provides protein-binding interface [376]. LIM domain plays an important role in targeting zyxin to focal adhesion and stress fiber [377, 378]. The interaction of LIM domains and

adaptors requires phosphorylation of zyxin at Ser142 [323]. Zyxin also interacts with  $\alpha$ -actinin to locate at focal adhesion and stress fiber [379]. Evidence shows that knockdown or inhibition of zyxin leads to blockade of cell spreading and migration [324]. Besides, zyxin is involved in stress fiber stabilization and remodeling through its recruitment to stress fibers and interaction with Ena/VASP and  $\alpha$ -actinin [325, 326]. P130Cas regulates the focal adhesion localization of zyxin and  $\alpha$ -actinin, and activation of MAPK pathway controls zyxin phosphorylation at stress fiber [325]. Here, we showed that inhibition of JNK activity gave rise to decreased phosphorylation of zyxin and stabilization of focal adhesion, indicating that JNK may control the regulation of zyxin in migration.

As cell migration is a crucial step in glioblastoma progression, inhibition of integrin/FAK/Src/PI3K/Rac1 and JNK/zyxin/Ena/VASP/ $\alpha$ -actinin signaling axes may be promising for GBM treatment.

### **6.3 Therapeutic implications of pharmacological inhibition and siRNA-induced gene silencing**

Pharmacological inhibition is an approach for studying protein functions, which utilizes chemical compounds to directly inhibit the activity of target protein without affecting its expression. Selective protein kinases inhibitor is not only a useful tool for investigating the role of the given target in diseases, but also a promising therapeutic approach. To date, more than 50 protein kinase are identified as oncoproteins, and more than 130 kinase inhibitors have entered into clinical trials for cancer treatment

[380, 381]. For example, gefitinib and erlotinib are selective tyrosine kinase inhibitor for EGFR are approved for the treatment of non-small cell lung cancer (NSCLC), and have entered phase I/II clinical trials for glioblastoma treatment [37, 38]. Most of the kinase inhibitors exert their roles in an ATP-competitive manner, through binding to the ATP-binding sites of kinases. Similar with siRNAs-induced gene silencing, kinase inhibitors also have off-target effects, since the capacity of blocking ATP binding may display the same effect on other classes of kinases [382]. To control this off-target effect,  $IC_{50}$  value of kinase inhibitor on target inhibition should be measured to ensure the specificity.

RNA interference (RNAi) is a post-transcriptional gene silencing approach which is carried out by synthetic siRNAs or endogenous microRNAs (miRNAs) to selectively silence target genes. The guide strand of siRNA or microRNA is incorporated into the RNA-induced silencing complex (RISC), and then guides the silencing complex to target mRNA, leading to mRNA degradation or translation attenuation [383, 384]. RNAi is now widely used to investigate gene functions and emerging as a novel approach for disease treatment. However, off-target effects and limitation of siRNA delivery *in vivo* greatly constrain its therapeutic application. The off-target effects are classified into three categories: microRNA-like off-target effects, immune response, and saturation of endogenous RNAi machinery [385, 386]. The microRNA-like off-target effect is the most common effect induced by the 5' end of siRNA guide strand mismatching to the 3'UTR of non-target mRNA, and the siRNA acts as a microRNA to prevent a number of genes from translating. This type of

off-target effect is able to trigger cytotoxicity and phenotype alternation, resulting in false-positive phenotypes and much more complicated outcomes [386]. Pooling of multiple siRNAs targeting the same gene and chemical modification of the seed region of siRNA have been shown to be favorable strategies to attenuate this off-target effect.

Immune response-mediated off-target effect is due to the siRNAs being recognized as foreign pathogen-associated molecules by Toll-like receptors [387]. The innate immune system is stimulated, followed by released of cytokines and interferons, leading to cytotoxicity in a nucleotide sequence-dependent manner. Therefore, optimized design of siRNA sequence and chemical modification such as 2'-O-methyl modification could suppress Toll-like receptors-mediated siRNA recognition and minimize the immune response [388, 389]. Exportin 5 is a dsRNA-binding protein that mediates nuclear export of pre-microRNA or shRNAs (short hairpin RNAs). Due to the limited capacity of this protein, it can be easily saturated by exogenous siRNAs or shRNAs, and thus affects endogenous miRNAs function. Moreover, the major barriers, including rapid degradation by nucleases, excretion by renal filtration, nonspecific accumulation and poor cellular uptake, can give rise to the low efficiency and specificity of siRNAs-mediated gene silencing *in vivo* [390, 391]. Owing to these limitations, there is still a long way to go before siRNA could be used as a therapeutic approach.

The phenotypes arising from pharmacological inhibition and siRNAs-induced gene silencing are different due to the distinct mechanisms involved. Selective

kinase inhibitor disrupts the functions of target protein through attenuating its activity, whereas the protein expression level is decreased by siRNAs via degradation of target mRNA. Therefore, protein-protein interaction and kinase-independent function mainly contribute to the divergent phenotypes. Some kinases still exert other functions even if their kinase domains are inhibited by selective inhibitors or expression of kinase-dead mutant. For example, FAK knockout mice show embryonic lethality, while expression of kinase-dead mutant of FAK in those mice is sufficient to support embryonic development, indicating that the kinase-independent function of FAK is crucial for embryogenesis [392]. Besides, kinase inhibitors and siRNAs have divergent effects on protein-protein interaction. This interaction is disrupted by siRNAs due to the reduced expression of the protein, whereas the protein treated with inhibitor still maintains the interaction with other proteins. It has been shown that the competitive interaction between p110 $\alpha$  and p110 $\beta$  for RTK binding sites gives rise to distinct phenotypes induced by p110 $\beta$  knockout and its selective inhibitor [301]. Knockout of p110 $\beta$  leads to more active p110 $\alpha$  binding to RTKs and elevated PI3K activity, which in turn potentiates tumorigenesis. Conversely, a p110 $\beta$  selective inhibitor suppresses tumor formation by inhibiting PI3K activity and Akt activation, since inactive p110 $\beta$  still occupies the binding sites of RTKs [301].

## 6.4 Drug resistance to single agent and implications for combination therapies

Emerging drug resistance to kinase inhibitors has become the major challenge for cancer treatment. Point mutation occurring at the gatekeeper residue, usually a threonine close to the active sites of protein kinases, influences the affinity for ATP binding, which is regarded as the main cause of resistance to kinase inhibitors [381]. The gatekeeper mutations at T670I residue in *c-Kit*, as well as at T315I residue in *BCR-ABL*, have been reported to confer resistance to imatinib in chronic myeloid leukemia (CML) and GIST patients [393, 394]. In addition, in response to the inhibition of target kinase, compensatory activation of other signaling pathways may restore downstream signaling and leads to drug resistance. For example, rapamycin and its analogs targeting mTOR complex 1 (mTORC1) trigger a negative feedback loop to augment Akt activation, leading to the resistance in glioblastoma [162, 395]. Inhibition of PI3K also results in the compensation of MEK/ERK signaling induced by activation of RTKs such as HER2 (human epidermal growth factor receptor 2) in breast cancer [396]. Amplification of *MET* proto-oncogene leads to activation of hepatocyte growth factor (HGF)/MET signaling, and confers resistance in colorectal cancer to anti-EGFR drugs cetuximab or panitumumab [397].

Since clinical response to a single drug may be limited in cancer treatment, combination of different kinase inhibitors is an attracting alternative to overcome drug resistance and achieve high efficacy. The inhibitors in the combination could simultaneously target kinases either in the same or different pathways. A well-known

combination therapy using inhibitors targeting PI3K/Akt/mTOR and Ras/MEK/ERK signaling pathways has been shown to overcome the resistance to PI3K inhibitor in a diverse range of cancers. Preclinical studies show that combined inhibition of PI3K and MEK has synergistic effect on blockade of tumor growth and induction of apoptosis in pancreatic cancer and nasopharyngeal carcinoma [398, 399]. This combination therapy has entered the phase I clinical trials [400].

In addition, dual blockade of PI3K and other kinases such as mTOR, cyclin-dependent kinase (CDK), MKK4, HER3 or JAK2 also exhibits synergism on cancer treatment [96, 97, 256, 401, 402]. Combination of CDK1/2 and PI3K inhibitors efficiently induces apoptosis in glioma cells *in vitro* and *in vivo* [97]. Inhibition of PI3K/mTOR also trigger a negative feedback loop in the activation of JAK2/STAT5 signaling pathway, and dual inhibition of PI3K/mTOR and JAK2 abrogates this feedback loop and display synergistic effect on suppressing tumor growth and metastasis in breast cancer [402]. Thus, the work focusing on kinase inhibitors is helpful to better understand the mechanism of emerging drug resistance and develop novel molecular targets for effective combination therapy.

## **6.5 Anti-cancer effect and therapeutic implications of natural flavonoids**

Paclitaxel, vinblastine and the derivative of camptothecin such as irinotecan and topotecan from natural plants have been widely used for cancer treatment, suggesting that natural chemical compounds could be promising anti-cancer drugs [403-406]. As a natural kinase inhibitor, flavonoids exhibit potent anti-cancer effect in

a wide range of cancers. Evidence shows that baicalein and myricetin among 11 flavonoids exhibit cytotoxic effect on CML cells rather than peripheral blood mononuclear cells [407]. The pro-apoptotic effect of 22 flavonoids on lymphoma cells has been evaluated, and chrysin, genistein, apigenin, quercetin, fisetin, luteolin,  $\alpha$ -naphthoflavone, galangin and 3,7-dihydroxyflavone significantly impede cell viability and promote apoptosis through activation of caspases-3 and -8 [408].

Preclinical studies also suggest the inhibitory effects of flavonoids on tumorigenesis, tumor growth and progression. Natural polyphenolic compounds quercetin and ellagic acid significantly decrease incidence of lung cancer in mice induced by N-Nitrosodiethylamine through inhibition of lipid peroxidation, highlighting the chemopreventive effect of flavonoids [409]. Quercetin and apigenin suppress melanoma growth and metastatic potential to the lung in mice [410]. Luteolin combined with ellagic acid and punicic acid from pomegranate juice inhibit prostate cancer growth, angiogenesis and metastasis *in vivo* by blocking IL-8 and VEGFR activation [411].

Several flavonoids have entered clinical trials due to the encouraging findings of their anti-cancer effects *in vitro* and from preclinical studies. Flavopiridol (Alvocidib™) is a synthetic flavone derived from rohitukine, which is isolated from an Indian plant *Dysoxylum binectariferum*. It is the first ATP-competitive CDKs inhibitor for clinical trials and has been approved by FDA for the treatment of acute myeloid leukemia (AML) [412]. To date, flavopiridol has been tested in numerous clinical trials for the treatment of a variety of cancers including non-Hodgkin's lymphoma, multiple

myeloma, melanoma, prostate, lung, pancreatic and ovarian carcinomas [413-419]. Other flavonoids such as quercetin, epigallocatechin-3-gallate and genistein have also been tested in clinical trials [420-422].

A number of flavonoids such as quercetin, myricetin, luteolin, wogonin and genistein have been shown to exert potent anti-cancer effect on glioma cells *in vitro* [279, 339, 423-425]. However, few studies have reported their effects *in vivo* or in clinical trials, suggesting that there are lots of challenges such as blood-brain barrier, systematic delivery and tissue specificity to be overcome before being used for GBM treatment.

## 6.6 Conclusions

In summary, the isoform-selective PI3K inhibitors displayed distinct effects on glioblastoma cell proliferation, migration and invasion *in vitro*. Inhibition of p110 $\alpha$  was sufficient to suppress glioblastoma cell viability, migration and invasion. The p110 $\beta$  and p110 $\delta$  inhibitors exhibited synergistic effects with JNK inhibitor to suppress glioblastoma cell proliferation and migration through inhibition of Akt, FAK and zyxin phosphorylation, resulting in the blockade of lamellipodia and membrane ruffles formation. More importantly, these inhibitors, either alone or in combination, are much less toxic to astrocytes than glioblastoma cells. Based on the results from this study, a competition model between p110 $\alpha$ , p110 $\beta$  and p110 $\delta$  was proposed, in which p110 $\beta$  and p110 $\delta$  compete with p110 $\alpha$  for RTK binding, and a crosstalk model between PI3K isoforms and JNK is suggested to illustrate the combination effects of

isoform-selective PI3K inhibitors and JNK inhibitor. A natural flavonoid myricetin targeting p110 $\alpha$ , p110 $\beta$ , p110 $\delta$  and JNK also showed inhibitory effects on glioblastoma cell proliferation, migration and invasion. Taken together, combination therapy via concurrent inhibition of PI3K/Akt and JNK pathways, especially p110 $\beta$  or p110 $\delta$  and JNK, is a promising approach for glioblastoma treatment.

### 6.7 Suggestions for future research

Synergistic effects of concurrent inhibition of p110 $\beta$ /p110 $\delta$  and JNK on glioblastoma cell viability and motility *in vitro* were observed in this study. However, SP600125 is a reversible ATP-competitive inhibitor with broad spectrum against JNK1, JNK2 and JNK3, and also has off-target effects on the activation of Aurora A, TrkA, FLT3 kinases with similar selectivities [288, 426]. It also inhibits the activities of MKK4 and p38 kinases at high concentrations [288, 427]. Therefore, it is important to clarify which JNK isoform(s) is(are) involved in the synergism with PI3K. In addition, *in vivo* study using a glioblastoma xenograft model in nude mice is required to further evaluate the combination effects of p110 $\beta$ /p110 $\delta$  and JNK inhibition on glioblastoma growth and progression.

Both JNK1 and JNK2 play important roles in cancer cell migration and invasion. Knockdown of both *JNK1* and *JNK2* sensitizes glioblastoma cells to cisplatin, leading to decreased cell viability and colony formation [428]. JNK2 $\alpha$ 2 isoform is constitutively activated and involved in the tumor formation and growth of glioblastoma [232]. In this study, inhibition of JNK was able to impede glioblastoma

cell migration and invasion. However, the role and mechanism of individual JNK isoform in glioblastoma cell motility is not fully elucidated. Novel strategies including zinc finger nuclease (ZFN), transcription activator-like effector nuclease (TALEN) and clusters of regularly interspaced short palindromic repeats and the Cas9 endonuclease (CRISPR/Cas9)-mediated systems become very effective and promising genome editing approaches *in vitro* and *in vivo* [429-431]. Therefore, knockout of *JNK1* and *JNK2* in glioblastoma cells can be performed using one of these gene editing systems to further investigate the individual role of JNK isoforms in glioblastoma cell motility.

Given that knockdown of *PIK3CD* showed inhibitory effects on glioblastoma cell proliferation, migration and invasion, p110 $\delta$  may be required for the development and progression of glioblastoma multiforme. Overexpression of p110 $\delta$  has been shown in glioblastoma cell lines and *ex vivo* culture of GBM specimens [104, 292]. However, the expression level of p110 $\delta$  in glioma tissues, as well as its correlation with prognosis and tumor grade have not been systematically determined. Therefore, future investigation into these will provide insights on the importance of p110 $\delta$  in glioblastoma multiforme.

The mechanism in which myricetin suppresses glioblastoma cell motility is unclear yet. Further evaluation of lamellipodia, membrane ruffles and invadopodia formation, as well as activation of related signaling pathway molecules such as FAK, paxillin, zyxin, Rac1, MMP family, and uPA is required. Although quercetin is able to cross the blood-brain barrier, whether myricetin can do the same needs further

investigation [259]. Considering that no study has reported the anti-cancer effect of myricetin on glioblastoma *in vivo*, future studies can be carried out using xenograft and allograft glioblastoma models.

## Appendix

### Source of materials and reagents

#### Antibodies

Anti-Akt (#9272)	Cell Signaling Technology
Anti-c-Jun (#9165)	Cell Signaling Technology
Anti-EGFR (C7489) (#2646)	Cell Signaling Technology
Anti-FAK (#3285)	Cell Signaling Technology
Anti-GAPDH (#2118)	Cell Signaling Technology
Anti-goat, HRP-conjugated antibody	Santa Cruz Biotechnology
Anti-mouse, HRP-conjugated antibody	Cell Signaling Technology
Anti-p110 $\alpha$ (#4255)	Cell Signaling Technology
Anti-p110 $\beta$ (C33D4) (#3011)	Cell Signaling Technology
Anti-p110 $\delta$ (#ab32401)	Abcam
Anti-p85 $\alpha$ (#GTX101106)	GeneTex
Anti-p85 $\beta$ (T15) (#GTX74710)	GeneTex
anti-phospho-Akt (Ser473) (#9271)	Cell Signaling Technology
anti-phospho-Akt (Thr308) (#9275)	Cell Signaling Technology
anti-phospho-c-Jun (Ser63) (#2361)	Cell Signaling Technology
anti-phospho-FAK (Tyr925) (#3284)	Cell Signaling Technology
anti-phospho-SAPK/JNK (Thr183/Tyr185) (#9251)	Cell Signaling Technology
anti-phospho-zyxin (Ser142/143) (#8467)	Cell Signaling Technology

## Appendix

---

Anti-PTEN (Ab-2) (#RB1-072-P1)	Lab Vision/Nemoarkers
Anti-rabbit, HRP-conjugated antibody	Cell Signaling Technology
Anti-Rac1 (#240106)	Cell Biolabs
Anti-RhoA (#2117)	Cell Signaling Technology
Anti-SAPK/JNK (#9258)	Cell Signaling Technology
Anti-zyxin (#3553)	Cell Signaling Technology

### Reagents

BSA	Sigma-Aldrich
CAL-101	Selleckchem
CNBr-activated Sepharose 4B	GE Healthcare
cOmplet protease inhibitor cocktail	Roche
DMSO (Tissue culture grade)	Sigma-Aldrich
FastStart Universal SYBR Green Master	Roche
FBS	Life Technologies
Fermentas RevertAid First Strand cDNA Synthesis Kit	Thermo Scientific
HEPES	Life Technologies
Lipofectamine 2000	Life Technologies
Mitomycin C	Life Technologies
MTT	Life Technologies
Myricetin	Cayman
Opti-MEM I Reduced Serum Medium	Life Technologies

PBS	Sigma-Aldrich
PhosSTOP phosphatase inhibitor cocktail	Roche
Pierce BCA Protein Assay Kit	Thermo Scientific
PIK-75	Selleckchem
Platinum Quantitative PCR SuperMix-UDG	Life Technologies
Polyester (PET)-Transwell insert	Corning
ProLong Gold antifade mountant with DAPI	Life Technologies
SP600125	Sigma-Aldrich
TGX-221	Selleckchem
Trizol reagent	Life Technologies
Trypsin-EDTA	Life Technologies
Tween-20	Sigma-Aldrich
$\alpha$ -MEM	Life Technologies
$\beta$ -mercaptoethanol	Sigma-Aldrich

### **Equipment**

ABI PRISM 7500 System	Applied Biosystems
BenchMark Plus™ microplate spectrophotometer	BioRad Laboratories
ChemiDoc MP Imaging System	BioRad Laboratories
DMI4000 B phase contrast microscope	Leica Microsystems
NanoDrop 2000 spectrophotometer	Thermo Scientific
TSC SP8 confocal laser scanning microscope	Leica Microsystems

## References

1. Dolecek TA, Propp JM, Stroup NE and Kruchko C. CBTRUS statistical report: primary brain and central nervous system tumors diagnosed in the United States in 2005-2009. *Neuro Oncol.* 2012; 14 Suppl 5:1-49.
2. Schwartzbaum JA, Fisher JL, Aldape KD and Wrensch M. Epidemiology and molecular pathology of glioma. *Nat Clin Pract Neurol.* 2006; 2(9):494-503.
3. Pu JKS, Ng GKB, Leung GKK and Wong CK. One-year review of the incidence of brain tumours in Hong Kong Chinese patients as part of the Hong Kong Brain and Spinal Tumours Registry. *Surg Pract.* 2012; 16(4):133-136.
4. Louis DN, Ohgaki H, Wiestler OD, Cavenee WK, Burger PC, Jouvet A, Scheithauer BW and Kleihues P. The 2007 WHO classification of tumours of the central nervous system. *Acta Neuropathol.* 2007; 114(2):97-109.
5. Ohgaki H and Kleihues P. Genetic Pathways to Primary and Secondary Glioblastoma. *The American Journal of Pathology.* 2007; 170(5):1445-1453.
6. Ohgaki H and Kleihues P. The definition of primary and secondary glioblastoma. *Clin Cancer Res.* 2013; 19(4):764-772.
7. Ohgaki H and Kleihues P. Genetic alterations and signaling pathways in the evolution of gliomas. *Cancer Science.* 2009; 100(12):2235-2241.
8. Rasheed BK, McLendon RE, Friedman HS, Friedman AH, Fuchs HE, Bigner DD and Bigner SH. Chromosome 10 deletion mapping in human gliomas: a common deletion region in 10q25. *Oncogene.* 1995; 10(11):2243-2246.
9. Ichimura K, Schmidt EE, Miyakawa A, Goike HM and Collins VP. Distinct patterns of deletion on 10p and 10q suggest involvement of multiple tumor suppressor genes in the development of astrocytic gliomas of different malignancy grades. *Genes, chromosomes & cancer.* 1998; 22(1):9-15.
10. Felsberg J, Erkwow A, Sabel MC, Kirsch L, Fimmers R, Blaschke B, Schlegel U, Schramm J, Wiestler OD and Reifenberger G. Oligodendroglial tumors: refinement of candidate regions on chromosome arm 1p and correlation of

- 1p/19q status with survival. *Brain Pathol.* 2004; 14(2):121-130.
11. Krex D, Klink B, Hartmann C, von Deimling A, Pietsch T, Simon M, Sabel M, Steinbach JP, Heese O, Reifenberger G, Weller M and Schackert G. Long-term survival with glioblastoma multiforme. *Brain.* 2007; 130(10):2596-2606.
  12. Das P, Puri T, Jha P, Pathak P, Joshi N, Suri V, Sharma MC, Sharma BS, Mahapatra AK, Suri A and Sarkar C. A clinicopathological and molecular analysis of glioblastoma multiforme with long-term survival. *J Clin Neurosci.* 2011; 18(1):66-70.
  13. Chang SM, Theodosopoulos P, Lamborn K, Malec M, Rabbitt J, Page M and Prados MD. Temozolomide in the treatment of recurrent malignant glioma. *Cancer.* 2004; 100(3):605-611.
  14. Stupp R, Mason WP, van den Bent MJ, Weller M, Fisher B, Taphoorn MJ, Belanger K, Brandes AA, Marosi C, Bogdahn U, Curschmann J, Janzer RC, Ludwin SK, Gorlia T, Allgeier A, Lacombe D, et al. Radiotherapy plus concomitant and adjuvant temozolomide for glioblastoma. *N Engl J Med.* 2005; 352(10):987-996.
  15. Zhang J, Stevens MF and Bradshaw TD. Temozolomide: mechanisms of action, repair and resistance. *Curr Mol Pharmacol.* 2012; 5(1):102-114.
  16. Friedman HS, Kerby T and Calvert H. Temozolomide and treatment of malignant glioma. *Clin Cancer Res.* 2000; 6(7):2585-2597.
  17. Wick W, Platten M, Meisner C, Felsberg J, Tabatabai G, Simon M, Nikkhah G, Papsdorf K, Steinbach JP, Sabel M, Combs SE, Vesper J, Braun C, Meixensberger J, Ketter R, Mayer-Steinacker R, et al. Temozolomide chemotherapy alone versus radiotherapy alone for malignant astrocytoma in the elderly: the NOA-08 randomised, phase 3 trial. *The Lancet Oncology.* 2012; 13(7):707-715.
  18. Malmstrom A, Gronberg BH, Marosi C, Stupp R, Frappaz D, Schultz H, Abacioglu U, Tavelin B, Lhermitte B, Hegi ME, Rosell J, Henriksson R and Nordic Clinical Brain Tumour Study G. Temozolomide versus standard 6-week radiotherapy versus hypofractionated radiotherapy in patients older than 60

- years with glioblastoma: the Nordic randomised, phase 3 trial. *The Lancet Oncology*. 2012; 13(9):916-926.
19. Hacibekiroglu I, Kodaz H, Erdogan B, Turkmen E, Ozcelik M, Esenkaya A, Saygi HM, Uzunoglu S and Cicin I. Single-agent bevacizumab is an effective treatment in recurrent glioblastoma. *Med Oncol*. 2015; 32(2):460.
  20. Gilbert MR, Dignam JJ, Armstrong TS, Wefel JS, Blumenthal DT, Vogelbaum MA, Colman H, Chakravarti A, Pugh S, Won M, Jeraj R, Brown PD, Jaeckle KA, Schiff D, Stieber VW, Brachman DG, et al. A randomized trial of bevacizumab for newly diagnosed glioblastoma. *N Engl J Med*. 2014; 370(8):699-708.
  21. Xu T, Chen J, Lu Y and Wolff JE. Effects of bevacizumab plus irinotecan on response and survival in patients with recurrent malignant glioma: a systematic review and survival-gain analysis. *BMC cancer*. 2010; 10:252.
  22. Vredenburgh JJ, Desjardins A, Herndon JE, 2nd, Marcello J, Reardon DA, Quinn JA, Rich JN, Sathornsumetee S, Gururangan S, Sampson J, Wagner M, Bailey L, Bigner DD, Friedman AH and Friedman HS. Bevacizumab plus irinotecan in recurrent glioblastoma multiforme. *J Clin Oncol*. 2007; 25(30):4722-4729.
  23. Hofland KF, Hansen S, Sorensen M, Engelholm S, Schultz HP, Muhic A, Grunnet K, Ask A, Costa JC, Kristiansen C, Thomsen C, Poulsen HS and Lassen U. Neoadjuvant bevacizumab and irinotecan versus bevacizumab and temozolomide followed by concomitant chemoradiotherapy in newly diagnosed glioblastoma multiforme: A randomized phase II study. *Acta Oncol*. 2014; 53(7):939-944.
  24. Chauffert B, Feuvret L, Bonnetain F, Taillandier L, Frappaz D, Taillia H, Schott R, Honnorat J, Fabbro M, Tennevet I, Ghiringhelli F, Guillamo JS, Durando X, Castera D, Frenay M, Campello C, et al. Randomized phase II trial of irinotecan and bevacizumab as neo-adjuvant and adjuvant to temozolomide-based chemoradiation compared with temozolomide-chemoradiation for unresectable glioblastoma: final results of the TEMAVIR study from ANOCEF dagger. *Ann Oncol*. 2014; 25(7):1442-1447.

25. Keunen O, Johansson M, Oudin A, Sanzey M, Rahim SA, Fack F, Thorsen F, Taxt T, Bartos M, Jirik R, Miletic H, Wang J, Stieber D, Stuhr L, Moen I, Rygh CB, et al. Anti-VEGF treatment reduces blood supply and increases tumor cell invasion in glioblastoma. *Proc Natl Acad Sci U S A*. 2011; 108(9):3749-3754.
26. Son MJ, Kim JS, Kim MH, Song HS, Kim JT, Kim H, Shin T, Jeon HJ, Lee DS, Park SY, Kim YJ, Kim JH and Nam DH. Combination treatment with temozolomide and thalidomide inhibits tumor growth and angiogenesis in an orthotopic glioma model. *Int J Oncol*. 2006; 28(1):53-59.
27. Escudier B, Eisen T, Stadler WM, Szczylik C, Oudard S, Siebels M, Negrier S, Chevreau C, Solska E, Desai AA, Rolland F, Demkow T, Hutson TE, Gore M, Freeman S, Schwartz B, et al. Sorafenib in advanced clear-cell renal-cell carcinoma. *N Engl J Med*. 2007; 356(2):125-134.
28. Tran TA, Kinch L, Pena-Llopis S, Kockel L, Grishin N, Jiang H and Brugarolas J. Platelet-derived growth factor/vascular endothelial growth factor receptor inactivation by sunitinib results in Tsc1/Tsc2-dependent inhibition of TORC1. *Mol Cell Biol*. 2013; 33(19):3762-3779.
29. Melichar B, Studentova H and Zezulova M. Pazopanib: a new multiple tyrosine kinase inhibitor in the therapy of metastatic renal cell carcinoma and other solid tumors. *J BUON*. 2011; 16(2):203-209.
30. Normanno N, De Luca A, Bianco C, Strizzi L, Mancino M, Maiello MR, Carotenuto A, De Feo G, Caponigro F and Salomon DS. Epidermal growth factor receptor (EGFR) signaling in cancer. *Gene*. 2006; 366(1):2-16.
31. Kalman B, Szep E, Garzuly F and Post DE. Epidermal growth factor receptor as a therapeutic target in glioblastoma. *Neuromolecular Med*. 2013; 15(2):420-434.
32. Rivera F, Vega-Villegas ME and Lopez-Brea MF. Cetuximab, its clinical use and future perspectives. *Anticancer Drugs*. 2008; 19(2):99-113.
33. Yang XD, Jia XC, Corvalan JR, Wang P and Davis CG. Development of ABX-EGF, a fully human anti-EGF receptor monoclonal antibody, for cancer therapy. *Crit Rev Oncol Hematol*. 2001; 38(1):17-23.
34. Karapetis CS, Khambata-Ford S, Jonker DJ, O'Callaghan CJ, Tu D, Tebbutt NC,

- Simes RJ, Chalchal H, Shapiro JD, Robitaille S, Price TJ, Shepherd L, Au HJ, Langer C, Moore MJ and Zalcborg JR. K-ras mutations and benefit from cetuximab in advanced colorectal cancer. *N Engl J Med.* 2008; 359(17):1757-1765.
35. Amado RG, Wolf M, Peeters M, Van Cutsem E, Siena S, Freeman DJ, Juan T, Sikorski R, Suggs S, Radinsky R, Patterson SD and Chang DD. Wild-type KRAS is required for panitumumab efficacy in patients with metastatic colorectal cancer. *J Clin Oncol.* 2008; 26(10):1626-1634.
36. Lv S, Teugels E, Sadones J, De Brakeleer S, Duerinck J, Du Four S, Michotte A, De Greve J and Neyns B. Correlation of EGFR, IDH1 and PTEN status with the outcome of patients with recurrent glioblastoma treated in a phase II clinical trial with the EGFR-blocking monoclonal antibody cetuximab. *Int J Oncol.* 2012; 41(3):1029-1035.
37. Cohen MH, Williams GA, Sridhara R, Chen G and Pazdur R. FDA drug approval summary: gefitinib (ZD1839) (Iressa) tablets. *The oncologist.* 2003; 8(4):303-306.
38. Cohen MH, Johnson JR, Chen YF, Sridhara R and Pazdur R. FDA drug approval summary: erlotinib (Tarceva) tablets. *The oncologist.* 2005; 10(7):461-466.
39. Chakravarti A, Wang M, Robins HI, Lautenschlaeger T, Curran WJ, Brachman DG, Schultz CJ, Choucair A, Dolled-Filhart M, Christiansen J, Gustavson M, Molinaro A, Mischel P, Dicker AP, Bredel M and Mehta M. RTOG 0211: a phase 1/2 study of radiation therapy with concurrent gefitinib for newly diagnosed glioblastoma patients. *Int J Radiat Oncol Biol Phys.* 2013; 85(5):1206-1211.
40. Peereboom DM, Shepard DR, Ahluwalia MS, Brewer CJ, Agarwal N, Stevens GH, Suh JH, Toms SA, Vogelbaum MA, Weil RJ, Elson P and Barnett GH. Phase II trial of erlotinib with temozolomide and radiation in patients with newly diagnosed glioblastoma multiforme. *J Neurooncol.* 2010; 98(1):93-99.
41. Kristiansen K. Molecular mechanisms of ligand binding, signaling, and regulation within the superfamily of G-protein-coupled receptors: molecular modeling and mutagenesis approaches to receptor structure and function.

- Pharmacol Ther. 2004; 103(1):21-80.
42. Schwindinger WF and Robishaw JD. Heterotrimeric G-protein betagamma-dimers in growth and differentiation. *Oncogene*. 2001; 20(13):1653-1660.
  43. Cantley LC. The phosphoinositide 3-kinase pathway. *Science*. 2002; 296(5573):1655-1657.
  44. Tzenaki N and Papakonstanti EA. p110delta PI3 kinase pathway: emerging roles in cancer. *Front Oncol*. 2013; 3:40.
  45. Stoyanov B, Volinia S, Hanck T, Rubio I, Loubtchenkov M, Malek D, Stoyanova S, Vanhaesebroeck B, Dhand R, Nurnberg B and et al. Cloning and characterization of a G protein-activated human phosphoinositide-3 kinase. *Science*. 1995; 269(5224):690-693.
  46. Stephens LR, Eguinoa A, Erdjument-Bromage H, Lui M, Cooke F, Coadwell J, Smrcka AS, Thelen M, Cadwallader K, Tempst P and Hawkins PT. The G beta gamma sensitivity of a PI3K is dependent upon a tightly associated adaptor, p101. *Cell*. 1997; 89(1):105-114.
  47. Vanhaesebroeck B, Guillermet-Guibert J, Graupera M and Bilanges B. The emerging mechanisms of isoform-specific PI3K signalling. *Nat Rev Mol Cell Biol*. 2010; 11(5):329-341.
  48. Hellyer NJ, Cheng K and Koland JG. ErbB3 (HER3) interaction with the p85 regulatory subunit of phosphoinositide 3-kinase. *Biochem J*. 1998; 333 ( Pt 3):757-763.
  49. Cuevas BD, Lu Y, Mao M, Zhang J, LaPushin R, Siminovitch K and Mills GB. Tyrosine phosphorylation of p85 relieves its inhibitory activity on phosphatidylinositol 3-kinase. *J Biol Chem*. 2001; 276(29):27455-27461.
  50. Chantry D, Vojtek A, Kashishian A, Holtzman DA, Wood C, Gray PW, Cooper JA and Hoekstra MF. p110delta, a novel phosphatidylinositol 3-kinase catalytic subunit that associates with p85 and is expressed predominantly in leukocytes. *J Biol Chem*. 1997; 272(31):19236-19241.
  51. Walker EH, Perisic O, Ried C, Stephens L and Williams RL. Structural insights

- into phosphoinositide 3-kinase catalysis and signalling. *Nature*. 1999; 402(6759):313-320.
52. Amzel LM, Huang CH, Mandelker D, Lengauer C, Gabelli SB and Vogelstein B. Structural comparisons of class I phosphoinositide 3-kinases. *Nat Rev Cancer*. 2008; 8(9):665-669.
53. Rodriguez-Viciana P, Warne PH, Dhand R, Vanhaesebroeck B, Gout I, Fry MJ, Waterfield MD and Downward J. Phosphatidylinositol-3-OH kinase as a direct target of Ras. *Nature*. 1994; 370(6490):527-532.
54. Campbell IG, Russell SE and Phillips WA. PIK3CA mutations in ovarian cancer. *Clin Cancer Res*. 2005; 11(19):7042-7043.
55. Lee JW, Soung YH, Kim SY, Lee HW, Park WS, Nam SW, Kim SH, Lee JY, Yoo NJ and Lee SH. PIK3CA gene is frequently mutated in breast carcinomas and hepatocellular carcinomas. *Oncogene*. 2005; 24(8):1477-1480.
56. Levine DA, Bogomolny F, Yee CJ, Lash A, Barakat RR, Borgen PI and Boyd J. Frequent mutation of the PIK3CA gene in ovarian and breast cancers. *Clin Cancer Res*. 2005; 11(8):2875-2878.
57. Ikenoue T, Kanai F, Hikiba Y, Obata T, Tanaka Y, Imamura J, Ohta M, Jazag A, Guleng B, Tateishi K, Asaoka Y, Matsumura M, Kawabe T and Omata M. Functional analysis of PIK3CA gene mutations in human colorectal cancer. *Cancer Res*. 2005; 65(11):4562-4567.
58. Broderick DK, Di C, Parrett TJ, Samuels YR, Cummins JM, McLendon RE, Fulst DW, Velculescu VE, Bigner DD and Yan H. Mutations of PIK3CA in anaplastic oligodendrogliomas, high-grade astrocytomas, and medulloblastomas. *Cancer Res*. 2004; 64(15):5048-5050.
59. Gallia GL, Rand V, Siu IM, Eberhart CG, James CD, Marie SK, Oba-Shinjo SM, Carlotti CG, Caballero OL, Simpson AJ, Brock MV, Massion PP, Carson BS, Sr. and Riggins GJ. PIK3CA gene mutations in pediatric and adult glioblastoma multiforme. *Mol Cancer Res*. 2006; 4(10):709-714.
60. Samuels Y, Wang Z, Bardelli A, Silliman N, Ptak J, Szabo S, Yan H, Gazdar A, Powell SM, Riggins GJ, Willson JK, Markowitz S, Kinzler KW, Vogelstein B and

- Velculescu VE. High frequency of mutations of the PIK3CA gene in human cancers. *Science*. 2004; 304(5670):554.
61. Gymnopoulos M, Elsliger MA and Vogt PK. Rare cancer-specific mutations in PIK3CA show gain of function. *Proc Natl Acad Sci U S A*. 2007; 104(13):5569-5574.
62. Zhao L and Vogt PK. Helical domain and kinase domain mutations in p110alpha of phosphatidylinositol 3-kinase induce gain of function by different mechanisms. *Proc Natl Acad Sci U S A*. 2008; 105(7):2652-2657.
63. Hooshmand-Rad R, Hajkova L, Klint P, Karlsson R, Vanhaesebroeck B, Claesson-Welsh L and Heldin CH. The PI 3-kinase isoforms p110(alpha) and p110(beta) have differential roles in PDGF- and insulin-mediated signaling. *J Cell Sci*. 2000; 113:207-214.
64. Jia S, Liu Z, Zhang S, Liu P, Zhang L, Lee SH, Zhang J, Signoretti S, Loda M, Roberts TM and Zhao JJ. Essential roles of PI(3)K-p110beta in cell growth, metabolism and tumorigenesis. *Nature*. 2008; 454(7205):776-779.
65. Foukas LC, Claret M, Pearce W, Okkenhaug K, Meek S, Peskett E, Sancho S, Smith AJ, Withers DJ and Vanhaesebroeck B. Critical role for the p110alpha phosphoinositide-3-OH kinase in growth and metabolic regulation. *Nature*. 2006; 441(7091):366-370.
66. Guillermet-Guibert J, Bjorklof K, Salpekar A, Gonella C, Ramadani F, Bilancio A, Meek S, Smith AJ, Okkenhaug K and Vanhaesebroeck B. The p110beta isoform of phosphoinositide 3-kinase signals downstream of G protein-coupled receptors and is functionally redundant with p110gamma. *Proc Natl Acad Sci U S A*. 2008; 105(24):8292-8297.
67. Vanhaesebroeck B, Welham MJ, Kotani K, Stein R, Warne PH, Zvelebil MJ, Higashi K, Volinia S, Downward J and Waterfield MD. P110delta, a novel phosphoinositide 3-kinase in leukocytes. *Proc Natl Acad Sci U S A*. 1997; 94(9):4330-4335.
68. Burke JE, Vadas O, Berndt A, Finegan T, Perisic O and Williams RL. Dynamics of the phosphoinositide 3-kinase p110delta interaction with p85alpha and

- membranes reveals aspects of regulation distinct from p110alpha. *Structure*. 2011; 19(8):1127-1137.
69. Whitehead MA, Bombardieri M, Pitzalis C and Vanhaesebroeck B. Isoform-selective induction of human p110delta PI3K expression by TNFalpha: identification of a new and inducible PIK3CD promoter. *Biochem J*. 2012; 443(3):857-867.
70. Kok K, Nock GE, Verrall EA, Mitchell MP, Hommes DW, Peppelenbosch MP and Vanhaesebroeck B. Regulation of p110delta PI 3-kinase gene expression. *PLoS One*. 2009; 4(4):e5145.
71. Venable JD, Ameriks MK, Blevitt JM, Thurmond RL and Fung-Leung WP. Phosphoinositide 3-kinase gamma (PI3Kgamma) inhibitors for the treatment of inflammation and autoimmune disease. *Recent Pat Inflamm Allergy Drug Discov*. 2010; 4(1):1-15.
72. Beer-Hammer S, Zebedin E, von Holleben M, Alferink J, Reis B, Dresing P, Degrandi D, Scheu S, Hirsch E, Sexl V, Pfeffer K, Nurnberg B and Piekorz RP. The catalytic PI3K isoforms p110gamma and p110delta contribute to B cell development and maintenance, transformation, and proliferation. *J Leukoc Biol*. 2010; 87(6):1083-1095.
73. Leopoldt D, Hanck T, Exner T, Maier U, Wetzker R and Nurnberg B. Gbetagamma stimulates phosphoinositide 3-kinase-gamma by direct interaction with two domains of the catalytic p110 subunit. *J Biol Chem*. 1998; 273(12):7024-7029.
74. Krugmann S, Hawkins PT, Pryer N and Braselmann S. Characterizing the interactions between the two subunits of the p101/p110gamma phosphoinositide 3-kinase and their role in the activation of this enzyme by G beta gamma subunits. *J Biol Chem*. 1999; 274(24):17152-17158.
75. Bohnacker T, Marone R, Collmann E, Calvez R, Hirsch E and Wymann MP. PI3Kgamma adaptor subunits define coupling to degranulation and cell motility by distinct PtdIns(3,4,5)P3 pools in mast cells. *Sci Signal*. 2009; 2(74):ra27.
76. Brazzatti JA, Klingler-Hoffmann M, Haylock-Jacobs S, Harata-Lee Y, Niu M,

- Higgins MD, Kochetkova M, Hoffmann P and McColl SR. Differential roles for the p101 and p84 regulatory subunits of PI3Kgamma in tumor growth and metastasis. *Oncogene*. 2012; 31(18):2350-2361.
77. Schmidt C, Schilli-Westermann M, Klinger R and Kirsch C. Phosphoinositide 3-kinase gamma has multiple phospholipid binding sites. *Protein J*. 2010; 29(2):127-135.
78. Philp AJ, Campbell IG, Leet C, Vincan E, Rockman SP, Whitehead RH, Thomas RJ and Phillips WA. The phosphatidylinositol 3'-kinase p85alpha gene is an oncogene in human ovarian and colon tumors. *Cancer Res*. 2001; 61(20):7426-7429.
79. Urlick ME, Rudd ML, Godwin AK, Sgroi D, Merino M and Bell DW. PIK3R1 (p85alpha) is somatically mutated at high frequency in primary endometrial cancer. *Cancer Res*. 2011; 71(12):4061-4067.
80. CancerGenomeAtlasResearchNetwork. Comprehensive genomic characterization defines human glioblastoma genes and core pathways. *Nature*. 2008; 455(7216):1061-1068.
81. Quayle SN, Lee JY, Cheung LW, Ding L, Wiedemeyer R, Dewan RW, Huang-Hobbs E, Zhuang L, Wilson RK, Ligon KL, Mills GB, Cantley LC and Chin L. Somatic mutations of PIK3R1 promote gliomagenesis. *PLoS One*. 2012; 7(11):e49466.
82. Miled N, Yan Y, Hon WC, Perisic O, Zvelebil M, Inbar Y, Schneidman-Duhovny D, Wolfson HJ, Backer JM and Williams RL. Mechanism of two classes of cancer mutations in the phosphoinositide 3-kinase catalytic subunit. *Science*. 2007; 317(5835):239-242.
83. Jaiswal BS, Janakiraman V, Kljavin NM, Chaudhuri S, Stern HM, Wang W, Kan Z, Dbouk HA, Peters BA, Waring P, Dela Vega T, Kenski DM, Bowman KK, Lorenzo M, Li H, Wu J, et al. Somatic mutations in p85alpha promote tumorigenesis through class IA PI3K activation. *Cancer Cell*. 2009; 16(6):463-474.
84. Park SW, Kang MR, Eom HS, Han JY, Ahn CH, Kim SS, Lee SH and Yoo NJ.

- Somatic mutation of PIK3R1 gene is rare in common human cancers. *Acta Oncol.* 2010; 49(1):125-127.
85. Fu Y, Zhang Q, Kang C, Zhang J, Zhang K, Pu P, Wang G and Wang T. Inhibitory effects of adenovirus mediated Akt1 and PIK3R1 shRNA on the growth of malignant tumor cells in vitro and in vivo. *Cancer Biol Ther.* 2009; 8(11):1002-1009.
86. Hartmann C, Bartels G, Gehlhaar C, Holtkamp N and von Deimling A. PIK3CA mutations in glioblastoma multiforme. *Acta Neuropathol.* 2005; 109(6):639-642.
87. Kita D, Yonekawa Y, Weller M and Ohgaki H. PIK3CA alterations in primary (de novo) and secondary glioblastomas. *Acta Neuropathol.* 2007; 113(3):295-302.
88. Knobbe CB, Trampe-Kieslich A and Reifenberger G. Genetic alteration and expression of the phosphoinositol-3-kinase/Akt pathway genes PIK3CA and PIKE in human glioblastomas. *Neuropathol Appl Neurobiol.* 2005; 31(5):486-490.
89. Parsons DW, Jones S, Zhang X, Lin JC, Leary RJ, Angenendt P, Mankoo P, Carter H, Siu IM, Gallia GL, Olivi A, McLendon R, Rasheed BA, Keir S, Nikolskaya T, Nikolsky Y, et al. An integrated genomic analysis of human glioblastoma multiforme. *Science.* 2008; 321(5897):1807-1812.
90. Guerreiro AS, Fattet S, Fischer B, Shalaby T, Jackson SP, Schoenwaelder SM, Grotzer MA, Delattre O and Arcaro A. Targeting the PI3K p110alpha isoform Inhibits medulloblastoma proliferation, chemoresistance, and migration. *Clinical Cancer Research.* 2008; 14(21):6761-6769.
91. Weber GL, Parat MO, Binder ZA, Gallia GL and Riggins GJ. Abrogation of PIK3CA or PIK3R1 reduces proliferation, migration, and invasion in glioblastoma multiforme cells. *Oncotarget.* 2011; 2(11):833-849.
92. Jeong JY, Kim KS, Moon JS, Song JA, Choi SH, Kim KI, Kim TH and An HJ. Targeted inhibition of phosphatidylinositol-3-kinase p110beta, but not p110alpha, enhances apoptosis and sensitivity to paclitaxel in chemoresistant ovarian cancers. *Apoptosis.* 2013; 18(4):509-520.
93. Yamaguchi H, Yoshida S, Muroi E, Yoshida N, Kawamura M, Kouchi Z,

- Nakamura Y, Sakai R and Fukami K. Phosphoinositide 3-kinase signaling pathway mediated by p110alpha regulates invadopodia formation. *J Cell Biol.* 2011; 193(7):1275-1288.
94. Jamieson S, Flanagan JU, Kolekar S, Buchanan C, Kendall JD, Lee WJ, Rewcastle GW, Denny WA, Singh R, Dickson J, Baguley BC and Shepherd PR. A drug targeting only p110alpha can block phosphoinositide 3-kinase signalling and tumour growth in certain cell types. *Biochem J.* 2011; 438(1):53-62.
95. Keam B, Kim S, Ahn YO, Kim TM, Lee SH, Kim DW and Heo DS. In Vitro Anticancer Activity of PI3K Alpha Selective Inhibitor BYL719 in Head and Neck Cancer. *Anticancer Res.* 2015; 35(1):175-182.
96. Garrett JT, Sutton CR, Kurupi R, Bialucha CU, Ettenberg SA, Collins SD, Sheng Q, Wallweber J, Defazio-Eli L and Arteaga CL. Combination of antibody that inhibits ligand-independent HER3 dimerization and a p110alpha inhibitor potently blocks PI3K signaling and growth of HER2+ breast cancers. *Cancer Res.* 2013; 73(19):6013-6023.
97. Cheng CK, Gustafson WC, Charron E, Houseman BT, Zunder E, Goga A, Gray NS, Pollok B, Oakes SA, James CD, Shokat KM, Weiss WA and Fan QW. Dual blockade of lipid and cyclin-dependent kinases induces synthetic lethality in malignant glioma. *Proc Natl Acad Sci U S A.* 2012; 109(31):12722-12727.
98. Chen H, Mei L, Zhou L, Shen X, Guo C, Zheng Y, Zhu H, Zhu Y and Huang L. PTEN restoration and PIK3CB knockdown synergistically suppress glioblastoma growth in vitro and in xenografts. *J Neurooncol.* 2011; 104(1):155-167.
99. Kang S, Denley A, Vanhaesebroeck B and Vogt PK. Oncogenic transformation induced by the p110beta, -gamma, and -delta isoforms of class I phosphoinositide 3-kinase. *Proc Natl Acad Sci U S A.* 2006; 103(5):1289-1294.
100. Carvalho S, Milanezi F, Costa JL, Amendoeira I and Schmitt F. PI3K the right isoform: the emergent role of the p110beta subunit in breast cancer. *Virchows Arch.* 2010; 456(3):235-243.
101. Cui B, Tao J and Yang Y. Studies on the expression patterns of class I PI3K catalytic subunits and its prognostic significance in colorectal cancer. *Cell*

- Biochem Biophys. 2012; 62(1):47-54.
- 102.Herman SE and Johnson AJ. Molecular Pathways: Targeting Phosphoinositide 3-Kinase p110-Delta in Chronic Lymphocytic Leukemia. Clin Cancer Res. 2012; 18(15):4013-4018.
- 103.Hoellenriegel J, Meadows SA, Sivina M, Wierda WG, Kantarjian H, Keating MJ, Giese N, O'Brien S, Yu A, Miller LL, Lannutti BJ and Burger JA. The phosphoinositide 3'-kinase delta inhibitor, CAL-101, inhibits B-cell receptor signaling and chemokine networks in chronic lymphocytic leukemia. Blood. 2011; 118(13):3603-3612.
- 104.Luk SK, Piekorz RP, Nürnberg B and To ST. The catalytic phosphoinositol 3-kinase isoform p110 $\delta$  is required for glioma cell migration and invasion. European Journal of Cancer. 2012; 48(1):149-157.
- 105.Knobbe CB and Reifenberger G. Genetic alterations and aberrant expression of genes related to the phosphatidyl-inositol-3'-kinase/protein kinase B (Akt) signal transduction pathway in glioblastomas. Brain Pathol. 2003; 13(4):507-518.
- 106.Boller D, Schramm A, Doepfner KT, Shalaby T, von Bueren AO, Eggert A, Grotzer MA and Arcaro A. Targeting the phosphoinositide 3-kinase isoform p110delta impairs growth and survival in neuroblastoma cells. Clin Cancer Res. 2008; 14(4):1172-1181.
- 107.Tzenaki N, Andreou M, Stratigi K, Vergetaki A, Makrigiannakis A, Vanhaesebroeck B and Papakonstanti EA. High levels of p110delta PI3K expression in solid tumor cells suppress PTEN activity, generating cellular sensitivity to p110delta inhibitors through PTEN activation. FASEB J. 2012; 26(6):2498-2508.
- 108.Jiang X, Chen S, Asara JM and Balk SP. Phosphoinositide 3-kinase pathway activation in phosphate and tensin homolog (PTEN)-deficient prostate cancer cells is independent of receptor tyrosine kinases and mediated by the p110beta and p110delta catalytic subunits. J Biol Chem. 2010; 285(20):14980-14989.
- 109.Hanada M, Feng J and Hemmings BA. Structure, regulation and function of PKB/AKT--a major therapeutic target. Biochim Biophys Acta. 2004;

- 1697(1-2):3-16.
110. Vanhaesebroeck B and Alessi DR. The PI3K-PDK1 connection: more than just a road to PKB. *Biochem J.* 2000; 346 Pt 3:561-576.
111. Toker A and Newton AC. Cellular signaling: pivoting around PDK-1. *Cell.* 2000; 103(2):185-188.
112. Sarbassov DD, Ali SM and Sabatini DM. Growing roles for the mTOR pathway. *Curr Opin Cell Biol.* 2005; 17(6):596-603.
113. Nojima H, Tokunaga C, Eguchi S, Oshiro N, Hidayat S, Yoshino K, Hara K, Tanaka N, Avruch J and Yonezawa K. The mammalian target of rapamycin (mTOR) partner, raptor, binds the mTOR substrates p70 S6 kinase and 4E-BP1 through their TOR signaling (TOS) motif. *J Biol Chem.* 2003; 278(18):15461-15464.
114. Zhang X, Tang N, Hadden TJ and Rishi AK. Akt, FoxO and regulation of apoptosis. *Biochim Biophys Acta.* 2011; 1813(11):1978-1986.
115. Datta SR, Brunet A and Greenberg ME. Cellular survival: a play in three Akts. *Genes Dev.* 1999; 13(22):2905-2927.
116. Viglietto G, Amodio N, Malanga D, Scrima M and De Marco C. Contribution of PKB/AKT signaling to thyroid cancer. *Front Biosci.* 2011; 16:1461-1487.
117. Xu CX, Jin H, Shin JY, Kim JE and Cho MH. Roles of protein kinase B/Akt in lung cancer. *Front Biosci (Elite Ed).* 2010; 2:1472-1484.
118. Haas-Kogan D, Shalev N, Wong M, Mills G, Yount G and Stokoe D. Protein kinase B (PKB/Akt) activity is elevated in glioblastoma cells due to mutation of the tumor suppressor PTEN/MMAC. *Curr Biol.* 1998; 8(21):1195-1198.
119. Lin HJ, Hsieh FC, Song H and Lin J. Elevated phosphorylation and activation of PDK-1/AKT pathway in human breast cancer. *Br J Cancer.* 2005; 93(12):1372-1381.
120. Altomare DA, Wang HQ, Skele KL, De Rienzo A, Klein-Szanto AJ, Godwin AK and Testa JR. AKT and mTOR phosphorylation is frequently detected in ovarian cancer and can be targeted to disrupt ovarian tumor cell growth. *Oncogene.* 2004; 23(34):5853-5857.

121. Rajasekhar VK, Viale A, Socci ND, Wiedmann M, Hu X and Holland EC. Oncogenic Ras and Akt signaling contribute to glioblastoma formation by differential recruitment of existing mRNAs to polysomes. *Mol Cell*. 2003; 12(4):889-901.
122. Holland EC, Celestino J, Dai C, Schaefer L, Sawaya RE and Fuller GN. Combined activation of Ras and Akt in neural progenitors induces glioblastoma formation in mice. *Nat Genet*. 2000; 25(1):55-57.
123. Sonoda Y, Ozawa T, Aldape KD, Deen DF, Berger MS and Pieper RO. Akt pathway activation converts anaplastic astrocytoma to glioblastoma multiforme in a human astrocyte model of glioma. *Cancer Res*. 2001; 61(18):6674-6678.
124. Robinson JP, Vanbrocklin MW, McKinney AJ, Gach HM and Holmen SL. Akt signaling is required for glioblastoma maintenance in vivo. *Am J Cancer Res*. 2011; 1(2):155-167.
125. Ohgaki H and Kleihues P. Population-based studies on incidence, survival rates, and genetic alterations in astrocytic and oligodendroglial gliomas. *J Neuropathol Exp Neurol*. 2005; 64(6):479-489.
126. Shinojima N, Tada K, Shiraishi S, Kamiryo T, Kochi M, Nakamura H, Makino K, Saya H, Hirano H, Kuratsu J, Oka K, Ishimaru Y and Ushio Y. Prognostic value of epidermal growth factor receptor in patients with glioblastoma multiforme. *Cancer Res*. 2003; 63(20):6962-6970.
127. Simmons ML, Lamborn KR, Takahashi M, Chen P, Israel MA, Berger MS, Godfrey T, Nigro J, Prados M, Chang S, Barker FG, 2nd and Aldape K. Analysis of complex relationships between age, p53, epidermal growth factor receptor, and survival in glioblastoma patients. *Cancer Res*. 2001; 61(3):1122-1128.
128. Frederick L, Wang XY, Eley G and James CD. Diversity and frequency of epidermal growth factor receptor mutations in human glioblastomas. *Cancer Res*. 2000; 60(5):1383-1387.
129. Sugawa N, Ekstrand AJ, James CD and Collins VP. Identical splicing of aberrant epidermal growth factor receptor transcripts from amplified rearranged genes in human glioblastomas. *Proc Natl Acad Sci U S A*. 1990; 87(21):8602-8606.

130. Katanasaka Y, Kodera Y, Kitamura Y, Morimoto T, Tamura T and Koizumi F. Epidermal growth factor receptor variant type III markedly accelerates angiogenesis and tumor growth via inducing c-myc mediated angiopoietin-like 4 expression in malignant glioma. *Mol Cancer*. 2013; 12:31.
131. Johnson H, Del Rosario AM, Bryson BD, Schroeder MA, Sarkaria JN and White FM. Molecular characterization of EGFR and EGFRvIII signaling networks in human glioblastoma tumor xenografts. *Mol Cell Proteomics*. 2012; 11(12):1724-1740.
132. Bonavia R, Inda MM, Vandenberg S, Cheng SY, Nagane M, Hadwiger P, Tan P, Sah DW, Cavenee WK and Furnari FB. EGFRvIII promotes glioma angiogenesis and growth through the NF-kappaB, interleukin-8 pathway. *Oncogene*. 2012; 31(36):4054-4066.
133. Narita Y, Nagane M, Mishima K, Huang HJ, Furnari FB and Cavenee WK. Mutant epidermal growth factor receptor signaling down-regulates p27 through activation of the phosphatidylinositol 3-kinase/Akt pathway in glioblastomas. *Cancer Res*. 2002; 62(22):6764-6769.
134. Weller M, Kaulich K, Hentschel B, Felsberg J, Gramatzki D, Pietsch T, Simon M, Westphal M, Schackert G, Tonn JC, von Deimling A, Davis T, Weiss WA, Loeffler M and Reifenberger G. Assessment and prognostic significance of the epidermal growth factor receptor vIII mutation in glioblastoma patients treated with concurrent and adjuvant temozolomide radiochemotherapy. *Int J Cancer*. 2014; 134(10):2437-2447.
135. Sun H, Lesche R, Li DM, Liliental J, Zhang H, Gao J, Gavrilova N, Mueller B, Liu X and Wu H. PTEN modulates cell cycle progression and cell survival by regulating phosphatidylinositol 3,4,5,-trisphosphate and Akt/protein kinase B signaling pathway. *Proc Natl Acad Sci U S A*. 1999; 96(11):6199-6204.
136. Song MS, Salmena L and Pandolfi PP. The functions and regulation of the PTEN tumour suppressor. *Nat Rev Mol Cell Biol*. 2012; 13(5):283-296.
137. Smith JS, Tachibana I, Passe SM, Huntley BK, Borell TJ, Iturria N, O'Fallon JR, Schaefer PL, Scheithauer BW, James CD, Buckner JC and Jenkins RB. PTEN

## Reference

---

- mutation, EGFR amplification, and outcome in patients with anaplastic astrocytoma and glioblastoma multiforme. *J Natl Cancer Inst.* 2001; 93(16):1246-1256.
138. Li YL, Tian Z, Wu DY, Fu BY and Xin Y. Loss of heterozygosity on 10q23.3 and mutation of tumor suppressor gene PTEN in gastric cancer and precancerous lesions. *World J Gastroenterol.* 2005; 11(2):285-288.
139. Reiss K, Wang JY, Romano G, Furnari FB, Cavenee WK, Morrione A, Tu X and Baserga R. IGF-I receptor signaling in a prostatic cancer cell line with a PTEN mutation. *Oncogene.* 2000; 19(22):2687-2694.
140. Forgacs E, Biesterveld EJ, Sekido Y, Fong K, Muneer S, Wistuba, II, Milchgrub S, Brezinschek R, Virmani A, Gazdar AF and Minna JD. Mutation analysis of the PTEN/MMAC1 gene in lung cancer. *Oncogene.* 1998; 17(12):1557-1565.
141. Yokomizo A, Tindall DJ, Hartmann L, Jenkins RB, Smith DI and Liu W. Mutation analysis of the putative tumor suppressor PTEN/MMAC1 in human ovarian cancer. *Int J Oncol.* 1998; 13(1):101-105.
142. Srividya MR, Thota B, Shailaja BC, Arivazhagan A, Thennarasu K, Chandramouli BA, Hegde AS and Santosh V. Homozygous 10q23/PTEN deletion and its impact on outcome in glioblastoma: a prospective translational study on a uniformly treated cohort of adult patients. *Neuropathology.* 2011; 31(4):376-383.
143. Pollack IF, Hamilton RL, James CD, Finkelstein SD, Burnham J, Yates AJ, Holmes EJ, Zhou T and Finlay JL. Rarity of PTEN deletions and EGFR amplification in malignant gliomas of childhood: results from the Children's Cancer Group 945 cohort. *J Neurosurg.* 2006; 105(5 Suppl):418-424.
144. Furnari FB, Huang HJ and Cavenee WK. The phosphoinositol phosphatase activity of PTEN mediates a serum-sensitive G1 growth arrest in glioma cells. *Cancer Res.* 1998; 58(22):5002-5008.
145. Li DM and Sun H. PTEN/MMAC1/TEP1 suppresses the tumorigenicity and induces G1 cell cycle arrest in human glioblastoma cells. *Proc Natl Acad Sci U S A.* 1998; 95(26):15406-15411.

## Reference

---

146. Freeman DJ, Li AG, Wei G, Li HH, Kertesz N, Lesche R, Whale AD, Martinez-Diaz H, Rozengurt N, Cardiff RD, Liu X and Wu H. PTEN tumor suppressor regulates p53 protein levels and activity through phosphatase-dependent and -independent mechanisms. *Cancer Cell*. 2003; 3(2):117-130.
147. Mayo LD, Dixon JE, Durden DL, Tonks NK and Donner DB. PTEN protects p53 from Mdm2 and sensitizes cancer cells to chemotherapy. *J Biol Chem*. 2002; 277(7):5484-5489.
148. Tamura M, Gu J, Matsumoto K, Aota S, Parsons R and Yamada KM. Inhibition of cell migration, spreading, and focal adhesions by tumor suppressor PTEN. *Science*. 1998; 280(5369):1614-1617.
149. Tamura M, Gu J, Takino T and Yamada KM. Tumor suppressor PTEN inhibition of cell invasion, migration, and growth: differential involvement of focal adhesion kinase and p130Cas. *Cancer Res*. 1999; 59(2):442-449.
150. Zhang LL, Liu J, Lei S, Zhang J, Zhou W and Yu HG. PTEN inhibits the invasion and metastasis of gastric cancer via downregulation of FAK expression. *Cell Signal*. 2014; 26(5):1011-1020.
151. Park MJ, Kim MS, Park IC, Kang HS, Yoo H, Park SH, Rhee CH, Hong SI and Lee SH. PTEN suppresses hyaluronic acid-induced matrix metalloproteinase-9 expression in U87MG glioblastoma cells through focal adhesion kinase dephosphorylation. *Cancer Res*. 2002; 62(21):6318-6322.
152. Cai XM, Tao BB, Wang LY, Liang YL, Jin JW, Yang Y, Hu YL and Zha XL. Protein phosphatase activity of PTEN inhibited the invasion of glioma cells with epidermal growth factor receptor mutation type III expression. *Int J Cancer*. 2005; 117(6):905-912.
153. Arcaro A and Wymann MP. Wortmannin is a potent phosphatidylinositol 3-kinase inhibitor: the role of phosphatidylinositol 3,4,5-trisphosphate in neutrophil responses. *Biochem J*. 1993; 296 ( Pt 2):297-301.
154. Vlahos CJ, Matter WF, Hui KY and Brown RF. A specific inhibitor of phosphatidylinositol 3-kinase,

## Reference

---

- 2-(4-morpholinyl)-8-phenyl-4H-1-benzopyran-4-one (LY294002). *J Biol Chem.* 1994; 269(7):5241-5248.
155. Gharbi SI, Zvelebil MJ, Shuttleworth SJ, Hancox T, Saghir N, Timms JF and Waterfield MD. Exploring the specificity of the PI3K family inhibitor LY294002. *Biochem J.* 2007; 404(1):15-21.
156. Rodon J, Dienstmann R, Serra V and Taberero J. Development of PI3K inhibitors: lessons learned from early clinical trials. *Nat Rev Clin Oncol.* 2013; 10(3):143-153.
157. Gobin B, Huin MB, Lamoureux F, Ory B, Charrier C, Lanel R, Battaglia S, Redini F, Lezot F, Blanchard F and Heymann D. BYL719, a new alpha-specific PI3K inhibitor: Single administration and in combination with conventional chemotherapy for the treatment of osteosarcoma. *Int J Cancer.* 2015; 136(4):784-796.
158. Lannutti BJ, Meadows SA, Herman SEM, Kashishian A, Steiner B, Johnson AJ, Byrd JC, Tyner JW, Loriaux MM, Deininger M, Druker BJ, Puri KD, Ulrich RG and Giese NA. CAL-101, a p110 selective phosphatidylinositol-3-kinase inhibitor for the treatment of B-cell malignancies, inhibits PI3K signaling and cellular viability. *Blood.* 2010; 117(2):591-594.
159. De Buck SS, Jakab A, Boehm M, Bootle D, Juric D, Quadt C and Goggin TK. Population pharmacokinetics and pharmacodynamics of BYL719, a phosphoinositide 3-kinase antagonist, in adult patients with advanced solid malignancies. *Br J Clin Pharmacol.* 2014; 78(3):543-555.
160. Brown JR, Byrd JC, Coutre SE, Benson DM, Flinn IW, Wagner-Johnston ND, Spurgeon SE, Kahl BS, Bello C, Webb HK, Johnson DM, Peterman S, Li D, Jahn TM, Lannutti BJ, Ulrich RG, et al. Idelalisib, an inhibitor of phosphatidylinositol 3-kinase p110delta, for relapsed/refractory chronic lymphocytic leukemia. *Blood.* 2014; 123(22):3390-3397.
161. Laplante M and Sabatini DM. mTOR signaling in growth control and disease. *Cell.* 2012; 149(2):274-293.
162. Fan QW and Weiss WA. Inhibition of PI3K-Akt-mTOR signaling in glioblastoma

- by mTORC1/2 inhibitors. *Methods Mol Biol.* 2012; 821:349-359.
163. Sarker D, Ang JE, Baird R, Kristeleit R, Shah K, Moreno V, Clarke PA, Raynaud FI, Levy G, Ware JA, Mazina K, Lin R, Wu J, Fredrickson J, Spoerke JM, Lackner MR, et al. First-in-human phase I study of pictilisib (GDC-0941), a potent pan-class I phosphatidylinositol-3-kinase (PI3K) inhibitor, in patients with advanced solid tumors. *Clin Cancer Res.* 2015; 21(1):77-86.
164. Ndubaku CO, Heffron TP, Staben ST, Baumgardner M, Blaquiére N, Bradley E, Bull R, Do S, Dotson J, Dudley D, Edgar KA, Friedman LS, Goldsmith R, Heald RA, Kolesnikov A, Lee L, et al. Discovery of 2-{3-[2-(1-isopropyl-3-methyl-1H-1,2,4-triazol-5-yl)-5,6-dihydrobenzo[f]imidazo[1,2-d][1,4]oxazepin-9-yl]-1H-pyrazol-1-yl}-2-methylpropanamide (GDC-0032): a beta-sparing phosphoinositide 3-kinase inhibitor with high unbound exposure and robust in vivo antitumor activity. *J Med Chem.* 2013; 56(11):4597-4610.
165. Rodon J, Brana I, Siu LL, De Jonge MJ, Homji N, Mills D, Di Tomaso E, Sarr C, Trandafir L, Massacesi C, Eskens F and Bendell JC. Phase I dose-escalation and -expansion study of buparlisib (BKM120), an oral pan-Class I PI3K inhibitor, in patients with advanced solid tumors. *Invest New Drugs.* 2014; 32(4):670-681.
166. Ando Y, Inada-Inoue M, Mitsuma A, Yoshino T, Ohtsu A, Suenaga N, Sato M, Kakizume T, Robson M, Quadt C and Doi T. Phase I dose-escalation study of buparlisib (BKM120), an oral pan-class I PI3K inhibitor, in Japanese patients with advanced solid tumors. *Cancer Sci.* 2014; 105(3):347-353.
167. Saura C, Bendell J, Jerusalem G, Su S, Ru Q, De Buck S, Mills D, Ruquet S, Bosch A, Urruticoechea A, Beck JT, Di Tomaso E, Sternberg DW, Massacesi C, Hirawat S, Dirix L, et al. Phase Ib study of Buparlisib plus Trastuzumab in patients with HER2-positive advanced or metastatic breast cancer that has progressed on Trastuzumab-based therapy. *Clin Cancer Res.* 2014; 20(7):1935-1945.
168. Mayer IA, Abramson VG, Isakoff SJ, Forero A, Balko JM, Kuba MG, Sanders ME, Yap JT, Van den Abbeele AD, Li Y, Cantley LC, Winer E and Arteaga CL. Stand up to cancer phase Ib study of pan-phosphoinositide-3-kinase inhibitor

- buparlisib with letrozole in estrogen receptor-positive/human epidermal growth factor receptor 2-negative metastatic breast cancer. *J Clin Oncol.* 2014; 32(12):1202-1209.
169. Bendell JC, Rodon J, Burris HA, de Jonge M, Verweij J, Birlle D, Demanse D, De Buck SS, Ru QC, Peters M, Goldbrunner M and Baselga J. Phase I, dose-escalation study of BKM120, an oral pan-Class I PI3K inhibitor, in patients with advanced solid tumors. *J Clin Oncol.* 2012; 30(3):282-290.
170. Levy B, Spira A, Becker D, Evans T, Schnadig I, Camidge DR, Bauman JE, Hausman D, Walker L, Nemunaitis J, Rudin CM, Halmos B and Bowles DW. A randomized, phase 2 trial of Docetaxel with or without PX-866, an irreversible oral phosphatidylinositol 3-kinase inhibitor, in patients with relapsed or metastatic non-small-cell lung cancer. *J Thorac Oncol.* 2014; 9(7):1031-1035.
171. Bowles DW, Ma WW, Senzer N, Brahmer JR, Adjei AA, Davies M, Lazar AJ, Vo A, Peterson S, Walker L, Hausman D, Rudin CM and Jimeno A. A multicenter phase 1 study of PX-866 in combination with docetaxel in patients with advanced solid tumours. *Br J Cancer.* 2013; 109(5):1085-1092.
172. Hong DS, Bowles DW, Falchook GS, Messersmith WA, George GC, O'Bryant CL, Vo AC, Klucher K, Herbst RS, Eckhardt SG, Peterson S, Hausman DF, Kurzrock R and Jimeno A. A multicenter phase I trial of PX-866, an oral irreversible phosphatidylinositol 3-kinase inhibitor, in patients with advanced solid tumors. *Clin Cancer Res.* 2012; 18(15):4173-4182.
173. Shapiro GI, Rodon J, Bedell C, Kwak EL, Baselga J, Brana I, Pandya SS, Scheffold C, Laird AD, Nguyen LT, Xu Y, Egile C and Edelman G. Phase I safety, pharmacokinetic, and pharmacodynamic study of SAR245408 (XL147), an oral pan-class I PI3K inhibitor, in patients with advanced solid tumors. *Clin Cancer Res.* 2014; 20(1):233-245.
174. Kahl BS, Spurgeon SE, Furman RR, Flinn IW, Coutre SE, Brown JR, Benson DM, Byrd JC, Peterman S, Cho Y, Yu A, Godfrey WR and Wagner-Johnston ND. A phase 1 study of the PI3Kdelta inhibitor idelalisib in patients with relapsed/refractory mantle cell lymphoma (MCL). *Blood.* 2014;

- 123(22):3398-3405.
175. Flinn IW, Kahl BS, Leonard JP, Furman RR, Brown JR, Byrd JC, Wagner-Johnston ND, Coutre SE, Benson DM, Peterman S, Cho Y, Webb HK, Johnson DM, Yu AS, Ulrich RG, Godfrey WR, et al. Idelalisib, a selective inhibitor of phosphatidylinositol 3-kinase-delta, as therapy for previously treated indolent non-Hodgkin lymphoma. *Blood*. 2014; 123(22):3406-3413.
176. Bendell JC, Kurkjian C, Infante JR, Bauer TM, Burris HA, 3rd, Greco FA, Shih KC, Thompson DS, Lane CM, Finney LH and Jones SF. A phase 1 study of the sachet formulation of the oral dual PI3K/mTOR inhibitor BEZ235 given twice daily (BID) in patients with advanced solid tumors. *Invest New Drugs*. 2015; 33(2):463-471.
177. Wise-Draper T, Moorthy G, Salkeni M, Thomas H, Mercer C, Kozma S, Thomas G, Rixe O, Desai P, Morris J and Olowokure O. P1.14A Dose Escalation Single Arm Phase Ib Combination Study of BEZ235 with Everolimus in Patients with Advanced Solid Malignancies. *Ann Oncol*. 2015; 26 Suppl 2:ii19.
178. Liu T, Sun Q, Li Q, Yang H, Zhang Y, Wang R, Lin X, Xiao D, Yuan Y, Chen L and Wang W. Dual PI3K/mTOR inhibitors, GSK2126458 and PKI-587, suppress tumor progression and increase radiosensitivity in nasopharyngeal carcinoma. *Mol Cancer Ther*. 2015; 14(2):429-439.
179. Janne PA, Cohen RB, Laird AD, Mace S, Engelman JA, Ruiz-Soto R, Rockich K, Xu J, Shapiro GI, Martinez P and Felip E. Phase I safety and pharmacokinetic study of the PI3K/mTOR inhibitor SAR245409 (XL765) in combination with erlotinib in patients with advanced solid tumors. *J Thorac Oncol*. 2014; 9(3):316-323.
180. Papadopoulos KP, Egile C, Ruiz-Soto R, Jiang J, Shi W, Bentzien F, Rasco D, Abrisqueta P, Vose JM and Taberero J. Efficacy, safety, pharmacokinetics and pharmacodynamics of SAR245409 (voxtalisib, XL765), an orally administered phosphoinositide 3-kinase/mammalian target of rapamycin inhibitor: a phase 1 expansion cohort in patients with relapsed or refractory lymphoma. *Leuk Lymphoma*. 2014:1-8.

181. De P, Dey N, Terakedis B, Bergsagel PL, Li ZH, Mahadevan D, Garlich JR, Trudel S, Makale MT and Durden DL. An integrin-targeted, pan-isoform, phosphoinositide-3 kinase inhibitor, SF1126, has activity against multiple myeloma in vivo. *Cancer Chemother Pharmacol.* 2013; 71(4):867-881.
182. Mahadevan D, Chiorean EG, Harris WB, Von Hoff DD, Stejskal-Barnett A, Qi W, Anthony SP, Younger AE, Rensvold DM, Cordova F, Shelton CF, Becker MD, Garlich JR, Durden DL and Ramanathan RK. Phase I pharmacokinetic and pharmacodynamic study of the pan-PI3K/mTORC vascular targeted pro-drug SF1126 in patients with advanced solid tumours and B-cell malignancies. *Eur J Cancer.* 2012; 48(18):3319-3327.
183. Bode AM and Dong Z. The functional contrariety of JNK. *Mol Carcinog.* 2007; 46(8):591-598.
184. Gupta S, Barrett T, Whitmarsh AJ, Cavanagh J, Sluss HK, Derijard B and Davis RJ. Selective interaction of JNK protein kinase isoforms with transcription factors. *EMBO J.* 1996; 15(11):2760-2770.
185. Barr RK and Bogoyevitch MA. The c-Jun N-terminal protein kinase family of mitogen-activated protein kinases (JNK MAPKs). *Int J Biochem Cell Biol.* 2001; 33(11):1047-1063.
186. Lopez-Illasaca M. Signaling from G-protein-coupled receptors to mitogen-activated protein (MAP)-kinase cascades. *Biochem Pharmacol.* 1998; 56(3):269-277.
187. Roskoski R, Jr. RAF protein-serine/threonine kinases: structure and regulation. *Biochem Biophys Res Commun.* 2010; 399(3):313-317.
188. Ichijo H, Nishida E, Irie K, ten Dijke P, Saitoh M, Moriguchi T, Takagi M, Matsumoto K, Miyazono K and Gotoh Y. Induction of apoptosis by ASK1, a mammalian MAPKKK that activates SAPK/JNK and p38 signaling pathways. *Science.* 1997; 275(5296):90-94.
189. Sun BK, Kim JH, Nguyen HN, Oh S, Kim SY, Choi S, Choi HJ, Lee YJ and Song JJ. MEK1/MEK4 are responsible for TRAIL-induced JNK/p38 phosphorylation. *Oncol Rep.* 2011; 25(2):537-544.

## Reference

---

190. Xu Z, Maroney AC, Dobrzanski P, Kukekov NV and Greene LA. The MLK family mediates c-Jun N-terminal kinase activation in neuronal apoptosis. *Mol Cell Biol.* 2001; 21(14):4713-4724.
191. Ip YT and Davis RJ. Signal transduction by the c-Jun N-terminal kinase (JNK)--from inflammation to development. *Curr Opin Cell Biol.* 1998; 10(2):205-219.
192. Kishimoto H, Nakagawa K, Watanabe T, Kitagawa D, Momose H, Seo J, Nishitai G, Shimizu N, Ohata S, Tanemura S, Asaka S, Goto T, Fukushi H, Yoshida H, Suzuki A, Sasaki T, et al. Different properties of SEK1 and MKK7 in dual phosphorylation of stress-induced activated protein kinase SAPK/JNK in embryonic stem cells. *J Biol Chem.* 2003; 278(19):16595-16601.
193. Tournier C, Dong C, Turner TK, Jones SN, Flavell RA and Davis RJ. MKK7 is an essential component of the JNK signal transduction pathway activated by proinflammatory cytokines. *Genes Dev.* 2001; 15(11):1419-1426.
194. Chiu R, Boyle WJ, Meek J, Smeal T, Hunter T and Karin M. The c-Fos protein interacts with c-Jun/AP-1 to stimulate transcription of AP-1 responsive genes. *Cell.* 1988; 54(4):541-552.
195. Shaulian E. AP-1--The Jun proteins: Oncogenes or tumor suppressors in disguise? *Cell Signal.* 2010; 22(6):894-899.
196. Engstrom W, Ward A and Moorwood K. The role of scaffold proteins in JNK signalling. *Cell Prolif.* 2010; 43(1):56-66.
197. Whitmarsh AJ, Cavanagh J, Tournier C, Yasuda J and Davis RJ. A mammalian scaffold complex that selectively mediates MAP kinase activation. *Science.* 1998; 281(5383):1671-1674.
198. Whitmarsh AJ, Kuan CY, Kennedy NJ, Kelkar N, Haydar TF, Mordes JP, Appel M, Rossini AA, Jones SN, Flavell RA, Rakic P and Davis RJ. Requirement of the JIP1 scaffold protein for stress-induced JNK activation. *Genes Dev.* 2001; 15(18):2421-2432.
199. Nihalani D, Meyer D, Pajni S and Holzman LB. Mixed lineage kinase-dependent JNK activation is governed by interactions of scaffold protein JIP with MAPK

- module components. *EMBO J.* 2001; 20(13):3447-3458.
200. Willoughby EA, Perkins GR, Collins MK and Whitmarsh AJ. The JNK-interacting protein-1 scaffold protein targets MAPK phosphatase-7 to dephosphorylate JNK. *J Biol Chem.* 2003; 278(12):10731-10736.
201. Sabapathy K, Hochedlinger K, Nam SY, Bauer A, Karin M and Wagner EF. Distinct roles for JNK1 and JNK2 in regulating JNK activity and c-Jun-dependent cell proliferation. *Mol Cell.* 2004; 15(5):713-725.
202. Sabapathy K and Wagner EF. JNK2: a negative regulator of cellular proliferation. *Cell Cycle.* 2004; 3(12):1520-1523.
203. Lin A. Activation of the JNK signaling pathway: Breaking the brake on apoptosis. *BioEssays.* 2003; 25(1):17-24.
204. Lin A and Dibling B. The true face of JNK activation in apoptosis. *Aging Cell.* 2002; 1(2):112-116.
205. Kato T, Noma H, Kitagawa M, Takahashi T, Oshitani N and Kitagawa S. Distinct role of c-Jun N-terminal kinase isoforms in human neutrophil apoptosis regulated by tumor necrosis factor-alpha and granulocyte-macrophage colony-stimulating factor. *J Interferon Cytokine Res.* 2008; 28(4):235-243.
206. Yujiri T, Ware M, Widmann C, Oyer R, Russell D, Chan E, Zaitso Y, Clarke P, Tyler K, Oka Y, Fanger GR, Henson P and Johnson GL. MEK kinase 1 gene disruption alters cell migration and c-Jun NH2-terminal kinase regulation but does not cause a measurable defect in NF-kappa B activation. *Proc Natl Acad Sci U S A.* 2000; 97(13):7272-7277.
207. Xia Y, Makris C, Su B, Li E, Yang J, Nemerow GR and Karin M. MEK kinase 1 is critically required for c-Jun N-terminal kinase activation by proinflammatory stimuli and growth factor-induced cell migration. *Proc Natl Acad Sci U S A.* 2000; 97(10):5243-5248.
208. Huang C, Jacobson K and Schaller MD. A role for JNK-paxillin signaling in cell migration. *Cell Cycle.* 2004; 3(1):4-6.
209. Huang C, Rajfur Z, Borchers C, Schaller MD and Jacobson K. JNK phosphorylates paxillin and regulates cell migration. *Nature.* 2003;

- 424(6945):219-223.
- 210.Lee MH, Koria P, Qu J and Andreadis ST. JNK phosphorylates beta-catenin and regulates adherens junctions. *FASEB J.* 2009; 23(11):3874-3883.
- 211.Lee MH, Padmashali R, Koria P and Andreadis ST. JNK regulates binding of alpha-catenin to adherens junctions and cell-cell adhesion. *FASEB J.* 2011; 25(2):613-623.
- 212.Zhang YH, Wang SQ, Sun CR, Wang M, Wang B and Tang JW. Inhibition of JNK1 expression decreases migration and invasion of mouse hepatocellular carcinoma cell line in vitro. *Med Oncol.* 2011; 28(4):966-972.
- 213.Mishra P, Senthivinayagam S, Rangasamy V, Sondarva G and Rana B. Mixed lineage kinase-3/JNK1 axis promotes migration of human gastric cancer cells following gastrin stimulation. *Mol Endocrinol.* 2010; 24(3):598-607.
- 214.Kaoud TS, Mitra S, Lee S, Taliaferro J, Cantrell M, Linse KD, Van Den Berg CL and Dalby KN. Development of JNK2-selective peptide inhibitors that inhibit breast cancer cell migration. *ACS Chem Biol.* 2011; 6(6):658-666.
- 215.Mitra S, Lee JS, Cantrell M and Van den Berg CL. c-Jun N-terminal kinase 2 (JNK2) enhances cell migration through epidermal growth factor substrate 8 (EPS8). *J Biol Chem.* 2011; 286(17):15287-15297.
- 216.Zhan Y, Abi Saab WF, Modi N, Stewart AM, Liu J and Chadee DN. Mixed lineage kinase 3 is required for matrix metalloproteinase expression and invasion in ovarian cancer cells. *Exp Cell Res.* 2012; 318(14):1641-1648.
- 217.Kimura R, Ishikawa C, Rokkaku T, Janknecht R and Mori N. Phosphorylated c-Jun and Fra-1 induce matrix metalloproteinase-1 and thereby regulate invasion activity of 143B osteosarcoma cells. *Biochim Biophys Acta.* 2011; 1813(8):1543-1553.
- 218.Sugioka Y, Watanabe T, Inagaki Y, Kushida M, Niioka M, Endo H, Higashiyama R and Okazaki I. c-Jun NH2-terminal kinase pathway is involved in constitutive matrix metalloproteinase-1 expression in a hepatocellular carcinoma-derived cell line. *Int J Cancer.* 2004; 109(6):867-874.
- 219.Nasrazadani A and Van Den Berg CL. c-Jun N-terminal Kinase 2 Regulates

- Multiple Receptor Tyrosine Kinase Pathways in Mouse Mammary Tumor Growth and Metastasis. *Genes Cancer*. 2011; 2(1):31-45.
220. Wang J, Kuitse I, Lee AV, Pan J, Giuliano A and Cui X. Sustained c-Jun-NH2-kinase activity promotes epithelial-mesenchymal transition, invasion, and survival of breast cancer cells by regulating extracellular signal-regulated kinase activation. *Mol Cancer Res*. 2010; 8(2):266-277.
221. Li JY, Wang H, May S, Song X, Fueyo J and Fuller GN. Constitutive activation of c-Jun N-terminal kinase correlates with histologic grade and EGFR expression in diffuse gliomas. *J Neurooncol*. 2008; 88(1):11-17.
222. Antonyak MA, Kenyon LC, Godwin AK, James DC, Emler DR, Okamoto I, Tnani M, Holgado-Madruga M, Moscatello DK and Wong AJ. Elevated JNK activation contributes to the pathogenesis of human brain tumors. *Oncogene*. 2002; 21(33):5038-5046.
223. Senger DL, Tudan C, Guiot MC, Mazzoni IE, Molenkamp G, LeBlanc R, Antel J, Olivier A, Snipes GJ and Kaplan DR. Suppression of Rac activity induces apoptosis of human glioma cells but not normal human astrocytes. *Cancer Res*. 2002; 62(7):2131-2140.
224. Shibata W, Maeda S, Hikiba Y, Yanai A, Sakamoto K, Nakagawa H, Ogura K, Karin M and Omata M. c-Jun NH2-terminal kinase 1 is a critical regulator for the development of gastric cancer in mice. *Cancer Res*. 2008; 68(13):5031-5039.
225. Lee SJ, Moon GS, Jung KH, Kim WJ and Moon SK. c-Jun N-terminal kinase 1 is required for cordycepin-mediated induction of G2/M cell-cycle arrest via p21WAF1 expression in human colon cancer cells. *Food Chem Toxicol*. 2010; 48(1):277-283.
226. Chang Q, Chen J, Beezhold KJ, Castranova V, Shi X and Chen F. JNK1 activation predicts the prognostic outcome of the human hepatocellular carcinoma. *Mol Cancer*. 2009; 8:64.
227. Nielsen C, Thastrup J, Bottzauw T, Jaattela M and Kallunki T. c-Jun NH2-terminal kinase 2 is required for Ras transformation independently of activator protein 1. *Cancer Res*. 2007; 67(1):178-185.

228. Potapova O, Gorospe M, Dougherty RH, Dean NM, Gaarde WA and Holbrook NJ. Inhibition of c-Jun N-terminal kinase 2 expression suppresses growth and induces apoptosis of human tumor cells in a p53-dependent manner. *Mol Cell Biol.* 2000; 20(5):1713-1722.
229. Bost F, McKay R, Bost M, Potapova O, Dean NM and Mercola D. The Jun kinase 2 isoform is preferentially required for epidermal growth factor-induced transformation of human A549 lung carcinoma cells. *Mol Cell Biol.* 1999; 19(3):1938-1949.
230. Potapova O, Gorospe M, Bost F, Dean NM, Gaarde WA, Mercola D and Holbrook NJ. c-Jun N-terminal kinase is essential for growth of human T98G glioblastoma cells. *J Biol Chem.* 2000; 275(32):24767-24775.
231. Tsuiki H, Tnani M, Okamoto I, Kenyon LC, Emlet DR, Holgado-Madruga M, Lanham IS, Joynes CJ, Vo KT and Wong AJ. Constitutively active forms of c-Jun NH2-terminal kinase are expressed in primary glial tumors. *Cancer Res.* 2003; 63(1):250-255.
232. Cui J, Han SY, Wang C, Su W, Harshyne L, Holgado-Madruga M and Wong AJ. c-Jun NH(2)-terminal kinase 2 $\alpha$ 2 promotes the tumorigenicity of human glioblastoma cells. *Cancer Res.* 2006; 66(20):10024-10031.
233. Yoshida S, Fukino K, Harada H, Nagai H, Imoto I, Inazawa J, Takahashi H, Teramoto A and Emi M. The c-Jun NH2-terminal kinase3 (JNK3) gene: genomic structure, chromosomal assignment, and loss of expression in brain tumors. *J Hum Genet.* 2001; 46(4):182-187.
234. Ying J, Li H, Cui Y, Wong AH, Langford C and Tao Q. Epigenetic disruption of two proapoptotic genes MAPK10/JNK3 and PTPN13/FAP-1 in multiple lymphomas and carcinomas through hypermethylation of a common bidirectional promoter. *Leukemia.* 2006; 20(6):1173-1175.
235. Gorogh T, Beress L, Quabius ES, Ambrosch P and Hoffmann M. Head and neck cancer cells and xenografts are very sensitive to palytoxin: decrease of c-jun n-terminale kinase-3 expression enhances palytoxin toxicity. *Mol Cancer.* 2013; 12:12.

236. Mielke K. Growth-arrest-dependent expression and phosphorylation of p27<sup>kip</sup> at serine10 is mediated by the JNK pathway in C6 glioma cells. *Mol Cell Neurosci.* 2008; 38(3):301-311.
237. Dajas-Bailador F, Bantounas I, Jones EV and Whitmarsh AJ. Regulation of axon growth by the JIP1-AKT axis. *J Cell Sci.* 2014; 127(Pt 1):230-239.
238. Kim AH, Sasaki T and Chao MV. JNK-interacting protein 1 promotes Akt1 activation. *J Biol Chem.* 2003; 278(32):29830-29836.
239. Pan J, Pei DS, Yin XH, Hui L and Zhang GY. Involvement of oxidative stress in the rapid Akt1 regulating a JNK scaffold during ischemia in rat hippocampus. *Neurosci Lett.* 2006; 392(1-2):47-51.
240. Kim AH, Yano H, Cho H, Meyer D, Monks B, Margolis B, Birnbaum MJ and Chao MV. Akt1 regulates a JNK scaffold during excitotoxic apoptosis. *Neuron.* 2002; 35(4):697-709.
241. Barthwal MK, Sathyanarayana P, Kundu CN, Rana B, Pradeep A, Sharma C, Woodgett JR and Rana A. Negative regulation of mixed lineage kinase 3 by protein kinase B/AKT leads to cell survival. *J Biol Chem.* 2003; 278(6):3897-3902.
242. Wen XR, Li C, Zong YY, Yu CZ, Xu J, Han D and Zhang GY. Dual inhibitory roles of geldanamycin on the c-Jun NH2-terminal kinase 3 signal pathway through suppressing the expression of mixed-lineage kinase 3 and attenuating the activation of apoptosis signal-regulating kinase 1 via facilitating the activation of Akt in ischemic brain injury. *Neuroscience.* 2008; 156(3):483-497.
243. Wang Q, Zhang QG, Wu DN, Yin XH and Zhang GY. Neuroprotection of selenite against ischemic brain injury through negatively regulating early activation of ASK1/JNK cascade via activation of PI3K/AKT pathway. *Acta Pharmacol Sin.* 2007; 28(1):19-27.
244. Kim AH, Khursigara G, Sun X, Franke TF and Chao MV. Akt phosphorylates and negatively regulates apoptosis signal-regulating kinase 1. *Mol Cell Biol.* 2001; 21(3):893-901.
245. Park HS, Kim MS, Huh SH, Park J, Chung J, Kang SS and Choi EJ. Akt (protein

- kinase B) negatively regulates SEK1 by means of protein phosphorylation. *J Biol Chem.* 2002; 277(4):2573-2578.
246. Murakami T, Takagi H, Suzuma K, Suzuma I, Ohashi H, Watanabe D, Ojima T, Suganami E, Kurimoto M, Kaneto H, Honda Y and Yoshimura N. Angiotensin-1 attenuates H<sub>2</sub>O<sub>2</sub>-induced SEK1/JNK phosphorylation through the phosphatidylinositol 3-kinase/Akt pathway in vascular endothelial cells. *J Biol Chem.* 2005; 280(36):31841-31849.
247. Logan SK, Falasca M, Hu P and Schlessinger J. Phosphatidylinositol 3-kinase mediates epidermal growth factor-induced activation of the c-Jun N-terminal kinase signaling pathway. *Mol Cell Biol.* 1997; 17(10):5784-5790.
248. Vivanco I, Palaskas N, Tran C, Finn SP, Getz G, Kennedy NJ, Jiao J, Rose J, Xie W, Loda M, Golub T, Mellinghoff IK, Davis RJ, Wu H and Sawyers CL. Identification of the JNK signaling pathway as a functional target of the tumor suppressor PTEN. *Cancer Cell.* 2007; 11(6):555-569.
249. Nitta RT, Del Vecchio CA, Chu AH, Mitra SS, Godwin AK and Wong AJ. The role of the c-Jun N-terminal kinase 2- $\alpha$ -isoform in non-small cell lung carcinoma tumorigenesis. *Oncogene.* 2011; 30(2):234-244.
250. Rong Y, Belozero V, Tucker-Burden C, Chen G, Durden DL, Olson JJ, Van Meir EG, Mackman N and Brat DJ. Epidermal growth factor receptor and PTEN modulate tissue factor expression in glioblastoma through JunD/activator protein-1 transcriptional activity. *Cancer Res.* 2009; 69(6):2540-2549.
251. Hettinger K, Vikhanskaya F, Poh MK, Lee MK, de Belle I, Zhang JT, Reddy SA and Sabapathy K. c-Jun promotes cellular survival by suppression of PTEN. *Cell Death Differ.* 2007; 14(2):218-229.
252. Lopez-Bergami P, Kim H, Dewing A, Goydos J, Aaronson S and Ronai Z. c-Jun regulates phosphoinositide-dependent kinase 1 transcription: implication for Akt and protein kinase C activities and melanoma tumorigenesis. *J Biol Chem.* 2010; 285(2):903-913.
253. Castellano E and Downward J. RAS Interaction with PI3K: More Than Just Another Effector Pathway. *Genes Cancer.* 2011; 2(3):261-274.

254. Xing Y and Hogge DE. Combined inhibition of the phosphoinosityl-3-kinase (PI3Kinase) P110delta subunit and mitogen-extracellular activated protein kinase (MEKinase) shows synergistic cytotoxicity against human acute myeloid leukemia progenitors. *Leukemia research*. 2013; 37(6):697-704.
255. Shimizu T, Tolcher AW, Papadopoulos KP, Beeram M, Rasco DW, Smith LS, Gunn S, Smetzer L, Mays TA, Kaiser B, Wick MJ, Alvarez C, Cavazos A, Mangold GL and Patnaik A. The clinical effect of the dual-targeting strategy involving PI3K/AKT/mTOR and RAS/MEK/ERK pathways in patients with advanced cancer. *Clin Cancer Res*. 2012; 18(8):2316-2325.
256. Lee HY, Oh SH, Suh YA, Baek JH, Papadimitrakopoulou V, Huang S and Hong WK. Response of non-small cell lung cancer cells to the inhibitors of phosphatidylinositol 3-kinase/Akt- and MAPK kinase 4/c-Jun NH2-terminal kinase pathways: an effective therapeutic strategy for lung cancer. *Clin Cancer Res*. 2005; 11(16):6065-6074.
257. Lee HY, Srinivas H, Xia D, Lu Y, Superty R, LaPushin R, Gomez-Manzano C, Gal AM, Walsh GL, Force T, Ueki K, Mills GB and Kurie JM. Evidence that phosphatidylinositol 3-kinase- and mitogen-activated protein kinase kinase-4/c-Jun NH2-terminal kinase-dependent Pathways cooperate to maintain lung cancer cell survival. *J Biol Chem*. 2003; 278(26):23630-23638.
258. Ren W, Qiao Z, Wang H, Zhu L and Zhang L. Flavonoids: promising anticancer agents. *Medicinal research reviews*. 2003; 23(4):519-534.
259. Youdim KA, Qaiser MZ, Begley DJ, Rice-Evans CA and Abbott NJ. Flavonoid permeability across an in situ model of the blood-brain barrier. *Free Radic Biol Med*. 2004; 36(5):592-604.
260. Wang ZH, Ah Kang K, Zhang R, Piao MJ, Jo SH, Kim JS, Kang SS, Lee JS, Park DH and Hyun JW. Myricetin suppresses oxidative stress-induced cell damage via both direct and indirect antioxidant action. *Environ Toxicol Pharmacol*. 2010; 29(1):12-18.
261. Heim KE, Tagliaferro AR and Bobilya DJ. Flavonoid antioxidants: chemistry, metabolism and structure-activity relationships. *J Nutr Biochem*. 2002;

- 13(10):572-584.
262. Cao G, Sofic E and Prior RL. Antioxidant and prooxidant behavior of flavonoids: structure-activity relationships. *Free Radic Biol Med.* 1997; 22(5):749-760.
263. Rice-Evans CA, Miller NJ and Paganga G. Structure-antioxidant activity relationships of flavonoids and phenolic acids. *Free Radic Biol Med.* 1996; 20(7):933-956.
264. Kempuraj D, Madhappan B, Christodoulou S, Boucher W, Cao J, Papadopoulou N, Cetrulo CL and Theoharides TC. Flavonols inhibit proinflammatory mediator release, intracellular calcium ion levels and protein kinase C theta phosphorylation in human mast cells. *Br J Pharmacol.* 2005; 145(7):934-944.
265. Blonska M, Czuba ZP and Krol W. Effect of flavone derivatives on interleukin-1beta (IL-1beta) mRNA expression and IL-1beta protein synthesis in stimulated RAW 264.7 macrophages. *Scand J Immunol.* 2003; 57(2):162-166.
266. Ding Y, Zhang ZF, Dai XQ and Li Y. Myricetin protects against cytokine-induced cell death in RIN-m5f beta cells. *J Med Food.* 2012; 15(8):733-740.
267. Wang SJ, Tong Y, Lu S, Yang R, Liao X, Xu YF and Li X. Anti-inflammatory activity of myricetin isolated from *Myrica rubra* Sieb. et Zucc. leaves. *Planta Med.* 2010; 76(14):1492-1496.
268. Kumamoto T, Fujii M and Hou DX. Akt is a direct target for myricetin to inhibit cell transformation. *Mol Cell Biochem.* 2009; 332(1-2):33-41.
269. Lee KW, Kang NJ, Rogozin EA, Kim HG, Cho YY, Bode AM, Lee HJ, Surh YJ, Bowden GT and Dong Z. Myricetin is a novel natural inhibitor of neoplastic cell transformation and MEK1. *Carcinogenesis.* 2007; 28(9):1918-1927.
270. Kumamoto T, Fujii M and Hou DX. Myricetin directly targets JAK1 to inhibit cell transformation. *Cancer Lett.* 2009; 275(1):17-26.
271. Jung SK, Lee KW, Byun S, Kang NJ, Lim SH, Heo YS, Bode AM, Bowden GT, Lee HJ and Dong Z. Myricetin suppresses UVB-induced skin cancer by targeting Fyn. *Cancer Res.* 2008; 68(14):6021-6029.
272. Ichimatsu D, Nomura M, Nakamura S, Moritani S, Yokogawa K, Kobayashi S, Nishioka T and Miyamoto K. Structure-activity relationship of flavonoids for

- inhibition of epidermal growth factor-induced transformation of JB6 Cl 41 cells. *Mol Carcinog.* 2007; 46(6):436-445.
273. Phillips PA, Sangwan V, Borja-Cacho D, Dudeja V, Vickers SM and Saluja AK. Myricetin induces pancreatic cancer cell death via the induction of apoptosis and inhibition of the phosphatidylinositol 3-kinase (PI3K) signaling pathway. *Cancer Lett.* 2011; 308(2):181-188.
274. Sun F, Zheng XY, Ye J, Wu TT, Wang J and Chen W. Potential anticancer activity of myricetin in human T24 bladder cancer cells both in vitro and in vivo. *Nutr Cancer.* 2012; 64(4):599-606.
275. Zang W, Wang T, Wang Y, Li M, Xuan X, Ma Y, Du Y, Liu K, Dong Z and Zhao G. Myricetin exerts anti-proliferative, anti-invasive, and pro-apoptotic effects on esophageal carcinoma EC9706 and KYSE30 cells via RSK2. *Tumour Biol.* 2014; 35(12):12583-12592.
276. Ko CH, Shen SC, Lee TJ and Chen YC. Myricetin inhibits matrix metalloproteinase 2 protein expression and enzyme activity in colorectal carcinoma cells. *Mol Cancer Ther.* 2005; 4(2):281-290.
277. Shih YW, Wu PF, Lee YC, Shi MD and Chiang TA. Myricetin suppresses invasion and migration of human lung adenocarcinoma A549 cells: possible mediation by blocking the ERK signaling pathway. *J Agric Food Chem.* 2009; 57(9):3490-3499.
278. Jung SK, Lee KW, Byun S, Lee EJ, Kim JE, Bode AM, Dong Z and Lee HJ. Myricetin inhibits UVB-induced angiogenesis by regulating PI-3 kinase in vivo. *Carcinogenesis.* 2010; 31(5):911-917.
279. Siegelin MD, Gaiser T, Habel A and Siegelin Y. Myricetin sensitizes malignant glioma cells to TRAIL-mediated apoptosis by down-regulation of the short isoform of FLIP and bcl-2. *Cancer Lett.* 2009; 283(2):230-238.
280. Chiu WT, Shen SC, Chow JM, Lin CW, Shia LT and Chen YC. Contribution of reactive oxygen species to migration/invasion of human glioblastoma cells U87 via ERK-dependent COX-2/PGE(2) activation. *Neurobiol Dis.* 2010; 37(1):118-129.

281. Sang DP, Li RJ and Lan Q. Quercetin sensitizes human glioblastoma cells to temozolomide in vitro via inhibition of Hsp27. *Acta Pharmacol Sin.* 2014; 35(6):832-838.
282. Jakubowicz-Gil J, Langner E, Badziul D, Wertel I and Rzeski W. Apoptosis induction in human glioblastoma multiforme T98G cells upon temozolomide and quercetin treatment. *Tumour Biol.* 2013; 34(4):2367-2378.
283. Kim JE, Kwon JY, Lee DE, Kang NJ, Heo YS, Lee KW and Lee HJ. MKK4 is a novel target for the inhibition of tumor necrosis factor-alpha-induced vascular endothelial growth factor expression by myricetin. *Biochem Pharmacol.* 2009; 77(3):412-421.
284. Ishii N, Maier D, Merlo A, Tada M, Sawamura Y, Diserens AC and Van Meir EG. Frequent co-alterations of TP53, p16/CDKN2A, p14ARF, PTEN tumor suppressor genes in human glioma cell lines. *Brain Pathol.* 1999; 9(3):469-479.
285. Di Tomaso E, Pang JC, Lam HK, Tian XX, Suen KW, Hui AB and Hjelm NM. Establishment and characterization of a human cell line from paediatric cerebellar glioblastoma multiforme. *Neuropathol Appl Neurobiol.* 2000; 26(1):22-30.
286. Zheng Z, Amran SI, Thompson PE and Jennings IG. Isoform-selective inhibition of phosphoinositide 3-kinase: identification of a new region of nonconserved amino acids critical for p110alpha inhibition. *Mol Pharmacol.* 2011; 80(4):657-664.
287. Jackson SP, Schoenwaelder SM, Goncalves I, Nesbitt WS, Yap CL, Wright CE, Kenche V, Anderson KE, Dopheide SM, Yuan Y, Sturgeon SA, Prabakaran H, Thompson PE, Smith GD, Shepherd PR, Daniele N, et al. PI 3-kinase p110beta: a new target for antithrombotic therapy. *Nat Med.* 2005; 11(5):507-514.
288. Bennett BL, Sasaki DT, Murray BW, O'Leary EC, Sakata ST, Xu W, Leisten JC, Motiwala A, Pierce S, Satoh Y, Bhagwat SS, Manning AM and Anderson DW. SP600125, an anthrapyrazolone inhibitor of Jun N-terminal kinase. *Proc Natl Acad Sci U S A.* 2001; 98(24):13681-13686.
289. Chou TC. Drug Combination Studies and Their Synergy Quantification Using the

- Chou-Talalay Method. *Cancer Research*. 2010; 70(2):440-446.
290. Yelskaya Z, Carrillo V, Dubisz E, Gulzar H, Morgan D and Mahajan SS. Synergistic inhibition of survival, proliferation, and migration of U87 cells with a combination of LY341495 and Iressa. *PLoS One*. 2013; 8(5):e64588.
291. Ohgaki H. Genetic pathways to glioblastomas. *Neuropathology*. 2005; 25(1):1-7.
292. Holand K, Boller D, Hagel C, Dolski S, Treszl A, Pardo OE, Cwiek P, Salm F, Leni Z, Shepherd PR, Styp-Rekowska B, Djonov V, von Bueren AO, Frei K and Arcaro A. Targeting class IA PI3K isoforms selectively impairs cell growth, survival, and migration in glioblastoma. *PLoS One*. 2014; 9(4):e94132.
293. Edgar KA, Wallin JJ, Berry M, Lee LB, Prior WW, Sampath D, Friedman LS and Belvin M. Isoform-specific phosphoinositide 3-kinase inhibitors exert distinct effects in solid tumors. *Cancer Res*. 2010; 70(3):1164-1172.
294. Denley A, Kang S, Karst U and Vogt PK. Oncogenic signaling of class I PI3K isoforms. *Oncogene*. 2008; 27(18):2561-2574.
295. Matheny RW, Jr. and Adamo ML. PI3K p110 alpha and p110 beta have differential effects on Akt activation and protection against oxidative stress-induced apoptosis in myoblasts. *Cell Death Differ*. 2010; 17(4):677-688.
296. Knight ZA, Gonzalez B, Feldman ME, Zunder ER, Goldenberg DD, Williams O, Loewith R, Stokoe D, Balla A, Toth B, Balla T, Weiss WA, Williams RL and Shokat KM. A pharmacological map of the PI3-K family defines a role for p110alpha in insulin signaling. *Cell*. 2006; 125(4):733-747.
297. Knight ZA and Shokat KM. Features of selective kinase inhibitors. *Chemistry & biology*. 2005; 12(6):621-637.
298. Bi L, Okabe I, Bernard DJ and Nussbaum RL. Early embryonic lethality in mice deficient in the p110beta catalytic subunit of PI 3-kinase. *Mammalian genome : official journal of the International Mammalian Genome Society*. 2002; 13(3):169-172.
299. Ciraolo E, Iezzi M, Marone R, Marengo S, Curcio C, Costa C, Azzolino O, Gonella C, Rubinetto C, Wu H, Dastru W, Martin EL, Silengo L, Altruda F, Turco E, Lanzetti L, et al. Phosphoinositide 3-kinase p110beta activity: key role in

- metabolism and mammary gland cancer but not development. *Sci Signal*. 2008; 1(36):ra3.
300. Iyengar S, Clear A, Bodor C, Maharaj L, Lee A, Calaminici M, Matthews J, Iqbal S, Auer R, Gribben J and Joel S. P110alpha-mediated constitutive PI3K signaling limits the efficacy of p110delta-selective inhibition in mantle cell lymphoma, particularly with multiple relapse. *Blood*. 2013; 121(12):2274-2284.
301. Utermark T, Rao T, Cheng H, Wang Q, Lee SH, Wang ZC, Iglehart JD, Roberts TM, Muller WJ and Zhao JJ. The p110alpha and p110beta isoforms of PI3K play divergent roles in mammary gland development and tumorigenesis. *Genes Dev*. 2012; 26(14):1573-1586.
302. Yip SC, El-Sibai M, Hill KM, Wu H, Fu Z, Condeelis JS and Backer JM. Over-expression of the p110beta but not p110alpha isoform of PI 3-kinase inhibits motility in breast cancer cells. *Cell Motil Cytoskeleton*. 2004; 59(3):180-188.
303. Huttenlocher A and Horwitz AR. Integrins in cell migration. *Cold Spring Harbor perspectives in biology*. 2011; 3(9):a005074.
304. Morozevich G, Kozlova N, Cheglakov I, Ushakova N and Berman A. Integrin alpha5beta1 controls invasion of human breast carcinoma cells by direct and indirect modulation of MMP-2 collagenase activity. *Cell Cycle*. 2009; 8(14):2219-2225.
305. Geiger B, Bershadsky A, Pankov R and Yamada KM. Transmembrane crosstalk between the extracellular matrix--cytoskeleton crosstalk. *Nat Rev Mol Cell Biol*. 2001; 2(11):793-805.
306. Gingras MC, Roussel E, Bruner JM, Branch CD and Moser RP. Comparison of cell adhesion molecule expression between glioblastoma multiforme and autologous normal brain tissue. *Journal of neuroimmunology*. 1995; 57(1-2):143-153.
307. Schnell O, Krebs B, Wagner E, Romagna A, Beer AJ, Grau SJ, Thon N, Goetz C, Kretschmar HA, Tonn JC and Goldbrunner RH. Expression of integrin alphavbeta3 in gliomas correlates with tumor grade and is not restricted to tumor

- vasculature. *Brain Pathol.* 2008; 18(3):378-386.
308. Zheng DQ, Woodard AS, Tallini G and Languino LR. Substrate specificity of alpha(v)beta(3) integrin-mediated cell migration and phosphatidylinositol 3-kinase/AKT pathway activation. *J Biol Chem.* 2000; 275(32):24565-24574.
309. Lei Y, Huang K, Gao C, Lau QC, Pan H, Xie K, Li J, Liu R, Zhang T, Xie N, Nai HS, Wu H, Dong Q, Zhao X, Nice EC, Huang C, et al. Proteomics identification of ITGB3 as a key regulator in reactive oxygen species-induced migration and invasion of colorectal cancer cells. *Mol Cell Proteomics.* 2011; 10(10):M110005397.
310. Meenderink LM, Ryzhova LM, Donato DM, Gochberg DF, Kaverina I and Hanks SK. P130Cas Src-binding and substrate domains have distinct roles in sustaining focal adhesion disassembly and promoting cell migration. *PLoS One.* 2010; 5(10):e13412.
311. Seidler J, Durzok R, Brakebusch C and Cordes N. Interactions of the integrin subunit beta1A with protein kinase B/Akt, p130Cas and paxillin contribute to regulation of radiation survival. *Radiotherapy and oncology : journal of the European Society for Therapeutic Radiology and Oncology.* 2005; 76(2):129-134.
312. Sansing HA, Sarkeshik A, Yates JR, Patel V, Gutkind JS, Yamada KM and Berrier AL. Integrin alphabeta1, alphavbeta, alpha6beta effectors p130Cas, Src and talin regulate carcinoma invasion and chemoresistance. *Biochem Biophys Res Commun.* 2011; 406(2):171-176.
313. Ricciardelli C, Frewin KM, Tan Ide A, Williams ED, Opeskin K, Pritchard MA, Ingman WV and Russell DL. The ADAMTS1 protease gene is required for mammary tumor growth and metastasis. *Am J Pathol.* 2011; 179(6):3075-3085.
314. Choi JE, Kim DS, Kim EJ, Chae MH, Cha SI, Kim CH, Jheon S, Jung TH and Park JY. Aberrant methylation of ADAMTS1 in non-small cell lung cancer. *Cancer genetics and cytogenetics.* 2008; 187(2):80-84.
315. Rocks N, Paulissen G, Quesada-Calvo F, Munaut C, Gonzalez ML, Gueders M, Hacha J, Gilles C, Foidart JM, Noel A and Cataldo DD. ADAMTS-1

- metalloproteinase promotes tumor development through the induction of a stromal reaction in vivo. *Cancer Res.* 2008; 68(22):9541-9550.
316. Freitas VM, do Amaral JB, Silva TA, Santos ES, Mangone FR, Pinheiro Jde J, Jaeger RG, Nagai MA and Machado-Santelli GM. Decreased expression of ADAMTS-1 in human breast tumors stimulates migration and invasion. *Mol Cancer.* 2013; 12:2.
317. Iruela-Arispe ML, Carpizo D and Luque A. ADAMTS1: a matrix metalloprotease with angioinhibitory properties. *Ann N Y Acad Sci.* 2003; 995:183-190.
318. Luque A, Carpizo DR and Iruela-Arispe ML. ADAMTS1/METH1 inhibits endothelial cell proliferation by direct binding and sequestration of VEGF165. *J Biol Chem.* 2003; 278(26):23656-23665.
319. Behm-Ansmant I, Rehwinkel J and Izaurralde E. MicroRNAs silence gene expression by repressing protein expression and/or by promoting mRNA decay. *Cold Spring Harbor symposia on quantitative biology.* 2006; 71:523-530.
320. Zhao HF, Wang J and Tony To SS. The phosphatidylinositol 3-kinase/Akt and c-Jun N-terminal kinase signaling in cancer: Alliance or contradiction? (Review). *Int J Oncol.* 2015.
321. Ridley AJ, Schwartz MA, Burridge K, Firtel RA, Ginsberg MH, Borisy G, Parsons JT and Horwitz AR. Cell migration: integrating signals from front to back. *Science.* 2003; 302(5651):1704-1709.
322. Drees B, Friederich E, Fradelizi J, Louvard D, Beckerle MC and Golsteyn RM. Characterization of the interaction between zyxin and members of the Ena/vasodilator-stimulated phosphoprotein family of proteins. *J Biol Chem.* 2000; 275(29):22503-22511.
323. Call GS, Chung JY, Davis JA, Price BD, Primavera TS, Thomson NC, Wagner MV and Hansen MD. Zyxin phosphorylation at serine 142 modulates the zyxin head-tail interaction to alter cell-cell adhesion. *Biochem Biophys Res Commun.* 2011; 404(3):780-784.
324. Nguyen TN, Uemura A, Shih W and Yamada S. Zyxin-mediated actin assembly is required for efficient wound closure. *J Biol Chem.* 2010;

- 285(46):35439-35445.
- 325.Hoffman LM, Jensen CC, Chaturvedi A, Yoshigi M and Beckerle MC. Stretch-induced actin remodeling requires targeting of zyxin to stress fibers and recruitment of actin regulators. *Mol Biol Cell*. 2012; 23(10):1846-1859.
- 326.Smith MA, Blankman E, Gardel ML, Luettjohann L, Waterman CM and Beckerle MC. A zyxin-mediated mechanism for actin stress fiber maintenance and repair. *Developmental cell*. 2010; 19(3):365-376.
- 327.Deramaudt TB, Dujardin D, Hamadi A, Noulet F, Kolli K, De Mey J, Takeda K and Ronde P. FAK phosphorylation at Tyr-925 regulates cross-talk between focal adhesion turnover and cell protrusion. *Mol Biol Cell*. 2011; 22(7):964-975.
- 328.Yao Y, Lin G, Xie Y, Ma P, Li G, Meng Q and Wu T. Preformulation studies of myricetin: a natural antioxidant flavonoid. *Pharmazie*. 2014; 69(1):19-26.
- 329.Hakkinen SH, Karenlampi SO, Heinonen IM, Mykkanen HM and Torronen AR. Content of the flavonols quercetin, myricetin, and kaempferol in 25 edible berries. *J Agric Food Chem*. 1999; 47(6):2274-2279.
- 330.Miean KH and Mohamed S. Flavonoid (myricetin, quercetin, kaempferol, luteolin, and apigenin) content of edible tropical plants. *J Agric Food Chem*. 2001; 49(6):3106-3112.
- 331.Noroozi M, Angerson WJ and Lean ME. Effects of flavonoids and vitamin C on oxidative DNA damage to human lymphocytes. *Am J Clin Nutr*. 1998; 67(6):1210-1218.
- 332.Srinivasan A, Thangavel C, Liu Y, Shoyele S, Den RB, Selvakumar P and Lakshmikuttyamma A. Quercetin regulates beta-catenin signaling and reduces the migration of triple negative breast cancer. *Mol Carcinog*. 2015.
- 333.Bhat FA, Sharmila G, Balakrishnan S, Arunkumar R, Elumalai P, Suganya S, Raja Singh P, Srinivasan N and Arunakaran J. Quercetin reverses EGF-induced epithelial to mesenchymal transition and invasiveness in prostate cancer (PC-3) cell line via EGFR/PI3K/Akt pathway. *J Nutr Biochem*. 2014; 25(11):1132-1139.
- 334.Mukherjee A and Khuda-Bukhsh AR. Quercetin Down-regulates IL-6/STAT-3 Signals to Induce Mitochondrial-mediated Apoptosis in a Nonsmall- cell

- Lung-cancer Cell Line, A549. *Journal of pharmacopuncture*. 2015; 18(1):19-26.
335. Shan BE, Wang MX and Li RQ. Quercetin inhibit human SW480 colon cancer growth in association with inhibition of cyclin D1 and survivin expression through Wnt/beta-catenin signaling pathway. *Cancer investigation*. 2009; 27(6):604-612.
336. Angst E, Park JL, Moro A, Lu QY, Lu X, Li G, King J, Chen M, Reber HA, Go VL, Eibl G and Hines OJ. The flavonoid quercetin inhibits pancreatic cancer growth in vitro and in vivo. *Pancreas*. 2013; 42(2):223-229.
337. Xu R, Zhang Y, Ye X, Xue S, Shi J, Pan J and Chen Q. Inhibition effects and induction of apoptosis of flavonoids on the prostate cancer cell line PC-3 in vitro. *Food chemistry*. 2013; 138(1):48-53.
338. Labbe D, Provencal M, Lamy S, Boivin D, Gingras D and Beliveau R. The flavonols quercetin, kaempferol, and myricetin inhibit hepatocyte growth factor-induced medulloblastoma cell migration. *The Journal of nutrition*. 2009; 139(4):646-652.
339. Michaud-Levesque J, Bousquet-Gagnon N and Beliveau R. Quercetin abrogates IL-6/STAT3 signaling and inhibits glioblastoma cell line growth and migration. *Exp Cell Res*. 2012; 318(8):925-935.
340. Wang G, Wang JJ, Chen XL, Du SM, Li DS, Pei ZJ, Lan H and Wu LB. The JAK2/STAT3 and mitochondrial pathways are essential for quercetin nanoliposome-induced C6 glioma cell death. *Cell Death Dis*. 2013; 4:e746.
341. Kim H, Moon JY, Ahn KS and Cho SK. Quercetin induces mitochondrial mediated apoptosis and protective autophagy in human glioblastoma U373MG cells. *Oxidative medicine and cellular longevity*. 2013; 2013:596496.
342. Walker EH, Pacold ME, Perisic O, Stephens L, Hawkins PT, Wymann MP and Williams RL. Structural determinants of phosphoinositide 3-kinase inhibition by wortmannin, LY294002, quercetin, myricetin, and staurosporine. *Mol Cell*. 2000; 6(4):909-919.
343. Rafiq RA, Quadri A, Nazir LA, Peerzada K, Ganai BA and Tasduq SA. A Potent Inhibitor of Phosphoinositide 3-Kinase (PI3K) and Mitogen Activated Protein (MAP) Kinase Signalling, Quercetin (3, 3', 4', 5, 7-Pentahydroxyflavone)

- Promotes Cell Death in Ultraviolet (UV)-B-Irradiated B16F10 Melanoma Cells. *PLoS One*. 2015; 10(7):e0131253.
344. Song NR, Chung MY, Kang NJ, Seo SG, Jang TS, Lee HJ and Lee KW. Quercetin suppresses invasion and migration of H-Ras-transformed MCF10A human epithelial cells by inhibiting phosphatidylinositol 3-kinase. *Food chemistry*. 2014; 142:66-71.
345. Dunn J, Baborie A, Alam F, Joyce K, Moxham M, Sibson R, Crooks D, Husband D, Shenoy A, Brodbelt A, Wong H, Liloglou T, Haylock B and Walker C. Extent of MGMT promoter methylation correlates with outcome in glioblastomas given temozolomide and radiotherapy. *Br J Cancer*. 2009; 101(1):124-131.
346. Jiang Z, Pore N, Cerniglia GJ, Mick R, Georgescu MM, Bernhard EJ, Hahn SM, Gupta AK and Maity A. Phosphatase and tensin homologue deficiency in glioblastoma confers resistance to radiation and temozolomide that is reversed by the protease inhibitor nelfinavir. *Cancer Res*. 2007; 67(9):4467-4473.
347. McEllin B, Camacho CV, Mukherjee B, Hahm B, Tomimatsu N, Bachoo RM and Burma S. PTEN loss compromises homologous recombination repair in astrocytes: implications for glioblastoma therapy with temozolomide or poly(ADP-ribose) polymerase inhibitors. *Cancer Res*. 2010; 70(13):5457-5464.
348. Carico C, Nuno M, Mukherjee D, Elramsisy A, Dantis J, Hu J, Rudnick J, Yu JS, Black KL, Bannykh SI and Patil CG. Loss of PTEN is not associated with poor survival in newly diagnosed glioblastoma patients of the temozolomide era. *PLoS One*. 2012; 7(3):e33684.
349. Hirose Y, Berger MS and Pieper RO. p53 effects both the duration of G2/M arrest and the fate of temozolomide-treated human glioblastoma cells. *Cancer Res*. 2001; 61(5):1957-1963.
350. Xu GW, Mymryk JS and Cairncross JG. Inactivation of p53 sensitizes astrocytic glioma cells to BCNU and temozolomide, but not cisplatin. *J Neurooncol*. 2005; 74(2):141-149.
351. Xu GW, Mymryk JS and Cairncross JG. Pharmaceutical-mediated inactivation of p53 sensitizes U87MG glioma cells to BCNU and temozolomide. *Int J Cancer*.

- 2005; 116(2):187-192.
352. Dinca EB, Lu KV, Sarkaria JN, Pieper RO, Prados MD, Haas-Kogan DA, Vandenberg SR, Berger MS and James CD. p53 Small-molecule inhibitor enhances temozolomide cytotoxic activity against intracranial glioblastoma xenografts. *Cancer Res.* 2008; 68(24):10034-10039.
353. Rossi M, Magnoni L, Miracco C, Mori E, Tosi P, Pirtoli L, Tini P, Oliveri G, Cosci E and Bakker A. beta-catenin and Gli1 are prognostic markers in glioblastoma. *Cancer Biol Ther.* 2011; 11(8):753-761.
354. Weller M, Felsberg J, Hartmann C, Berger H, Steinbach JP, Schramm J, Westphal M, Schackert G, Simon M, Tonn JC, Heese O, Krex D, Nikkhah G, Pietsch T, Wiestler O, Reifenberger G, et al. Molecular predictors of progression-free and overall survival in patients with newly diagnosed glioblastoma: a prospective translational study of the German Glioma Network. *J Clin Oncol.* 2009; 27(34):5743-5750.
355. Wang X, Chen JX, Liu JP, You C, Liu YH and Mao Q. Gain of function of mutant TP53 in glioblastoma: prognosis and response to temozolomide. *Ann Surg Oncol.* 2014; 21(4):1337-1344.
356. Hermisson M, Klumpp A, Wick W, Wischhusen J, Nagel G, Roos W, Kaina B and Weller M. O6-methylguanine DNA methyltransferase and p53 status predict temozolomide sensitivity in human malignant glioma cells. *J Neurochem.* 2006; 96(3):766-776.
357. Roos WP, Batista LF, Naumann SC, Wick W, Weller M, Menck CF and Kaina B. Apoptosis in malignant glioma cells triggered by the temozolomide-induced DNA lesion O6-methylguanine. *Oncogene.* 2007; 26(2):186-197.
358. Malkoun N, Chargari C, Forest F, Fotso MJ, Cartier L, Auberdiac P, Thorin J, Pacaut C, Peoc'h M, Nuti C, Schmitt T and Magne N. Prolonged temozolomide for treatment of glioblastoma: preliminary clinical results and prognostic value of p53 overexpression. *J Neurooncol.* 2012; 106(1):127-133.
359. Birner P, Piribauer M, Fischer I, Gatterbauer B, Marosi C, Ungersbock K, Rössler K, Budka H and Hainfellner JA. Prognostic relevance of p53 protein

- expression in glioblastoma. *Oncol Rep.* 2002; 9(4):703-707.
360. Pozsgai E, Bellyei S, Cseh A, Boronkai A, Racz B, Szabo A, Sumegi B and Hocsak E. Quercetin increases the efficacy of glioblastoma treatment compared to standard chemoradiotherapy by the suppression of PI-3-kinase-Akt pathway. *Nutr Cancer.* 2013; 65(7):1059-1066.
361. Li N, Sun C, Zhou B, Xing H, Ma D, Chen G and Weng D. Low concentration of quercetin antagonizes the cytotoxic effects of anti-neoplastic drugs in ovarian cancer. *PLoS One.* 2014; 9(7):e100314.
362. Gaspar N, Marshall L, Perryman L, Bax DA, Little SE, Viana-Pereira M, Sharp SY, Vassal G, Pearson AD, Reis RM, Hargrave D, Workman P and Jones C. MGMT-independent temozolomide resistance in pediatric glioblastoma cells associated with a PI3-kinase-mediated HOX/stem cell gene signature. *Cancer Res.* 2010; 70(22):9243-9252.
363. Lin F, de Gooijer MC, Roig EM, Buil LC, Christner SM, Beumer JH, Wurdinger T, Beijnen JH and van Tellingen O. ABCB1, ABCG2, and PTEN determine the response of glioblastoma to temozolomide and ABT-888 therapy. *Clin Cancer Res.* 2014; 20(10):2703-2713.
364. Vicente-Manzanares M, Webb DJ and Horwitz AR. Cell migration at a glance. *J Cell Sci.* 2005; 118(Pt 21):4917-4919.
365. Lauffenburger DA and Horwitz AF. Cell migration: A physically integrated molecular process. *Cell.* 1996; 84(3):359-369.
366. Nagano M, Hoshino D, Koshikawa N, Akizawa T and Seiki M. Turnover of focal adhesions and cancer cell migration. *Int J Cell Biol.* 2012; 2012:310616.
367. Humphries JD, Wang P, Streuli C, Geiger B, Humphries MJ and Ballestrem C. Vinculin controls focal adhesion formation by direct interactions with talin and actin. *J Cell Biol.* 2007; 179(5):1043-1057.
368. Schaller MD, Otey CA, Hildebrand JD and Parsons JT. Focal adhesion kinase and paxillin bind to peptides mimicking beta integrin cytoplasmic domains. *J Cell Biol.* 1995; 130(5):1181-1187.
369. Parsons JT, Martin KH, Slack JK, Taylor JM and Weed SA. Focal adhesion

- kinase: a regulator of focal adhesion dynamics and cell movement. *Oncogene*. 2000; 19(49):5606-5613.
370. Mitra SK, Hanson DA and Schlaepfer DD. Focal adhesion kinase: in command and control of cell motility. *Nat Rev Mol Cell Biol*. 2005; 6(1):56-68.
371. Chang F, Lemmon CA, Park D and Romer LH. FAK potentiates Rac1 activation and localization to matrix adhesion sites: a role for betaPIX. *Mol Biol Cell*. 2007; 18(1):253-264.
372. Ilic D, Furuta Y, Kanazawa S, Takeda N, Sobue K, Nakatsuji N, Nomura S, Fujimoto J, Okada M and Yamamoto T. Reduced cell motility and enhanced focal adhesion contact formation in cells from FAK-deficient mice. *Nature*. 1995; 377(6549):539-544.
373. Bear JE, Svitkina TM, Krause M, Schafer DA, Loureiro JJ, Strasser GA, Maly IV, Chaga OY, Cooper JA, Borisy GG and Gertler FB. Antagonism between Ena/VASP proteins and actin filament capping regulates fibroblast motility. *Cell*. 2002; 109(4):509-521.
374. Bear JE and Gertler FB. Ena/VASP: towards resolving a pointed controversy at the barbed end. *J Cell Sci*. 2009; 122(Pt 12):1947-1953.
375. Breitsprecher D, Kiesewetter AK, Linkner J, Urbanke C, Resch GP, Small JV and Faix J. Clustering of VASP actively drives processive, WH2 domain-mediated actin filament elongation. *EMBO J*. 2008; 27(22):2943-2954.
376. Kadmas JL and Beckerle MC. The LIM domain: from the cytoskeleton to the nucleus. *Nat Rev Mol Cell Biol*. 2004; 5(11):920-931.
377. Smith MA, Blankman E, Deakin NO, Hoffman LM, Jensen CC, Turner CE and Beckerle MC. LIM domains target actin regulators paxillin and zyxin to sites of stress fiber strain. *PLoS One*. 2013; 8(8):e69378.
378. Nix DA, Fradelizi J, Bockholt S, Menichi B, Louvard D, Friederich E and Beckerle MC. Targeting of zyxin to sites of actin membrane interaction and to the nucleus. *J Biol Chem*. 2001; 276(37):34759-34767.
379. Reinhard M, Zumbunn J, Jaquemar D, Kuhn M, Walter U and Trueb B. An alpha-actinin binding site of zyxin is essential for subcellular zyxin localization

- and alpha-actinin recruitment. *J Biol Chem.* 1999; 274(19):13410-13418.
380. Blume-Jensen P and Hunter T. Oncogenic kinase signalling. *Nature.* 2001; 411(6835):355-365.
381. Fabbro D. 25 years of small molecular weight kinase inhibitors: potentials and limitations. *Mol Pharmacol.* 2015; 87(5):766-775.
382. Weiss WA, Taylor SS and Shokat KM. Recognizing and exploiting differences between RNAi and small-molecule inhibitors. *Nature chemical biology.* 2007; 3(12):739-744.
383. Martinez J, Patkaniowska A, Urlaub H, Luhrmann R and Tuschl T. Single-stranded antisense siRNAs guide target RNA cleavage in RNAi. *Cell.* 2002; 110(5):563-574.
384. Carthew RW and Sontheimer EJ. Origins and Mechanisms of miRNAs and siRNAs. *Cell.* 2009; 136(4):642-655.
385. Singh S, Narang AS and Mahato RI. Subcellular fate and off-target effects of siRNA, shRNA, and miRNA. *Pharm Res.* 2011; 28(12):2996-3015.
386. Jackson AL and Linsley PS. Recognizing and avoiding siRNA off-target effects for target identification and therapeutic application. *Nat Rev Drug Discov.* 2010; 9(1):57-67.
387. Judge AD, Sood V, Shaw JR, Fang D, McClintock K and MacLachlan I. Sequence-dependent stimulation of the mammalian innate immune response by synthetic siRNA. *Nat Biotechnol.* 2005; 23(4):457-462.
388. Judge AD, Bola G, Lee AC and MacLachlan I. Design of noninflammatory synthetic siRNA mediating potent gene silencing in vivo. *Mol Ther.* 2006; 13(3):494-505.
389. Eberle F, Giessler K, Deck C, Heeg K, Peter M, Richert C and Dalpke AH. Modifications in small interfering RNA that separate immunostimulation from RNA interference. *J Immunol.* 2008; 180(5):3229-3237.
390. Whitehead KA, Langer R and Anderson DG. Knocking down barriers: advances in siRNA delivery. *Nat Rev Drug Discov.* 2009; 8(2):129-138.
391. Shim MS and Kwon YJ. Efficient and targeted delivery of siRNA in vivo. *The*

- FEBS journal. 2010; 277(23):4814-4827.
392. Zhao X, Peng X, Sun S, Park AY and Guan JL. Role of kinase-independent and -dependent functions of FAK in endothelial cell survival and barrier function during embryonic development. *J Cell Biol.* 2010; 189(6):955-965.
393. Tamborini E, Bonadiman L, Greco A, Albertini V, Negri T, Gronchi A, Bertulli R, Colecchia M, Casali PG, Pierotti MA and Pilotti S. A new mutation in the KIT ATP pocket causes acquired resistance to imatinib in a gastrointestinal stromal tumor patient. *Gastroenterology.* 2004; 127(1):294-299.
394. Gorre ME, Mohammed M, Ellwood K, Hsu N, Paquette R, Rao PN and Sawyers CL. Clinical resistance to STI-571 cancer therapy caused by BCR-ABL gene mutation or amplification. *Science.* 2001; 293(5531):876-880.
395. Rodrik-Outmezguine VS, Chandarlapaty S, Pagano NC, Poulikakos PI, Scaltriti M, Moskatel E, Baselga J, Guichard S and Rosen N. mTOR kinase inhibition causes feedback-dependent biphasic regulation of AKT signaling. *Cancer Discov.* 2011; 1(3):248-259.
396. Serra V, Scaltriti M, Prudkin L, Eichhorn PJ, Ibrahim YH, Chandarlapaty S, Markman B, Rodriguez O, Guzman M, Rodriguez S, Gili M, Russillo M, Parra JL, Singh S, Arribas J, Rosen N, et al. PI3K inhibition results in enhanced HER signaling and acquired ERK dependency in HER2-overexpressing breast cancer. *Oncogene.* 2011; 30(22):2547-2557.
397. Bardelli A, Corso S, Bertotti A, Hobor S, Valtorta E, Siravegna G, Sartore-Bianchi A, Scala E, Cassingena A, Zecchin D, Apicella M, Migliardi G, Galimi F, Lauricella C, Zanon C, Perera T, et al. Amplification of the MET receptor drives resistance to anti-EGFR therapies in colorectal cancer. *Cancer Discov.* 2013; 3(6):658-673.
398. Alagesan B, Contino G, Guimaraes AR, Corcoran RB, Deshpande V, Wojtkiewicz GR, Hezel AF, Wong KK, Loda M, Weissleder R, Benes C, Engelman JA and Bardeesy N. Combined MEK and PI3K inhibition in a mouse model of pancreatic cancer. *Clin Cancer Res.* 2015; 21(2):396-404.
399. Wong CH, Ma BB, Cheong HT, Hui CW, Hui EP and Chan AT. Preclinical

- evaluation of PI3K inhibitor BYL719 as a single agent and its synergism in combination with cisplatin or MEK inhibitor in nasopharyngeal carcinoma (NPC). *Am J Cancer Res.* 2015; 5(4):1496-1506.
400. Tolcher AW, Patnaik A, Papadopoulos KP, Rasco DW, Becerra CR, Allred AJ, Orford K, Aktan G, Ferron-Brady G, Ibrahim N, Gauvin J, Motwani M and Cornfeld M. Phase I study of the MEK inhibitor trametinib in combination with the AKT inhibitor afuresertib in patients with solid tumors and multiple myeloma. *Cancer Chemother Pharmacol.* 2015; 75(1):183-189.
401. Liu T, Sun Q, Li Q, Yang H, Zhang Y, Wang R, Lin X, Xiao D, Yuan Y, Chen L and Wang W. Dual PI3K/mTOR inhibitors, GSK2126458 and PKI-587, suppress tumor progression and increase radiosensitivity in nasopharyngeal carcinoma. *Mol Cancer Ther.* 2014.
402. Britschgi A, Andraos R, Brinkhaus H, Klebba I, Romanet V, Muller U, Murakami M, Radimerski T and Bentires-Alj M. JAK2/STAT5 inhibition circumvents resistance to PI3K/mTOR blockade: a rationale for cotargeting these pathways in metastatic breast cancer. *Cancer Cell.* 2012; 22(6):796-811.
403. Menzin AW, King SA, Aikins JK, Mikuta JJ and Rubin SC. Taxol (paclitaxel) was approved by FDA for the treatment of patients with recurrent ovarian cancer. *Gynecol Oncol.* 1994; 54(1):103.
404. Young SD, Whissell M, Noble JC, Cano PO, Lopez PG and Germond CJ. Phase II clinical trial results involving treatment with low-dose daily oral cyclophosphamide, weekly vinblastine, and rofecoxib in patients with advanced solid tumors. *Clin Cancer Res.* 2006; 12(10):3092-3098.
405. Liu Y, Luan L and Wang X. A randomized Phase II clinical study of combining panitumumab and bevacizumab, plus irinotecan, 5-fluorouracil, and leucovorin (FOLFIRI) compared with FOLFIRI alone as second-line treatment for patients with metastatic colorectal cancer and KRAS mutation. *OncoTargets and therapy.* 2015; 8:1061-1068.
406. McNeil C. Topotecan: after FDA and ASCO, what's next? *J Natl Cancer Inst.* 1996; 88(12):788-789.

407. Romanouskaya TV and Grinev VV. Cytotoxic effect of flavonoids on leukemia cells and normal cells of human blood. *Bulletin of experimental biology and medicine*. 2009; 148(1):57-59.
408. Monasterio A, Urdaci MC, Pinchuk IV, Lopez-Moratalla N and Martinez-Irujo JJ. Flavonoids induce apoptosis in human leukemia U937 cells through caspase- and caspase-calpain-dependent pathways. *Nutr Cancer*. 2004; 50(1):90-100.
409. Khanduja KL, Gandhi RK, Pathania V and Syal N. Prevention of N-nitrosodiethylamine-induced lung tumorigenesis by ellagic acid and quercetin in mice. *Food Chem Toxicol*. 1999; 37(4):313-318.
410. Caltagirone S, Rossi C, Poggi A, Ranelletti FO, Natali PG, Brunetti M, Aiello FB and Piantelli M. Flavonoids apigenin and quercetin inhibit melanoma growth and metastatic potential. *Int J Cancer*. 2000; 87(4):595-600.
411. Wang L, Li W, Lin M, Garcia M, Mulholland D, Lilly M and Martins-Green M. Luteolin, ellagic acid and punicic acid are natural products that inhibit prostate cancer metastasis. *Carcinogenesis*. 2014; 35(10):2321-2330.
412. Senderowicz AM. Flavopiridol: the first cyclin-dependent kinase inhibitor in human clinical trials. *Invest New Drugs*. 1999; 17(3):313-320.
413. Jones JA, Rupert AS, Poi M, Phelps MA, Andritsos L, Baiocchi R, Benson DM, Blum KA, Christian B, Flynn J, Penza S, Porcu P, Grever MR and Byrd JC. Flavopiridol can be safely administered using a pharmacologically derived schedule and demonstrates activity in relapsed and refractory non-Hodgkin's lymphoma. *American journal of hematology*. 2014; 89(1):19-24.
414. Bible KC, Peethambaram PP, Oberg AL, Maples W, Groteluschen DL, Boente M, Burton JK, Gomez Dahl LC, Tibodeau JD, Isham CR, Maguire JL, Shridhar V, Kukla AK, Voll KJ, Mauer MJ, Colevas AD, et al. A phase 2 trial of flavopiridol (Alvocidib) and cisplatin in platin-resistant ovarian and primary peritoneal carcinoma: MC0261. *Gynecol Oncol*. 2012; 127(1):55-62.
415. Burdette-Radoux S, Tozer RG, Lohmann RC, Quirt I, Ernst DS, Walsh W, Wainman N, Colevas AD and Eisenhauer EA. Phase II trial of flavopiridol, a cyclin dependent kinase inhibitor, in untreated metastatic malignant melanoma.

- Invest New Drugs. 2004; 22(3):315-322.
416. Hofmeister CC, Poi M, Bowers MA, Zhao W, Phelps MA, Benson DM, Kraut EH, Farag S, Efebera YA, Sexton J, Lin TS, Grever M and Byrd JC. A phase I trial of flavopiridol in relapsed multiple myeloma. *Cancer Chemother Pharmacol.* 2014; 73(2):249-257.
417. Liu G, Gandara DR, Lara PN, Jr., Raghavan D, Doroshow JH, Twardowski P, Kantoff P, Oh W, Kim K and Wilding G. A Phase II trial of flavopiridol (NSC #649890) in patients with previously untreated metastatic androgen-independent prostate cancer. *Clin Cancer Res.* 2004; 10(3):924-928.
418. Shapiro GI, Supko JG, Patterson A, Lynch C, Lucca J, Zaccarola PF, Muzikansky A, Wright JJ, Lynch TJ, Jr. and Rollins BJ. A phase II trial of the cyclin-dependent kinase inhibitor flavopiridol in patients with previously untreated stage IV non-small cell lung cancer. *Clin Cancer Res.* 2001; 7(6):1590-1599.
419. Carvajal RD, Tse A, Shah MA, Lefkowitz RA, Gonen M, Gilman-Rosen L, Kortmanský J, Kelsen DP, Schwartz GK and O'Reilly EM. A phase II study of flavopiridol (Alvocidib) in combination with docetaxel in refractory, metastatic pancreatic cancer. *Pancreatology : official journal of the International Association of Pancreatology.* 2009; 9(4):404-409.
420. Ferry DR, Smith A, Malkhandi J, Fyfe DW, deTakats PG, Anderson D, Baker J and Kerr DJ. Phase I clinical trial of the flavonoid quercetin: pharmacokinetics and evidence for in vivo tyrosine kinase inhibition. *Clin Cancer Res.* 1996; 2(4):659-668.
421. Lazarevic B, Boezelijn G, Diep LM, Kvernrod K, Ogren O, Ramberg H, Moen A, Wessel N, Berg RE, Egge-Jacobsen W, Hammarstrom C, Svindland A, Kucuk O, Saatcioglu F, Tasken KA and Karlsen SJ. Efficacy and safety of short-term genistein intervention in patients with localized prostate cancer prior to radical prostatectomy: a randomized, placebo-controlled, double-blind Phase 2 clinical trial. *Nutr Cancer.* 2011; 63(6):889-898.
422. Zhao H, Zhu W, Xie P, Li H, Zhang X, Sun X, Yu J and Xing L. A phase I study of concurrent chemotherapy and thoracic radiotherapy with oral

- epigallocatechin-3-gallate protection in patients with locally advanced stage III non-small-cell lung cancer. *Radiotherapy and oncology : journal of the European Society for Therapeutic Radiology and Oncology*. 2014; 110(1):132-136.
- 423.Cheng WY, Chiao MT, Liang YJ, Yang YC, Shen CC and Yang CY. Luteolin inhibits migration of human glioblastoma U-87 MG and T98G cells through downregulation of Cdc42 expression and PI3K/AKT activity. *Molecular biology reports*. 2013; 40(9):5315-5326.
- 424.Khaw AK, Yong JW, Kalthur G and Hande MP. Genistein induces growth arrest and suppresses telomerase activity in brain tumor cells. *Genes, chromosomes & cancer*. 2012; 51(10):961-974.
- 425.Lee DH, Lee TH, Jung CH and Kim YH. Wogonin induces apoptosis by activating the AMPK and p53 signaling pathways in human glioblastoma cells. *Cell Signal*. 2012; 24(11):2216-2225.
- 426.Colombo R, Caldarelli M, Mennecozzi M, Giorgini ML, Sola F, Cappella P, Perrera C, Depaolini SR, Rusconi L, Cucchi U, Avanzi N, Bertrand JA, Bossi RT, Pesenti E, Galvani A, Isacchi A, et al. Targeting the mitotic checkpoint for cancer therapy with NMS-P715, an inhibitor of MPS1 kinase. *Cancer Res*. 2010; 70(24):10255-10264.
- 427.Vaishnav D, Jambal P, Reusch JE and Pugazhenti S. SP600125, an inhibitor of c-jun N-terminal kinase, activates CREB by a p38 MAPK-mediated pathway. *Biochem Biophys Res Commun*. 2003; 307(4):855-860.
- 428.Parra E, Gutierrez L and Ferreira J. Inhibition of basal JNK activity by small interfering RNAs enhances cisplatin sensitivity and decreases DNA repair in T98G glioblastoma cells. *Oncol Rep*. 2015; 33(1):413-418.
- 429.Bibikova M, Golic M, Golic KG and Carroll D. Targeted chromosomal cleavage and mutagenesis in *Drosophila* using zinc-finger nucleases. *Genetics*. 2002; 161(3):1169-1175.
- 430.Cho SW, Kim S, Kim JM and Kim JS. Targeted genome engineering in human cells with the Cas9 RNA-guided endonuclease. *Nat Biotechnol*. 2013; 31(3):230-232.

## Reference

---

431. Morbitzer R, Romer P, Boch J and Lahaye T. Regulation of selected genome loci using de novo-engineered transcription activator-like effector (TALE)-type transcription factors. *Proc Natl Acad Sci U S A*. 2010; 107(50):21617-21622.